INVESTIGATION OF THE OCCURRENCE, BIOSORPTION, AND PHYTOREMEDIATION OF SELECTED ENDOCRINE DISRUPTING CHEMICALS FROM WASTEWATER USING *MORINGA OLEIFERA* AND *EICHHORNIA CRASSIPES*

Emily Chelangat Ngeno

A thesis submitted to the School of Natural Sciences in partial fulfillment of the requirements for the degree of Doctor of Philosophy (Ph.D.) in Chemistry of Masinde Muliro University of Science and Technology.

OCTOBER 2024

DECLARATION

This thesis is my original work prepared with no other than the indicated sources and support and has not been presented elsewhere for a degree or any other award.

Signature..... Date….....

Emily Chelangat Ngeno

SCH/H/01-56335/2017

CERTIFICATION

The undersigned certify that they have read and hereby recommend for acceptance of Masinde Muliro University of Science and Technology a thesis entitled: "**Investigation of the Occurrence, Biosorption, and Phytoremediation of Selected Endocrine Disrupting Chemicals from Wastewater using *Moringa oleifera* and *Eichhornia crassipes***"

Signature……... Date…….

Prof. Francis Orata Omoto,

Associate Professor, Department of Pure and Applied Chemistry,

Masinde Muliro University of Science and Technology.

Signature……... Date…….

Dr. Roselyn Ongulu,

Lecturer, Department of Pure and Applied Chemistry,

Masinde Muliro University of Science and Technology.

Signature……. Date……....

Dr. Patrick Ssebugere,

Senior Lecturer,

Department of Chemistry,

Makerere University.

COPYRIGHT

DEDICATION

I dedicate this work to my husband Mr. Charles Kiprono, and children Ryan Kiptoo, Renee Cheruto, and Ruby Cherop. Thank you.

ACKNOWLEDGMENT

My sincere gratitude goes to my supervisors Prof. Francis Orata, Dr. Roselyn Ongulu, and Dr. Patrick Ssebugere for their tireless support, valuable criticism, encouragement, and guidance throughout this study. Special appreciation goes to Dr. Victor Shikuku for his expertise in adsorption. My sincere thanks also go to all staff of the Pure and Applied Chemistry Department, Masinde Muliro University of Science and Technology, and those of Makerere University, Department of Chemistry. Specifically, I wish to thank Mr. Manoah Opanga and Mr. Stephen Mulinda for their laboratory technical guidance; Mr. Agnitius Akala who assisted in sample clean-up and extraction of the selected EDCs; Mr. Fred Ssepuya and Ms. Resty Alexandra who carried out the analysis of the samples; Mr. Deo Ssentongo who assisted in the adsorption experiments and finally Mr. Silver Odongo and Ms. Afuwa Kagoya who provided orientation during my stay in Makerere university.

This study would not have been accomplished without the financial support of the Organization for Women Scientists for the Developing World (OWSD), Kenya National Research Fund (NRF), International Foundation for Science (1I2_W_042583_REV), TWAS-SIDA (20-267 RG/CHE/AF/AC_G), Makerere University Research and Innovation Fund (MAKRIF/CH/01/21) and APPEAR Academic Partnership (Project 249). I also thank the African-German Network of Excellence in Science (AGNES) for granting me a Mobility Grant in 2021 to Makerere University; the Grant is supported by the German Federal Ministry of Education and Research through the Alexander von Humboldt Foundation. My sincere appreciation goes to Mawazo for their professional fellowship program and their financial support.

ABSTRACT

Endocrine disrupting chemicals (EDCs) cause adverse health effects to biota. They are not effectively removed by conventional wastewater treatment options and advanced methods are costly. This study investigated the levels, mass loadings, removal efficiency, and associated ecotoxicological risks of selected EDCs, namely, dibutyl phthalate (DBP), diethylhexyl phthalate (DEHP), dimethyl phthalate (DMP), linuron (LNR) and progesterone (PGT) in wastewater, sludge, and untreated dry biosolid (UDBS) samples from twelve wastewater treatment plants (WWTPs) in nine major towns in Kenya. Analysis was done using high-performance liquid chromatography coupled with triple quadrupole mass spectrometry (HPLC-MS/MS). All the wastewater influents had quantifiable levels of EDCs with DBP being the most abundant (37.5%) with a mean range of 4.3−9.7 μg L^{-1}. DEHP was the most abundant in sludge and accounted for 48.2% ranging between 278.7 and 9243.5 ng g^{-1} dry weight (dw). In the UDBS samples, DEHP was also the most abundant (40%) of the total EDCs detected with levels ranging from 78.8–3938.5 ng g^{-1} dw. The average removal efficiency per pollutant was as follows: DMP (98.7%) > DEHP (91.7%) > PGT (88.3%) > DBP (77.9%) > LNR (72.2%). The mass loadings were as high as 373.3 g day^{-1} of DBP in WWTPs in densely populated cities. DEHP and PGT had their Risk Quotients (RQs) > 1, posing a high risk to biota. DMP, DBP, and LNR posed medium risks as their RQ values were between 0.1 and 1. Removal of these toxicants was carried out via adsorption using chemically activated fat-free powdered *Moringa oleifera* seed biomass (*MOSB*) which was pretreated, characterized, and used as a low-cost biosorbent for the abstraction of PGT and LNR from synthetic wastewater. The process parameters, contact time, pH, adsorbate concentration, temperature, and adsorbent dosage were set and optimized using central composite design (CCD) and response surface methodology (RSM) in Design Expert Software. For biosorption of both PGT and LNR, the proposed model was quadratic. The optimum parameters for PGT adsorption to *MOSB* were: 86.8 min, 500 μg L^{-1} adsorbate concentration, 298 K and 0.1 g adsorbent dosage while for LNR were: 154 min, 500 μg L^{-1} adsorbate concentration, 298K and 0.1 g adsorbent dosage. pH was not a significant factor in the removal of both PGT and LNR. The kinetics, isotherms, and thermodynamics were analyzed further using OriginPro. The equilibrium data were best described by the Langmuir isotherm for PGT and Sips model for LNR, with maximum monolayer adsorption capacities of 135.8 μg g^{-1} and 144.0 μg g^{-1}, respectively. Adsorption kinetics followed pseudo-first order (PFO) for PGT and pseudo-second order (PSO) for LNR predicting physisorption and chemisorption rate-determining steps, respectively. The thermodynamics functions (PGT: $\Delta G < 0$, ΔH = -9.3 kJ mol^{-1} and ΔS = +44.2 J mol^{-1} and LNR: $\Delta G < 0$, ΔH = -10.3 kJ mol^{-1} and ΔS = +41.5 J mol^{-1}) confirmed that the adsorption of PGT and LNR onto *MOSB* was a spontaneous and exothermic process with randomness and affinity experienced at the surface of the adsorbent. The adsorption mechanism was non-electrostatic and may have involved π-π interactions. The results from this study show that the *MOSB* is a promising alternative for an ecofriendly, low-cost biosorbent that can effectively remove PGT and LNR from aqueous solutions. Phytoremediation of LNR and PGT using *Eichhornia crassipes* was also carried out. The concentrations of EDCs abstracted using phytoremediation were however below the quantification levels.

TABLE OF CONTENTS

LIST OF FIGURES

LIST OF TABLES

TABLE OF APPENDICES

ABBREVIATIONS AND ACRONYMS

ACs	Activated carbons
AF	Assessment factor
ANOVA	analysis of variance
BOD_5	Biochemical oxygen demand
$CaCl_2$	Calcium chloride
CCD	Central composite design
CNTs	Carbon nanotubes
COD	Chemical oxygen demand
DBP	dibutyl phthalate
DDT	Dichlorodiphenyltrichloroethane
DEHP	diethylhexyl phthalate
DMP	dimethyl phthalate
EC	Electrical conductivity
EC_{50}	Lowest short-term concentration causing 50% effect
ECOTOX	Ecotoxicology
E. Crassipes	*Eichhornia crassipes*
EDCs	Endocrine disrupting chemicals
ESI^+	Positive electrospray ionization
ESI^-	Negative electrospray ionization
HPLC-MS/MS	High-Performance Liquid Chromatography tandem Mass Spectrometry
HCl	Hydrochloric acid
H_2SO_4	Sulphuric acid
H_3PO_4	phosphoric acid
KCNS	potassium thiocyanate
$KMnO_4$	Potassium permanganate
KOH	potassium hydroxide
K_2S	potassium sulphide
LC_{50}	Lowest short-term concentration causing 50% death
LC-MS	Liquid Chromatography - Mass spectrometry

LOD	Limit of detection
LOEC	Lowest observed effect concentration
LOQ	Limit of quantification
LNR	linuron
µg g^{-1}	Micrograms per gram
µg L^{-1}	Micrograms per Litre
µg ml^{-1}	Microgram per millimetre
MEC	Maximum measured environmental concentration
mL	millilitres
mM	Millimole
mg L^{-1}	Milligrams per Litre
M.O	*Moringa oleifera*
MOSB	*Moringa oleifera* seed biomass
MRM	Multiple reaction monitoring
MTBE	Methyltertbutyl ether
MMUST	Masinde Muliro University of Science and Technology
NaOH	Sodium Hydroxide
NOEC	long term no observed effect concentration
O_2	Oxygen
Rpm	Revolutions per minute
PAEs	Phthalic acid esters
PAHs	Polycyclic aromatic hydrocarbons
PBBs	Polybrominated biphenyls
PCBs	polychlorinated biphenyls
PFASs	Per- and polyfluoroalkyl substances
PFO	Pseudo first-order
PGT	Progesterone
pH_{pzc}	pH at a point of zero charge
PNEC	Predicted No effect concentration
PVC	Polyvinyl chloride
PSO	Pseudo second order
R^2	Coefficient of determination

RSM	Response surface methodology
RQ	Risk Quotient
SD	Standard deviation
SPE	Solid Phase Extraction
TCE	Trichloroethylene
TDS	Total dissolved solids
TNT	Trinitrotoluene
WSPs	Wastewater stabilization ponds
WWTPs	Wastewater treatment plants
WHO	World Health Organization
χ^2	Chi-square
UDBS	Untreated dry biosolids
UNEP	United Nations Environmental Programme
UN-SDG	United Nations-Sustainable Development Goals
$ZnCl_2$	Zinc chloride

CHAPTER ONE

INTRODUCTION

1.1 Background of the study

Endocrine disrupting chemicals (EDCs) are natural or exogenous chemicals that can interfere with the normal functioning of the natural blood-borne hormones in the body (Zoeller et al., 2012). Hormones are found in the endocrine glands and circulate in trace, time-dependent concentrations. They are responsible for homeostasis, reproduction, regulating the body's response to various nutritional needs, and brain and body development processes (Bergman et al., 2013). Every gland secretes one or more hormones, that are subsequently released into the bloodstream where they travel until they reach a specific tissue or organ. There, they attach to particular receptors, generating a response such as synthesis of another hormone, metabolism alteration, a change in behavior, or other reactions, based upon the specific hormone and its target (Gore et al., 2014). The endocrine system is crucial for numerous key biological and physiological activities, regulating the quality of life, and any deficiency can result in diseases or fatalities (Gore et al., 2014).

Exposure to EDCs can impair the endocrine system in both human beings and animals. This interference with the production, secretion, biosynthesis, metabolism, transport, or supplementary action of endogenous hormones causes a deviation from routine homeostatic control or reproduction, which has a negative impact on the organism's health (Diamanti-Kandarakis et al., 2009). In addition to reproductive health issues, congenital anomalies, cardiovascular and respiratory diseases, tumors, cancer, neurological and

behavioral disorders, Alzheimer's, thyroid issues, and obesity, hormonal dysfunctions also hurt the immune system, the cardiopulmonary system, and the nervous system (Bergman et al., 2013; Kasonga et al., 2021). EDCs include selected pesticides, plastics, plasticizers, hormones, pharmaceutical agents, and industrial chemicals and their byproducts [polychlorinated biphenyls (PCBs), polybrominated biphenyls (PBBs), dioxins, per- and polyfluoroalkyl substances (PFASs)] (Diamanti-Kandarakis et al., 2009; Olujimi et al., 2012; Ssebugere et al., 2020). These chemicals are originally designed for specific beneficial actions but negatively affect the body's normal functions when absorbed into the body (Schug et al., 2011).

EDCs and other emerging contaminants are chemically stable to biodegradation and can form complexes, hazardous derivatives, and byproducts (Kumar et al., 2022); therefore making their removal by conventional wastewater treatment methods such as coagulation, flocculation, and settling processes complicated and ineffective (Kasonga et al., 2021; Mukherjee et al., 2021; Ng et al., 2021; Orata, 2018). Moreover, advanced methods like oxidation processes, nanofiltration, reverse osmosis, and membranes are costly for developing countries (Mukherjee et al., 2021). As a result, these compounds may escape from the wastewater treatment plants (WWTPs) *via* effluents into the aquatic environment (Ojoghoro et al., 2021) and subsequently to drinking water (Orata, 2018) potentially posing detrimental effects to aquatic life, wildlife, and human beings. Furthermore, untreated dry biosolids (UDBS) from WWTPs applied in farmlands as fertilizer (Grassi et al., 2013), seepage from septic tanks, landfilling areas, surface waters (Ng et al., 2021) and a wide range of consumer products are other sources of EDCs (Lee & Ji, 2022; Rachoń, 2015).

Despite the detrimental impacts of EDCs, there is scant data on their prevalence, fate, and environmental impact in developing countries. Consequently, they are inadequately monitored and inventoried (Gavrilescu et al., 2015; K'oreje et al., 2020). Although numerous studies in other countries have documented EDCs in merchandise and other environmental matrices (Basile et al., 2011; Bergman et al., 2013), there is a dearth of literature about the contaminant levels of EDCs in East Africa. A few studies have focused on legacy contaminants such as PFASs (Chirikona et al., 2022) and dioxins (Omwoma et al., 2015). Those who have investigated the occurrence of emerging pollutants like pharmaceuticals and personal care products (K'oreje et al., 2020; Ngigi et al., 2020) did not investigate how the contaminants are introduced into the environment. Only one study by Onchiri et al. (2021) has so far reported on the prevalence of target emerging pollutants such as phthalates in only three WWTPs in Kenya.

1.2 Selected EDCs

The present study entailed target screening and aimed to investigate the levels, mass loadings, removal efficiency, and associated ecotoxicological risks of representative EDCs; dibutyl phthalate (DBP), diethylhexyl phthalate (DEHP), and dimethyl phthalate (DMP) which are industrial chemicals; linuron (LNR) an herbicide, and progesterone (PGT), a hormone. The structures of these selected compounds and their physicochemical properties are presented in **Table 1.1.**

Table 1.1: Physicochemical properties of selected EDCs

EDCs	Structure	Molecular formulae	Molecular weight (g mol^{-1})	Log K_{OW}	Water Solubility (mg L^{-1} at 25 °C)
Dibutyl phthalate	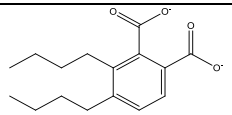	$C_{16}H_{22}O_4$ or $C_6H_4(COOC_4H_9)_2$	278.4	4.5	13
Dimethyl phthalate	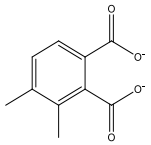	$C_{10}H_{10}O_4$ or $C_6H_4(COOCH_3)_2$	194.2	1.6	4,000
Diethylhexyl phthalate	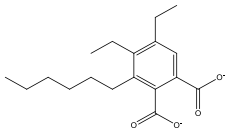	$C_{24}H_{38}O_4$	390.6	7.6	0.3
Linuron (3-(3,4-dichlorophenyl)-1-methoxy-1-methylurea)	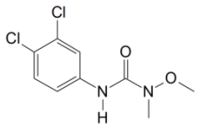	$C_9H_{10}Cl_2N_2O_2$	249.1	3.2	75
Progesterone (Pregn-4-ene-3,20-dione)	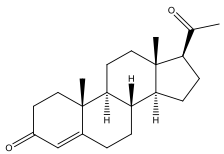	$C_{21}H_{30}O_2$	314.5	3.9	8.8

Adopted from the National Centre for Biotechnology Information (2022)

DBP, DMP, and DEHP are phthalic acid esters (PAEs) used as plasticizers in polymeric materials to ease production and improve flexibility and toughness (Nantaba et al., 2021). Plastic production in Kenya is a significant investment of around USD 50 million as of 2013 (the latest data is unavailable) and it influences all sectors of the economy (Nyagah, 2013). Approximately 10% of plastics wind up in the environment resulting in environmental distress due to their persistence. Numerous research has implicated PAEs as endocrine disruptors, and they have been extensively investigated with some plasticizers having been already banned or are subject to stricter regulation (Gore et al., 2014; Soto & Sonnenschein, 2010; Staples et al., 1998).

PGT is a steroid hormone that belongs to a class of hormones called progestogens. Synthetic PGT is approved for the regulation of the menstrual cycle by correcting dysfunctional uterine bleeding or amenorrhea. It also aids with contraception by facilitating the implantation of the blastocyst in the uterus and sustaining the pregnancy. PGT has also been given to menopausal and post-menopausal women as a component of hormone replacement treatment (Almazrouei et al., 2023; Cui et al., 2021; Ojoghoro et al., 2021). Further to this, it is a major naturally occurring human progestogen. It is introduced to the environment through human excretion, and mainly via WWTPs' effluent release, UDBS from WWTPs that are applied in farmlands as fertilizer and seepage from septic tanks and landfills (Golovko et al., 2018; Moulahcene et al., 2015). This has led to the detection of progestogens in surface waters (Almazrouei et al., 2023; Chang et al., 2011; Golovko et al., 2018; Šauer et al., 2018). In the environment, PGT is known to be an EDC with adverse health effects on biota.

LNR is used as an herbicide to promote productivity in the agricultural sector. Whereas some pesticides have been steadily outlawed and replaced by environmentally benign alternatives, several pesticides and herbicides are still occasionally found in surface and groundwater (Guillette, 2000; Johnson et al., 2000). Biologically active, hazardous pesticide metabolites that are frequently found in higher concentrations in water sources and wastewater effluents are the focus of current research (Amoros et al., 2000). Kenya imports a variety of herbicides for weed control in the agricultural sector, including LNR. According to information found in the literature, the nation imported 7708 tons of different pesticides and herbicides in 2005. Whereas recent data is unavailable, the statistics on these imports demonstrate an annual increase (Loha et al., 2018).

1.3 Cost-effective removal of selected pollutants through adsorption

The importance of successfully removing EDCs from aquatic systems is monumentally significant. Since EDCs and other organic contaminants are typically ineffectively removed from water by conventional wastewater or drinking water treatment (Tong et al., 2010) and advanced methods are costly for developing countries (Rossner et al., 2009), the best alternative strategies for wastewater treatment will include low-cost technologies, especially those that make use of locally accessible resources. The quest for these novel technologies that can be used in the removal of toxic metals and other pollutants from wastewater has drawn attention to adsorption, a low-cost method that utilizes the binding abilities of multiple biological materials (Ahalya et al., 2006). The process of adsorption consists of a biological solid phase (adsorbent) and a liquid phase holding the adsorbates, or dissolved species to be removed. Due to the adsorbent's increased affinity for the adsorbates, the latter is attracted and attached to the adsorbent surface by multiple

mechanisms. The cycle repeats until a balance is reached between the species of sorbates that are bound to the solid and those that are still present in the solution (Igwe et al., 2008; Tarley & Arruda, 2004; Volesky, 1999). The sorbates' distribution between the solid and liquid phases is determined by their sorbent affinity.

During the biosorption process, the percentage removal is dependent on operational processes such as temperature, pH, contact time, initial concentration, and biosorbent dosage. The adsorption process is typically studied by changing one variable while maintaining the other relevant factors at an undetermined or predetermined constant level. The limitation of this is that it does not consider the synergistic or antagonistic effect, if any, of all the variables involved. Furthermore, it is costly both time-wise and in the use of reagents, and optimal conditions are not guaranteed (Jayan et al., 2021; Ong et al., 2011). These can be avoided by using statistical experimental designs such as response surface methodology (RSM). RSM is a multivariate approach for designing experiments, modeling, evaluating factor interactions, and collectively optimizing all parameters affecting adsorption (Ani et al., 2019; Korde et al., 2021) thus giving the system's ideal operating conditions or an area that meets the optimum operational specifications. The application of RSM in adsorption has been noted to be cost-effective while improving adsorption efficiency and reducing process variability (Aly-Eldeen et al., 2018; Ani et al., 2019). In addition, the analysis of variance (ANOVA) establishes each process parameter’s significance, if any, in controlling adsorbent performance. Second-order polynomials serve as the fundamental component of RSM. The influence of every variable on response is assessed via full factorial design, along with how the effect of each factor varies when the amount of the other factors changes (Ani et al., 2019).

The biosorbent in this study was *Moringa oleifera (M.O)* seed biomass (**Figure 1.1**). Numerous studies as listed in the literature review have explored the capability of different parts of *M.O* (bark, leaves, seed, and seed pods) as a biosorbent for the sequestration of contaminants from aqueous solutions and have reported positive results.

(a)  (b)  (c) 

Figure 1.1: (a) *M.O* tree; (b) *M.O* seeds with shells (c) deshelled *M.O* seeds.

A survey of the literature showed that few studies have investigated PGT removal using adsorption. Ragab et al. (2016) reported a 95% removal efficiency of PGT using polytetrafluoroethylene (PTFE) double-layer microfiltration membrane modified with zeolite imidazolate metal-organic frameworks-8. Another study by Moulahcene et al. (2015) reported a 98.2% removal efficiency of PGT using cyclodextrin polymers cross-linked with citric acid. A recent study by Ghasemi et al. (2017) demonstrated that 4 g L^{-1} of PGT required 10 g cellulose for removal (no percent given) while Ifelebuegu et al. (2016) reported a 60% PGT removal using UV photo-assisted Fenton-like degradation.

Some studies have investigated LNR sequestration using various adsorbents. For instance, Rissouli et al. (2016) reported a 56.2% and 63.0% removal efficiency of LNR using chitin and chitosan biopolymers. González-Pradas et al. (1999) reported a 15.9% removal of LNR for the untreated bentonite and up to 41.5% of LNR for the treated bentonite. Sirival

et al. (2020) also reported 63.5% LNR removal using synthetic zeolite combined with activated carbon (AC) and a 78.0% removal of LNR using synthetic zeolite with AC and modified with hexadecyltrimethylammonium (HDTMA) surfactant. The same study also reported a 66.6% removal of LNR by synthetic zeolite and 38.5% by synthetic zeolite modified with HDTMA surfactant. Yang et al. (2021b) reported a 95.1% removal of LNR while using a modified sludge-based biochar.

However, to the best of my knowledge, the acid-activated, fat-free *M.O* seeds have not been explored for the abstraction of PGT and LNR from aqueous solutions with RSM being used for experimental design and optimization. The adsorption kinetics, thermodynamics, and general mechanistic studies were also investigated and are herein reported. In addition to being proven to be effective, the adsorption method does not introduce harmful byproducts into the environment (Tong et al., 2010).

1.4 Sequestration of selected pollutants through phytoremediation

Several physical and chemical methods of eliminating micropollutants have several drawbacks, notably extensive work, costly expenses, irreversible changes in soil characteristics, disruption of soil native microflora, and secondary pollution. With these constraints, the study, therefore, explored another technology where the practicality of using a local *Eichhornia crassipes* (*E. crassipes*) plant for wastewater treatment in urban areas using phytoremediation was investigated. Phytoremediation provides a green alternative solution to these limitations, and it comprises the use of different plant species and the affiliated soil microbes to restore polluted soil and water by reducing the amounts or the toxicity of pollutants in the environment by use of a constructed wetland (Tripathi

et al., 2020). This could be through the following mechanisms which may as well occur simultaneously:

- Phytostabilization where plants serve as hydraulic barriers or trapping through adsorption to avert runoff or leaching of inorganic or organic pollutants (Tripathi et al., 2020).
- Rhizofiltration where plants are used as filters in a hydroponic setup up majorly used indoors for radionuclides.
- Phytovolatilization is a phenomenon, especially for volatile organic carbons (VOCs) where they are taken up in the plant tissue and released as volatiles.
- Phytoextraction where plants can be employed to siphon contaminants through phytoaccumulation, phytoabsorption, or phytosequestration in their tissues, succeeded by reaping of the plant material (Tripathi et al., 2020). This is mainly used for metals and other inorganics.
- Phytostimulation or rhizodegradation, in which plants can aid in the biodegradation of organic pollutants to non-toxic metabolites through the use of microorganisms in their root zone/rhizosphere, and is primarily employed for hydrophobic organics that plants cannot absorb but can be digested by bacteria (Pilon-Smits, 2005; Tripathi et al., 2020).
- In rare occasions, phytodegradation may occur where contaminants can be absorbed upwards, subsequently undergoing degradation or sequestration in the plant's other tissues.

Different mechanisms work for different contaminants and different plant species. Phytoremediation is viewed as an effective, novel, economically viable, green, solar-

powered technology that is usable in situ and has widespread public acceptability. It can also be used extensively in locations where other remediation options are unaffordable. Since it does not affect the topsoil, the soil's function and fertility are maintained. It could even boost soil fertility while reducing soil erosion. The expenses for setup and maintenance are likewise quite low. Moreover, the plants employed typically have high biomass and could be utilized for energy production in the future (Ali et al., 2013).

The use of *E. crassipes* in constructed wetlands can not only remediate wastewater but may save aquatic ecosystems in East Africa and the region. Its harvest to be replanted in constructed wetlands will consequently clear up lakes thus enabling fishing and boating activities. This will consequently bring back the socio-economic activities of the major lakes, thereby improving livelihoods and reducing the crime rate in East Africa. This study therefore investigated the potential of *E. crassipes* in phytoremediation of PGT and LNR from water.

1.5 Statement of the problem

The United Nations-Sustainable Development Goals (UN-SDGs) target 6.3 demands countries to improve water quality and reverse the declining water quality. Inevitably, due to the increased global usage of EDCs, there is a greater incidence of contamination in surface and groundwater, which has negative impacts on both aquatic and terrestrial life. The various effects of EDCs on experimental animals are well recognized, and people are also susceptible to these effects (Cevasco et al., 2008). These adverse health effects have been extensively listed in section 1.1. Although the majority of EDCs are not acutely hazardous to biota at their typical environmental concentrations, little is known regarding potential chronic health effects linked to exposure to the

combinations of these compounds over an extended period. Indeed, the synergistic or antagonistic effects of chemicals can have a bigger influence than the individual impacts of each chemical. As global use of EDCs increases, an inevitable consequence is an increased level of contamination of surface and ground waters with these biologically active chemicals, and thus a greater potential for adverse effects in both aquatic and terrestrial organisms. There is however paucity of data regarding their occurrence in Kenya and East Africa therefore limiting their monitoring and regulation.

Furthermore, the Kenya National Water and Sewage Corporations use traditional wastewater treatment procedures that are insufficient in eliminating EDCs from wastewater. The alternative effective treatment methods such as advanced oxidation processes, reverse osmosis, and membrane filtration are estimated to cost 10-450 US dollars per cubic meter of water. Contrastingly, adsorption costs 5-200 US dollars per cubic meter of water (Ali et al., 2012). This gap prompts the exploration of adsorption as a cheaper alternative especially when the adsorbents are locally available. There is also a research gap in terms of elaborating the interaction between the adsorbate and adsorbent synergistically or antagonistically during adsorption. The use of RSM displays the interaction of varied factors affecting adsorption. It also gives the optimum parameters required to obtain maximum efficiency. The use of live plants is also another cheaper alternative that remains less explored.

This study was conducted first to evaluate the concentrations, removal efficiency, mass loading rates, and ecological impacts of EDCs. Secondly, the performance of *M.O* seed biomass as a potential adsorbent for removing PGT and LNR from simulated wastewater was studied. In addition, the kinetic, isothermal, thermodynamic, and mechanistic studies

were also determined. Finally, *E. crassipes* as a potential phytoremedant for abstraction of PGT and LNR from water was also investigated.

1.6 Objectives of the study

1.6.1 General objective

To determine the levels, mass loadings, removal efficiency, and associated ecotoxicological risks of selected EDCs from twelve WWTPs in nine major towns in Kenya, and their potential removal from aqueous solutions by biosorption onto chemically activated fat-free *MOSB* and phytoremediation using *E. crassipes*.

1.6.2 Specific objectives

1. To determine concentration levels, mass loadings, removal efficiency, and associated ecotoxicological risks of selected EDCs (DBP, DEHP, DMP, LNR, PGT) in sludge, UDBS, and wastewater samples from WWTPs in nine major towns of Kenya.
2. To determine the potential of chemically modified fat-free *M.O* seed biomass in adsorbing PGT and the kinetics, thermodynamics, isotherms, and mechanisms involved during the process.
3. To evaluate the practicality of utilizing chemically modified fat-free *M.O* seed biomass in adsorbing LNR and the kinetics, thermodynamics, isotherms, and mechanisms involved during the process.
4. To evaluate the phytoremediation capacity of *E. crassipes* in removing PGT and LNR from simulated wastewater and the mechanism involved.

1.7 Justification

Over the last three decades, there has been rapid industrialization, urbanization and increased agricultural activities in Kenya consequently resulting in increased pollution in major towns. Since the conventional removal methods applied in WWTPs do not work in abstracting EDCs, it implies that towns in the larger western region (Kisumu, Kakamega, Bungoma, Busia, Kisii, Kericho, and Eldoret) could be releasing EDCs to Lake Victoria. Effective determination of their concentration and removal is paramount especially in the western region of Kenya since WWTPs in this region release their effluent to rivers and streams that drain into Lake Victoria, the largest freshwater lake in Africa. Nairobi region is also included in the study due to its large population and therefore exposure level is expected to be high.

Regardless of their adverse health effects, EDCs are chemicals in common use for example PAEs are added to plastics and are therefore expected to be in the environment. The use of pesticides and hormones has skyrocketed in the recent past. Excessive application especially for herbicides and their improper disposal has resulted in their detection in different environmental compartments. Most EDCs are at trace concentrations in the environment. They have thus remained unregulated in most countries due to the paucity of information and knowledge regarding their presence, fate, and effects on the environment. With scarce data on their levels and the unclear effects on biota, this study was both timely and relevant.

Information on the concentration levels of EDCs is a prerequisite to remediating the environment. The adsorption procedure is considered among the most efficient and cost-effective methods for eliminating these EDCs from the environment. A cost analysis

carried out on the utilization of agricultural products for adsorption was found to be much lower when compared to conventional methods of wastewater treatment (Sharma & Ayub, 2019). Abstraction of pollutants using *M.O* and *E. crassipes* for removal of pollutants such as heavy metals and dyes has been reported (Ongulu et al., 2015; Shah et al., 2010), however, scanty data is available for their use in the removal of EDCs. According to published research, AC is a powerful adsorbent that is capable of eliminating both organic and inorganic contaminants from wastewater (Akinbiyi, 2000). However, the prohibitive price of AC has restricted its application as an adsorbent, necessitating the investigation of alternative, less expensive adsorbents.

Traditionally, the biosorption process is investigated by varying one operating factor while holding other variables at an unspecified or specified constant level. The limitation of this is that it does not consider the synergistic or antagonistic effect, if any, of all the variables involved. Furthermore, it is costly both time-wise and in the use of reagents, and optimal conditions are not guaranteed (Jayan et al., 2021; Ong et al., 2011). These can be avoided by using RSM. RSM is a multivariate approach for designing experiments, modeling, evaluating factor interactions, and collectively optimizing all parameters affecting biosorption (Ani et al., 2019; Korde et al., 2021) thus giving the system's ideal operating conditions or an area that meets the optimum operational specifications. The application of RSM to optimize parameters further decreases the cost. Furthermore, understanding kinetics and thermodynamics is relevant for design purposes. Additionally, after removing useful oils from *M.O*, the remaining biomass is usually discarded. In this study, the use of acid-activated fat free *M.O* seed biomass makes use of an otherwise wasted resource.

Moreover, *M.O* seed biomass used as an adsorbent was easily available and it does not generate toxicants to the environment.

Phytoremediation is yet another technology where live plants are monitored for uptake, degradation, or immobilization of pollutants. Though *E. crassipes* is a problem in major water resources in East Africa, it can be used in the efficient removal of toxic EDCs from wastewater through harvesting and replanting them in constructed wetlands. It has been used for the uptake of other toxic pollutants, especially metals and this study used it in the phytoremediation of PGT and LNR. The plant was also picked because it grows locally and is widespread near polluted locations suggesting that the species will be appropriate in withstanding and eliminating the contaminants. *M.O* and *E. crassipes* are inexpensive and are widely abundant in Kenya.

1.8 Significance of the study

The study generated data on the levels of EDCs in wastewater from WWTPs in Kenya (for the first time for PGT and LNR). This provided scientific literature on the scope of pollution and the efficiency of the WWTPs in EDCs' remediation. Furthermore, the environmental mass loadings and the toxicological data therein could be used in policy formulation by the relevant government agencies such as the ministries of water, health, and agriculture which will help in meeting the UN-SDGs especially target 6 on water and sanitation.

The study has also illustrated the potentiality of *E. crassipes* and *MOSB* in the elimination of PGT and LNR from aqueous solutions. This has therefore provided cost-effective alternatives that can be used in the treatment of contaminated water systems. This can thus inform policymakers in putting up structures to help remediate wastewater using cheap

locally available materials. This will be in line with Kenya's Vision 2030 which aims to transform Kenya into an industrialized, middle-income country providing a high quality of life to all its citizens by 2030 in a clean and secure environment. Furthermore, The use of RSM in biosorption has been noted to be cost-effective while improving biosorption efficiency, reducing process variability, and determining the significance of each process parameter, if any, in controlling adsorbent performance (Aly-Eldeen et al., 2018; Ani et al., 2019). This therefore bridges the scientific gap experienced in adsorption during the optimization of parameters.

The applicability of *E. crassipes* in phytoremediation has also been reported. This information informs future research on appropriate plants to be used in sequestering specific pollutants.

CHAPTER TWO

LITERATURE REVIEW

2.1 Sources and Fate of EDCs

EDCs are a worldwide and ubiquitous concern encountered in our living places, and in our work areas, we inhale them on outdoors, consume them in food and drinks, encounter them in industrial products, or are passed from a mother to a fetus through the placenta or from a mother to a baby through lactation (Diamanti-Kandarakis et al., 2009). They include polychlorinated biphenyls (PCBs), polybrominated biphenyls (PBBs), and dioxins which are synthetic substances used as furniture and floor coverings, industrial solvents, lubricants, and flame retardants. Among them are also plasticizers e.g., phthalates used in children's products, food containers, and medical tubing used intravenously enabling direct interaction with the circulatory system. Some pharmaceutical active compounds (e.g. diethylstilbestrol and *N*-acetyl-*p*-aminophenol (paracetamol)) (Darbre, 2019) and personal care products (such as ingredients including benzophenones and parabens added to UV-filters (sunscreens) and synthetic musks (fragrances)) are also classified as EDCs (Martín-Pozo et al., 2021). This list also includes pesticides such as fungicides, algaecides, and herbicides sprayed on buildings, fields, and water reservoirs that emit airborne and sedimented chemicals that can be absorbed through the skin, breathed, or swallowed through treated food. Those used for pest control are neurotoxicants or reproductive toxicants to animals and it is expected that human beings will be affected in the same manner (Longnecker et al., 2002). Examples are methoxychlor, chlorpyrifos, dichlorodiphenyltrichloroethane, vinclozolin, atrazine, linuron, and glyphosate. Lastly, natural chemicals found in human bodies but also their synthetic counterparts being

prescribed *e.g*., progestogens are also classified as EDCs (Diamanti-Kandarakis et al., 2009).

The major pathway of EDCs to biota is WWTPs' effluents and dried sludge usually given out as fertilizer to farmers. In highly polluted environments, EDCs may leach into both soil and waterways and then become absorbed by plants, algae, and microorganisms; resulting in bioaccumulation and biomagnification in the tissues of bigger animals and human beings which are at the apex of the food chain. Evidence that certain chemicals are transferred by air and water currents to other parts of the world that are far from their initial source is extremely concerning (Diamanti-Kandarakis et al., 2009). As a result, 100% of tested persons worldwide have now shown evidence of EDCs in their blood, urine, placenta, umbilical cord blood, and bodily tissues such as adipose tissue (Calafat et al., 2007; Gore et al., 2014).

2.2 Impact of EDCs to living organisms

Environmental factors are thought to be responsible for 24% of all human diseases and disorders worldwide (Fingerhut et al., 2006). It is also postulated that 80% of fatal diseases which include cardiovascular ailments, cancer, and respiratory disorders are linked to pollutants in the environment (Prüss-Üstün & Corvalán, 2006). Most of these diseases stem from perturbation of the endocrine system implying that EDCs may be the primary contributors. Studies have established that the prevalence of endocrine disorders and the manufacturing of chemicals are directly proportional. Worldwide manufacture of plastics has grown tremendously over the years (Nyagah, 2013), a situation similarly experienced in the chemical industry with the production of pesticides, fire retardants,

solvents, and surfactants skyrocketing in recent decades. This has also seen a rise in endocrine disorders (Gore et al., 2014).

It is worrying since lifelong exposure to specific EDCs not only affects the vulnerable individual but also impairs the offspring. This is because some of these EDCs are persistent and bioaccumulate in the fatty tissues of the body where they are fat-soluble. They are then passed during pregnancy across the placenta affecting the developing embryo or through breastfeeding. In addition, there is emerging proof that EDCs alter germ cells, which are the building blocks of sperm and egg cells, leaving their impacts heritable for multiple generations even after the chemical is cleared up or degrades (Cevasco et al., 2008).

There are several endocrine disorders associated with EDCs. Early life exposure mainly leads to disease and disorder later in life (Schug et al., 2011). To begin with, we have pediatric disorders including early female puberty, brain cancer, leukemia, neurobehavioral disorders, and male reproductive problems such as cryptorchidism, testicular cancer, and hypospadias, which have all increased significantly over the years and are connected to elevated amounts of EDCs in the environment (Sharpe, 2011). Additionally, the prevalence of preterm births and developmental disabilities in US children increased from 12.8% to 15.0% between 1997-2008 (Boyle et al., 2011) and this can be linked to consumer products that have EDCs. There is also data linking EDCs' exposure to retardation of child development and other human health disorders (Meeker, 2012). Numerous studies and public health agencies including the World Health Organization (WHO) and the United Nations Environmental Programme (UNEP) have expressed concern about EDCs' effects on the brain and behavior of children (Bergman

et al., 2013). Exposure to brominated flame retardants, perfluorinated compounds, and pesticides (organophosphates like chlorpyrifos and organochlorines) has been linked to an increase in childhood neuropsychiatric disorders such as attention deficit hyperactivity disorder, autism spectrum disorder, depression, executive function deficits, learning disabilities, and conduct disorders (De Cock et al., 2012; Gore & Dickerson, 2012). Experimental animal data demonstrate multiple neurobiological alterations brought by EDCs, including impacts on the maturing brain's structure and organization, synaptic characteristics, neurotransmitter synthesis and release, and neuronal growth (Gore & Dickerson, 2012). These studies highlight the brain as an especially susceptible target of EDCs, which is supported by a growing body of literature on the behavioral effects of EDC exposures, particularly during development.

EDCs also have an impact on adults, and research has suggested a connection between exposure to pesticides and neurological diseases including Parkinson's disease and depressed tendencies (Baldi et al., 2003). Accumulating evidence suggests that obesity is aggravated by chemical exposures even though primarily caused by lifestyle factors such as choice of diet and physical activity (Baillie-Hamilton, 2002). Obesogens are chemicals that are considered to trigger weight gain by altering or resetting important endocrine system components that control metabolism, energy balance, and hunger, leading to obesity and its associated negative health outcomes (Gore & Dickerson, 2012). Due to the thyroid gland's crucial part in the regular maintenance of metabolism, interference with thyroid hormone activity is another way that obesogenic substances might work. Certain chemical pesticides, phthalates, perfluorinated chemical compounds, dioxins, and various

other EDCs have recently been identified as probable obesogens (Grün & Blumberg, 2009).

The strongest positive correlations are those between exposure to EDCs and reproductive health diseases such as low fertility levels, preteen puberty, reduced sperm counts, abnormalities of the sex organs, uterine fibroids, ovarian disorders, and perturbations of sex ratios (Crain et al., 2008).

Cancer cases have ballooned over the years and studies have shown that they are linked to environmental pollutants (Siddiqua et al., 2022). Most carcinogens among them industrial chemicals, pharmaceutical agents, hormones, and pesticides are EDCs. A study in Pakistan has linked pesticides to several cancer cases (de Graaf et al., 2022). Most cancers that affect the reproductive system such as prostate, breast, uterine, testicular, and other reproductive tissues involve hormones, justifying the fact that chemicals that interfere with the endocrine system such as phthalates, synthetic hormones, and certain pesticides, are carcinogens (Diamanti-Kandarakis et al., 2009). The chance of developing cancer later in life is also increased by early exposure to chemicals like phthalates and some pesticides, according to research employing cellular and animal models (Soto & Sonnenschein, 2010). Additionally, occupational exposure increases the risk of developing cancer, making certain occupations more susceptible than others, such as painting, firefighting, working in the coal, steel, or rubber sectors, manufacturing textiles and papers, and mining. Minimizing chemical exposures will significantly reduce the chance of developing cancer and increase the likelihood of survival based on the significant and widespread impacts of environmental contaminants on cancer occurrence and manifestation.

Epidemiological studies on human beings and animals show that exposure to EDCs is also a factor in diabetes and cardiovascular disease (Schug et al., 2011). The immunological and inflammatory consequences of EDCs are a new area of study. Numerous chronic conditions, such as obesity, cognitive impairment, cardiovascular disease, respiratory ailments, and autism, are linked to inflammation. When reacting to environmental threats, the immune and endocrine systems frequently collaborate, and part of the inflammatory consequences may be explained by the convergence of their signaling routes (Schug et al., 2011).

To summarize the effects of EDCs on well-being, it is critical to recognize that children are considerably more susceptible to EDCs than adults since their bodies are immature and can take up these toxins that are easily dissolved in the fat of their mother's milk or infant formula. Furthermore, besides playing and living close to the ground with little awareness of hazards, they also put their hands and items in their mouths significantly more frequently than adults. Additionally, compared to adults, kids have skin that is larger per unit of body mass resulting in increased chemical uptake. They also have a longer life expectancy with a much longer period for exposure to manifest as disease (Landrigan & Etzel, 2013). Children's adverse reactions differ based on their developmental vulnerabilities and the paths of exposure. This study is therefore paramount and timely in protecting the younger generation by providing data on EDCs and providing cheaper options for their removal.

2.3 Safe dosage levels

It is universally established that every chemical has a safe dosage, and exposures that fall below that limit are considered acceptable. Such thresholds accentuate a

carcinogenic/survival index and are obtained by testing only single pure compounds, overlooking concomitant effects and postulating a linear dose-toxicity association, where large doses are more harmful while small doses are less hazardous (Gore et al., 2014). This gives a threshold dosage under which it is assumed there is no observed adverse effect. This is inaccurate because subtle perturbations including affected hormone levels, which might affect the predisposition to developing a disease, may be induced even at levels below the threshold dosage. Furthermore, EDCs exist in the body as a complex mixture due to continual environmental exposures to different chemicals and their degradation products throughout the life cycle with symptoms being manifested long after exposure. One significant problem of this method of risk assessment is the failure of toxicological testing to quantify such unobservable effects. Endogenous hormones regulate body systems and cause adjustments at trace quantities (usually in the part-per-trillion to part-per-billion scale). At certain phases of life, a person may not need any of these natural hormones. This implies that any exposure to an extrinsic EDC that mimics their effects will overwhelm the organism's intrinsic hormone threshold limits, which are nil at that life phase, and any trace levels will result in tremendous interference leading to adverse effects in that organism (Zoeller et al., 2012). Safe levels of exposure in EDCs are therefore toxicological misinformation. To represent EDCs' synergistic (or antagonistic) effects on human health even at the low levels encountered in daily life, an entirely novel testing incorporating low levels of combinations is required. We must also be aware that specific life phases, especially from conception to early childhood, are more susceptible to EDCs than others. This implies that EDCs' effects on exposed fetuses or infants will be more pronounced and extrapolating the effects of EDCs on adults to such early phases may not be viable.

2.4 EDCs of interest in this study

2.4.1 Phthalic acid esters (PAEs)- Phthalates

To facilitate production, and improve flexibility and toughness, plasticizers are added to polymers (Nantaba et al., 2021). Monomeric plasticizers with low molecular weight are the major plasticizers that are most frequently utilized. Esters made from phthalic acid, generally known as phthalates, are the most popular monomeric plasticizers. These non-halogenated phthalates are widely utilized in an assortment of merchandise, including packaging, electric wire insulators, children's toys, fabrics, and smart screens (Nantaba et al., 2021). Phthalate content ranges from 10 to 60% by weight of a finished plastic product. Plasticizers have a history of leaching from objects made of plastic into the gas, liquid, or solid that they are in contact with (Rivera-Utrilla et al., 2012).

Typically, PAEs are odorless, colorless, or liquids with a yellowish oily appearance. Except for DMP (5.5 ^{o}C), they all have melting points below -25 ^{o}C. Their boiling points range from 230 ^{o}C to 486 ^{o}C. PAEs' relatively low melting points and substantial boiling points impart their utilization as plasticizers, heat transfer fluids, and carriers. PAEs biodegradation, bioaccumulation, removal from WWTPs, leachate from landfills and sludge-amended soils, and environmental distribution are dependent on their water solubility. The fate of PAEs (whether hydrophobic or hydrophilic phases) is determined by their octanol-water partitioning factor, (Kow) while vapor pressure predicts its fate in the atmosphere. As the alkyl chain of PAEs lengthens from 1 to 13 carbon atoms, there is a consequential increase in Kow by eight orders of magnitude and a decrease in vapor pressure by four orders of magnitude (Rivera-Utrilla et al., 2012).

Low-molecular-weight PAEs such as DBP and DMP are commonly used in personal care products and cosmetics. DMP, for example, decreases volatility in perfume fragrances thus lengthening the duration of the scent. DBP imparts a chip-resistant property to nail polish. DBP is also used in printing inks and adhesives. In the polymer sector, high molecular weight PAEs with longer phthalate molecules, for instance, DEHP, are utilized as plasticizers to enhance agility, ease of manufacture, and excellent handling qualities. For example, DEHP is majorly used for polyvinylchloride (PVC) plasticization which is a major component in toy and medical equipment (catheters, bottles, and blood bags) manufacture. This gives a low-cost, flexible, and durable final product (Bider et al., 2020).

Phthalates have increasingly become widespread pollutants since they are not chemically bonded to polymer matrixes and can easily diffuse into the surroundings during manufacture, consumption, and disposal (Bider et al., 2020). As a result, they wind up in municipal landfills alongside waste PVC and have the potential to be transferred into groundwater and surface water. Additionally, through the sewer line, PAEs are present in WWTPs, and due to low solubilities, phthalates will adsorb to the sewage sludge which is then dried and used in agricultural farms as fertilizers. Consequently, these chemicals are introduced into the food chain through soil microbial populations, plants, and animals. It is therefore critical to verify that sludge is free of these contaminants before usage. PAEs are also introduced into foodstuffs, and both indoor and outdoor atmospheres through releases from materials containing them. The resultant accumulation of PAEs in the environment poses a growing threat to ecosystems and human health since they are considered EDCs (Rivera-Utrilla et al., 2012).

2.4.2 Progestogen hormones

Progestogens are steroid hormones that are naturally produced throughout life in people and animals, such as PGT (**Table 1.1**). These compounds are introduced to the environment through human and animal excretion, and mainly via WWTPs' effluent release (Moulahcene et al., 2015), UDBS from WWTPs applied in farmlands as fertilizer and seepage from septic tanks and landfilling areas. The bio-activity of these compounds results in their capacity to disrupt the normal function of endocrine systems thus potentially affecting the reproduction and development of aquatic and terrestrial organisms in the environments where these compounds are introduced (Tyler et al., 2005). Synthetic progestogens have been reported to cause disorders in fish by affecting their offspring's sexual development, reducing egg production, and decreasing the spawning rate via increasing masculinity in female fish (Almazrouei et al., 2023; Golovko et al., 2018). Further, zebrafish exposed to PGT showed altered liver function and ocular growth in addition to neurodevelopmental consequences. These effects are thought to translate to human beings through fish consumption (Almazrouei et al., 2023). In this regard, it is therefore monumentally significant to abstract this pollutant using effective low-cost technologies especially those that utilize locally available materials.

2.4.3 Pesticides

Persistent pesticides such as dichlorodiphenyltrichloroethane (DDT) (an organochlorine) have since been banned in most countries. Pesticides that are currently available as insecticides, herbicides, fungicides, and rodenticides are non-persistent and include organophosphates, carbamates, and pyrethroids. Despite having no lasting effects on the environment, the pervasive use of pest control in numerous contexts exposes a significant

portion of the general population to some of these chemical toxicants that have been associated with endocrine disruption in addition to other adverse health effects.

Inhalation, cutaneous contact, or ingesting foods with low amounts of pesticide residue are the main ways that people are exposed to pesticides in or around the house and other indoor areas. Surface run-offs from farms can also result in these chemicals being detected in water bodies and WWTPs' effluents and dried sludge. Atmospheric depositions are other sources. Consequently, LNR has been detected in surface and underground waters and WWTPs since it is slow to biodegradation and hence is recalcitrant to conventional wastewater treatments (Bachir et al., 2021).

Workplace investigations involving concurrent exposure to varied pesticides point to a link between non-persistent pesticide exposure and lowered semen quality (Diamanti-Kandarakis et al., 2009). Pesticides have also been associated with benign and malignant tumors, birth defects, genetic disorders, reproductive disorders, nerve and blood disorders, and endocrine disruption (Caioni et al., 2021; Rissouli et al., 2016).

The pesticide of interest in this study is linuron (**Table 1.1**), (3-(3,4-dichlorophenyl)-1-methoxy-1-methylurea) which is a phenylurea herbicide that is used to suppress the proliferation of grass and weeds while enhancing the growth of crops like soybeans.

2.5 The adsorption process for wastewater treatment, commonly used adsorbents, and studies on wastewater treatment

2.5.1 The adsorption processes

The inefficiency of conventional WWTPs and the cost associated with advanced methods have led environmental chemists and material scientists to look into various cheaper alternatives for eliminating environmental contaminants (Omo-Okoro et al., 2018).

Adsorption is a better alternative to all others because of its ease of use, availability, cost-effectiveness, no increase in the chemical oxygen demand of water, and the fact that it does not leave behind toxic by-products (Chaudhuri et al., 2008; Kanamarlapudi et al., 2018). In the search for eco-friendly and efficient materials for wastewater treatment, several household, agro-industrial wastes, and by-products have been investigated and proven to be viable alternatives to their conventional counterparts, including commercial activated carbons (ACs) produced from non-renewable feedstocks such as lignite and coal. In the African context, and for economic and availability reasons, the use of waste materials as adsorbents for wastewater treatment is the main ongoing trend in this field. These waste materials are majorly used as adsorbents in the adsorption process.

Adsorption is a physiochemical interface mass-transfer phenomenon applied for wastewater treatment and pollution removal, among other applications (**Figure 2.1**). It is an established technology with proven advantageous features such as versatility, low cost, high efficiency, prone to recycling, and relatively smoother implementation and operations (Awad et al., 2020; Dotto & McKay, 2020; Fazal et al., 2021). Overall, during an adsorption-based wastewater treatment process, organic and/or inorganic pollutants (adsorbates) are attracted to the outer and inner surfaces of the porous materials (adsorbents), through mass transfer and diffusion processes from the aqueous media to the active adsorbing sites of the adsorbents.

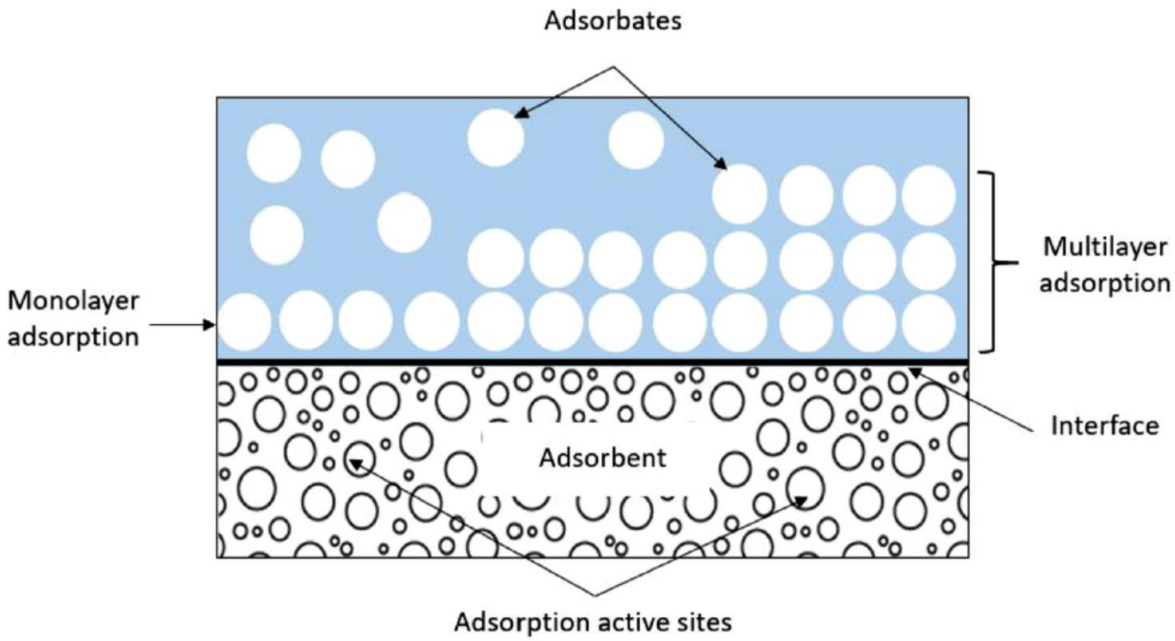

Figure 2.1: Mechanism of the adsorption process.

The involved mechanism is either chemisorption (ionic interactions for instance) or physisorption or both (such as Van der Waals and π–π interactions) (Al-Ghouti & Da'ana, 2020). The sorbate species have a higher affinity for the sorbent consequently being bound to the sorbent *via* diverse mechanisms (Adeniyi & Ighalo, 2019; Al-Ghouti & Da'ana, 2020).

For adsorption to be successful, the sorbate molecules and the surface of the sorbents should have approximately similar pore sizes since finer pore sizes take up smaller molecules and vice versa (Wang et al., 2017). Low molecular weight pollutants can also be displaced by high-weight molecular species (Nguyen et al., 2020). It has also been observed that adsorbents show preferences for certain sorbates in a complex system due to other properties such as hydrophobicity, kinetic diameters, dissociation constants, and chemical structure among others (Ali et al., 2012). Other parameters that affect the

adsorption process are sorbate concentration, the textural characteristics of the adsorbent, temperature, the presence of competing ions, and pH (Ngeno et al., 2016).

2.5.2 Waste-derived adsorbents for water treatment

Numerous waste materials have been investigated as raw or modified adsorbents for the removal of various pollutants (dyes, surfactants, heavy metals, emerging contaminants, etc.) from domestic, municipal, and industrial wastewater. In **Table 2.1**, a selection of recent investigations (2017-2022) related to the use of wastes as adsorbents in wastewater treatment is presented to showcase the versatility and abundance of such waste-derived materials, and their widespread utilization throughout the world (except Africa which is featured in section 2.5.6).

Table 2.1: Worldwide selection of waste-derived adsorbents of the removal of organic and inorganic pollutants from aqueous solutions

Location	Pollutants	Adsorbents	Adsorbates	Max adsorption capacity	Key operating conditions Time (hr)	pH	T (^oC)	References
USA	Dyes	AC from Cashew nut shells	Methylene Blue (MB)	476.0 mg g^{-1}	24	7	25	Spagnoli et al. (2017)
Turkey		AC from active sludge	Crystal violet	62.1 mg g^{-1}	2.5	6	25	Sahbaz et al. (2019)
Malaysia		Modified coffee waste	Reactive Black 5 Congo Red	77.5 mg g^{-1} 34.4 mg g^{-1}	2	7	Room temperature	Wong et al. (2020)
Brazil		AC from Palm Fibres	MB dye	110.8-162.5 mg g^{-1}	1	6	30	Maia et al. (2021)
USA/South Korea	Heavy metals	Biochar from loblolly pine	Cd^{2+}	167.0 mg/g	24	7.5	25	Park et al. (2017)
Viet Nam		AC from banana peel	Cu^{2+} Ni^{2+} Pb^{2+}	14.3 mg g^{-1} 27.4 mg g^{-1} 34.5 mg g^{-1}	24	6.1 - 6.5	25	Van Thuan et al. (2017)

Location	Pollutants	Adsorbents	Adsorbates	Max adsorption capacity	Key operating conditions Time (hr)	pH	T (^{o}C)	References
Turkey		Brewed tea waste	Pb^{2+}	1.2 mg g^{-1}	0.5	4.0	25	Çelebi et al. (2020)
			Zn^{2+}	1.4 mg g^{-1}		-		
			Ni^{2+}	1.1 mg g^{-1}		-		
			Cd^{2+}	2.4 mg g^{-1}		5.0		
Brunei		AC from sugarcane bagasse	Cr^{6+}	9.7 mg g^{-1}	2	6.5	26	Karri et al. (2020)
Japan	Fertilizers / Pesticides	Waste glass and shells' composite	Phosphate	73 mg g^{-1}	120	3 - 7	25	Jiang et al. (2017)
Hungary		Pomegranate peel powder	Ammonium	2.5 mg g^{-1}	2	6	25	Hodúr et al. (2020)
China		AC from tangerine seed	Metolcarb	9.1 mg g^{-1}	0.25	7	30	Wang et al. (2020)
			Pirimicarb	39.4 mg g^{-1}				
			Methiocarb	93.4 mg g^{-1}				
Spain		AC from sludge	Acetamiprid	129.0 mg g^{-1}	24-144	7	25	Sanz-Santos et al. (2021)
			Thiamethoxam	127.0 mg g^{-1}				

Location	Pollutants	Adsorbents	Adsorbates	Max adsorption capacity	Key operating conditions Time (hr)	pH	T (^{o}C)	References
			Imidacloprid	166.0 mg g^{-1}				
China	Emerging pollutants	Waste tea-based AC	Oxytetracycline	286.0–345.0 mg g^{-1}	30	-	30	Kan et al. (2017)
Hong Kong		AC from palm kernel shel	Atenolol	0.7 mmol g^{-1}	24	7	25	To et al. (2017)
			Acebutolol	0.7 mmol g^{-1}				
			Carbamazepine	0.7 mmol g^{-1}				
Brazil		AC from Macauba palm	Bisphenol A	0.2 mmol g^{-1}	24	5.5	25	Moura et al. (2018)
			Ethinylestradiol	0.1 mmol g^{-1}				
			Amoxicillin	0.1 mmol g^{-1}				
USA		Biochar from agricultural wastes	Sulfapyridine	1.2 mg g^{-1}	24	7 - 10	25	Ndoun et al. (2021)
			Docusate	19.7 mg g^{-1}				
			Erythromycin	17.1 mg g^{-1}				

Overall, among these various waste-derived adsorbents, carbonaceous porous materials including powdered materials, biochars, ACs, and carbon nanotubes (CNTs) are being subjected to a special focus from researchers all over the world using highly available and low-cost agro-industrial wastes and household residues as feedstocks. These carbonaceous materials have been widely investigated and reported as efficient adsorbents for various pollutants mainly due to well-developed porous structure, variable pore size distribution, and high surface area with functional groups that can be used as-prepared or after chemical modification to provide binding sites for adsorption of various contaminants in water.

2.5.3 Classification of waste-derived adsorbents

Various adsorbents have been employed in the adsorption process, and **Table 2.2** illustrates how they are classified.

Table 2.2: Classification of waste-derived adsorbents, and selected examples

Classification	Examples
Household wastes	Scrap tires.
Agricultural by-products	Pearl millet husk, peanut husk, rice, coconut and almond husks, silkworm pupa, hen feathers, tendu leaf, papaya wood, neem leaf, fertilizer wastes, barks of trees, seeds of plants, silk cotton hull, sawdust, oak dust, potato peels, orange, citrus and banana peels, maize cobs, cocoa and coconut shells, carrot residues, barley straw, cassava wastes, eggshells.
Sea materials	Seaweed and algae, seafood processing wastes, peat moss, chitosan, fish scales, and crab shells.
Industrial products	Fuel oil fly ash, bagasse fly ash, coal ash, petroleum wastes, sugar industry wastes, blast furnace slag, thermosensitive gel or polymer

Classification	Examples
Soil and ore materials	Silica gel, natural and synthetic zeolites, ore minerals, modified red mud, clays, sediment, and soil.
Metal compounds	Activated alumina, bauxite, activated and novel phosphate, and synthetic iron sulphides.

From **Table 2.2,** various biological materials especially agricultural-based waste products have been used to remove water contaminants by adsorption, then referred to as biosorption (Eletta & Ighalo, 2019).

2.5.4 Desirable properties of sorbents

As alternatives to industrial adsorbents generally derived from finite resources such as coal, lignite, and peat, the precursors to sorbents should be easily accessible, affordable, and non-toxic. The carbon or oxygen content should also be high to increase bonding possibilities between the sorbent and the sorbate. Other attributes include thermal resistance, resistance to wear, recyclability, and narrow pore diameters (Ali et al., 2012). This leads to increased exposed surface area and, hence, an elevated surface capacity and fast kinetics for adsorption. Further, the sorbents should also be easily desorbed thereafter thus enabling regeneration without releasing undesirable substances into the aqueous media (Kumar et al., 2019; Omo-Okoro et al., 2018).

Most waste biomaterials have been found to fulfill most, if not all, of those desired properties for the preparation of carbonaceous adsorbents. Additionally, they are a renewable resource. Usually, these waste materials, often bio-based ones, are used without thermal or chemical pretreatment or are pyrolyzed to obtain low-cost biochars that are alternatives to activated carbon. These carbonaceous chars can further be activated to improve their porosity and surface chemistry (Ali et al., 2012).

2.5.5 Processing and activation of carbonaceous sorbents

In general, sorbents are processed and/or activated using both physical and chemical methods. Some bio-based sorbents (biosorbents) are used directly as dried powdered biomass (Adeniyi & Ighalo, 2019). The majority, however, are transformed into carbonaceous materials through pyrolysis, a process of decomposing organic material through heating at elevated temperatures in the absence of oxygen and halogen. This converts the material to carbon (Omo-Okoro et al., 2018). The heating rate and duration of carbonization and activation are the most significant variables during pyrolysis since they influence the ultimate pore structure, surface area, and chemical properties of the resultant carbon (Ali et al., 2012). The resultant material constitutes an inflexible carbonaceous char containing pores packed with tarry pyrolysis deposits and necessitates activation to expand the internal surface area of the char thus increasing porosity. Activation may be achieved chemically or physically consequently obtaining activated carbons with diverse forms and dimensions given the varying pathways of activation (Adeniyi & Ighalo, 2019).

In chemical activation, chemical modifiers are infused into the biomass. Chemical activators in common use are zinc chloride ($ZnCl_2$) (Agarry et al., 2020), phosphoric acid (H_3PO_4), sulphuric acid (H_2SO_4), potassium hydroxide (KOH), sodium hydroxide (NaOH), potassium sulphide (K_2S) and potassium thiocyanate (KSCN) (Ali et al., 2012; Omo-Okoro et al., 2018). These chemically modifying groups which most of them contain oxygen, sulphur, and nitrogen are known to improve the adsorption and cation-exchange capacities. Once the biomass is saturated with the activators, it is then dehydrated to minimize tar formation and volatilization during pyrolysis. The chemical activation

technique has some strengths including minimal temperatures of activation, shorter reaction time, reduced energy costs, and increased yield of material. The used material may however be environmentally hazardous and its choice should be well thought out (Omo-Okoro et al., 2018). Noteworthy, the cost of adsorbent development depends on the method of chemical activation, duration of pyrolysis, and temperatures used.

Physical activation is the direct reaction between the carbonized char and an activator, which are mostly oxidizing agents like steam, carbon dioxide (CO_2), and air. Physical activators are clean, easy to handle, and environmentally friendly but have a lower yield. Just like chemical activation, the main aim is to rid the structure of tarry amorphous carbon in the interstitial layers thus increasing the porosity and making the internal surface area accessible (Ali et al., 2012).

Nanotechnology has also been employed in producing nanocomposites from waste materials. Nanoscale structures are those whose atomic and molecular sizes are within 1-100 nm. Nanocomposites are materials synthesized from varied materials put together and structured into nanoscale size to increase their functionality and reactivity (Omo-Okoro et al., 2018). Most nanocomposites have been manufactured from metals and agricultural waste materials and have been found to work exceptionally well in water treatment (Okello et al., 2017).

2.5.6 Recent studies using different waste-derived sorbents for pollutant removal from aqueous solutions in Africa

Using a bibliometric approach based on the method described in Olisah et al. (2019), it was observed that more research has been dedicated to the use of bio-based sorbents in the recent past in Africa. In general, the last decade (2011–2020) produced the highest

number of studies with an approximate number of 373 publications on the use of biosorbents in wastewater treatment. It is worth noting that records for 2024 (n = 92) are underestimated as these indicate the output for five months only (January to May).

The many international initiatives and funding agencies established to reduce water pollution in Africa may be responsible for the high research outputs in the last two decades. Some of the funding initiatives include the establishment of Rural Water Supply and Sanitation Initiative (RWSSI) in 2003, funded by the African Development Bank Group (ADBG) and other international agencies, and the adoption of the UN-SDGs in 2015, particularly the Clean Water and Sanitation Goal. Other reasons for the high research output may be linked to the emergence of sophisticated analytical instruments for scientific research, the advent of new research ideas, and the establishment of international collaboration programs between the governments of African countries and high-income countries. A strong positive correlation was observed between the number of publications and the year of article production. This fitted into a polynomial model (R^2 = 0.835, $y = 0.333x^2 - 1333x + 1.335$ as shown in **Figure 2.2**. This suggests that articles in this area of study are likely to increase in the future.

On the other hand, **Table 2.3** illustrates, with relevant information like country, and maximum adsorption capacity, varied bio-based and waste-derived materials used in the removal of various pollutants from selected studies from the year 2016 to 2024.

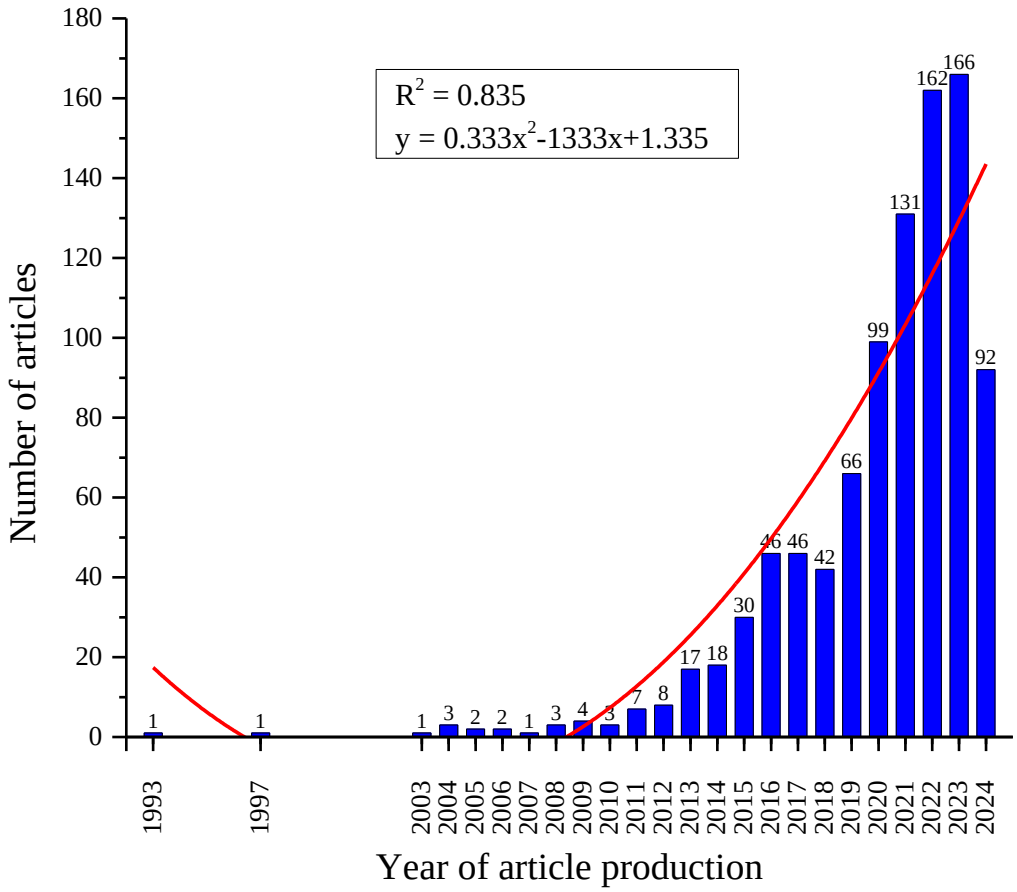

Figure 2.2: The annual production of articles related to the usage of adsorbents in wastewater treatment in Africa published between 1993 to 2024.

Table 2.3: Recent studies that have used different sorbents from waste materials to remove various pollutants in Africa

Sorbents and precursors	Pollutants	Country	Removal rate (%) or Maximum adsorption capacity (mg g^{-1})	Reference
Vinegar-treated eggshell waste biomass	Nickel (II) and Cobalt (II) ions	Botswana	78.7% and 76.5% respectively	Stevens and Batlokwa (2017)
Sugarcane bagasse-derived biochar	Sulfamethoxazole	Kenya	78.0%	Shikuku and Jemutai-Kimosop (2020)
Banana peels	Lead (II) ions	South Africa	98.1%	F. O. Afolabi et al. (2021)
Pulp and paper sludge biochar nanocomposite	Methylene blue	Zimbabwe	50.0 and 33.0 mg g^{-1} respectively	Chaukura et al. (2017)
Sawdust activated carbon	dye	Nigeria	98.5%	Eletta et al. (2018)
Tyre-based activated carbon	microcystin-LR	South Africa	100%	Mashile et al. (2018)
Fish scales	Heavy Metals	Nigeria	Above 50.0%	Eletta and Ighalo (2019)
Eggshells and fish scales	Chromium (VI) ions	Uganda	Not indicated	Bamukyaye and Wanasolo (2017)

Sorbents and precursors	Pollutants	Country	Removal rate (%) or Maximum adsorption capacity (mg g^{-1})	Reference
Agro-waste (*Musa paradisiaca* peels)	Toxic metal ions	Nigeria	Above 90.0%	Ibisi and Asoluka (2018)
Magnetic iron modified carbonized bagasse	Carbamazepine pharmaceutical	Kenya	60.9%	Okello et al. (2017)
Corn and rice husks in raw form, pyrolyzed form, and chemically modified form	Lead (II) ions	Tanzania	>90.0%	Rwiza et al. (2018)
Fish scales biochar	Copper (II) ions	Kenya	39.4 mg g^{-1}	Achieng and Shikuku (2020)
Rice husk, rice straw, sugarcane bagasse, sawdust; cement kiln bypass dust, and marble powder.	Chromium (III) ions	Egypt	>99.0% for cement kiln	Abdelkader et al. (2021)

Sorbents and precursors	Pollutants	Country	Removal rate (%) or Maximum adsorption capacity (mg g^{-1})	Reference
Raw coconut shell, activated carbon, and activated nanocomposite	Lead, copper, and color	Nigeria	Not indicated	Sarkingobir et al. (2020)
Water hyacinth biochar	Caffeine and ciprofloxacin pharmaceuticals	Kenya	>60%	Ngeno et al. (2016)
Moringa stenopetala seeds	Antibiotics	South Africa	>70.4% for all samples.	Kebede et al. (2019)
Raw and modified *Adansonia digitata* fruit pericarp	Fluorides	Tanzania	67.6 and 91.9% respectively	Mihayo et al. (2021)
Banana peels nanosorbent	Radioactive minerals from real mine water	South Africa	27.1 mg g^{-1}, 34.1 mg g^{-1} for uranium; 45.5 mg g^{-1}, 10.1 mg g^{-1} for thorium in synthetic and real mine water, respectively	Oyewo et al. (2016)

Sorbents and precursors	Pollutants	Country	Removal rate (%) or Maximum adsorption capacity (mg g^{-1})	Reference
Chemically and thermally modified coconut (Cocos nucifera) husks	Crude oil	Nigeria	Between 12.1 g g^{-1} and 16.8 g g^{-1}	Agarry et al. (2020)
Banana peels	Methylene Blue	South Africa	5.1 mg g^{-1}	Ramutshatsha-Makhwedzha et al. (2023)
Mandarin peels	Acid brown 14 dye	Egypt	416.67 mg g^{-1}	Eldeeb et al. (2024)

2.5.7 Adsorbent of choice in the study

M.O. is a tropical tree (**Figure 1.1(a)**) which is a species of a monogeneric family, the Moringaceae (Idris et al., 2016). Also called the drumstick, horseradish or benzolive tree, it can withstand drought and is available all year round. It has medicinal applications such as analgesic, anti-inflammatory, and antihypertensive properties, as well as weight loss, etc. (Grosshagauer et al., 2021; Jayan et al., 2021). In terms of nutritive value, the *M.O* leaves are rich in protein, vitamin C, potassium, and calcium (Anwar et al., 2007). The seed kernels contain oils high in tocopherols while the leaves contain vitamins, proteins, and minerals. *M.O*'s spherical, 1 cm-diameter seeds have three papery wings and a brownish, semi-permeable seed hull. The seed hulls range from brown to black, although they can sometimes turn white if the viability of the kernels is poor. A tree's annual seed production ranges from 15,000 to 25,000. A seed's average weight is 0.3 grams. They are known to contain alkaloids, resins, tannins, flavonoids, saponins, steroidal rings, glycosides, and crude proteins among others. The most crucial component utilized in water treatment is the inexpensive, easily available defatted cake, which is a waste product of the seed after edible oil removal. The defatted cake is known to treat turbidity, soften hard water, and as a dewatering agent. The defatted cake can be used in adsorption as a seed powder or AC. The adsorptive capacity is due to the presence of proteins and a cellulosic component called lignin. Lignin is a heterogeneous, complex bipolymeric molecule that possesses many functional groups, including carboxyl, hydroxyl-aliphatic, methoxyl, and phenolic groups. Additionally, it favors biosorption due to its aromatic, three-dimensional polymer structure and infinite apparent molecular weight (Idris et al., 2016).

Numerous research has explored the capability of the other different parts of *M.O* (bark, leaves, seed, and seed pods) as a biosorbent for the sequestration of contaminants from aqueous solutions and have reported positive results. Imran et al. (2019) reported 98.6% removal efficiency of lead while Jayan et al. (2021) reported 95.6% and 89.4% removal efficiency of lead and zinc ions, respectively, both using unmodified leaves of *M.O*. Keereerak and Chinpa (2020) reported 86.2% removal of crystal violet using pod husks while Maina et al. (2016) and Ongulu et al. (2015) reported higher removal efficiencies of trace heavy metals (lead, cadmium, copper, manganese, iron, zinc, magnesium, and chromium) using acid treated seed pods. These studies, though using different parts with varied treatments of *M.O,* agree that *M.O* is an excellent water purifier. It is also easily available, cost-effective, has a biodegradable sludge, is non-toxic, non-corrosive and has low sludge volume.

2.5.8 Methods used for the characterization of the adsorbents

Adsorbents are characterized to determine their textural and surface characteristics before and after adsorption. This involves analyzing their size, morphology, crystallinity, porosity, specific surface area, polarity, chemical structure, thermal stability, and the functional groups present (Oyewo et al., 2016). High porosity and consequently larger surface area with more specific adsorption sites and hence faster kinetics are the fundamental characteristics of good adsorbent. Surface polarity corresponds to affinity with polar substances such as water or alcohol. Polar adsorbents are hydrophilic and aluminosilicates such as zeolites, porous alumina, geopolymers, silica gel or silica-alumina are examples of adsorbents of this type. Carbonaceous adsorbents and polymer

adsorbents are typical non-polar adsorbents that are generally hydrophobic. These adsorbents have more affinity with oil or hydrocarbons than water (Schoutteten, 2012).

Several characterization methods can be conducted on adsorbents including X-ray diffraction (XRD), which has been employed for mineralogical phase identification and quantification and measurement of crystallite size. The scanning electron microscope (SEM), and transmission electron microscopy (TEM) are used for inspecting surface morphology, and Fourier Transform infrared spectrometry (FTIR) has also been used for the determination of surface functional groups of adsorbents pre- and post-adsorption (Choina et al., 2015; Onwuka et al., 2016; Oyewo et al., 2016; Souza et al., 2017). Further elaboration on their working principles is given in the subsequent sections.

2.5.8.1 X-ray diffraction (XRD)

XRD is a methodology used for phase analysis and measurement of crystallite size whereby X-rays, similar to electron beams, are scattered by a crystal lattice. The X-rays can also be reflected (diffracted) at the net plane of a crystal lattice (Al-Khateeb et al., 2014). X-ray beams are used because their wavelength is similar to the spacing between atoms in the sample as opposed to longer wavelengths. As a result, the angle of diffraction will be altered by the spacing of the atoms in the molecule. As the X-rays pass through the sample, the direction of the beam is changed at an angle, theta, from the original beam (**Figure 2.3**).

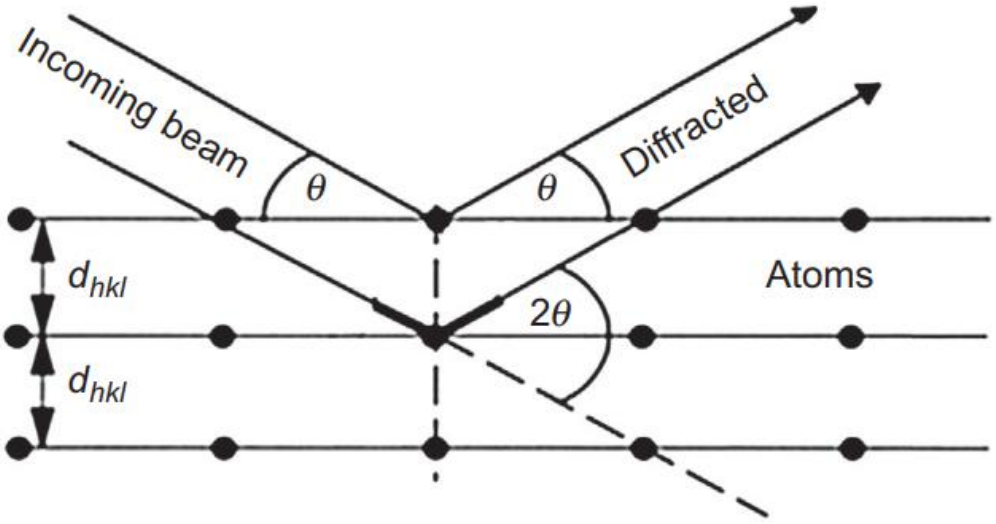

Figure 2. 3: Diffraction from lattice planes (Epp, 2016)

While some of these diffracted beams cancel each other out, positive interference happens when the beams have wavelengths in common. The angle of diffraction can then be used to determine the difference between atomic planes using Bragg's law,

$$n\lambda = 2d \sin\theta \qquad \text{(Equation 2. 1)}$$

where; λ is the wavelength of the x-rays, d is the inter-lattice spacing, θ is the incident angle and n is an integer. The distance between atomic plates can then be used to determine composition or crystalline structure.

2.5.8.2 Fourier Transform infrared (FT-IR) spectrometry

FT-IR spectrometry gives information on fundamental vibrations of characteristic functional groups in adsorbents and therefore the identification of functional groups. The electromagnetic spectrum's far infrared region and energies between 4000 and 400 cm^{-1} are often the only regions that can be studied using IR spectroscopy (Choina et al., 2015).

A molecule is IR active if it has a net dipole moment and therefore, observable functional groups common in organic materials include: hydroxyl, carbonyl, ester, methyl, epoxy, phenol, and aromatic ring. The absorbance or the percent transmittance of light as a function of wavelength (λ) or, more frequently, its inverse, which is the wave number (cm^{-1}), is captured as the FT-IR spectrum. Quantitatively, molecular concentration and molecular structure both affect how much energy is absorbed at a particular frequency. Characteristic band data interpretation is done by basic visual inspection and comparison with generalized characteristic group frequency charts (Khan et al., 2018).

2.5.8.3 Brunner-Emmet-Teller (BET)

The specific surface area (SSA, in $m^2\ g^{-1}$) of a material is the total surface area (SA) of a sample divided by its mass, M. The BET method, which is mostly employed, is based on the measurement of nitrogen adsorption to measure the total (gas-accessible) inner and outer surface area of a given sample at low temperatures (Barret et al., 1951). The BET model allows for multilayer adsorption, as an extension of the Langmuir isotherm and is anchored on the following assumptions:

- The adsorption surface is energetically homogeneous,
- The amount of surface coverage has no bearing on the heat of adsorption,
- Van der Waals interactions between the various layers control multilayer adsorption. The heat of condensation is equivalent to the energy released by multilayer adsorption. There is no interaction between adsorbed gas molecules of the same layer, and
- It is feasible for an endless number of layers to be adsorbed (Gibson et al., 2020).

During BET analysis, known amounts of preferable nitrogen are allowed to step wisely adsorb and desorb at low temperatures and partial vacuum. A BET isotherm, which shows the volume of gas adsorbed as a function of relative pressure, is used to display the data. Using the data from the isotherm, the BET **Equation, 2.2**, calculates the sample's surface area.

$$\frac{1}{X[(P_0/P)-1]} = \frac{1}{X_m C} + \frac{C-1}{X_m C}\left(\frac{P}{P_0}\right)$$

(Equation 2. 2)

In this equation, C is constant, X_m is the monolayer capacity or the volume of gas adsorbed at standard temperature and pressure (STP), and X is the weight of nitrogen adsorbed at a given relative pressure (P/P_o). The definition of STP is 273 K and 1 atm (Gibson et al., 2020).

2.5.8.4 Scanning Electron Microscopy–Energy Dispersive Spectroscopy, (SEM-EDS)

An electron beam is emitted from an electron cannon and then passed through one or more condenser lenses to reduce its size to about 0.4-5 nm in diameter in a scanning electron microscope. Before the beam interacts with the sample, it first travels through two deflection coils in the electron column to deflect the beam in the x and y axes. By ensuring that the scan is in raster fashion—that is, a rectangular image capture pattern of the sample—this deflection guarantees accuracy. The electron beam loses energy as it interacts with the sample because of random scattering and absorption by the material. Different signals, such as secondary electrons, back-scattered electrons, and characteristic X-rays, are produced by the interaction between the electron beam of a scanning electron

microscope and atoms at varying depths within the sample. In the SEM, each of these signals has an own detector. When the electron beam interacts with the sample, it takes one electron from the inner shell. This causes a higher-energy electron to occupy the shell and release energy, which causes the characteristic X-rays to be released. For elemental analysis, Energy-dispersive X-ray spectroscopy can detect the energy or wavelength of these X-rays. An image of the sample distribution is produced by detecting and utilizing the electron beam that the sample absorbs giving an image as a map showing the signal intensity radiated from the sample's scanning area (Inkson, 2016).

2.5.9 Commonly used adsorption models

To fully comprehend adsorption, the kinetics, isotherms, and mechanisms involved should be elaborated by fitting the data obtained to commonly used adsorption models.

2.5.9.1 Adsorption isotherms

Adsorption is usually described through an isotherm. An adsorption isotherm is the presentation of the amount of solute adsorbed per unit weight of adsorbent as a function of the equilibrium concentration in the bulk solution at a constant temperature. Two non-linearized two-parameter isotherm models, namely, Langmuir and Freundlich, and two other non-linearized three-parameter isotherm models, namely, Redlich–Peterson and Sips are commonly used. The Redlich–Peterson model combines Langmuir and Freundlich models (Redlich & Peterson, 1959) and if data fits the model, then the adsorption is hybrid implying that ideal monolayer sorption is not feasible. Due to its versatility, it applies to homogeneous or heterogeneous surfaces. The model can be expressed as in **Equation 2.3**.

$$q_e = \frac{AC_e}{1 + BC_e^g}$$

(Equation 2. 3)

where C_e denotes the equilibrium concentration of the solute (µg L^{-1}), q_e depicts equilibrium uptake capacity (µg g^{-1}), A (L μg^{-1}), B (L g^{-1}) signify the constants of the Redlich–Peterson model and g denotes an exponent reflecting the heterogeneity of the sorbent and its values range between 0 and 1. When g values are equal to zero and one, the Redlich-Peterson isotherm converges to the Henry and Langmuir isotherms, respectively. Further, when the isotherm parameters A and B >> 1 and g < 1, the Redlich–Peterson isotherm will represent the Freundlich isotherm (**Equation 2.4 & 2.5**) (Freundlich, 1906) which is possible at very high solute concentrations in the liquid phase. The three parameters cannot be obtained by linearizing without overestimating or underestimating thus the use of the non-linearized format.

$$q_e = \frac{A}{B} C_e^{1-g}$$

(Equation 2. 4)

where $A/B = K_F$ and $(1-g) = 1/n$ of the Freundlich model translating to:

$$q_e = K_f C_e^{\frac{1}{n}}$$

(Equation 2. 5)

When $g = 1$, **Equation 2.4** becomes the Langmuir isotherm with $b = B$ [Langmuir constant (L g^{-1}) which is associated with the adsorption energy]. $A = bq_m$, but q_m refers to Langmuir's optimum uptake capacity of the solid (µg g^{-1}) (Langmuir, 1916).

$$q_e = \frac{q_{max} C_e}{1 + K_L C_e}$$

(Equation 2. 6)

Where q_e (µg g^{-1}) and C_e (µg L^{-1}) are the solute uptake and the solution concentration at equilibrium, respectively and q_{max} (µg g^{-1}) is the monolayer adsorption capacity. The K_L (L mg^{-1}) and K_f (L g^{-1}) are the Langmuir and Freundlich constants and 1/n is related to the adsorption affinity or surface heterogeneity.

When β=0, **Equation 2.4** becomes Henry's model having *A/B* as Henry's constant (K_{HE}).

$$q_e = K_{He} Ce$$

(Equation 2. 7)

In heterogeneous adsorption, where the adsorbed molecule has numerous adsorption sites, the Sips isotherm (**Equation 2.8**), which combines the Freundlich and Langmuir isotherms is the most appropriate (Sips, 1948). Adsorbate-adsorbate synergy, however, is not taken into account by the model. The Sips isotherm is expressed as:

$$q_e = \frac{q_{MS} a_s C_e^{B_s}}{1 + a_s C_e^{B_s}}$$

(Equation 2. 8)

Where q_{ms}, a_s and B_s are the isotherm constants. The constant B_s is the heterogeneity index whose magnitude increases with heterogeneity.

2.5.9.2 Kinetic models

There are two widely used kinetic models, namely, pseudo-first-order (PFO) (**Equation 2.9**) (Ho & McKay, 1998), and pseudo-second-order (**Equation 2.10**) (PSO) (Ho, 2006) models represented in the equations below:

$$\boldsymbol{q_t = q_e(1 - e^{k_1 t})}$$

(Equation 2. 9)

$$q_t = \frac{q_e^2 k_2 t}{1 + k_2 q_e t}$$

(Equation 2. 10)

Where t (min) and q_t (µg g^{-1}) are time and amount adsorbed at equilibrium time, respectively, while q_e is the equilibrium adsorption capacity. k_1 (min^{-1}) and k_2 (g/µg/min) are rate constants. Assuming PFO kinetics, the initial adsorption rate (S_{rate}) and adsorption half-life ($t_{1/2}$) were calculated using **Equations 2.11**, and **2.12**, respectively.

$$S_{rate} = K_1 q_e$$

(Equation 2. 11)

$$t_{1/2} = \frac{ln2}{K_1}$$

(Equation 2. 12)

The initial sorption rate and adsorption half-life for PSO were obtained using **Equations 2.13,** and **2.14**, respectively.

$$S_{rate} = K_2 q_e^2$$

(Equation 2. 13)

$$t_{1/2} = \frac{1}{K_2 q_e}$$

(Equation 2. 14)

2.5.9.3 Adsorption Thermodynamics

Temperature changes affect the adsorption process. To determine the thermodynamics of the process, the thermodynamic parameter change in Gibb's free energy (ΔG) is estimated using the following equations:

$$\Delta G = -RTlnK_c$$

(Equation 2. 15)

$$K_c = 1000K_d$$

(Equation 2. 16)

$$K_d = \frac{C_{ads}}{C_e}$$

(Equation 2. 17)

Where K_c is the equilibrium constant, C_e is the equilibrium concentration in the solution (μg L^{-1}) and C_{ads} is the equilibrium solid phase concentration (μg L^{-1}). R is the gas constant (8.314 J $mol^{-1}K^{-1}$) and T is the temperature in Kelvin. K_d is the distribution coefficient (L g^{-1}), and the density of water is 1,000 g L^{-1} (Luttah et al., 2023). The changes in enthalpy (ΔH) (kJ mol^{-1}) and entropy (Δs) (J mol^{-1}) are obtained from the slope and intercept of the Van't Hoff plot (**Equation 2.18**), respectively.

$$ln\, K_c = \frac{\Delta S}{R} - \frac{\Delta H}{R}\frac{1}{T}$$

(Equation 2. 18)

2.5.10 Merits and challenges of using waste materials in Africa

Large quantities of bio-based materials that can be used as sorbents are in most cases readily available. The reuse of these bulky biowastes, which are currently a public health concern due to disposal problems, causes waste minimization and reduces waste loads in landfills (Bhatnagar & Sillanpää, 2010). Biowastes have also been found to be highly efficient in dilute solutions with high possibilities of regeneration (Omo-Okoro et al., 2018). Another advantage is the conservation of limited and valuable feedstock such as coal, lignite, and petroleum coke, which are mostly used for commercial activated carbon production. These merits align with the millennium development goals of sustainable development and zero waste (Schoutteten, 2012).

The disposal of the used adsorbents is the main challenge that researchers are still grappling with. Incineration and landfilling could be considered options. However, disposal of the so-produced pollutant-laden ash presents another unresolved environmental challenge. Other uses of the used biosorbents include being used as fillers in road surfacing and in amending soils (Chaukura et al., 2016) or as precursors for eco-cement (geopolymers) development (Tome et al., 2020). Most of the adsorbents do not work in natural conditions (Ali et al., 2012) and that is why parameters like pH and temperature must be varied. Some may also require a longer contact period for maximum adsorption. They may also require larger concentrations of pollutants, that is, in the mg mL^{-1} range contrary to the µg mL^{-1} concentration range in real environmental media.

Large-scale applications of adsorption can be costly and require capital investment. Furthermore, over time, the adsorption beds age and become saturated and less efficient, and no amount of regeneration can salvage the adsorption sites. This requires replacement

with new sorbents. There can also be an issue of desorption especially if the contaminant concentration is low to maintain equilibrium. Desorption can also be caused by competition for the adsorption sites by different pollutants and other adsorbed species (Grandclément et al., 2017).

It is also important to note that removal efficiencies of organic micro-pollutants rely on several factors including the physico-chemical properties of the compound for example water solubility, hydrophobicity and degradation among others. Further, process-specific parameters like batch versus continuous, temperature, pH, Ultra-Violet radiation, and precipitation rate also alter the adsorption process (Grandclément et al., 2017). These variables may affect removal efficiencies with some variables, if not optimized well, affecting the adsorption negatively.

2.6 Phytoremediation studies using *E. crassipes*

Phytoremediation is another emerging green technology that uses certain plant species to sequester pollutants from different environmental compartments or render them harmless (Ajayi & Ogunbayio, 2012; Chaudhuri et al., 2008; Sudarsan et al., 2012). Research has shown that plants display good sorption performance for heavy metals, nitrates, phosphates, and organic pollutants including herbicides such as atrazine, organic solvents such as trichloroethylene, explosives such as trinitrotoluene, petroleum hydrocarbons such as oil, gasoline, benzene, toluene, and polycyclic aromatic hydrocarbons, the fuel additive methyl tert-butyl ether, and PCBs (Farrag & Fawzy, 2012; Pilon-Smits, 2005; Trueman & Erber, 2013). Several plants such as water lotus, saltgrass, water hyacinth, cattail, parrot feather, duckweed, pickleweed, sunflower, indian mustard, azolla, mulberry trees, ryegrass, poplar, and willow have been used to eliminate harmful environmental

pollutants from water systems (Christwardana & Soetrisnanto, 2013; Dipu et al., 2011; Ibezute & Tawari-Fufeyin, 2012; Madhurina et al., 2014; Pilon-Smits, 2005). For phytoextraction to be successful, the plants used must be quickly growing, rich in biomass, competitive, hardy, tolerant to pollutants, and with a high capacity for pollutant absorption, translocation, and accumulation in harvestable tissues. They should grow broad, dense roots with abundant degrading enzymes for phytodegradation to be applied. An extensive root surface area also promotes phytostimulation, as it provides for microbial growth. Moreover, plants that can allow the flourishing of microbes around the root region can facilitate the production of specific exudate compounds that are vital in enhancing rhizodegradation through particular interactions between the plant and the microbes (Pilon-Smits, 2005). Because they grow more quickly, produce more biomass, and have a higher relative capacity for pollutant uptake than terrestrial plants, aquatic macrophytes are more suited for wastewater treatment than terrestrial plants. They are more efficient at phytoremediation when there is no barrier between them and the polluted water. These plants could be emergent, floating, or submerged aquatic species. Floating aquatic plants absorb contaminants through their roots, whereas submerged plants accumulate pollutants through their entire bodies. Emergent plants grow on banks and have deep dense roots. Plant roots may release exudates that enhance biotransformation and microbial degradation of these chemicals (Michelini et al., 2012).

The construction of a phytoremediation site exploits the ability of plants to adsorb, uptake, stabilize, concentrate, chelate, degrade, volatilize, or transform organic and inorganic pollutants (Dipu et al., 2011; Pilon-Smits, 2005; Sukumaran et al., 2013; Vymazal, 2002). These phytoremediation sites have been shown to significantly lower the amounts of

tetracycline and sulfamethazine antibiotics in wastewater, with mass removal rates of 85%-95% and 11%-95% for the two compounds, respectively (Liu et al., 2014).

E. crassipes has been largely used for adsorption of pollutants (Buasri et al., 2012; Isichei & Okieimen, 2014; Ngeno et al., 2016; Wanyonyi et al., 2013). Its' use for phytoremediation of pollutants however remains largely ignored even with its huge potential of eliminating a vast range of organic and inorganic contaminants from wastewater due to its capacity to thrive in severely contaminated waterways (So et al., 2003).

While studying phytoremediation, Liao and Chang (2004) investigated the use of *E. crassipes* to absorb and translocate cadmium (Cd), lead (Pb), copper (Cu), zinc (Zn), and nickel (Ni) in the Erh-Chung wetlands. The study reported high bioconcentration of these trace elements to *E. crassipes* when grown in water environments with low concentrations of the five elements. Generally, the concentration of these five elements in the roots was 3 to 15 times higher than those in the shoots. The study further established that the absorption capacity for *E. crassipes* was estimated at 0.24 kg ha^{-1} for Cd, 5.42 kg ha^{-1} for Pb, 21.62 kg ha^{-1} for Cu, 26.17 kg ha^{-1} for Zn, and 13.46 kg ha^{-1} for Ni, concluding that *E. crassipes* is a promising candidate for phytoremediation of wastewater. Shah et al. (2010) also reported the potential of *E. crassipes* in treating industrial dye effluent. The authors found a considerable drop in the pH, TDS, conductivity, hardness, DO, BOD, COD, nitrate nitrogen, and ammonium nitrogen in different wastewater concentrations. The water hyacinth was most effective in wastewater concentrations of 25–50%, but not in wastewater concentrations of 75–100%. Dar et al. (2011) also demonstrated that this wonder plant can be used to treat sewage effluent. They reported that *E. crassipes* was

able to reduce all the physico-chemical and biological parameters significantly (25%, 50%, 75%, and 100% wastewaters) except the DO which displayed an upward trend.

Rapidly-growing *E. crassipes* is a floating plant with a substantial biomass and a well-established fibrous root system. It also readily conforms to a variety of aquatic circumstances and is crucial in the process of removing contaminants from water (Ali et al., 2012). Because of its rapid spread and crowded growth, which cause major issues with navigation, irrigation, power generation, and death to aquatic life, it has garnered attention from all around the world (Ajayi & Ogunbayio, 2012; Buasri et al., 2012). It is a plentiful bioresource that, despite being viewed by many as an environmental nuisance, is useful in the treatment of wastewater (Isichei & Okieimen, 2014). It is widespread throughout Kenya, including the Lake Victoria region, and has caused a national calamity. This can be harvested, and in line with the golden rules of sustainable development, used for the sustainable treatment of wastewater by replanting them in constructed wetlands (Ajayi & Ogunbayio, 2012). This will also lead to the reduction of this plant in Lake Victoria, which is the largest major freshwater lake in Africa. After phytoremediation, the used plants can then be removed and used for making useful products like furniture and baskets which are not for ingestion. They could also be used for biogas production and the remaining residue incinerated.

Phytoremediation offers a cost-effective and technically feasible technology and has proven effective and successful in the remediation of wastewater (Ali et al., 2012) since it is solar-driven and can be performed *in situ*. Phytoremediation may also have its shortcomings. For instance, the plants that execute the remediation must be in contact with the toxicant and should have the capacity to carry out the intended function. Accordingly,

wastewater characteristics, toxic levels, and climatic conditions should all promote plant development. Phytoremediation may also be constrained by root depth since the plants and the contaminants should be in contact. Additionally, it may be seen to be a slow process as it can take years for plants to take up contaminants (Pilon-Smits, 2005).

2.7 Previously used methods of extraction and analysis

There are various recent advances in EDCs extraction and analysis as recorded by Singh et al. (2014). Before analysis, clean-up and extraction methods may involve liquid-liquid extraction, microwave-assisted extraction, ultrasonic extraction, liquid-phase microextraction, solid-phase microextraction, or solid-phase extraction (SPE). The most popular method is SPE due to its many benefits, including its simplicity, high recovery rates, minimal use of organic solvents, high pre-concentration factors, and ease of mechanization and operation. For analysis, the most common ones employed include ultra-violet and visible spectrophotometry (UV-Vis), high-performance liquid chromatography (HPLC), high-performance liquid chromatography-tandem mass spectrometry (HPLC-MS/MS) and Gas chromatography hyphenated to mass spectrometry (GC-MS/MS) (Benijts et al., 2004; Kelly, 2000; Trenholm et al., 2006; Vanderford et al., 2003). Quantitative analysis using UV-Vis is usually based on Beer Lambert's law and in many cases the presence of stray radiation makes the direct application of Beer's law inaccurate. Therefore, GC-MS and HPLC-MS/MS methods have been employed due to their low detection limits (Trenholm et al., 2006; Vanderford et al., 2003). The use of GC-MS technique limits the spectrum of the analyzed chemicals to non-ionic and thermally stable substances. However, derivatization methods such as acylation or methylation and hydrolysis can be employed to enable analysis by GC-MS (Adelaja, 2011).

CHAPTER THREE

MATERIALS AND METHODS

3.1 Research Design

The research design was experimental and it was achieved through laboratory experiments.

3.2 Chemicals, standards, and reagents

DBP and DMP reference standards were purchased from Dr. Ehrenstorfer GmbH (Augsburg, Germany). DEHP, LNR, and PGT were purchased from Sigma Aldrich. All the standards were above 99% purity. Analytical grade and high-performance liquid chromatography (HPLC) grade solvents for extraction and analysis were purchased from Fluka Chemicals, Germany. SPE cartridges and nylon microfilters were procured from Merck Chemicals. Analytical grade anhydrous sodium sulfate (Na_2SO_4) was supplied by Sigma-Aldrich. All the glassware was thoroughly washed by first soaking it for 2 hours in warm tap water combined with a phosphate-free detergent. It was then rinsed with hot water, followed by de-ionized water and finally acetone. Before use, the glassware was subsequently dried in an oven at 105 °C for 3 hours.

3.3 Determination of concentration levels of the selected EDCs

3.3.1 Study area

The study was carried out in twelve (12) WWTPs of Nairobi and the major towns in the larger western region of Kenya, namely, Kisumu, Kakamega, Bungoma, Busia, Kisii, Kericho, Eldoret, and Nakuru (**Figure 3.1**).

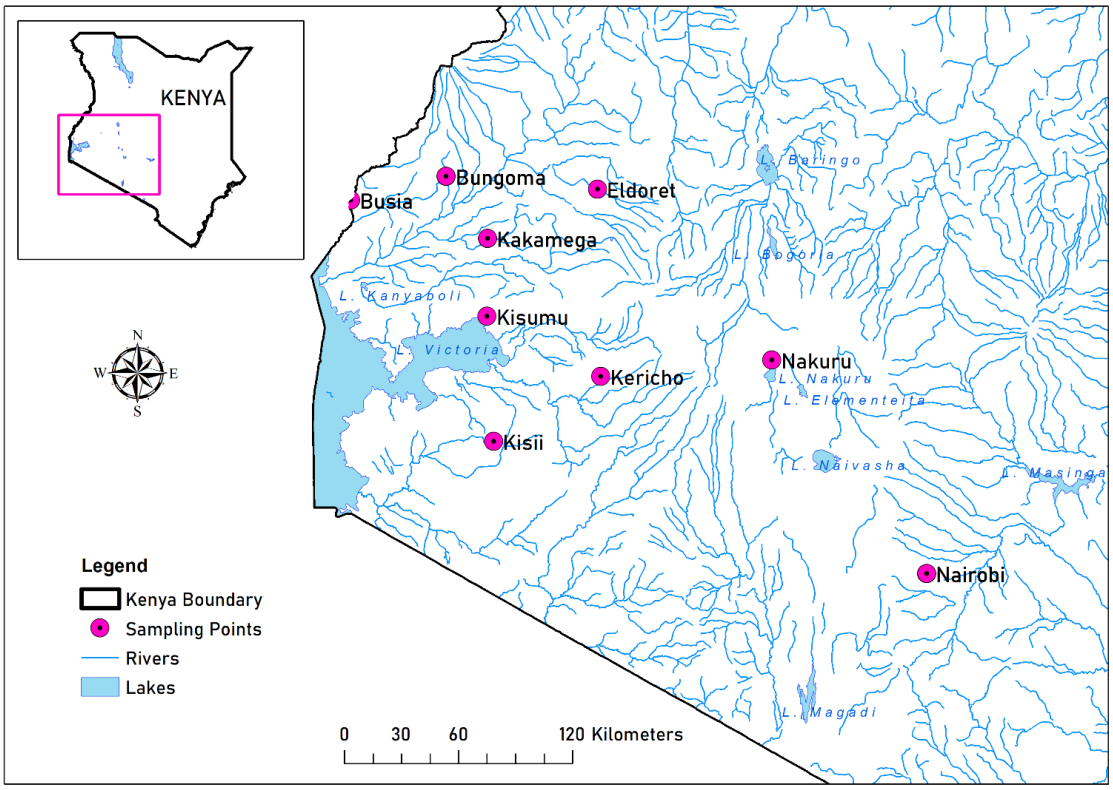

Figure 3.1: Map showing the study area.

These sites were purposely selected because the WWTPs in these towns (except Nairobi and Nakuru) release their effluents directly into streams and rivers that eventually drain and are major tributaries to Lake Victoria, the largest freshwater lake in Africa. These major towns in western Kenya have moderately dense human settlements, various agricultural and industrial activities, and open illegal dumpsites which are probable sources of EDCs to the lake through effluent release and rainwater runoff. The high-intensity agricultural activities were also a major factor in collecting samples from Kericho, Kisii, Nakuru, and Eldoret. Nairobi was included because it is highly urbanized, heavily industrialized, and densely populated with informal settlements that harbor open dumpsites for waste management.

The WWTPs in the sampling areas were either using conventional treatment systems (trickling filters) or wastewater stabilization ponds (WSPs) (aerated lagoons). Due to the high cost of maintenance and complexity of conventional WWTPs, most towns have constructed WSPs in addition to the conventional WWTPs. Examples of such towns are Nairobi, Nakuru, Eldoret, and Kisumu. The conventional WWTPs were in Kisat (Kisumu), Kericho, Eldoret, and Kariobangi (Nairobi). The lagoons were in Nyalenda (Kisumu), Kisii, Ruai (Nairobi), Bungoma, Busia, Shirere, and Masinde Muliro University of Science and Technology (MMUST) (both in Kakamega). **Table 3.1** indicates the characteristics of the WWTPs sampled.

Table 3.1: Characteristics of the WWTPs where samples were collected

WWTPs' location	City population	Type of wastewater treated	Treatment type	Capacity (C_{wwtp}) (M^3 day^{-1})
Bungoma	298,696	Domestic	Wastewater stabilization ponds	9,200
Busia	113,753	Domestic	Wastewater stabilization ponds	2,150
Kisii	112,417	Domestic and Agricultural runoffs	Wastewater stabilization ponds	4,000
Kisat	397,957	Domestic and industrial	Conventional treatment system	8,000
Kisumu-Nyalenda	397,957	Domestic and industrial	Wastewater stabilization ponds	18,000

WWTPs' location	City population	Type of wastewater treated	Treatment type	Capacity (C_{wwtp}) (M^3 day^{-1})
Kakamega-Shirere	252,611	Domestic	Waste stabilization ponds	2,000
MMUST	21,000	Domestic	Wastewater stabilization ponds	425
Eldoret-Kipkenyo	165,450	Domestic and Agricultural runoffs	Conventional treatment system	8,000
Nakuru Old town	409,908	Domestic and industrial	Conventional treatment system	6,600
Nairobi Kariobangi	4,397,073	Domestic and industrial	Conventional treatment system	23,000
Nairobi-Ruai	4,397,073	Domestic and industrial	Wastewater stabilization ponds	80,000
Kericho	228,318	Domestic and Agricultural runoffs	Conventional treatment system	990

Source of data: Adopted from (Chirikona et al. (2015); Kenya Population Census (2019); Kimosop et al. (2016)) .

3.3.2 Sampling

One-liter water samples (N = 60) were collected in triplicate into pre-cleaned amber glass bottles which were then tightly covered and preserved in an icebox to limit microbial activities (Sampling pictures are in **Appendix 1-3**). From the conventional treatment systems, water samples were picked from the influents, primary ponds, secondary ponds, tertiary ponds, and effluent. From the WSPs, the sampling locations were identified as

influent, anaerobic ponds, facultative ponds, maturation ponds, and effluent release. In the laboratory, the water samples were spiked with 10 mL formaldehyde (86% v/v) and stored in a refrigerator below 4 ^{o}C to avoid microbial degradation before extraction. Extraction was carried out within 48 hours of sample collection.

Sludge samples were collected from the anaerobic ponds (for the lagoons) and primary ponds (for the conventional treatment plants) just below the influent flow of the twelve WWTPs. Approximately 2 kgs of the wet weight of the sludge samples were wrapped in aluminum foil then placed in a cool box packed with ice and transported directly to the laboratory. Once in the laboratory, the samples were air-dried under a shade for two weeks. Dried UDBS (approximately 1 kg dry weight) was collected from the drier beds of the WWTPs. They were wrapped in aluminum foil and ferried to the laboratory where they were immediately air-dried.

3.3.3 Determination of water quality parameters

Water quality parameters such as pH, chemical oxygen demand (COD), total dissolved solids (TDS), biochemical oxygen demand (BOD_5), and electrical conductivity (EC) were determined *in situ* on the influent locations using a Hydrolab Quanta Multi-Probe Meter**.** BOD_5 was determined by measuring the O_2 content in a representative sample, then repeating the process after a 5-day incubation period and calculating the difference (Ahmad et al., 2015).

3.3.4 Extraction and clean-up of wastewater samples

Wastewater samples were extracted following the method described by Olaniyan and Okoh (2020) with slight modifications. Briefly, 250 mL aliquots of each sample were vacuum filtered through 0.45 µm glass microfiber filters to eliminate suspended particles

and particulate debris. The residue was eluted with 10 mL of methanol to extract any EDC that may have adsorbed to the residue. The eluate obtained was put aside. The filtrate was then extracted using SPE on an SPE manifold (Supelco Visiprep™ SepPack) system and Supelclean Envi-18 SPE cartridges (500 mg/6 mL) and an external PerkinElmer vacuum pump at a rate of 8 L min^{-1} (**Appendix 4**). Before extraction, the SPE cartridges were preconditioned with 10 mL of HPLC-grade methanol followed by equilibration with 10 mL of HPLC-grade water. When the entire sample had passed through the SPE cartridges, the cartridges were first washed with 10 mL of HPLC-grade water and then air dried for 60 minutes. The analytes were then eluted with 10 mL of methanol. The resulting eluate was combined with the eluate from the residue and dried using anhydrous sodium sulphate then concentrated using a rotary evaporator to 2 mL with a heating bath set at 40 ^{o}C. The eluate was further concentrated to 1 mL using a nitrogen stream and filtered using 0.45 μm nylon microfilters as they were transferred to glass vials. The clean sample was then stored in a refrigerator below 4 ^{o}C awaiting analysis using a HPLC-MS/MS.

3.3.5 Extraction and clean-up of sludge and UDBS samples

Sludge and UDBS samples were extracted and cleaned using the method reported by George et al. (2019) with modifications. Briefly, the air-dried sludge and UDBS samples were ground using a mortar and a pestle, homogenized, and sieved through 220 μm sieves. Twenty grams of the fine sample was placed in a glass fiber extraction thimble and Soxhlet extracted with 200 mL methanol for 8 hours (**Appendix 5**). The supernatant solution was filtered through glass wool pre-conditioned with 10 mL of HPLC-grade methanol. The filtrate was then concentrated to dryness using a rotary evaporator at 40 ^{o}C. The sample was then re-dissolved in 100 mL distilled water and clean-up was performed by SPE

following the same procedure for wastewater samples in section 3.2.4. The drying and concentration also followed the wastewater procedure.

3.3.6 Instrumental analysis

HPLC-MS/MS analysis was done using an Agilent 1200 Infinity system hyphenated with tandem MS detector (Agilent MS quadrupole 6420). The machine is fitted with an automatic sampler model G7129A. The draw speed was set at 200 µL min^{-1} while the eject speed was set at 400 µL min^{-1}. The wait time after the draw was 1.2 sec. The injection was accompanied with needle wash at the flush port for 3 sec and the injection volume was 3 µL. The equipment was connected to a binary pump system (G1312B) at a set flow rate of 0.3 mL min^{-1}. The low-pressure limit was set at 0.00 bar while the high pressure was set at 500.00 bar. The maximum flow gradient was 100 mL min^{-1}. The stop time was after 15 min and the post time was 1.90 min. The analytes were separated on an Agilent Zorbax Eclipse (XDB C18, RP18, ODS, Octadecyl) column, 80 Å pore size, 5 µm particle size, 4.6 mm inner diameter and 150 mm length. The column temperature was set at 45 ^{o}C.

The solvent composition was set as follows; channel A was for solvent 1, and composed of H_2O, with 5 mM Ammonium formate + 0.1% formic acid used at 95.0%. Channel B was for solvent 2 and composed of methanol with 5 mM Ammonium formate + 0.1% formic acid used at 5.0%. The gradient used was as follows: at 0.5 min, A was 95% and B was 5%; at 5 min, A was 15% and B was 85%; at 5.5 min, A was 0% and B was 100%; at 12.5 min, A was 95% and B was 5%; and at 15 min, A was 95% and B was 5%.

The ion source on the mass spectrometer detector was in electrospray Ionization (ESI) mode and the scan type was multiple reaction monitoring (MRM). The source parameters

for both positive (ESI^+) and negative (ESI^-) values were gas temperature 325 (^oC), gas flow 10 L min^{-1}), nebulizer 45 psi, and the capillary was 4000 V. All target compounds were optimized in both positive electrospray ionization (ESI^+) and negative electrospray ionization (ESI^-) ion modes. For all of the chemicals tested, higher abundances of ion transitions were obtained in the ESI^+ mode than in the ESI^- mode. As a result, all of the compounds of interest were analyzed in the ESI^+ mode. All the representative compounds were analyzed in the MRM mode. The identification of EDCs in the sample extracts was determined by a comparison of the retention times and fragmentation patterns of the peaks in measured sample extract chromatograms to those in calibration standards (R^2 = 0.992 or better) (**Appendix 6**). Quantification was computed by integrating the chromatograms (**Appendix 7**).

3.3.7 Removal efficiency of selected EDCs in the sampled WWTPs

The percentages of EDCs removed during treatment by the conventional/aerated lagoon method were calculated from the concentrations in the effluent and influent using **Equation 3.1**. This gives the efficiency of the treatment method.

$$\%\ \boldsymbol{Removal\ Efficiency} = \frac{\left(\boldsymbol{C_{influent}} - \boldsymbol{C_{effluent}}\right)\boldsymbol{x\ 100}}{\boldsymbol{C_{influent}}}$$

(Equation 3.1)

Where $C_{influent}$ is the concentration of EDCs in the raw sewage and $C_{effluent}$ is the concentration of EDCs in the treated sewage (Kairigo et al., 2020).

3.3.8 Mass loading of EDCs into the environment

The daily EDC mass loadings from WWTPs were calculated assuming that the EDC levels in the effluent wastewater reported were constant throughout the day and that the WWTPs were operating at full capacity (Kimosop et al., 2016). This was done using **Equation 3.2**.

$$\boldsymbol{Dd = C_W \times C_{WWTP} \times 1000 \times 10^{-3} (mg day^{-1})}$$

(Equation 3.2)

Where: Dd = Daily discharge of EDCs (mg day^{-1}),

C_w = Concentration of individual EDC in the effluents (µg L^{-1})

C_{WWTP} = Capacity of WWTP (M^3 day^{-1}) (**Table 3.1**),

1000 = Conversion factor from cubic meters to liters,

10^{-3} = Conversion from microgram to milligram.

3.3.9 Potential health risks to the recipient aquatic ecosystem

The toxic risks posed by the compounds of interest were assessed by calculating the Risk Quotients (RQ) (**Equation 3.3**) for three different trophic levels (fish, crustaceans *(Daphnia)* and algae) following the European Commission's Technical Guidance Document on risk assessment (European Commission, 2003).

$$\boldsymbol{RQ = \frac{MEC}{PNEC}}$$

(Equation 3. 3)

Where MEC is the maximum measured environment concentration and PNEC is the Predicted No Effect Concentration. A PNEC is regarded as a concentration below which an unacceptable effect will most likely not occur. It is calculated (**Equation 3.4**) by

dividing the lowest short-term concentration causing 50% death (LC50) or effect (EC50) or lowest observed effect concentration (LOEC) or long-term no observed effect concentration (NOEC) value for the most sensitive indicator species by an appropriate assessment factor (AF). The AF reflects the degree of uncertainty in extrapolation from laboratory toxicity test data for a limited number of species to the natural environment. AF applied for long-term tests is lower and is preferred as the uncertainty of the extrapolation from laboratory data to the natural environment is minimal (European Commission, 2003). AF of 100 was utilized for PNEC calculations for detected EDCs where NOEC data for species representing only one trophic level (*Daphnia* or fish) were available. AFs 50 and 10 were used when NOEC values were available for species representing two trophic levels (fish, and/or *Daphnia*, and/or algae) and three trophic levels (usually fish, *Daphnia*, and algae) respectively. Additionally, an AF of 1000 was used for acute toxicity data (European Commission, 2003).

$$\boldsymbol{PNEC = \frac{NOEC(or\ L(E)C50)}{AF}}$$

(Equation 3. 4)

For every EDC, RQ was calculated based on the worst-case scenario, by considering the maximum concentration detected among all the sites, as well as the lowest NOECs or E(L)C50. The RQ for chronic cases was also calculated for every EDC per site. An RQ value > 1 indicated a suspected high ecotoxicological risk, and 0.1 < RQ < 1 and RQ < 0.1 represented possible medium and low risks respectively (Huang et al., 2018). Data (**Table 3.2**) were obtained from the Norman network and ECOTOX database.

Table 3.2: Toxicological data for selected EDCs in effluents released to surface water

EDC	Trophic level	Scientific name	Acute or Chronic	Exposure regime	Effect measurement	Endpoint	Duration	Effect value (mg L^{-1})
DEHP	Algae	*Stephanodiscus hantzschii*	Chronic	Static	Growth, general	EC50	4 days	0.3
	Crustacean	*Daphnia magna*	Chronic	Flow-through	Mortality	NOEC	7 days	0.2
	Fish	*Oryzias latipes*	Chronic	Renewal	Growth length	NOEC	91.3 days	0.05
DBP	Algae	*Skeletonema costatum*	Chronic	Static	Population	NOEC	4 days	200.0
	Crustacean	*Daphnia magna*	Chronic	Renewal	Mortality	NOEC	24 days	0.5
	Fish	*Danio rerio*	Chronic	Renewal	Mortality	NOEC	95 days	0.4
DMP	Algae	*Raphidocelis subcapitata*	Chronic	Static	Chlorophyll concentration	NOEC	4 days	35.8
	Crustacean	*Daphnia magna*	Chronic	Static	Mortality	NOEC	2 days	1.7
	Fish	*Oryzias latipes*	Chronic	Static	Mortality	EC50	1 day	180.0
PGT	Crustacean	*Daphnia magna*	Acute	Renewal	Immobile	NOEC	48 hours	0.2
			Chronic	Renewal	Survival	NOEC	26 days	0.1

EDC	Trophic level	Scientific name	Acute or Chronic	Exposure regime	Effect measurement	Endpoint	Duration	Effect value (mg L^{-1})
	Fish	*Lepomis macrochirus*	Acute	Flow-through	Mortality	NOEC	96 hours	0.07
		Pimephales promelas	Chronic	Flow-through	Growth, general	NOEC	35 days	0.009
LNR	Algae	*Chlorella vulgaris*	Chronic	Static	Population growth rate	NOEC	96 hours	0.001
	Crustacean	*Daphnia magna*	Acute	Static	Survivorship	NOEC	144 hours	0.1
			Chronic	static	Survival	NOEC	21 days	0.1
	Fish	*Lepomis macrochirus*	Acute	Static	Mortality	NOEC	96 hours	4.9
		Oncorhynchus mykiss	Chronic	Flow through	Histological changes, general	LOEC	28 days	0.06

PAEs data was adopted from (Olker, 2022), while PGT and LNR data were adopted from (NORMAN Network, 2023). (DBP = dibutyl phthalate, DEHP = diethylhexyl phthalate, DMP = dimethyl phthalate, LNR = linuron and PGT = progesterone; LC50 = lowest short-term concentration, EC50 = effect causing 50% death, LOEC = lowest observed effect concentration, NOEC= long term no observed effect concentration)

3.3.10 Quality control and assurance

External standards calibration was used for quantification. Calibration curves (6-8 points) were obtained by preparing individual standards at different concentrations (5-150 μg L^{-1}) using blank solvents. The linearity of the calibration was evaluated based on the coefficients of determination (R^2) of the calibration curves. In all cases, R^2 was ≥ 0.99. The precision of the HPLC–MS/MS method for each EDC analyte investigated was determined by analyzing all the samples in triplicates. Since phthalates are ubiquitous, maximum care had to be taken to avoid the risk of contamination from laboratory equipment, glassware, solvents, reagents, and personnel. These procedures included minimal sample manipulation, careful choice of equipment, and proper cleaning and baking of glassware at high temperatures before use.

Procedural blanks (250 mL of ultrapure Milli-Q water and river sediments deemed uncontaminated for the sludge and UDBS) were analyzed to monitor for background contamination. Signals were observed with the phthalates' procedural blanks and the data were therefore blank corrected by calculating the mean of all procedural blanks and subtracting from the sample values for every analyte. Analytes were deemed to be non-detectable (n.d.) if their concentrations after blank correction were less than three times the blank values' standard deviation. Additionally, n.d. was assigned to any analyses in samples that were not detected prior to blank correction.

Two blank spike recoveries (250 mL of ultrapure Milli-Q water and river sediments deemed uncontaminated for the sludge and UDBS) spiked with 50 μL of the target analytes at known concentrations of 20 μg L^{-1} and 50 μg L^{-1}, and two spike recovery samples (actual wastewater, sludge, and UDBS samples spiked with the target compounds at known

concentrations of 20 μg $L^{-1}$and 50 μg L^{-1}) were included to check for recovery and method performance. The spiked blanks and samples were analyzed using the same procedure as the samples. The recoveries ranged from 74-109% which are within the acceptable values of 60-120% and therefore, the data were not corrected for recoveries.

The limits of detection (LOD) and limits of quantification (LOQ) for each analyte were determined statistically by obtaining calibration curves of increasingly low concentrations of the analyte. The LOD and LOQ were then determined using the following **Equation 3.5 a & b**):

$$\boldsymbol{LOD = \frac{3SD}{b}}$$

$$\boldsymbol{LOQ = \frac{10SD}{b}}$$

(Equation 3.5 a & b)

Where SD is the standard deviation of the y-residuals (residual standard error) and b is the slope of the signal (Desimoni & Brunetti, 2015; Uhrovčík, 2014).

3.3.11 Statistical data analysis

Descriptive statistics reporting means, standard deviations, and ranges were calculated for only positive quantifiable samples. For further statistical analysis, half the LOD was assigned to the n.d. Normality of the data was assessed using Shapiro-Wilk's test and visual inspections of their histograms and box plots. The data for the sludge samples were approximately normally distributed. Therefore, parametric tests (one sample and paired sample t-tests) were applied to check for statistical differences among levels of EDCs in each location. One-way analysis of variance (ANOVA) was used to evaluate the differences in levels among sites and the different matrices. For the data that were not

normally distributed, (levels of EDCs in water and UDBS samples) non-parametric tests were applied. These included the Kruskal-Wallis tests and the Friedman tests which were used to compare the levels of EDCs among themselves, between sites, and among the different matrices. All differences were deemed significant if $p < 0.05$. Spearman's rank-order correlation coefficients (r_s) were calculated to evaluate bivariate associations between WWTPs' water quality parameters and the pollutant levels, as well as those amongst the different pollutants. All statistical analyses were conducted using Excel, SPSS version 20 (IBM, Chicago IL, USA), and OriginPro, version 9 (OriginLab Corporation, Northampton, MA, USA).

3.4 Adsorption studies

3.4.1 Choice of adsorbates

PGT and LNR were used for adsorption experiments. Although the PAEs had higher concentrations in the environmental matrices, they could not be used for adsorption since they are found in most apparatus in the laboratory and they tend to leach out of them. For this same reason, even after careful handling, procedural blanks during the determination of the levels were found to have signals and therefore the results were blank corrected. Further, PGT had a high RQ implying that its abstraction from environmental matrices should be treated with urgency. Kenya being an agricultural country means that more herbicides like LNR are in use. It is thus imperative to find an inexpensive way of sequestering them from the environment.

3.4.2 Pretreatment of the adsorbent

M.O seeds were purchased from Nakasero market, Kampala, Uganda due to the proximity to the laboratory and the cost. The seeds were manually de-shelled to remove the outer

coat. The pretreatment of *M.O* seed was done as reported by Kituyi et al. (2013) and Ongulu et al. (2015) but with modification. Briefly, 500 g of the kernel was washed in deionized water to remove dirt, and then soaked in 1000 mL of 0.1 M HCl for 3 days, to remove impurities and increase the surface area (Adelaja et al., 2011). The seeds were then washed again with ultra-pure water, dried in air then ground using a domestic blender. The biomass is supposed to be used as an agro-waste product after the removal of useful oils and fats. Fat was therefore eliminated using 200 ml of n-hexane. n-hexane dissolved the fat and floated. The mixture was centrifuged (2010D Centurion Scientific, West Sussex, UK) at 5000 revolutions per minute (rpm) for 10 minutes at room temperature. The supernatant was disposed of, and the fat-free *M.O* sediment was air-dried to evaporate the remaining hexane. 200 g of the fat-free *M.O* powder was soaked in 0.5 M phosphoric acid for 2 hours to increase the pores. The sample was then oven-dried at 105 ^{o}C for 24 hours, sieved through a 75 µm sieve, and labelled *MOSB* (**Figure 3.2).**

Figure 3.2: *M.O* treated seed biomass.

3.4.3 Characterization of *MOSB*

To obtain the sample crystallinity of *MOSB*, a Bruker D8 Advance X-ray diffractometer with copper Kα monochromator at the voltage of 15kV, scanned at wavelength λ=1.54Å with 2θ angle range from 5^{o} to 90^{o} was used. Morphology, microstructure, and percentage elemental composition of *MOSB* were obtained by scanning electron microscopy–energy dispersive spectroscopy, (SEM-EDS) (JSM-IT500). Fourier Transform Infra-red (FT-IR) spectroscopy (NICOLET iS50 FT-IR) at 400–4000 cm^{-1} wavenumbers was used to determine the surface functional groups of the biosorbent before and after sorption (Adelaja et al., 2011; Shikuku et al., 2015).

3.4.4 Experimental design and statistical analysis

Five experimental variables (solution contact time: 10–180 min; pH: 2–10; adsorbent dosage: 0.1–2.0 g; temperature: 298 K–338 K; and initial EDC concentration: 20–500 µg L^{-1}) were evaluated based on a central composite design (CCD). To achieve the aforementioned range of independent input variables, preliminary tests were conducted. The interaction between these variables and their relative significance were studied and optimized collectively by applying RSM. Design Expert Version 13 (Stat-Ease, USA) was used for the experimental planning and statistical analysis of the data. The number of input variables influences the plan matrix. Every parameter has three distinct levels, which are denoted by the numerical values: -1 for low, 0 for center, and +1 for high (**Table 3.3**).

Table 3.3: Plan matrix used in the present study

Levels	Time (mins)	Temperature (K)	pH	Initial concentration (µg L^{-1})	Mass of adsorbent (g)
-1	10	298	2	20	0.1

0	95	318	6	260	0.55
+1	180	338	10	500	1

The total experimental runs conducted are computed according to **Equation 3.6** (Bayuo et al., 2020).

$$N = 2^n + 2n + n_c \qquad \text{(Equation 3. 6)}$$

$$N = 2^5 + 2(5) + 8 = 32+10+8=50$$

where n is the number of independent factors, n_c is the number of center points and N is the overall total of experimental runs. 50 experimental runs (**Table 3.5**) were used for modeling and optimization and comprised 32 factorial runs, 10 axial runs, and 8 center runs (**Table 3.4**). The quantification of the residual EDCs was determined using HPLC-MS/MS as described in section 3.2.6.

Table 3. 4: Experimental domain indicating the 50 runs obtained from CCD

Run	Factor 1 (A): Time (Mins)	Factor 2 (B): Temperature (K)	Factor 3 (C): pH	Factor 4 (D): Adsorbate (µg L^{-1})	Factor 5 (E): Adsorbent (g)
1	180	298	2	20	0.1
2	10	298	2	20	0.1
3	10	298	2	500	0.1
4	95	318	6	260	0.55
5	180	298	10	500	1.0
6	180	298	10	20	0.1
7	180	338	10	20	0.1
8	10	338	10	20	1.0
9	10	338	10	500	1.0

Run	Factor 1 (A): Time (Mins)	Factor 2 (B): Temperature (K)	Factor 3 (C): pH	Factor 4 (D): Adsorbate (µg L^{-1})	Factor 5 (E): Adsorbent (g)
10	95	318	6	260	0.55
11	180	338	10	20	1.0
12	95	298	6	260	0.55
13	180	338	2	500	1.0
14	10	298	10	20	1.0
15	95	318	2	260	0.55
16	10	338	2	500	0.1
17	95	318	6	260	0.1
18	10	318	6	260	0.55
19	95	318	6	20	0.55
20	95	318	6	260	0.55
21	180	338	2	20	0.1
22	95	318	10	260	0.55
23	10	338	10	500	0.1
24	180	338	10	500	0.1
25	10	338	2	20	0.1
26	95	338	6	260	0.55
27	10	298	2	500	1.0
28	180	338	2	20	1.0
29	10	338	2	500	1.0
30	10	298	10	500	0.1
31	180	318	6	260	0.55
32	180	298	2	20	1.0
33	10	338	10	20	0.1

Run	Factor 1 (A): Time (Mins)	Factor 2 (B): Temperature (K)	Factor 3 (C): pH	Factor 4 (D): Adsorbate (µg L^{-1})	Factor 5 (E): Adsorbent (g)
34	10	338	2	20	1.0
35	95	318	6	260	1.0
36	10	298	10	20	0.1
37	180	298	10	20	1.0
38	95	318	6	260	0.55
39	180	338	2	500	0.1
40	180	338	10	500	1.0
41	180	298	2	500	0.1
42	95	318	6	260	0.55
43	95	318	6	260	0.55
44	95	318	6	260	0.55
45	10	298	10	500	1.0
46	180	298	10	500	0.1
47	10	298	2	20	1.0
48	95	318	6	260	0.55
49	180	298	2	500	1.0
50	95	318	6	500	0.55

The Design Expert program was also used for statistical, regression, and graphical analysis of the acquired data. The batch method was employed to obtain the dependent variable (response), which is the percent adsorption (R), and it was subsequently used to build an empirical mathematical model. If the entire regression equation, taking into account the interaction among each of the factors under consideration, we would obtain the proposed **Equation 3.7** (Aly-Eldeen et al., 2018):

$$R = b_0 + \sum_{i=1}^{n} b_i X_i + \sum_{i=1}^{n-1} \sum_{j=i+1}^{n} b_{ij} X_i X_j + \sum_{i=1}^{n} b_{ii} X_i^2$$

(Equation 3. 7)

where R is PGT or LNR removal efficiency (%); b_0 is the model constant; X_i and X_j are independent variables and b_i, b_{ij}, and b_{ii} are linear coefficients, interaction effect coefficients, and quadratic coefficients, respectively (Bayuo et al., 2020).

3.4.5 Optimization of parameters

Maximum values for percent (%) removal and amount adsorbed (qe), the dependent parameters, were established as the aim criterion in the optimization study using RSM. For the independent factors, the temperature was minimized to depict experiments carried out at room temperature; the pH was set at 7 to depict neutral conditions; the adsorbent was minimized to ease disposal after use; the adsorbate was maximized while the contact time was left in range. The goal was to find the best settings that would result in the best response.

3.4.6 Batch adsorption experiments

A stock solution of 1000 mg L^{-1} of PGT and LNR standards was used to prepare standard solutions of desired concentrations. All experiments were carried out in batch mode in 250 mL conical flasks in a temperature-controlled magnetic heat stirrer (Stuart heat-stirrer SB162). During these batch experiments, a predetermined adsorbent mass was added to a 25 mL aqueous solution in a conical flask containing PGT and LNR at a concentration, pH, and temperature according to CCD. The pH values of the solutions were altered using 1 M HCl and 1 M NaOH and determined using a pH meter (691, Metrohm, Herisau, Switzerland). The solid matrix was separated from the rest of the solution by filtration

using the Whatman number 0.45 µm filter paper after the contact time recommended by the experimental domain. This was followed by centrifugation to get the supernatant solution. The remaining concentration after adsorption was quantified using HPLC-MS/MS (Agilent 1200 Infinity system hyphenated with tandem MS detector (Agilent MS quadruple 6420). The difference between the amount spiked and the residual concentration following equilibration as determined by HPLC-MS/MS quantification was used to compute the concentration of PGT and LNR adsorbed on the *MOSB.* Values were obtained from blank solvents and therefore solvent correction was done. Furthermore, procedural blanks were carried out to determine if PGT and LNR were lost to the apparatus used during adsorption. The average recovery was found to be 89.3% for PGT and 94.8% for LNR and this too was factored into the data analysis. The amount of adsorbate adsorbed (µg L^{-1}), percentage uptake, and equilibrium adsorption amount (µg g^{-1}) of the EDC were taken as responses. The percentage removal (R) of PGT and LNR were however taken as the dependent variable for further analysis and optimization.

The percentage removal (R) of each EDC from aqueous solutions was obtained using **Equation 3.8.**

$$R = \frac{(C_o - C_e)}{C_o} \times 100\% \quad \text{(Equation 3.8)}$$

The equilibrium adsorption amount (q_e) was computed based on the mass balance **Equation 3.9**.

$$q_e = \frac{(C_o - C_e)V}{M} \quad \text{(Equation 3.9)}$$

where q_e is the equilibrium amount (µg g^{-1}) of PGT or LNR adsorbed per gram of *MOSB*, C_o and C_e are the PGT or LNR concentrations (µg L^{-1}) in the solution initially and after adsorption, respectively, V is the volume (L) of the solution, and M is the mass (g) of the adsorbent used in the experiment.

3.4.7 Adsorption Isotherm studies

To obtain the adsorption isotherms, initial EDC concentration (20-500 µg L^{-1}) was varied as all the parameters obtained from optimization were kept constant (PGT: pH-7; contact time- 87 min; adsorbent dosage of 0.1g and 298 K; LNR: pH-7; contact time- 154 min; adsorbent dosage of 0.1g and 298 K). After equilibration, the equilibrium adsorption capacity, q_e at different initial adsorbate concentrations was obtained using **Equation 3.9**.

The experimental data was fitted to non-linearized two-parameter isotherm models, namely, Freundlich **(Equation 2.5)**, and Langmuir **(Equation 2.6),** and non-linearized three-parameter isotherm models, namely, Redlich–Peterson **(Equation 2.3)** and Sips **(Equation 2.8)** with the sole aim of selecting the most appropriate model that would best describe the biosorption of each EDC onto the *MOSB*.

3.4.8 Effect of contact time on Biosorption

Having optimized the parameters required (pH-7; initial PGT concentration-500 ug L^{-1}; adsorbent dosage of 0.1g and room temperature for PGT and pH-7; initial LNR concentration-500 ug L^{-1}; adsorbent dosage of 0.1g and 298 K for LNR), the adsorption kinetic experiments were performed by varying the contact time (0-180 min). The amount of EDC adsorbed per unit mass at the time (t) was calculated using **Equation 3.10**.

$$q_t = \frac{(C_{o-}C_t)V}{M}$$

(Equation 3. 10)

Where C_o and C_t are the initial and equilibrium concentration (µg L^{-1}), M is the mass of the adsorbent (g) and V is the volume of the solution (L). To generate the kinetic parameters, the kinetic data was fitted to two widely used kinetic models, namely, pseudo-first-order (PFO) (**Equation 2.9**) (Ho & McKay, 1998), and pseudo-second-order (**Equation 2.10**) (PSO) (Ho, 2006) models.

3.4.9 Effect of temperature on biosorption

The effect of temperature changes on the adsorption was studied in a temperature range of 298-338 K. Here, 0.1 g of *MOSB* biomass was dispersed into 25 mL of 500 µg L^{-1} of EDC and then stirred using a temperature-controlled magnetic stirrer at different temperatures (298, 308, 318, 328 and 338 K), until equilibration at 87 min for PGT and 154 min for LNR. The thermodynamic parameter change in Gibb's free energy (ΔG) was estimated using **Equations 2.15, 2.16, and 2.17**.

The changes in enthalpy (ΔH) (kJ mol^{-1}) and entropy (Δs) (J mol^{-1}) were obtained from the slope and intercept of the Van't Hoff plot (**Equation 2.18**).

3.4.10 Effect of pH on EDC Removal

Over a pH range of 2 to 12, the effect of pH on the amount of EDC removal was analyzed. In this case, 25 mL (500 µg L^{-1}) of each EDC and 0.1 g *MOSB* were placed in a stopper glass conical flask and the pH was adjusted using 1 M HCl and 1 M NaOH solutions. The solution was then agitated at 298 K until equilibration at 87 min for PGT and 154 min for LNR.

The pH at the point of zero surface charge (pH_{pzc}) of the adsorbent was also investigated and compared to the pKa values of PGT and LNR to determine the mechanism of interaction. The pH_{zpc} measurements were obtained using the pH drift method (Jemutai-Kimosop et al., 2020; Padhiyar et al., 2020). This technique involved preparing cohorts of 25 mL of 0.01 M NaCl solutions with initial pH varied between 2 and 12 by adding appropriate amounts of 0.1 M HCl or 0.1 M NaOH. It was followed by dissolving 0.1 g of *MOSB* powder in each and then agitating at 130 rpm in a shaker at 25 °C for 24 hours. Thereafter, the ΔpH (final pH (pH_f) -initial pH (pH_i)) values were plotted against initial pH (pH_i), and pH_{zpc} was determined as the x-intercept.

3.5 Phytoremediation studies

Water hyacinth *(E. crassipes)* was investigated for uptake of PGT and LNR. For phytoremediation experiments, fully mature *E. crassipes* plants were collected from areas deemed less contaminated in Lake Victoria (**Figure 3.3**). Before use, sample plants with similar weight and height were selected, rinsed, and air-dried for analysis to check for background concentrations of EDCs.

Figure 3.3: Collection of the Water Hyacinth (*E. crassipes*) plant.

Phytoremediation experiments were conducted using polyvinyl chloride (PVC) pots and to avoid different climatic conditions, the experiments were run in Kisumu where the plants were picked, and not in MMUST. Two sets of experiments for each EDC (PGT and LNR giving a total of four sets) containing four PVC buckets (**Figure 3.4**) were set for the *E. crassipes* plants as designed by Vymazal (2002) and Sudarsan et al. (2012). In each set, one bucket was without the plants and was used to establish the concentration levels of the EDCs in the sediments and lake water used. The second bucket contained plants spiked with the standards. A third bucket was the control experiment, with plants but without the EDCs. The fourth bucket was used for stage monitoring to check for aging of the plants. The other set of each EDC was a duplicate. Three *E. crassipes* plants were placed in each of the four buckets and cultured for one month to establish favorable

conditions. Lake water was collected from unpolluted sections of the lake to be used in replanting the *E. crassipes*. Some soil sediments from sites near the lake, deemed uncontaminated, were also placed in the pots. Periodically, the mixture was amended using a suitable fertilizer.

Figure 3.4: Planted *E. crassipes*.

After the plants had fully settled in the pots with favorable conditions established, which took three months, 10 mg L^{-1} of each EDC was spiked. Sample plants were picked, air-dried, and stored in a cool dry place monthly for six months. After running the experiments for nine months, the plants displayed old age and started withering off. The plants were then harvested and together with the ones harvested monthly, the roots, stem, and leaves were put aside and air-dried for three weeks before extraction. Ignoring the bucket for stage monitoring in each set, the samples obtained from each set after nine months were

nine (9), that is, three buckets each having roots, stem, and leaves separated. The ones obtained monthly for six months from the three buckets were fifty-four (54), that is, each month had each bucket yielding three samples from the roots, stem, and leaves. This gave a sub-total of sixty-three samples per set and considering the duplicate, the total number of samples for each EDC was one hundred and twenty-six (126).

To determine the concentration taken up by the plants, 1 g of each part of the plant (N = 126 for each EDC) was extracted using 50 mL of methanol. This was carried out by shaking the mixture in a shaker for 8 hours. Filtration was then carried out using 0.45 µm filter paper. Concentration was carried out using a rotary evaporator. Further clean-up was done using 0.45 µm nylon microfilters before analysis with HPLC-MS/MS.

CHAPTER FOUR

RESULTS AND DISCUSSION

4.1 Determination of concentration levels in WWTPs

4.1.1 Water quality parameters

Water quality parameters influence the sorption and degradation of organic pollutants thus determining their aqueous concentrations (K'Oreje et al., 2012). Mean water quality parameters (pH, TDS, COD, BOD_5, and EC) determined (in triplicate) *in situ* on the influent locations, are reported in **Table 4.1.**

Table 4.1: Water quality parameters of different sites during the sampling period

Site	pH	TDS (mg L^{-1})	BOD_5 (mg L^{-1})	COD (mg L^{-1})	EC (µS cm^{-1})
Nakuru	6.8	758.2	55.1	162.7	1532
Eldoret	6.8	759.5	54.9	163.6	1518
Bungoma	6.9	754.3	52.9	155.9	1513
Busia	7.0	749.4	52.4	154.5	1514
Kisii	6.8	756.1	53.3	158.1	1520
MMUST	6.8	755.6	51.8	154.2	1504
Ruai	6.7	764.8	59.5	172.0	1541
Shirere	6.8	756.4	53.7	161.3	1527
Kisat	6.7	760.5	57.6	165.4	1519
Nyalenda	6.7	762.3	55.4	167.6	1533
Kericho	7.0	753.2	53.3	159.1	1500
Kariobangi	6.7	765.7	58.5	170.8	1554

(TDS = total dissolved solids; COD = chemical oxygen demand; BOD_5 = biochemical oxygen demand and EC = electrical conductivity).

There was not much variation in the pH with the values ranging between 6.7 (Ruai) and 7.0 (Kericho). These values are comparable to those obtained by K'oreje et al. (2018) which ranged between 6.5 and 7.1. Lower pH values are reported in WWTPs serving larger populations (Ruai) implying that an increase in contamination increases acidity. WWTPs serving smaller and less industrious populations like Kericho displayed reduced pH. TDS was lowest in smaller WWTPs (749.4 mg L^{-1}-Busia) implying lesser solid deposition and highest in a larger WWTP (765.7 mg L^{-1}, Kariobangi) due to more solids being deposited in the plant, including those from soil erosion. BOD_5 followed the same trend with 51.8 mg L^{-1} in MMUST and 59.5 mg L^{-1} in Ruai indicating a lesser organic load in MMUST than in Ruai. TDS and BOD_5 are comparable to those reported by Shikuku et al. (2017). The lowest value of COD was in Busia (154.5 mg L^{-1}) while the highest was in Ruai (172.0 mg L^{-1}), indicative of increased contamination. The variance in EC was minimal (1500-1554 μS cm^{-1}). The East African standards for effluent discharge are COD = 50 mg L^{-1}; BOD_5 = 30 mg L^{-1}; pH = 6.5 – 8.5; TDS = 1200 mg L^{-1}; EC = 15000 μS cm^{-1} (K'oreje et al., 2018). The elevated values of COD and BOD_5 could be due to the impact of increased waste brought about by the increasing population, and commercial and industrial activities discharging enormous amounts of their wastes to the larger WWTPs, especially Ruai and Kariobangi. In smaller towns like Kericho, Kisii, Busia and Bungoma, there could be less sewerage connectivity with an increased number of households using latrines and septic tanks.

4.1.2 LOD and LOQ values

The LOD and LOQ for the target analytes are summarized in **Table 4.2**.

Table 4. 2: LOD and LOQ values

	DBP	DEHP	DMP	LNR	PGT
LOD (sludge & UDBS-ng g^{-1})	8.4	6.3	7.9	3.9	6.0
LOQ (Sludge and UDBS-ng g^{-1})	27.9	21.1	26.3	12.9	19.8
LOD (water samples-μg L^{-1})	0.03	0.03	0.004	0.003	0.003
LOQ (water samples-μg L^{-1})	0.1	0.1	0.01	0.01	0.01

PAEs showed high LODs in all the matrices ranging from 6.3 to 8.4 ng g^{-1} (sludge/UDBS) to 0.004 μg L^{-1} (wastewater) and LOQs ranging from 21.1 to 27.9 ng g^{-1} (sludge/UDBS). LNR had the least LOD (3.9 ng g^{-1} (sludge/UDBS); 0.003 μg L^{-1} (wastewater) and the LOQ was 12.9 ng g^{-1} (sludge/UDBS); 0.01 μg L^{-1} (wastewater).

4.1.3 Levels of EDCs in wastewater samples

The levels of the selected EDCs are represented in **Table 4.3** and **Appendix 8**. In the influents, DBP was the most abundant PAE congener (37.5%) as well as EDC detected in the 12 WWTPs (∑12WWTPs) ranging from 4.3 ± 0.6 μg L^{-1} in Bungoma to 19.7 ± 1.2 μg L^{-1} in Ruai. DEHP was the second most abundant EDC (26.2%) with levels ranging from 2.7 ± 0.2 μg L^{-1} in Nakuru to 14.3 ± 1.5 μg L^{-1} in Kariobangi. Levels of DMP in the influents were between 1.1 ± 0.3 μg L^{-1} in Shirere to 15.9 ± 1.4 μg L^{-1} in Nakuru, contributing 19.6%. PGT (15.7%) ranged from 0.9 ± 0.2 μg L^{-1} in Nakuru to 14.7 ± 1.1 μg L^{-1} in Ruai. LNR ranged between 0.05 ± 0.01 μg L^{-1} in Nyalenda to 2.5 ± 0.6 μg L^{-1} in Eldoret giving a 1.0% of the ∑12WWTPs. The total means ± standard deviations (SD) (μg L^{-1}) of the EDCs in all the influents were as follows: DBP = 10.1 ± 5.0; DEHP = 7.1 ± 3.0; DMP = 5.3 ± 4.2; PGT = 4.2 ± 6.3 and LNR = 0.3 ± 0.7.

Table 4.3: Levels of EDCs (µg L^{-1}) in the wastewater samples

	Location	DBP	DEHP	DMP	LNR	PGT
Nakuru	Influent	8.3 ± 1.0	2.9 ± 0.2	15.9 ± 1.4	0.1 ± 0.02	0.9 ± 0.2
	Primary ponds	6.8 ± 0.8	1.8 ± 0.1	1.0 ± 0.1	0.04 ± 0.01	0.8 ± 0.2
	Secondary ponds	5.0 ± 0.4	1.0 ± 0.04	1.1 ± 0.1	0.03 ± 0.01	0.6 ± 0.2
	Tertiary ponds	2.1 ± 0.3	0.2 ± 0.1	0.2 ± 0.1	0.02 ± 0.01	0.5 ± 0.2
	Effluent	1.6 ± 0.3	< LOQ	0.02 ± 0.01	0.02 ± 0.01	0.3 ± 0.2
Eldoret	Influent	10.5 ± 0.8	6.9 ± 1.1	7.5 ± 0.7	2.5 ± 0.6	20.3 ± 1.5
	Primary ponds	7.2 ± 0.9	6.1 ± 1.0	5.2 ± 0.4	1.0 ± 0.01	11.5 ± 1.0
	Secondary ponds	7.1 ± 0.8	5.8 ± 0.6	1.9 ± 0.2	0.1 ± 0.01	3.1 ± 0.4
	Tertiary ponds	3.8 ± 0.5	2.2 ± 0.34	1.6 ± 0.2	0.02 ± 0.01	1.8 ± 0.1
	Effluent	2.5 ± 0.5	1.8 ± 0.2	0.2 ± 0.1	0.02 ± 0.01	1.3 ± 0.2
Bungoma	Influent	4.6 ± 0.6	7.0 ± 1.0	8.4 ± 1.0	0.1 ± 0.01	1.0 ± 0.1
	Anaerobic ponds	4.4 ± 0.5	6.4 ± 0.8	2.8 ± 0.4	0.04 ± 0.01	0.6 ± 0.1
	Facultative ponds	4.1 ± 0.5	2.4 ± 0.1	2.6 ± 0.4	0.03 ± 0.01	0.4 ± 0.1
	Maturation ponds	3.4 ± 0.6	< LOQ	0.1 ± 0.01	0.03 ± 0.01	0.3 ± 0.1
	Effluent	2.6 ± 0.4	< LOQ	0.1 ± 0.02	0.02 ± 0.01	0.3 ± 0.1
Busia	Influent	5.5 ± 0.5	6.7 ± 1.1	3.7 ± 0.7	0.1 ± 0.01	2.2 ± 0.3
	Anaerobic ponds	3.7 ± 0.6	2.7 ± 0.7	3.1 ± 0.6	0.1 ± 0.01	1.8 ± 0.1
	Facultative ponds	3.5 ± 0.3	2.1 ± 0.4	1.8 ± 0.4	0.04 ± 0.01	1.7 ± 0.3
	Maturation ponds	2.1 ± 0.2	2.0 ± 0.3	< LOQ	0.03 ± 0.01	0.4 ± 0.03
	Effluent	1.9 ± 0.2	1.6 ± 0.4	0.03 ± 0.01	0.03 ± 0.01	0.4 ± 0.04
Kisii	Influent	13.6 ± 1.2	4.6 ± 0.6	1.4 ± 0.3	0.1 ± 0.01	0.9 ± 0.1
	Anaerobic ponds	1.9 ± 0.3	4.1 ± 0.5	0.2 ± 0.02	0.04 ± 0.01	0.8 ± 0.1
	Facultative ponds	1.1 ± 0.2	2.4 ± 0.3	0.03 ± 0.01	0.04 ± 0.01	0.5 ± 0.1
	Maturation ponds	< LOQ	1.0 ± 0.2	0.02 ± 0.01	0.03 ± 0.01	0.2 ± 0.1
	Effluent	< LOQ	0.8 ± 0.2	0.02 ± 0.01	0.02 ± 0.01	0.1 ± 0.04
MMUST	Influent	5.8 ± 0.9	8.0 ± 1.0	2.0 ± 0.4	0.06 ± 0.01	1.3 ± 0.3
	Anaerobic ponds	7.3 ± 0.6	3.5 ± 0.7	0.3 ± 0.1	0.05 ± 0.01	0.8 ± 0.1
	Facultative ponds	6.1 ± 0.6	1.7 ± 0.7	0.04 ± 0.01	0.03 ± 0.01	0.6 ± 0.2
	Maturation ponds	4.6 ± 0.5	1.3 ± 0.4	0.02 ± 0.01	0.03 ± 0.01	0.4 ± 0.03
	Effluent	4.8 ± 0.5	< LOQ	0.02 ± 0.01	0.03 ± 0.01	0.4 ± 0.02
Ruai	Influent	19.7 ± 1.2	9.2 ± 0.9	4.4 ± 1.2	0.1 ± 0.01	14.7 ± 1.1
	Anaerobic ponds	17.3 ±1.0	9.1 ± 0.8	4.8 ± 1.1	0.1 ± 0.01	1.3 ± 0.2
	Facultative ponds	13.7 ± 0.8	2.9 ± 0.3	4.6 ± 1.0	0.1 ± 0.01	1.1 ± 0.1
	Maturation ponds	10.5 ± 0.9	2.7 ± 0.3	2.3 ± 0.7	0.1 ± 0.01	1.0 ± 0.04
	Effluent	4.7 ± 0.6	2.0 ± 0.1	0.1 ± 0.1	0.1 ± 0.01	0.9 ± 0.10
Shirere	Influent	7.9 ± 1.0	5.6 ± 0.8	1.1 ± 0.3	0.1 ± 0.1	2.1 ± 0.21
	Anaerobic ponds	7.5 ± 0.9	3.7 ± 0.5	0.7 ± 0.2	0.1 ± 0.01	1.4 ± 0.33

	Location	DBP	DEHP	DMP	LNR	PGT
	Facultative ponds	4.6 ± 0.6	1.1 ± 0.3	0.1 ± 0.01	0.1 ± 0.01	0.2 ± 0.05
	Maturation ponds	< LOQ	< LOQ	0.04 ± 0.01	0.03 ± 0.01	0.02 ± 0.01
	Effluent	< LOQ	< LOQ	0.02 ± 0.01	0.02 ± 0.01	0.01 ± 0.01
Kisat	Influent	5.6 ± 0.9	4.2 ± 0.8	5.0 ±1.0	0.1 ± 0.03	0.9 ± 0.1
	Primary ponds	3.5 ± 0.5	4.2 ± 0.7	0.1 ± 0.01	0.02 ± 0.01	0.3 ± 0.1
	Secondary ponds	0.9 ± 0.1	3.8 ± 0.5	0.04 ± 0.01	0.03 ± 0.01	0.1 ± 0.01
	Tertiary ponds	0.8 ±0.1	0.8 ± 0.1	0.02 ± 0.01	0.02 ± 0.01	0.02 ± 0.01
	Effluent	< LOQ	< LOQ	0.01 ± 0.01	0.02 ± 0.01	0.01 ± 0.01
Nyalenda	Influent	11.2 ± 1.0	6.6 ± 1.0	1.7 ± 0.5	0.1 ± 0.01	2.7 ± 0.4
	Anaerobic ponds	3.8 ± 0.3	3.7 ± 0.4	1.3 ± 0.4	0.03 ± 0.01	0.5 ± 0.1
	Facultative ponds	6.5 ± 0.6	2.1 ± 0.2	0.3 ± 0.03	0.03 ± 0.01	0.4 ± 0.1
	Maturation ponds	3.7 ± 0.5	< LOQ	0.12 ± 0.1	0.03 ± 0.01	0.2 ± 0.1
	Effluent	3.6 ± 0.6	< LOQ	0.1 ± 0.01	0.02 ± 0.01	0.1 ± 0.1
Kericho	Influent	10.1 ± 1.0	8.9 ± 1.1	5.1 ± 0.9	0.1± 0.02	2.2 ± 0.3
	Primary ponds	5.7 ± 0.9	6.8 ± 0.8	1.3 ± 0.4	0.1 ± 0.02	1.7 ± 0.4
	Secondary ponds	4.2 ± 0.7	3.9 ± 0.6	0.1 ± 0.01	0.1 ± 0.02	1.1 ± 0.2
	Tertiary ponds	4.1 ± 0.4	0.8 ± 0.1	0.02 ± 0.01	0.03 ± 0.01	0.7 ± 0.2
	Effluent	< LOQ	0.6 ± 0.1	0.01 ± 0.01	0.02 ± 0.01	0.1 ± 0.01
Kariobangi	Influent	18.5 ± 1.1	14.3 ± 1.5	7.1 ± 0.7	0.1 ± 0.02	1.8 ± 0.2
	Primary ponds	11.1 ± 1.0	1.3 ± 0.3	4.8 ± 0.5	0.04 ± 0.01	1.1 ± 0.2
	Secondary ponds	9.4 ± 0.8	1.3 ± 0.1	4.6 ± 0.4	0.04 ± 0.01	1.9 ± 0.1
	Tertiary ponds	7.1 ± 0.5	1.4 ± 0.2	3.1 ± 0.2	0.02 ± 0.01	0.8 ± 0.1
	Effluent	3.4 ± 0.3	0.7 ± 0.1	0.1 ± 0.01	0.02 ± 0.01	0.6 ± 0.1

(DBP = dibutyl phthalate, DEHP = diethylhexyl phthalate, DMP = dimethyl phthalate, LNR = linuron and PGT = progesterone). Values represent means ± standard deviation; n=3.

From **Table 4.3**, it is observed that Nakuru and MMUST had all the sampled points containing quantifiable levels of EDCs except DEHP which was below LOQ in the effluent wastewater. Almost a similar scenario was observed in Bungoma, Shirere, and Nyalenda where DEHP was not quantifiable in the maturation ponds and the effluents but all other EDCs were measurable. In Kisat however, DEHP and DBP were below LOQ in the effluent ponds while in Kericho, DBP was not quantifiable in the effluent. In Kisii,

DBP was not quantified in both the maturation pond and effluent while in Busia, it was DMP that was not quantified in the effluent. Eldoret, Ruai, and Kariobangi had all the sampled points containing the targeted EDCs. The lower LOQ values of DMP and DBP in some maturation ponds and effluents could be attributed to photodegradation and sorption to sludge. The lower than LOQ levels of DEHP in most effluents and some maturation ponds could be attributed to its high log K_{OW} (**Table 1.1**) making it more likely to adsorb to the majorly organic sludge and thus being less likely detected in the wastewater of the effluents and maturation ponds.

There were significant spatial variations ($p < 0.05$; Friedman) in the levels of EDCs detected in the influent wastewater samples at different sites. For example, high levels of EDCs were detected in Ruai (Total sum of five EDCs per site, $\sum$5EDCs = 48.0 μg L^{-1}) while lower levels were detected at Kisat ($\sum$5EDCs = 15.9 μg L^{-1}). Therefore, EDCs loading to the WWTP was a function of the location (industrial activities, population density, agricultural activities, etc.), the maintenance of the wastewater treatment system, and connectivity to the sewer line. Elevated levels of PAEs were noted in Kariobangi and Ruai influents which are both located in Nairobi, a city with dense human habitation, and a wide array of commercial, industrial, and manufacturing activities. There is also a paucity of stringent measures of waste disposal, a case in point being that of Dandora open dumpsite. Kisat is in Kisumu, a city with lower levels of EDCs regardless of a medium population. This could be attributed to better waste management by the county, which in recent years has invested in getting rid of open dumpsites. The other locations (Busia, Kisii, Kericho, etc.) registering less concentration have lower populations and lesser

industrial, commercial, and manufacturing activities. Additionally, decreased sewerage connectivity with some households using septic tanks and pit latrines is another factor.

The levels of EDCs in the influent water samples (**Figure 4.1 (a)**) were significantly higher than those in the effluents (**Figure 4.1 (b)** ($p < 0.05$; Kruskal-Walis)). Generally, the levels kept reducing at the different ponds as the wastewater moved towards the effluent within each WWTP. The higher concentrations in the influents than the effluents are because they are entry points to the WWTPs. Further, the target EDCs have a high Log K_{OW} (**Table 1.1**) implying that they are more likely to adsorb onto the sludge consequently giving less detection in the effluents.

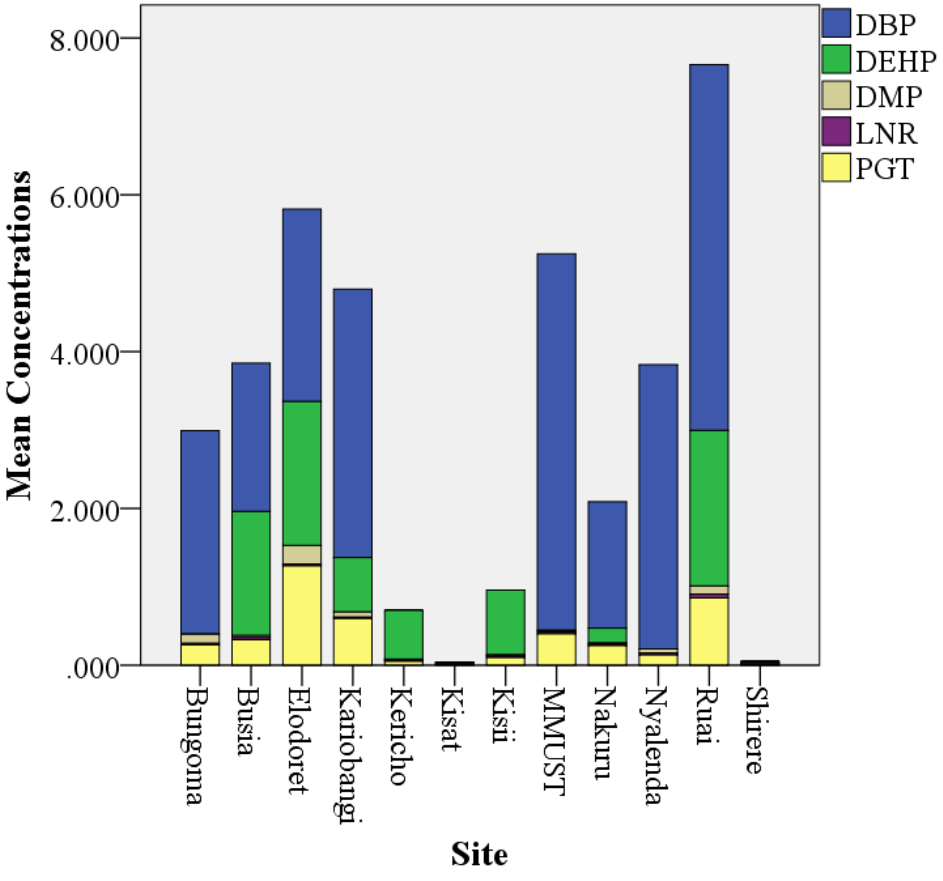

Figure 4.1(a): Levels of EDCs at the influents.

The effluents are a concern since they are point sources of pollutants to receiving waters that act as habitats for aquatic organisms and may find their way into drinking water, especially in emerging economies. In the effluents, EDCs were dominated by DBP (65.9%), followed by DEPH (20.3%), PGT (11.2%), DMP (1.8%), and LNR (0.7%). The levels of DBP, DEHP, PGT, DMP, and LNR (in μg L^{-1}) were between < LOQ - 4.8 ± 0.5, < LOQ – 2.0 ± 0.1, 0.01 ± 0.01 - 1.3 ± 0.2, 0.01 ± 0.01-0.2 ± 0.1, and 0.02 ± 0.01 -0.1 ± 0.01, respectively. The means ± SD of the EDCs in the effluents were as follows: DBP = 2.01 ± 1.8; DEHP = 0.6 ± 0.8; DMP = 0.1 ± 0.1; PGT = 0.4 ± 0.4 and LNR = 0.02 ± 0.01. The standard deviations are larger for some EDCs because the data values are more spread out from the mean.

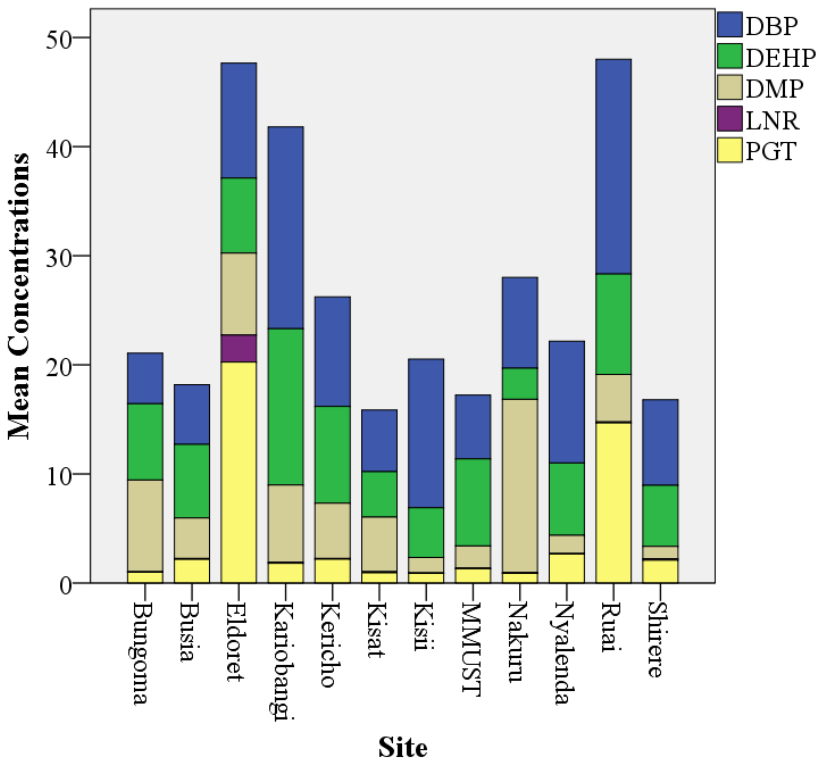

Figure 4.1 (b): Levels of EDCs at effluents.

As noted, some maturation ponds and effluents had less concentration than the LOQ. This can be ascribed to EDCs' adsorption to the sludge that is eventually dried and used as UDBS. The adsorption could be due to the hydrophobicity of the EDCs due to their high log K_{OW}. A general rule used to frequently predict the sorption capacity of micro-pollutants on solids is: log $K_{OW} < 2.5$ indicates low sorption potential, $2.5 <$ log $K_{OW} < 4$ indicates medium sorption potential and log $K_{OW} > 4$ indicates high sorption potential (Orata, 2018). The levels of EDCs in the effluent samples displayed no significant differences ($p > 0.05$; Kruskal-Walis) suggesting that the WWTPs have comparable efficiency, regardless of the concentration, in reducing the EDCs in wastewater.

For both influents and effluents, PAEs had higher concentrations than PGT and LNR. This is attributed to the PAEs' widespread use in industry and within households, as additives in plastic containers and pipes. PAEs are also not chemically bonded to plastics (Cong et al., 2022) and are leached out of plastic packaging and containers (Metcalfe et al., 2022) into the environment. Plastic manufacturing is a major investment in Kenya estimated at USD 50 million as of the year 2013 (Nyagah, 2013) and the latest data is unavailable though it is projected to be higher. However, there is poor plastic waste disposal potentially exposing environmental compartments to EDCs. This is noted in the presence of DEHP, DMP, and DBP in the nine towns studied.

It is noteworthy that PGT's mean for all sites was detected at higher levels than LNR. As of October 2021, Volza Grow Global (2021) indicated that Kenya had a yearly import of 211 shipments of PGT either from South Africa, Germany, or India. On the contrary, LNR levels were high in agricultural areas (Eldoret and Kericho). This is attributed to extensive farming activities (wheat, maize, and tea) in the locations where LNR is used for weed

control. Rain runoffs from farmlands, atmospheric deposition during aerial sprays, and wastewater effluents are significant sources of LNR in the ecosystem which has been found to disrupt thyroid, androgen, and estrogen signaling in human beings (Spirhanzlova et al., 2017).

The levels of EDCs in wastewater in this study were higher than those reported in the study by Onchiri et al. (2021) which recorded influent mean levels of DMP in Kisumu, Homabay, and Kisii of 0.1 and 0.08 μg L^{-1} during the wet and dry seasons, respectively. The lower values in the aforementioned study can be attributed to few sampling areas and less populous towns. In South Africa, Salaudeen et al. (2018) reported higher DBP influent ranges (2.7 and 2488.0 μg L^{-1}) and effluent (4.9 – 8.9 μg L^{-1}) than our study in three WWTPs in Eastern Cape. Kenya banned plastic bag packaging in February 2017, and this could explain the lower ranges in addition to Kenya being less populous and industrialized. The same can be said of Nigeria since Adeogun et al. (2015) reported much higher concentrations of DBP and DEHP concentrations in water at the Lagos lagoon at 130 ± 4 and 180 ± 10 μg L^{-1}, respectively. Weizel et al. (2018) detected much lower values of PGT in the range of 0.0003 – 0.001 μg L^{-1} in the municipal waters of Germany. Šauer et al. (2018) recorded progestogenic activities in all effluents ranging from 0.00006 to 0.0005 μg L^{-1} indicating the presence of PGT in the municipal waters of the Czech and Slovak Republic. Appa et al. (2018) found the range of PGT to be 0.02– 0.20 μg L^{-1} in treated and non-treated sewage water in Central India. Khazri et al. (2022) investigated the presence of LNR in the Bizerte wastewater, Tunisia, and reported a mean value of 3.94 μg L^{-1} (**Table 4.4**).

Table 4.4: Concentrations of EDCs in wastewater, sludge, and UDBS in other studies

Compound	Region	Environmental matrix	Concentration	Reference(s)
DBP	South Africa (Eastern Cape)	Wastewater	2.7-2488.0 μg L^{-1} influent ranges; and 4.9–8.9 μg L^{-1} effluent ranges	Salaudeen et al. (2018)
	Nigeria (Lagos)	Wastewater	130.0 ± 4.0 μg L^{-1}	Adeogun et al. (2015)
	China	Sludge	957.0 ng g^{-1}	Zhu et al. (2019)
	Nigeria (Epe)	Sludge	0.2 ± 0.01 mg g^{-1}	Adeogun et al. (2015)
	Kenya	Wastewater	10.1± 5.0 μg L^{-1} (influent); 2.01 ± 1.8 μg L^{-1} (effluent)	This study
		Sludge	1498.6 ± 993.0 ng g^{-1}	
		UDBS	656.1 ± 724. 3 ng g^{-1}	
DEHP	Nigeria (Lagos)	Wastewater	180.0 ± 10.0 μg L^{-1}	Adeogun et al. (2015)
	China	Sludge	14700.0 ng g^{-1}	Zhu et al. (2019)
	Taiwan	Sludge	1569.0 ng g^{-1}- 35670.0 ng g^{-1} dw	Dong et al. (2020)
	Nigeria (Epe)	Sludge	0.3 ± 0.02 mg g^{-1}	Adeogun et al. (2015)
	Kenya	Wastewater	7.1 ± 3.0 μg L^{-1} (influent); 0.6 ± 0.8 μg L^{-1} (effluent)	This study
		Sludge	3181.2 ± 2772.9 ng g^{-1}	
		UDBS	1153.1 ± 1159.9 ng g^{-1}	

Compound	Region	Environmental matrix	Concentration	Reference(s)
DMP	Kenya	Wastewater	0.1 and 0.08 μg L^{-1} (wet and dry seasons, respectively)	Onchiri et al. (2021)
	China	Sludge	195.0 ng g^{-1}	
	Kenya	Wastewater	5.3 ± 4.2 μg L^{-1} (influent); 0.1 ± 0.1 μg L^{-1} (effluent)	Zhu et al. (2019)
		Sludge	991.6 ± 424.9 ng g^{-1}	This study
		UDBS	474.4 ± 398.0 ng g^{-1}	
LNR	Tunisia (Bizerte)	Wastewater	3.9 μg L^{-1}	Khazri et al. (2022)
	Kenya	Wastewater	0.3 ± 0.7 μg L^{-1} (influent); 0.02 ± 0.01 μg L^{-1} (effluent)	This study
		Sludge	65.1 ± 29.1 ng g^{-1}	
		UDBS	42.2 ± 23.5 ng g^{-1}	
PGT	Germany	Municipal waters	0.0003-0.0013 μg L^{-1}	Weizel et al. (2018)
	Czech and Slovak Republic	Municipal waters	0.00006 to 0.0005 μg L^{-1}	Šauer et al. (2018)
	Central India	Sewage water	0.02– 0.20 μg L^{-1}	Appa et al. (2018)
	Kenya	Wastewater	4.2 ± 6.3 μg L^{-1} (influent); 0.4 ± 0.4 μg L^{-1} (effluent)	This study
		Sludge	865.6 ± 265.8 ng g^{-1}	
		UDBS	556.7 ± 290.4 ng g^{-1}	

4.1.4 Levels of EDCs in sludge samples

All the sludge samples collected had quantifiable levels of EDCs and the spatial distribution is represented in **Figure 4.2** and further illustrated in **Figure 4.3**.

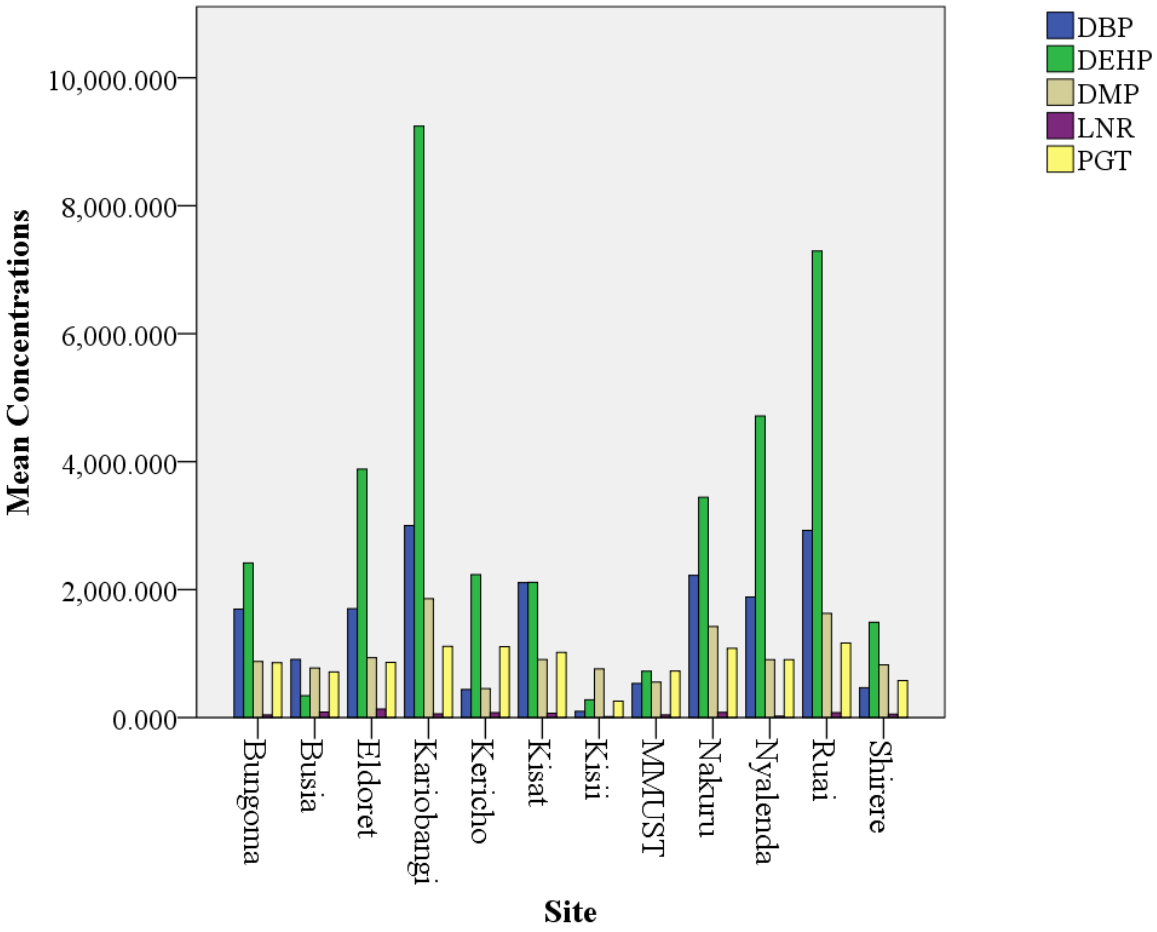

Figure 4.2: Bar graph depicting the spatial distribution of EDCs in sludge samples.

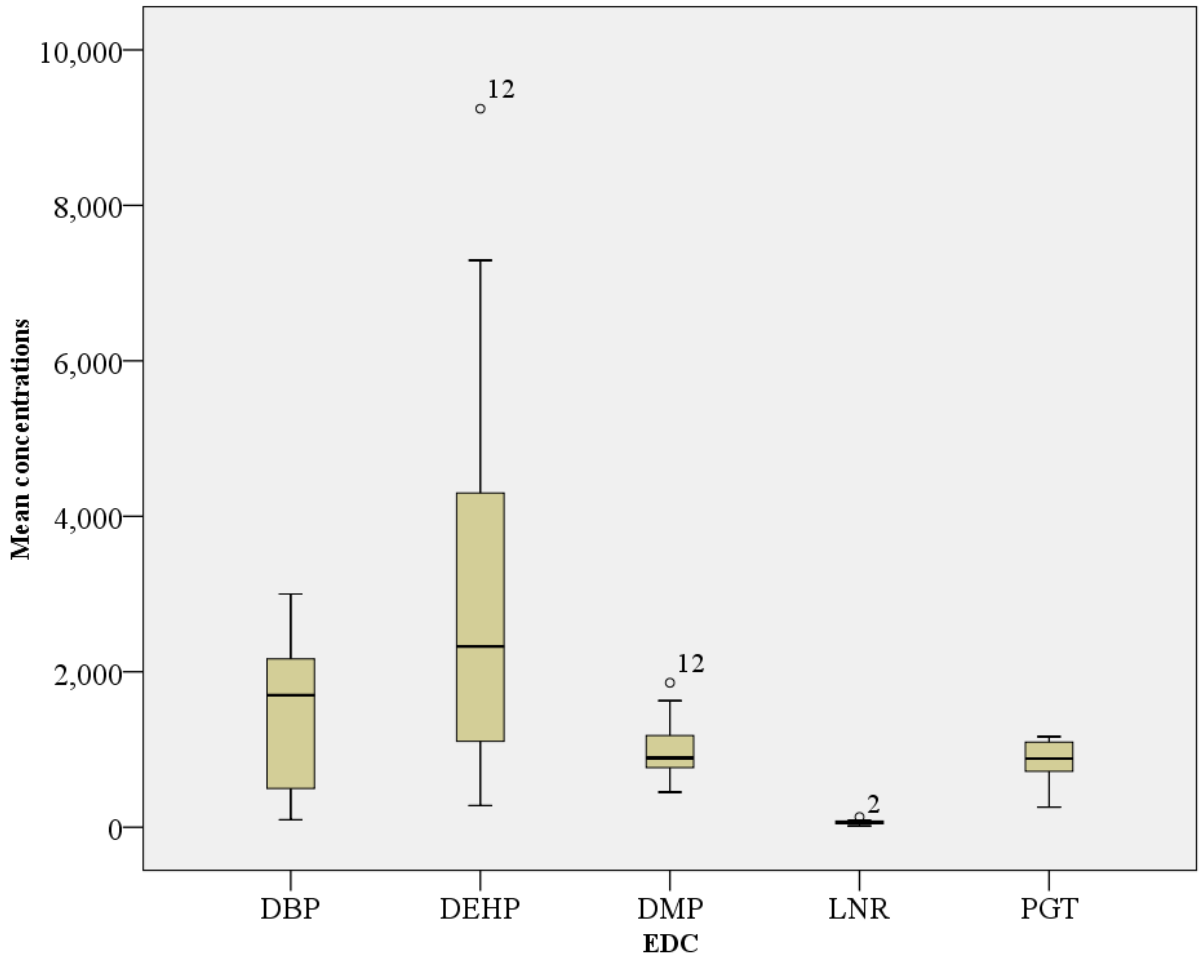

Figure 4.3: Box plots for EDCs in sludge (The small circles represent sites with high concentrations of EDCs).

DEHP was the most abundant and accounted for 48.2% of the sum of the pollutants detected in the sludge. It ranged between 278.7 ng g^{-1} dw in Kisii to 9243.5 ng g^{-1} dw in Kariobangi. This was followed by DBP (22.7%), with ranges of 97.1 ng g^{-1} dw in Kisii to 3000.0 ng g^{-1} dw in Kariobangi. DMP contributed 15.0% with ranges between 452.5 ng g^{-1} dw in Kericho to 1858.5 ng g^{-1} dw in Kariobangi. PGT represented 13.1% with ranges between 257.4 ng g^{-1} dw in Kisii to 1165.5 ng g^{-1} dw in Ruai. LNR was the least recorded

representing 0.99% with ranges of 18.5 ng g^{-1} dw in MMUST to 132.7 ng g^{-1} dw in Eldoret. The means ± SD of the EDCs in the sludge are given in **Table 4.5.**

Table 4.5: Descriptives for sludge samples

Compound	% Frequency	Min	Max	Median	Mean ± SD
DBP	100	97.1	3000.0	1699.0	1498.6 ± 993.0
DEHP	100	278.7	9243.5	2325.1	3181.2 ± 2772.9
DMP	100	452.5	1858.5	890.6	991.6 ± 424.9
LNR	100	18.5	132.7	62.8	65.1 ± 29.1
PGT	100	257.4	1165.5	882.9	865.6 ± 265.8

These values displayed significant differences ($p < 0.05$; ANOVA) among the EDCs. The high concentrations of the PAEs in sludge samples as compared to PGT and LNR, reflect increased plastic use (toys, water pipes, smart screens, packaging films, etc.). Furthermore, it is noted that DEHP concentrations were higher than DMP and DBP. This can be explained by the fact that DMP and DBP are classified as low-molecular-weight PAEs used in the production of packaging bags, finishing materials, personal care products, and insecticides. Plastic packaging bags were banned in Kenya, and this could explain the lower concentrations of DBP and DMP. Conversely, DEHP is a high-molecular-weight PAE used for the manufacturing of vinyl-based products, toys, construction materials, polyethylene terephthalate bottles, food packages, medical devices (bags and tubing used for blood transfusion, kidney dialysis or dosing antibiotics intravenously) (Cong et al., 2022; Zhu et al., 2019). All these products of DEHP are still in use in Kenya but are poorly disposed off. Additionally, from **Table 1.1**, it is noted that

DEHP has a lower water solubility and a higher log K_{OW} than other PAEs implying that it partitions more to the sludge and is more resistant to biodegradation.

Kariobangi and Ruai sludge, both in Nairobi, recorded higher concentrations in most EDCs except LNR than the rest of the sampled WWTPs. This can be attributed to the two WWTPs receiving domestic and industrial wastewater from the populous city, which is highly industrialized, and urbanized with a dense population. It is also often contaminated by runoff and stormwater drainages, open landfills, agricultural practices, and pesticide use. The highest concentration of LNR was observed in Eldoret, an agricultural area with large-scale pesticide-intensive wheat and maize farming.

The ∑5EDCs in sludge (μg g^{-1} dry weight (dw)), decreased in the following order: Kariobangi (15.3) > Ruai (13.1) > Nyalenda (8.5) > Nakuru (8.2) > Eldoret (7.5) > Kisat (6.2) > Bungoma (5.9) > Kericho (4.3) > Shirere (3.4) > Busia (2.8) > MMUST (2.6) > Kisii (1.5). The order depicts the effect of urbanization, population density, and industrialization of the city where the WWTP is located. For instance, Kariobangi and Ruai recorded higher concentrations in the ∑5EDCs reflecting the fact that the two WWTPs are in a populous city, Nairobi. Conversely, the lesser urbanized regions like Shirere (Kakamega), Busia, and Kisii had low levels of EDCs, mirroring their low populations and less industrialization. The low levels can also be associated with poor sewerage connectivity in some towns (Kenya Population Census, 2019).

The levels of EDCs in sludge in the present study were compared to those reported elsewhere (**Table 4.4**). In China, Zhu et al. (2019) reported an abundance of DEHP congener in sludge samples which is consistent with the current study. In their study, PAEs were detected in the same order (DEHP > DBP > DMP). However, the mean

concentrations of DEHP (14700 ng g^{-1}) were higher than that observed in our study while DBP and DMP were detected at lower levels (means of 957.0 and 195.0 ng g^{-1} respectively). This could be attributed to less use of low molecular weight plastics and better waste management. Dong et al. (2020) also confirmed the ubiquity of DEHP in their study that found out that 99% of the PAEs found in the sludge of some WWTPs in Taiwan were DEHP with ranges between 1569.0 ng g^{-1} and 35670.0 ng g^{-1} dw. More literature searches, however, yielded studies on other environmental matrices like sediment samples. For example, in Nigeria, Adeogun et al. (2015) reported much higher concentrations in sediments in Epe lagoon (DBP and DEHP were 0.2 ± 0.01 mg g^{-1} and 0.3 ± 0.02 mg g^{-1}, respectively). Additionally, Cong et al. (2022) also noted that DEHP had slightly higher concentrations with a mean of 4594.0 ng g^{-1} dw from sediment samples obtained from the Eastern Indian Ocean.

4.1.5 Levels of EDCs in UDBS samples

All the UDBS samples collected from the different locations had quantifiable levels of the EDCs (**Figure 4.4** and **Figure 4.5)**. DEHP was the most abundant (40%) of the total EDCs detected with levels ranging from 78.8 ng g^{-1} dw in Kisii to 3938.5 ng g^{-1} dw in Kariobangi. This was followed by DBP (22.8%) with levels ranging from 69.4 ng g^{-1} dw in Kisii to 2320.5 ng g^{-1} dw in Kariobangi. PGT represented 19.3% with its levels ranging from 167.0 ng g^{-1} dw in Shirere to 984.6 ng g^{-1} dw in Ruai. DMP represented 16.5% with its levels ranging from 57.8 ng g^{-1} dw in Kericho to 1084.9 ng g^{-1} dw in Kariobangi. LNR had the lowest levels (1.5%) with levels ranging from 13.5 ng g^{-1} dw in Kisat to 88.8 ng g^{-1} dw in Eldoret.

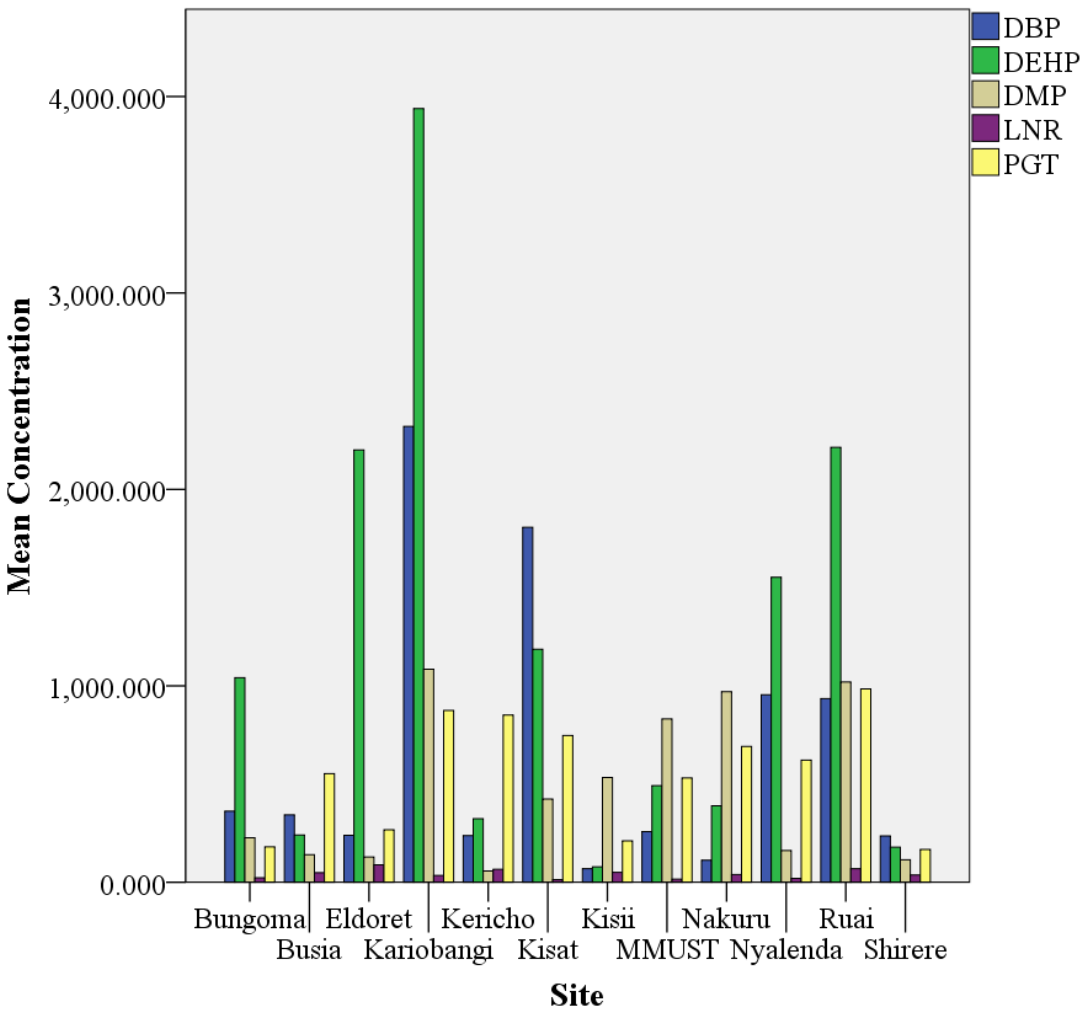

Figure 4.4: The spatial variations in the levels of EDCs in ng g^{-1} in UDBS samples.

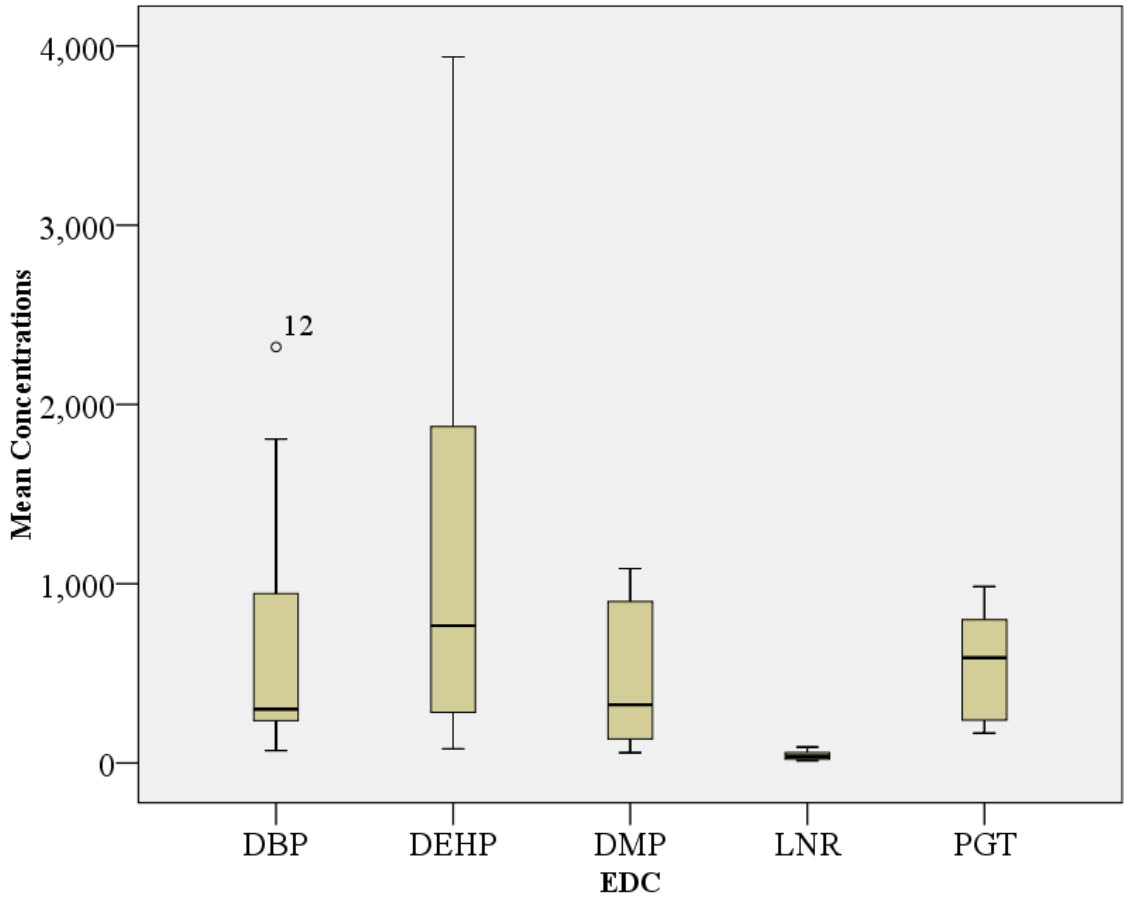

Figure 4.5: Box plots for EDCs in UDBS (The small circle represents sites with high concentrations of EDCs).

The means ± SD of the EDCs in the UDBS are given in **Table 4.6.**

Table 4.6: Descriptives for UDBS samples

Compound	%Frequency	Min	Max	Median	Mean ±SD
DBP	100	69.4	2320.5	300.5	656.1 ± 724. 3
DEHP	100	78.8	3938.5	766.6	1153.1 ± 1159.9
DMP	100	57.8	1084.9	325.1	474.4 ± 398.0
LNR	100	13.5	88.8	38.0	42.2 ± 23.5
PGT	100	167.0	984.6	587.6	556.7 ± 290.4

The data displayed significant differences ($p < 0.05$; Kruskal-Wallis) between the EDCs in the different sites sampled. The high levels of the PAEs, especially in the more urbanized Nairobi city are consistent with their use, effluent release from plastic manufacturing industries, and less stringent measures in their disposal. DEHP concentration is much higher than DMP and DBP due to its use in a wide array of plastic consumer products. PGT, from medical facilities, was higher in UDBS samples than DMP implying less biodegradation capacity and stronger sorption capacity in the WWTPs. LNR had elevated concentrations in areas with high-intensity agricultural activities, e.g., Eldoret.

There was decrease in the total concentration of EDCs (∑5EDCs) in UDBS samples in the following order (μg g^{-1} dw): Kariobangi (8.3) > Ruai (5.2 > Kisat (4.2) > Nyalenda (3.3) > Eldoret (2.9) > Nakuru (2.2) > MMUST (2.1) > Bungoma (1.8) > Kericho (1.5) > Busia (1.3) > Kisii (0.9) > Shirere (0.7). The arrangement illustrates the impact of population density, urbanization, and industry on the city housing the WWTP. For example, Kariobangi and Ruai showed greater concentrations in the ∑5EDCs, which is consistent with the two WWTPs being located in Nairobi, a populated city. On the other hand, lower levels of EDCs were found in less urbanized areas like Kericho, Busia, Kisii and Shirere (Kakamega), which is consistent with their lower population and less industrialization. In some towns, poor sewerage connectivity, with more homes using latrines and septic tanks, may also be linked to the low levels. Nationwide research related to EDCs in UDBS may help to determine the quality of UDBS in land application consequently supplementing the data concerning human exposure to EDCs.

The literature survey did not yield studies that reported on the concentration levels of EDCs in the UDBS from the drier beds of WWTPs. However, some studies have reported PAEs in soil and street dust. For example, Škrbić et al. (2016) analyzed soils and dust from Novi Sad, Serbia, and found the ranges to be from 0.2 ng g^{-1} dw to 4820 ng g^{-1} dw, with the highest level being DEHP, which was the most dominant (70 – 96%). The presence of these EDCs in UDBS is of great concern since they are used as fertilizers causing potential toxicological risks to terrestrial life.

4.1.6 Association between sludge, UDBS, and wastewater

There was a positive correlation between the concentrations of EDCs in the influents and sludge (**Table 4.7**).

Table 4.7: Paired Samples Correlations between influents and sludge

		N	Correlation	Sig.
Pair 1	DBP_s & DBP_i	12	.48	.12
Pair 2	$DEHP_s$ & $DEHP_i$	12	.67	.02
Pair 3	DMP_s & DMP_i	12	.46	.14
Pair 4	LNR_s & LNR_i	12	.73	.007
Pair 5	PGT_s & PGT_i	12	.22	.49

(Subscript s = sludge; i = influent).

However, the levels of EDCs in some influent wastewaters were significantly lower ($p < 0.05$; ANOVA) than those observed in sludge with DEHP being ubiquitous in bio-solids. From **Table 4.7**, there is no correlation between PGT_s and PGT_i while there are low correlations between DBP_s and DBP_i, DMP_s and DMP_i. However, there are moderate correlations between $DEHP_s$ and $DEHP_i$ and LNR_s and LNR_i. This could be attributed to the accumulation of the pollutants over time in the receiving ponds, atmospheric

deposition and surface runoffs, and storm waters from neighboring farmlands and polluted sites thus increasing the concentrations in sludge and therefore displaying minimal correlations (Kumar et al., 2020).

The UDBS, however, had considerably lower concentrations relative to those in the sludge. The UDBS from the drier beds also had higher concentrations than the effluents. This suggests that EDCs partition more to the sludge than to the water. This is also confirmed through Spearman's Rank order correlation coefficient. Correlation coefficients run between -1 and 1 where positive correlation is used to describe when two variables move in the same direction. A negative correlation is when one variable moves positively while a second variable moves in the opposite direction. When the correlation coefficient range is between 0.0 and 0.25, there is no correlation; when the correlation coefficient range is between 0.25 and 0.50, there is a low degree of correlation; when the correlation coefficient range is between 0.50 and 0.75, there is moderate correlation; when the correlation coefficient range is above 0.75, there is a high degree of correlation. In this study, it was noted that there were positive correlations between the EDCs' concentration levels and the TDS, COD, $BOD_{5,}$ and EC (**Table 4.8**). This can be attributed to their low water solubility and high log K_{OW} hence stronger sorption and lower degradation capacity (Cong et al., 2022; Mukherjee et al., 2021). Therefore, sludge is a sink to the EDCs, which are then consequently used as fertilizer in the form of UDBS, posing a risk in agricultural farmlands.

Table 4.8: Correlations between the Influents and the water quality parameters

			pH	TDS (mg L^{-1})	BOD5 (mg L^{-1})	COD (mg L^{-1})	EC (µS cm^{-1})	DBP	DEHP	DMP	LNR	PGT
Spearman's rho	pH	Correlation Coefficient	1.0	-.96**	-.90**	-.87**	-.86**	-.53	-.03	-.05	-.44	-.09
		Sig. (2-tailed)	.	.00	.00	.00	.00	.08	.92	.87	.16	.79
		N	12	12	12	12	12	12	12	12	12	12
	TDS (mg L^{-1})	Correlation Coefficient	-.96**	1.0	.92**	.92**	.88**	.66*	.10	.07	.43	.18
		Sig. (2-tailed)	.00	.	.00	.00	.00	.02	.76	.83	.17	.57
		N	12	12	12	12	12	12	12	12	12	12
	BOD5 (mg L^{-1})	Correlation Coefficient	-.90**	.92**	1.00	.98**	.86**	.63*	.05	.18	.49	.19
		Sig. (2-tailed)	.00	.00	.	.00	.00	.03	.89	.59	.11	.55
		N	12	12	12	12	12	12	12	12	12	12

		pH	TDS (mg L^{-1})	BOD5 (mg L^{-1})	COD (mg L^{-1})	EC (µS cm^{-1})	DBP	DEHP	DMP	LNR	PGT
COD (mg L^{-1})	Correlation Coefficient	-.87**	.92**	.98**	1.00	.84**	.68*	.13	.15	.48	.34
	Sig. (2-tailed)	.00	.00	.00	.	.001	.02	.68	.63	.12	.28
	N	12	12	12	12	12	12	12	12	12	12
EC	Correlation Coefficient	-.86**	.88**	.86**	.84**	1.00	.66*	.01	.02	.38	.07
	Sig. (2-tailed)	.00	.00	.00	.001	.	.02	.97	.95	.23	.83
	N	12	12	12	12	12	12	12	12	12	12
DBP	Correlation Coefficient	-.53	.66*	.63*	.68*	.66*	1.00	.32	-.13	.20	.35
	Sig. (2-tailed)	.08	.02	.03	.02	.02	.	.31	.70	.54	.27
	N	12	12	12	12	12	12	12	12	12	12
DEHP	Correlation Coefficient	-.03	.10	.05	.13	.01	.32	1.00	.15	-.02	.53
	Sig. (2-tailed)	.92	.76	.89	.68	.97	.31	.	.63	.95	.08

		pH	TDS (mg L^{-1})	BOD5 (mg L^{-1})	COD (mg L^{-1})	EC (µS cm^{-1})	DBP	DEHP	DMP	LNR	PGT
	N	12	12	12	12	12	12	12	12	12	12
DMP	Correlation Coefficient	-.05	.07	.18	.15	.02	-.13	.15	1.00	.13	-.12
	Sig. (2-tailed)	.87	.83	.59	.63	.95	.70	.63	.	.68	.71
	N	12	12	12	12	12	12	12	12	12	12
LNR	Correlation Coefficient	-.44	.43	.49	.48	.38	.20	-.02	.13	1.00	.26
	Sig. (2-tailed)	.16	.17	.11	.12	.23	.54	.95	.68	.	.42
	N	12	12	12	12	12	12	12	12	12	12
PGT	Correlation Coefficient	-.09	.18	.19	.34	.07	.35	.53	-.12	.26	1.00
	Sig. (2-tailed)	.79	.57	.55	.28	.83	.27	.08	.71	.42	.
	N	12	12	12	12	12	12	12	12	12	12

**. Correlation is significant at the 0.01 level (2-tailed); *. Correlation is significant at the 0.05 level (2-tailed).

To single out an exception observed, DEHP was more abundant in the sludge and UDBS while DBP was highest in the influent wastewater. This is consistent with their physico-chemical parameters (**Table 1.1**). As noted in section 4.1.3, log K_{OW} < 2.5 indicates low sorption potential, 2.5 < log K_{OW} < 4 indicates medium sorption potential and log K_{OW} > 4 indicates high sorption potential (Orata, 2018), thereby indicating why DEHP (log K_{OW}: 7.6) had greater concentrations in sludge and UDBS while DBP (log K_{OW}: 4.5) had greater concentrations in the wastewater samples.

4.1.7 Association between EDC Concentrations and Water Quality Parameters

Spearman's rank order correlation was used to show the association between the water quality parameters and the concentration of the EDCs at the influents (**Table 4.8**). The pH was negatively correlated with all the EDCs detected at the influent points (r_s values ranged from -0.03 to -0.53). This implies that increased contamination increases acidity thus lowering the pH but increasing the rest of the parameters. This may be attributed to increased solubility, an observation made in other pollutants like heavy metals (Kumar et al., 2020). Therefore, contaminants increase the acidity of wastewater making them undesirable. Conversely, for TDS, BOD_5, COD, and EC, there were positive correlations (r_s values 0.01-0.68) implying that the greater the water quality parameter the higher the concentration of the EDCs. The correlations, however, were not significant ($p > 0.05$; $p > 0.01$*) in most of the compounds except for DBP which was strongly significant ($p < 0.05$) for TDS, BOD_5, COD, and EC. Pollution is thus often associated with the worst water quality metrics.

Among the EDCs, there were majorly positive correlations between the PAEs and negative correlations to PGT and LNR. PGT and LNR were however positively correlated. This implies the same sources of PAEs as compared to PGT and LNR.

4.1.8 Removal efficiency of selected EDCs in the sampled WWTPs

The removal efficiencies for each analyte were calculated as illustrated in section 3.2.7. The percentages of efficiencies are shown in **Table 4.9** and the ranges were between 30.2% and 100%. The average removal per pollutant (treating 30.2% removal in Kariobangi as an outlier) was as follows: DMP (98.7%) > DEHP (91.7%) > PGT (88.3%) > DBP (77.9%) > LNR (72.2%). DMP had greater removal percentages while WWTPs displayed less efficiency in removing LNR. DEHP removal efficiency was slightly lower than that reported by Marttinen et al. (2003) at 94%. Up to 95% of DMP and DBP have been attributed to biotransformation and adsorption to sludge (Zhu et al., 2019). The average removal for individual WWTPs for all the selected EDCs was as follows: Shirere (96.3%) > Kisat (96.0%) > Kericho (93.3%) > Eldoret (92.2%) > Kisii (86.2%) > Kariobangi (84.0%) > Ruai (83.5%) > Busia (82.7%) > MMUST (82.1%) > Nakuru (77.7) > Bungoma (75.8%). The removal efficiencies were independent of the type of WWTP, that is, lagoons or conventional. This may be attributed to some conventional WWTPs being old with little to no servicing done periodically. They may have also been built using old technologies which cannot remove emerging pollutants.

Sorption, biological degradation, photolysis, and phytoremediation may be factors affecting dissipation, as these mechanisms can be effective in elimination (Chen et al., 2012). Sorption ensures the transfer of the pollutants to the sludge and then to the UDBS due to the EDCs partitioning onto the biosolid. Plastics can also undergo biodegradation

and photodegradation (Zeenat et al., 2021) explaining the higher ranges of DMP dissipation. Some EDCs (LNR) showed relative stability over the whole treatment process, possibly due to their chemical structure and physiochemical properties making them persistent with weak adsorbility. These values are largely important to regulators as they serve to inform them of the efficiencies of WWTPs and the presence of pollutants in UDBS obtained from WWTPs.

Table 4.9: Percent (%) removal efficiencies of EDCs

Site	DBP	DEHP	DMP	LNR	PGT
Nakuru	58.9	93.3	99.9	65.1	71.5
Eldoret	76.7	89.9	98.5	98.2	97.1
Bungoma	43.9	100.0	99.2	61.8	73.8
Busia	65.4	100.0	99.3	63.7	85.0
Kisii	100	81.9	98.9	61.2	89.0
MMUST	72.4	100.0	99.2	69.5	69.4
Ruai	76.3	78.5	97.6	71.0	94.2
Shirere	100	100	98.6	83.3	99.4
Kisat	100	100	99.9	81.2	98.7
Nyalenda	67.5	76.1	96.7	57.8	95.1
Kericho	100	93.0	99.8	76.0	97.7
Kariobangi	74.0	87.2	96.7	78.1	30.2

4.1.9 Mass loading of EDCs into the environment

The daily discharges (Dds) of the EDCs are shown in **Table 4.10** and were calculated only for the analytes above the LOQ. The Dd loads from the twelve WWTPs varied depending on the pollutant and the geographical difference. The Dd in densely populated areas like Nairobi, represented by Kariobangi and Ruai were considerably high. DBP recorded at Ruai was the highest (373.3 g day^{-1}). This implies that large quantities of EDCs are being

released into receiving waters eventually finding their way into surface waters, potable water, and drinking water. The potential risks to human beings and biota are not in dispute. The synergistic effects of the combination of varied EDCs are unknown. More studies should be carried out to investigate the concentrations of other EDCs in different environmental compartments and their mass loadings into the environment. Some attempts, however, have been made on pharmaceutical mass loadings (K'oreje et al., 2018; Kimosop et al., 2016) but more needs to be done especially in East Africa.

Table 4.10: Daily discharge of EDCs (mg day^{-1}) to the environment through the effluents

Location	DBP	DEHP	DMP	LNR	PGT
Nakuru	22606.9	1256.5	104.2	175.7	1658.3
Eldoret	19641.4	5551.67	926.0	366.2	4760.5
Bungoma	23881.2	–	609.0	181.1	2388.4
Busia	4069.0	–	59.5	55.7	701.7
Kisii	–	3298.6	62.6	84.3	389.7
MMUST	685.0	–	6.7	7.3	170.6
Ruai	373327.8	158716.1	8408.9	1878.2	68680.7
Shirere	–	–	31.6	42.9	23.8
Kisat	–	–	44.8	153.8	95.2
Nyalenda	65270.4	28465.5	995.2	406.3	2357.2
Kericho	–	615.5	10.1	17.4	49.5
Kariobangi	110468.1	42220.7	5439.6	420.8	29149.7

(- represents those areas whose effluents were below the LOQ)

4.1.10 Potential ecotoxicological risks to the recipient aquatic ecosystem

Three trophic levels were chosen to assess the ecotoxicological risks for the selected EDCs in effluents released to surface water. **Table 4.11** shows the calculated RQs for the

selected EDCs based on the worst-case scenario obtained by considering maximum concentrations detected among all the sites and the lowest NOECs or E(L)C50. DEHP (chronic) and PGT (acute and chronic) had their RQs > 1 posing a high risk to biota. DMP, DBP, and LNR posed medium risks as their RQ values were between 0.1 and 1.

Table 4.11: Calculated RQs for the selected EDCs

EDC	Maximum recorded effluent concentration (μg L^{-1})	Effect value used (mg L^{-1})	No. of trophic levels	Acute or Chronic	AF	PNEC converted to μg L^{-1}	RQ
DEHP	1.984	0.3 (EC50)	3	Chronic	1000	0.3	6.2
DBP	4.803	0.4 (lowest NOEC)	3	Chronic	10	40	0.1
DMP	0.237	180 (EC50)	3	Chronic	1000	180	0.001
PGT	0.859	0.1 (lowest NOEC)	2	Acute	1000	0.1	12.5
		0.009 (lowest NOEC)	2	Chronic	50	0.2	5.1
LNR	0.046	0.1 (lowest NOEC)	2	Acute	1000	0.1	0.5
		0.001 (Lowest NOEC)	3	Chronic	10	0.1	0.5

The RQs for chronic cases were also calculated for every EDC per site (**Figure 4.6**).

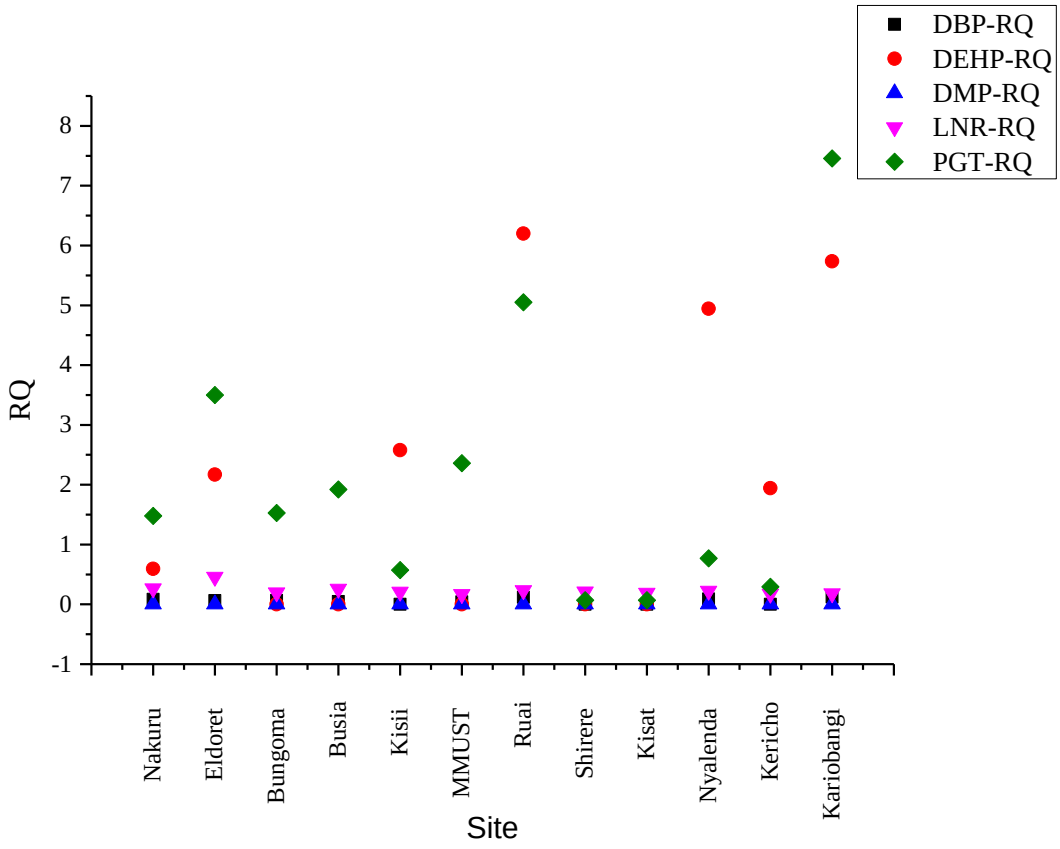

Figure 4.6: RQs for chronic cases calculated for every EDC per site.

DBP displayed medium risks in Ruai and Kariobangi and low to no observed risks in the rest of the sites. DEHP posed high risks in Eldoret, Kisii, Ruai, Nyalenda, Kericho, and Kariobangi while recording medium risks in Nakuru and low risks in the rest of the sites. DMP posed low to no observed risks in all the sites due to recorded low levels in the effluents. LNR displayed medium risks in all the sites while PGT posed high risks in Nakuru, Eldoret, Bungoma, Busia, MMUST, Ruai, and Kariobangi. It is worth noting that sites that recorded high concentrations of EDCs due to denser populations and industrial activities also displayed high risks. Furthermore, low EDC levels at the effluents displayed

minimal values of RQs. More risk assessments should be carried out on more pollutants and more sites to fully comprehend their health impacts on aquatic organisms. Sadly, there is limited data on adverse effects e.g., behavioral effects, and neurotoxicity due to minimal testing strategy. Minimal studies have reported hormonal changes on only one trophic level (fish) and for a few EDCs. Ecotoxicological risks to the terrestrial ecosystem should also be studied.

4.2 Adsorption experiments

4.2.1 Characterization of the adsorbents

4.2.1.1 X-ray diffractometry (XRD)

Figure **4.7** displays the XRD diffractograms of both the treated and untreated *MOSB.* The X-ray diffractogram showed weak and unresolved peaks, indicating the predominance of the amorphous nature of the biosorbent, a characteristic that helps the penetration of the adsorbates. A high amount of lignin, cellulose, and tannin provides a heterogeneous and complex nature of the biosorbent (A. Afolabi et al., 2021; Jayan et al., 2021). For the untreated *MOSB*, there were characteristics peaks at $2\theta = 16.5^{o}$, 17.3^{o}, 22.5^{o} and 34.93^{o} which are in agreement with isolated cellulose from *M.O* seeds carried out by (A. Afolabi et al., 2021). For the treated *MOSB,* the peaks at $2\theta = 16.5^{o}$, and 17.3^{o} were suppressed, those at $2\theta = 22.5^{o}$ and 34.9^{o} were enhanced and there was an additional peak at 27.3^{o} which could be attributed to phosphoric acid hydrolysis.

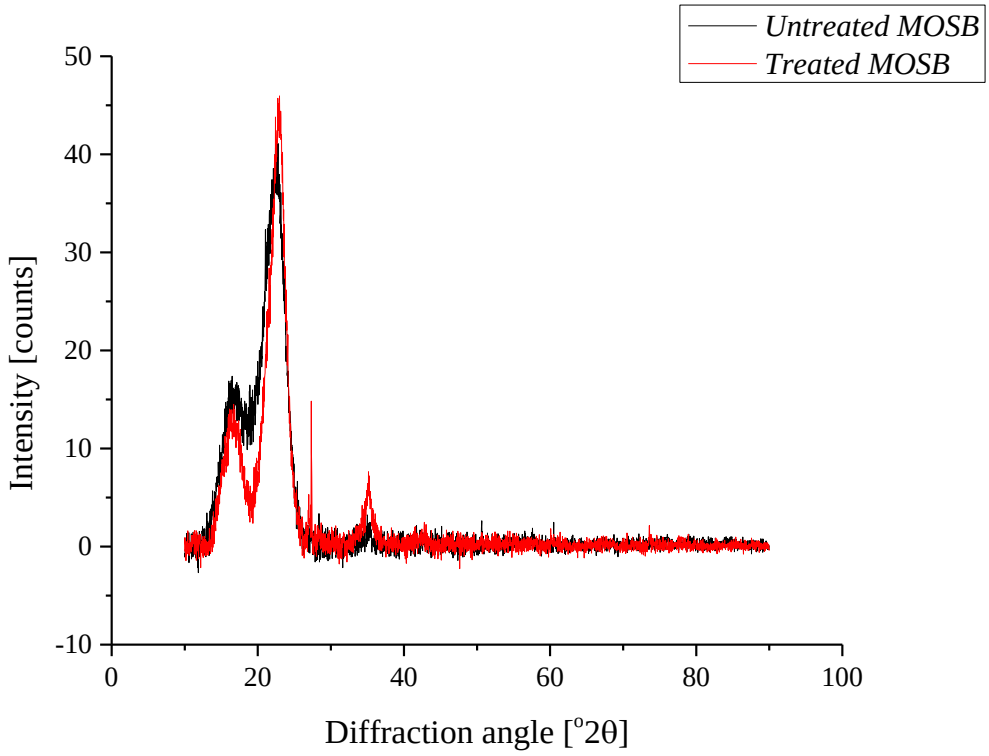

Figure 4.7: XRD analysis of treated and untreated *MOSB*.

4.2.1.2 Scanning electron microscopy–energy dispersive spectroscopy (SEM-EDS)

Figure 4.8 (a) shows the scanning electron micrographs of the untreated *MOSB* while **Figure 4.8 (b)** displays the micrographs of the treated *MOSB* (More micrographs with different magnifications are in **Appendices 9-12**). The morphology of the treated *MOSB* shows a porous complex fiber matrix with no particular shape, a situation observed by other studies such as Araujo et al. (2010) and Bagheri et al. (2020). After treatment, the phosphate-modified *MOSB* revealed micropores and irregular trough-like patterns displaying interstices in the structure that facilitate the biosorption processes. This gives the material adequate morphological characteristics for retaining the EDCs.

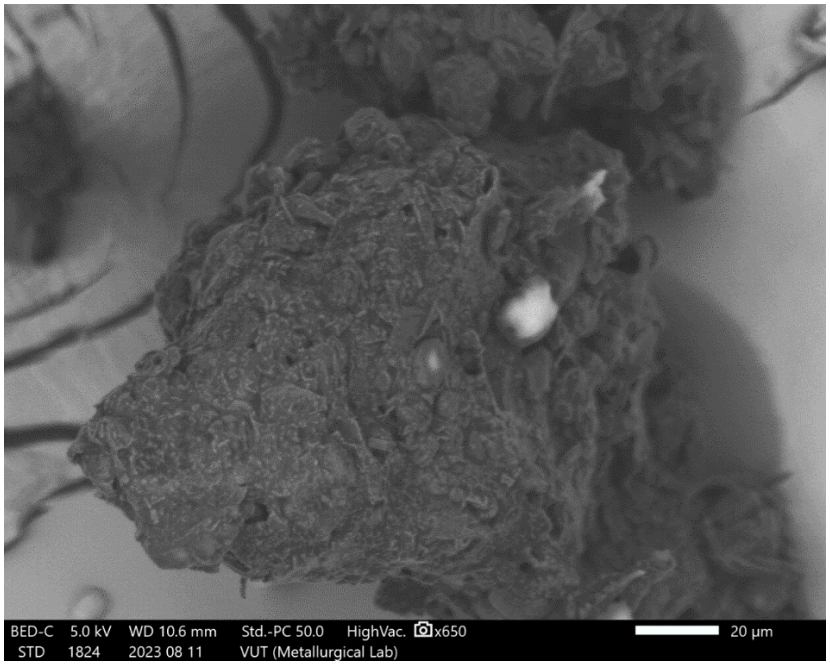

Figure 4.8 (a): SEM images for untreated *MOSB.*

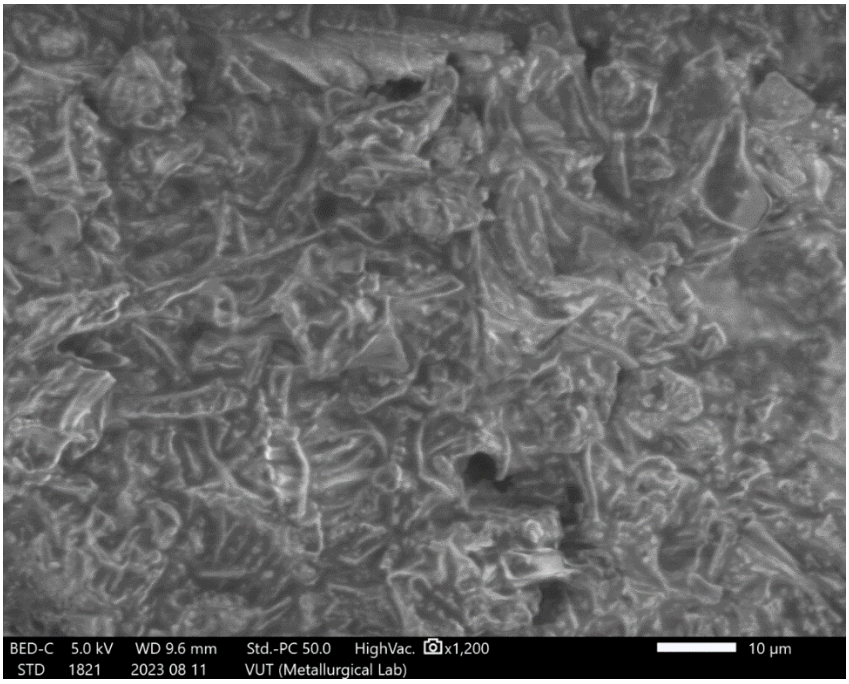

Figure 4.8 (b): SEM images for treated *MOSB.*

The major elemental composition of the synthesized materials (atomic %) was analyzed by EDS (**Figure 4.9 a & b**). The EDS analysis of untreated *MOSB* showed 72.5% carbon

and 22.5% oxygen. After the treatment of *MOSB*, 70.1% of the biomass was found to be carbon while 29.8% was oxygen. The major elemental composition is characteristic of carbonaceous materials. The percentage of oxygen is enhanced in the treated *MOSB* due to modification by weak H_3PO_4 which introduced more oxygen.

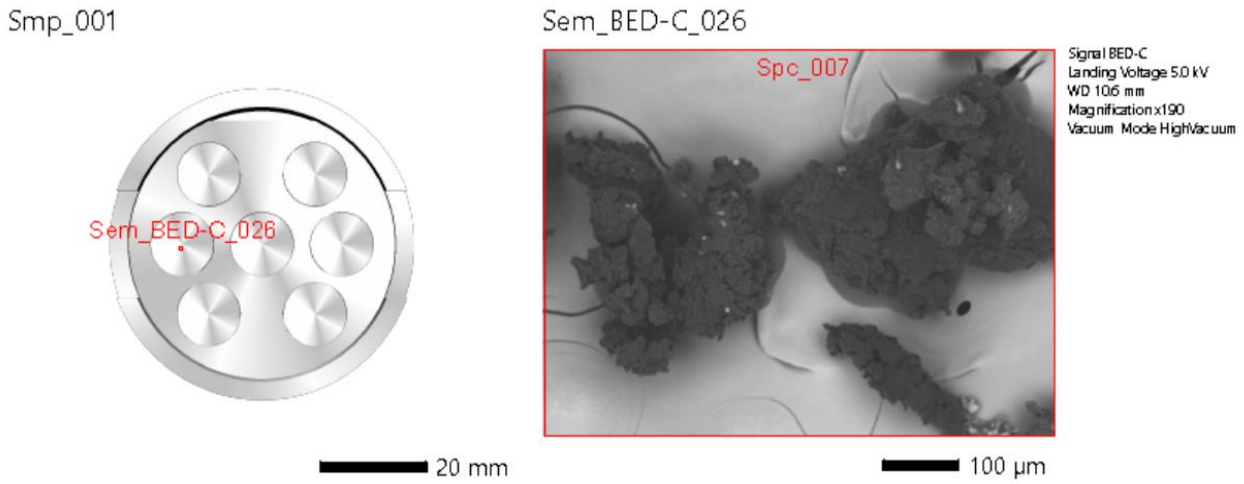

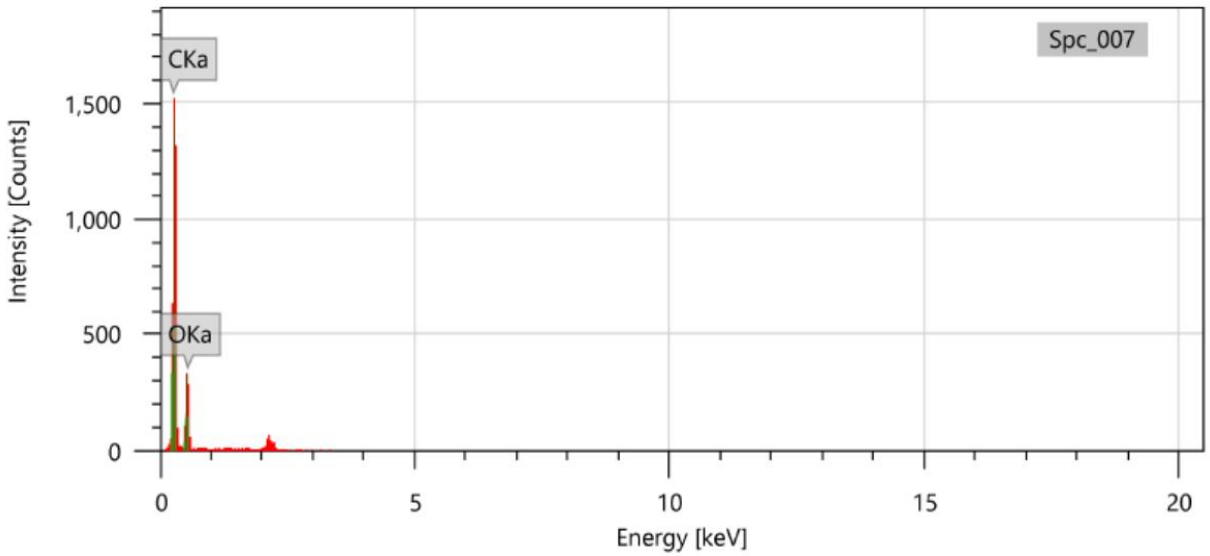

Items	Value
measurement conditions	
Acceleration voltage	5.00 kV
Probe current	-
Magnification	x 190
Process time	T3
Measurement detector	First
Live time	30.00 seconds
Real time	30.19 seconds
Dead time	1.00 %
Count rate	542.00 CPS

Display name	Standard data	Quantification method	Result Type
Spc_007	Standardless	ZAF	Metal

Element	Line	Mass%	Atom%
C	K	72.50±0.34	77.83±0.36
O	K	27.50±0.50	22.17±0.40
Total		100.00	100.00
Spc_007			Fitting ratio 0.0351

Figure 4.9 (a): EDS for untreated *MOSB.*

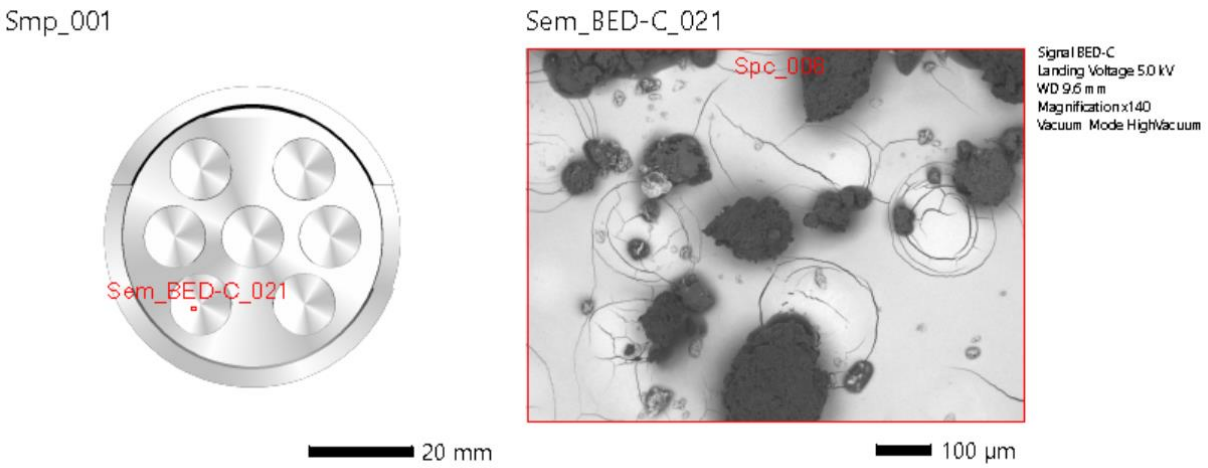

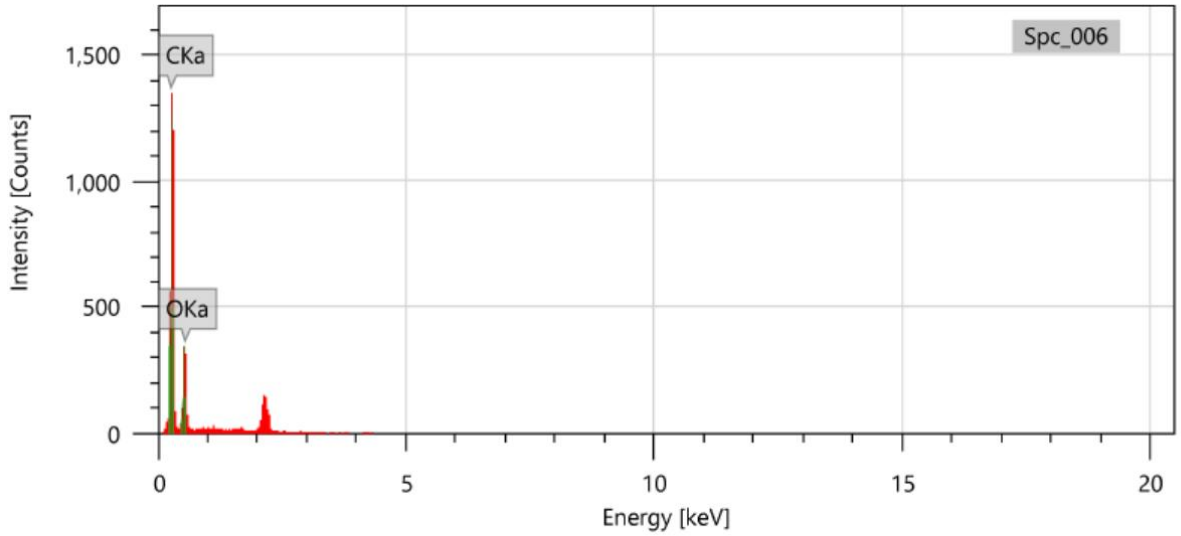

Items	Value
measurement conditions	
Acceleration voltage	5.00 kV
Probe current	-
Magnification	x 140
Process time	T3
Measurement detector	First
Live time	30.00 seconds
Real time	30.16 seconds
Dead time	1.00 %
Count rate	642.00 CPS

Display name	Standard data	Quantification method	Result Type
Spc_006	Standardless	ZAF	Metal

Element	Line	Mass%	Atom%
C	K	70.17±0.35	75.80±0.37
O	K	29.83±0.54	24.20±0.44
Total		100.00	100.00
Spc_006			Fitting ratio 0.0736

Figure 4.9 (b): EDS for treated *MOSB.*

4.2.1.3 Fourier Transform Infra-Red (FT-IR) spectroscopic analysis

The FT-IR technique was used to study the main functional groups present in *MOSB*. **Figure 4.10 (a)** and **(b)** show the FT-IR spectra for untreated and treated *MOSB* respectively. **Figure 4.10 (c)** displays combined spectra for both untreated and treated *MOSB*. A general observation from the spectra showed a broad band centered at 3,288 cm^{-1} assigned to O-H stretching. This functional group is a major bond in proteins, fatty acids, carbohydrates, phenolics, silanols (SiOH), and lignin units present in *M.O* seeds. Due to the high content of protein present in seeds, there may have also been a contribution in this region from the N-H stretching of amide groups. The peak at 2,916 cm^{-1} was assigned to the asymmetrical stretching of the C-H of the CH_2 group which indicated the presence of methylcellulose. The peak at 2,849 cm^{-1} was due to the symmetrical stretching of the C–H bond of the CH_3 group. In the region between 1800 and 1600 cm^{-1}, there were intense bands assigned to C=O bond stretching and C=C of the aromatic bonds. The carbonyl group is present in the fatty acid and protein structures and thus the band at 1,708 cm^{-1} could be associated with the asymmetrical C=O stretching of the carboxyl found in fatty acids. The band at 1,649 cm^{-1} could be attributed to the amide group in the protein. The presence of a peak at 1,541 cm^{-1} could be assigned to C-N stretching and/or N-H deformation. The presence of this band confirmed the protein structure in *MOSB*. The peak at 1,460 cm^{-1} could have been due to the C-O of carboxylic acids while the peak at 1,238 cm^{-1} referred to the C-O stretching of carboxylic acids (Araujo et al., 2018). After treatment, there was not much shifting of the functional groups nor the creation of new peaks. The intensities of the bands were however enhanced for example the O-H band may have been slightly enhanced by phosphoric acid hydrolysis.

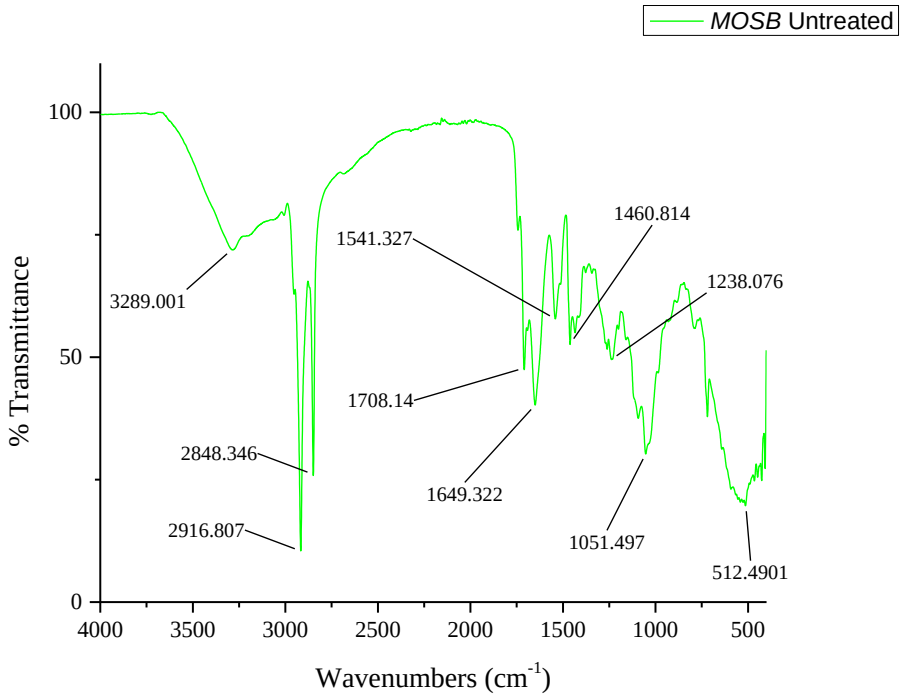

Figure 4.10 (a): FT-IR spectra for untreated *MOSB*.

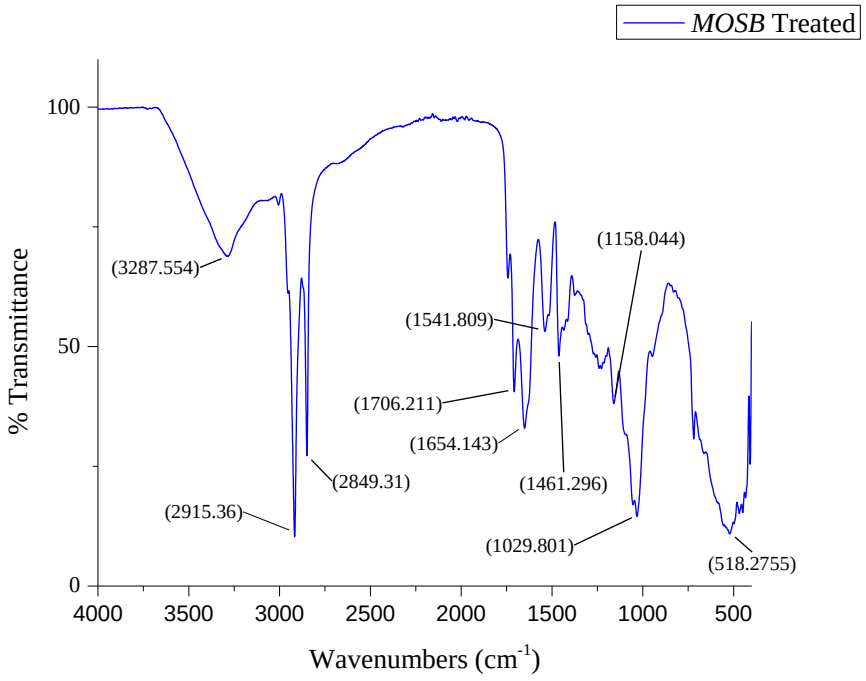

Figure 4.10 (b): FT-IR spectra for treated *MOSB*.

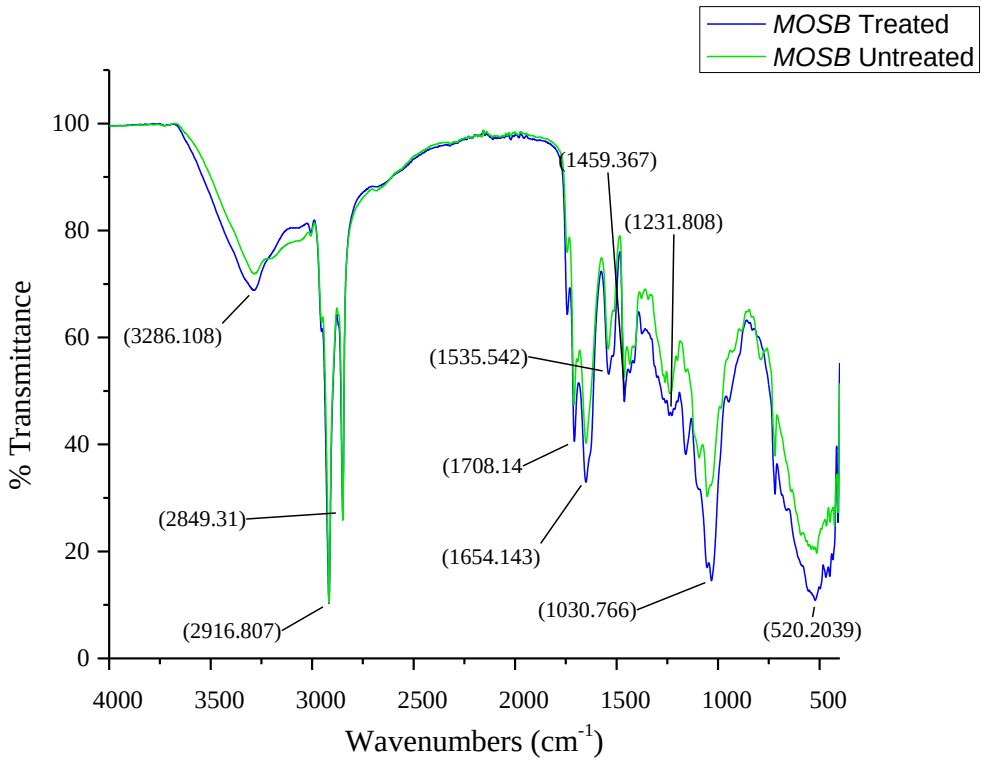

Figure 4.10 (c): FT-IR spectra for combined untreated and treated *MOSB.*

After biosorption of both PGT and LNR (**Figure 4.11 a & b**), the functional groups -OH (3288 cm^{-1}), the C-H of CH_2 (2649 cm^{-1}), the C–H bond of the CH_3 group (2916 cm^{-1}) the C=O bond and the C=C (between 1800-1600 cm^{-1}), the C-N stretching and/or N-H (541 cm^{-1}) and the C-O of carboxylic acids (1460 cm^{-1}) were greatly affected. This change could be related to the stretching of COO^- bonds present in the heterocyclic rings of both PGT and LNR and part of the N–H deformation of secondary amine groups present in LNR. This implied that these are the groups involved in the biosorption of both PGT and LNR.

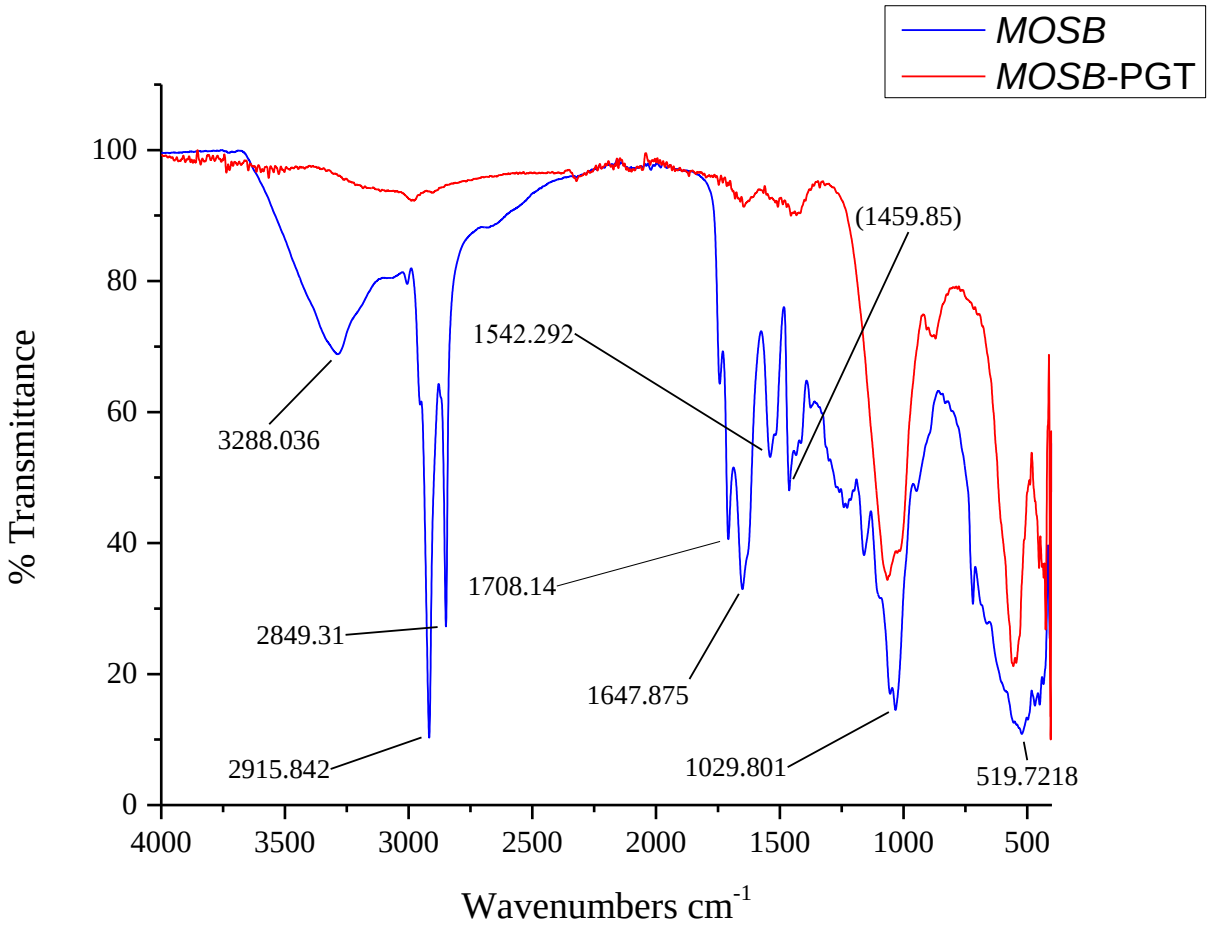

Figure 4.11 (a): FT-IR spectra for *MOSB* with PGT.

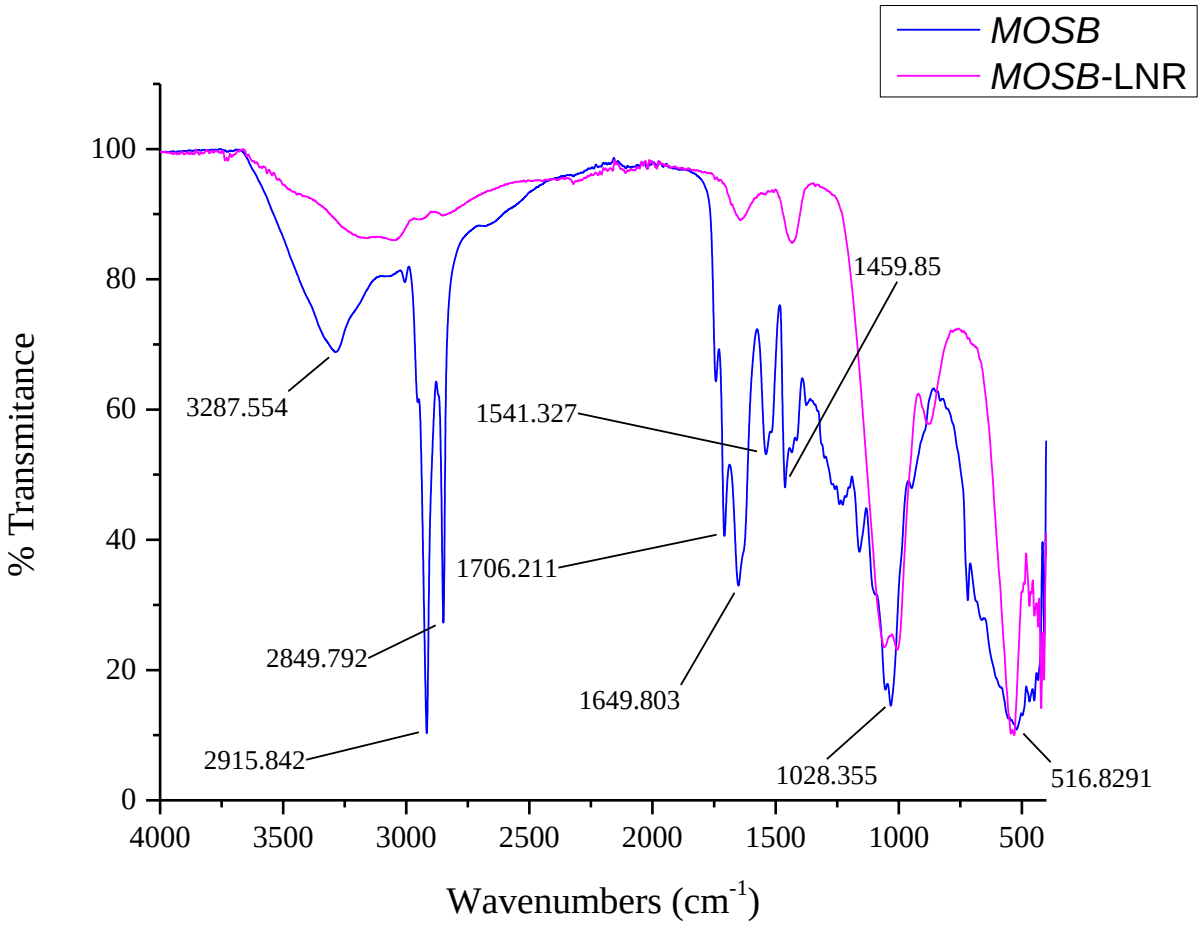

Figure 4.11 (b): FT-IR spectra for *MOSB* with LNR.

4.2.2 PGT adsorption experiments

4.2.2.1 Central composite design (CCD) and data analysis for PGT biosorption

The adsorption of PGT to *MOSB* was run based on the experimental design plan and the results are represented in **Table 4.12**. The calibration curves and the chromatograms used for quantification are displayed in **Appendix 13**.

Table 4.12: PGT Results obtained from the experimental design matrix

Run	Factor A: Time (Mins)	Factor B: Temp. (K)	Factor C: pH	Factor D: Adsorbate (ppb)	Factor E: Adsorbent (g)	Response 1: Concentration adsorbed (µg L^{-1})	Response 2: Percentage removal (R)	Response 3: Amount adsorbed (qe) ug g^{-1}
1	180	298	2	20	0.1	17.2	85.8	4.3
2	10	298	2	20	0.1	16.4	82.0	4.1
3	10	298	2	500	0.1	441.6	88.3	110.4
4	95	318	6	260	0.55	233.1	89.7	10.6
5	180	298	10	500	1.0	445.6	89.1	11.1
6	180	298	10	20	0.1	17.3	86.4	4.3
7	180	338	10	20	0.1	14.2	71.0	3.5
8	10	338	10	20	1.0	16.7	83.5	0.4
9	10	338	10	500	1.0	445.7	89.1	11.1
10	95	318	6	260	0.55	231.4	89.0	10.5
11	180	338	10	20	1.0	17.8	89.1	0.4
12	95	298	6	260	0.55	240.7	92.6	10.9
13	180	338	2	500	1.0	445.1	89.0	11.1
14	10	298	10	20	1.0	16.5	82.5	0.4
15	95	318	2	260	0.55	232.0	89.2	10.5
16	10	338	2	500	0.1	423.3	84.7	105.8
17	95	318	6	260	0.1	226.1	87.0	56.5

Run	Factor A: Time (Mins)	Factor B: Temp. (K)	Factor C: pH	Factor D: Adsorbate (ppb)	Factor E: Adsorbent (g)	Response 1: Concentration adsorbed (µg L^{-1})	Response 2: Percentage removal (R)	Response 3: Amount adsorbed (qe) ug g^{-1}
18	10	318	6	260	0.55	218.3	84.0	9.9
19	95	318	6	20	0.55	17.7	88.7	0.8
20	95	318	6	260	0.55	229.6	88.3	10.4
21	180	338	2	20	0.1	14.5	72.5	3.6
22	95	318	10	260	0.55	232.0	89.2	10.5
23	10	338	10	500	0.1	424.9	85.0	106.2
24	180	338	10	500	0.1	383.1	76.6	95.8
25	10	338	2	20	0.1	14.9	74.5	3.7
26	95	338	6	260	0.55	230.3	88.6	10.5
27	10	298	2	500	1.0	413.1	82.6	10.3
28	180	338	2	20	1.0	17.2	86.0	0.4
29	10	338	2	500	1.0	435.7	87.1	10.9
30	10	298	10	500	0.1	437.8	87.6	109.5
31	180	318	6	260	0.55	216.3	83.2	9.8
32	180	298	2	20	1.0	17.8	89.1	0.4
33	10	338	10	20	0.1	14.2	71.0	3.5
34	10	338	2	20	1.0	16.0	80.0	0.4
35	95	318	6	260	1.0	235.0	90.4	5.9

Run	Factor A: Time (Mins)	Factor B: Temp. (K)	Factor C: pH	Factor D: Adsorbate (ppb)	Factor E: Adsorbent (g)	Response 1: Concentration adsorbed (µg L^{-1})	Response 2: Percentage removal (R)	Response 3: Amount adsorbed (qe) ug g^{-1}
36	10	298	10	20	0.1	16.0	80.0	4.0
37	180	298	10	20	1.0	18.0	90.0	0.5
38	95	318	6	260	0.55	226.4	87.1	10.3
39	180	338	2	500	0.1	386.2	77.2	96.5
40	180	338	10	500	1.0	442.6	88.5	11.1
41	180	298	2	500	0.1	442.8	88.6	110.7
42	95	318	6	260	0.55	235.1	90.4	10.7
43	95	318	6	260	0.55	232.7	89.5	10.6
44	95	318	6	260	0.55	228.0	87.7	10.4
45	10	298	10	500	1.0	416.3	83.3	10.4
46	180	298	10	500	0.1	441.5	88.3	110.4
47	10	298	2	20	1.0	15.5	77.5	0.4
48	95	318	6	260	0.55	232.0	89.2	10.5
49	180	298	2	500	1.0	445.3	89.1	11.1
50	95	318	6	500	0.55	449.5	89.9	20.4

The percentage removal depicting adsorption efficiency of *MOSB* for the abstraction of PGT from aqueous solutions depends on whether there is significant variation in the combination of the process parameters. The proposed model for PGT biosorption to *MOSB* was quadratic and ANOVA was used to determine the significant variation of the model terms and consequently the adequacy of the proposed model (**Table 4.13).**

Table 4.13: ANOVA for PGT's quadratic model

Source	Sum of Squares	df	Mean Square	F-value	p-value	
Model	1364.22	20	68.21	43.18	< 0.0001	significant
A-Time	39.94	1	39.94	25.28	< 0.0001	
B-Temperature	140.45	1	140.45	88.91	< 0.0001	
C-pH	1.42	1	1.42	0.90	0.35	
D-Adsorbate	163.05	1	163.05	103.21	< 0.0001	
E-Adsorbent	186.32	1	186.32	117.94	< 0.0001	
AB	70.25	1	70.25	44.47	< 0.0001	
AC	0.36	1	0.36	0.23	0.64	
AD	50.26	1	50.26	31.81	< 0.0001	
AE	80.99	1	80.99	51.27	< 0.0001	
BC	0.06	1	0.06	0.037	0.85	
BD	21.38	1	21.38	13.53	0.0010	
BE	218.87	1	218.87	138.54	< 0.0001	
CD	0.86	1	0.86	0.55	0.47	
CE	15.78	1	15.78	9.99	0.004	
DE	33.78	1	33.78	21.38	< 0.0001	
A^2	83.11	1	83.11	52.61	< 0.0001	
B^2	3.57	1	3.57	2.26	0.14	
C^2	0.05	1	0.05	0.03	0.86	
D^2	0.01	1	0.01	0.01	0.93	
E^2	1.19	1	1.19	0.75	0.39	
Residual	45.81	29	1.58			

Source	Sum of Squares	df	Mean Square	F-value	p-value	
Lack of Fit	37.33	22	1.70	1.40	0.34	not significant
Pure Error	8.48	7	1.21			
Cor Total	1410.04	49				

The Model F-value of 43.18 implied that the model was significant. There was only a 0.01% chance that an F-value this large could occur due to noise. P-values less than 0.05 indicate that the model terms are significant while values greater than 0.10 indicate the model terms are not significant. The linear effects of A (time), B (temperature), D (adsorbate concentration), and E (adsorbent dosage), the interactive effects of AB, AD, AE, BD, BE, CE, and DE, and the quadratic effects of A^2 were significant model terms. C (pH), AC, BC, CD, B^2, C^2, $D^{2,}$ and E^2 had no significant effect on the biosorption process of PGT. The F-value of 1.40 suggests that the lack of fit was not statistically significant compared to the pure error. There was a 33.90% probability that a lack of fit F-value of this magnitude could occur due to noise. When there is a non-significant lack of fit, the model fits. Model reduction was performed to enhance the model because of a few insignificant model terms. **Table 4.14** displays the reduced quadratic model.

Table 4.14: ANOVA for Reduced Quadratic model

Source	Sum of Squares	df	Mean Square	F-value	p-value	
Model	1358.90	13	104.53	73.59	< 0.0001	significant
A-Time	39.94	1	39.94	28.12	< 0.0001	
B-Temperature	140.45	1	140.45	98.88	< 0.0001	
C-pH	1.42	1	1.42	1.00	0.32	
D-Adsorbate	163.05	1	163.05	114.79	< 0.0001	

Source	Sum of Squares	df	Mean Square	F-value	p-value	
E-Adsorbent	186.32	1	186.32	131.18	< 0.0001	
AB	70.25	1	70.25	49.46	< 0.0001	
AD	50.26	1	50.26	35.38	< 0.0001	
AE	80.99	1	80.99	57.02	< 0.0001	
BD	21.38	1	21.38	15.05	0.0004	
BE	218.87	1	218.87	154.09	< 0.0001	
CE	15.78	1	15.78	11.11	0.0020	
DE	33.78	1	33.78	23.78	< 0.0001	
A^2	336.42	1	336.42	236.86	< 0.0001	
Residual	51.13	36	1.42			
Lack of Fit	42.65	29	1.47	1.21	0.42	not significant
Pure Error	8.48	7	1.21			
Cor Total	1410.04	49				

The model F-value of 73.59 was large enough implying that the model was significant. There was only a 0.01% chance that an F-value this large could occur due to noise. In this case, A, B, D, E, AB, AD, AE, BD, BE, CE, DE, and A^2 were significant model terms. The parameter coded C (pH) was not significant implying that PGT removal was unaffected by varying pH. This is because PGT is not dissociated under varying pH values, a scenario observed by Moulahcene et al. (2015) and Banasiak and Schäfer (2010). This therefore implied that electrostatic interactions did not contribute significantly to a higher retention of PGT or their effect was neglected. The lack of fit F-value of 1.21 implied that the lack of fit was not significant relative to the pure error. There was a 42.43% chance that a lack of fit F-value this large could occur due to noise. Non-significant lack of fit is

good since it implies that the reduced quadratic model fits. The fit statistics gave the coefficient of determination (R^2) as 0.96 which was good enough. The predicted R^2 of 0.9275 was in reasonable agreement with the adjusted R^2 of 0.9506; i.e., the difference was less than 0.2. This reduced quadratic model can be used to navigate the design space and the empirical relationship between adsorption efficiency (*R*) and the five process variables is given in **Equation 4.1**.

$$R=89.15 + 1.08 * A + -2.03 * B + 0.20 * C + 2.20 * D + 2.34 * E + -1.50 * AB + -1.25 * AD + 1.59 * AE + 0.82 * BD + 2.62 * BE + 0.70 * CE + -1.03 * DE + -5.56 * A^2$$

(Equation 4. 1)

where A-E are the coded values for the independent variables, and R is the percentage removal indicating adsorption efficiency. Coefficients featuring a single factor demonstrate the influence of that specific component, whereas coefficients containing multiple variables describe the interaction of those variables. Synergistic effects are indicated by a positive sign before the terms, and antagonistic effects are indicated by a negative sign (Ani et al., 2019). For specific levels of each coded factor, **Equation 4.1** can be applied in computing the response. The high values of the factors are coded as +1, while the low levels are coded as -1. By comparing the factor coefficients, **Equation 4.1** can be used to determine the significance of the process variables. **Figure 4.12,** of actual experimental values versus predicted values, displays a reasonable distribution along a straight line implying a good relationship.

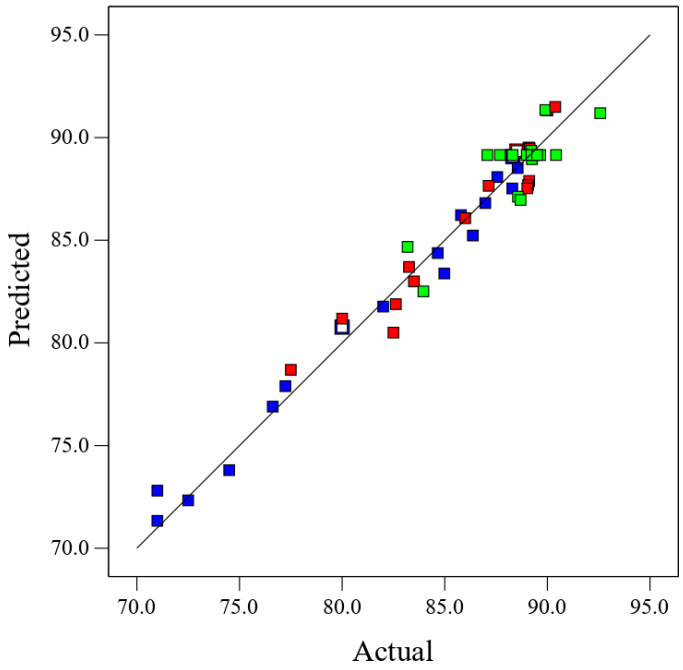

Figure 4.12: Predicted values versus actual experimental values for PGT biosorption.

Diagnostic plots further indicating the fitness of the model by correlating the experimental and predicted values of adsorption of PGT to *MOSB* are shown in **Figure 4.13 (a-d)**. **Figure 4.13 (a)** displays a straight line when the normal percentage probability was plotted against internally studentized residuals demonstrating that the error terms were normally distributed. This confirmed the goodness of fit of the model predictions**.** In **Figure 4.13 (b)**, the random scatter along a center line of the residuals of the predicted values of PGT biosorption illustrated that the observed and predicted values were in agreement, and this was corroborated by **Figure 4.13 (c**) showing a distribution along a center line in the residuals of the run. The Box-Cox plot (**Figure 4.13 (d**)) for power transform did not recommend any data transformation. Cook's distance (**Figure 4.13 (e**))

is considered high if it is greater than 0.5 and extreme if it is greater than 1. The values in the biosorption of PGT were much less and thus satisfactory.

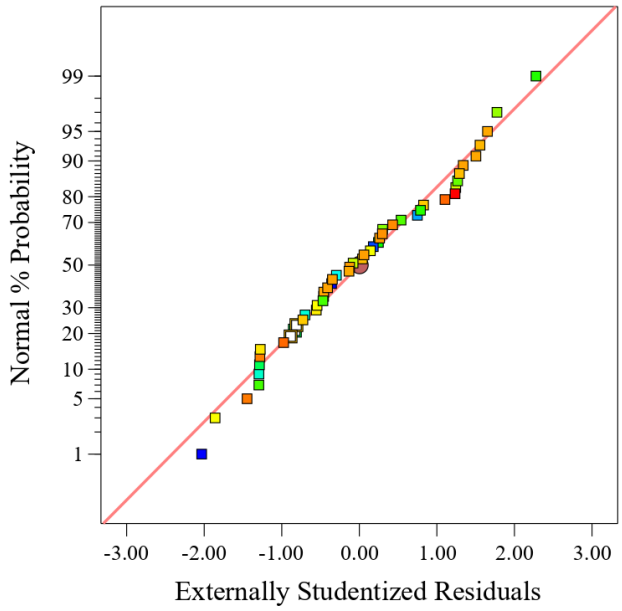

Figure 4.13 (a): Normal plot of residuals for PGT biosorption.

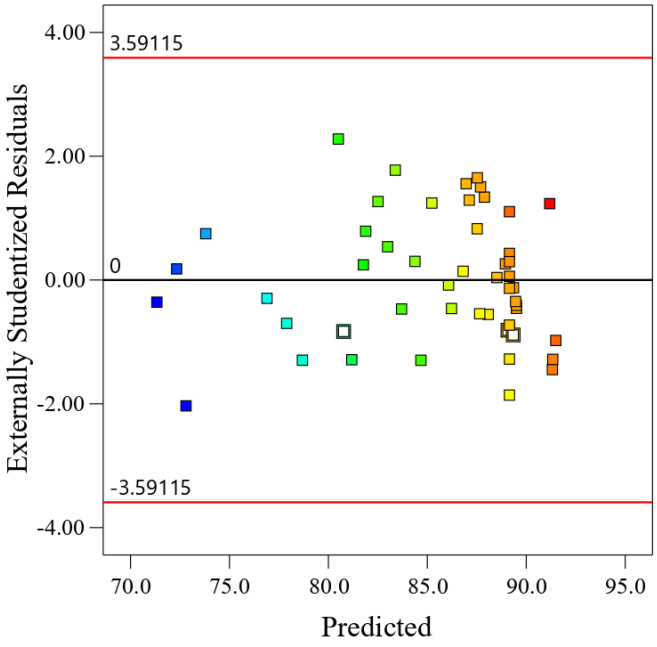

Figure 4.13 (b): Residual versus predicted during PGT biosorption.

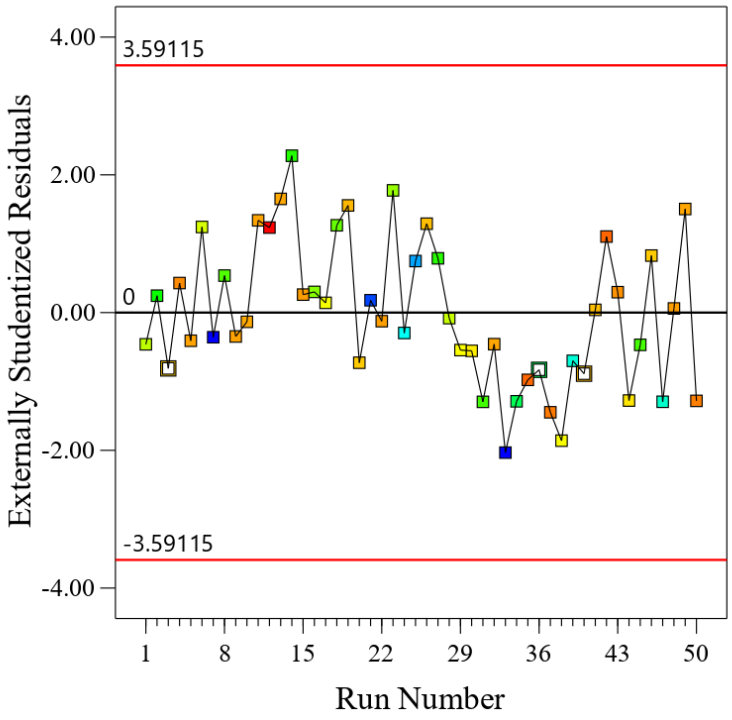

Figure 4.13 (c): Residuals versus run for PGT biosorption.

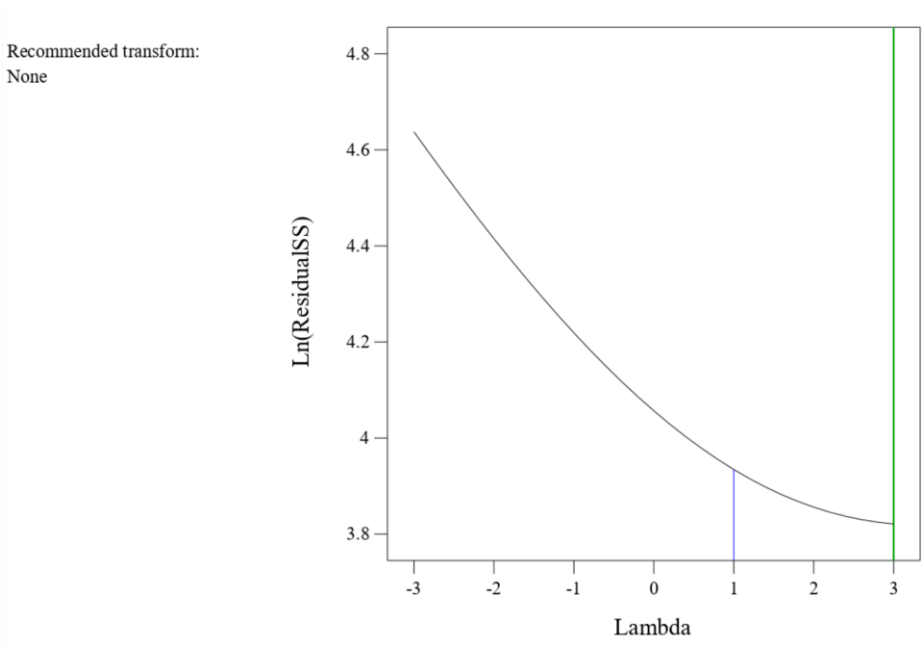

Figure 4.13 (d): Box Co plot for power transforms for PGT biosorption.

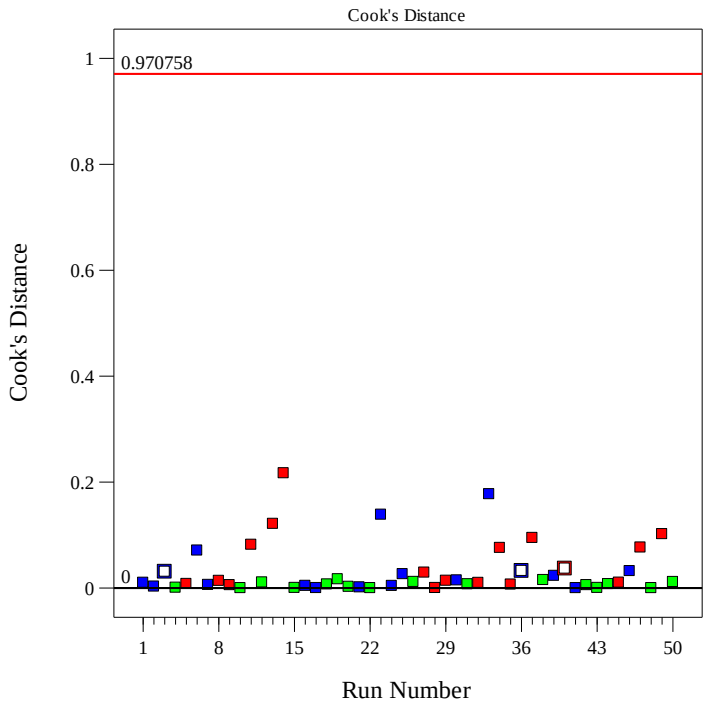

Figure 4.13 (e): Cooks distance for PGT biosorption.

4.2.2.2 Model Graphs for all factor interactions

Figure 4.14 (a) displays all factor perturbation around a reference point of contact time-95 min, temperature-318 K, adsorbate concentration of 260 µg L^{-1}, pH-6, and 0.55 g of biosorbent. **Figures 4.14 (b-f)** show the influence of the independent variables on the biosorption process, taking into consideration all the factor interactions. The dotted lines represent the 95% confidence band on the mean prediction. As contact time was varied from 10-180 min, there was a faster initial increase reaching a peak before a decrease in percentage removal (**Figure 4.14 (b)**). As the temperature varied from 298 to 338 K, the removal efficiency decreased (**Figure 4.14 (c)**). **Figure 4.14 (d)** corroborates the ANOVA tests displaying PGT removal being unaffected by pH and the percentage removal remaining practically constant. **Figure 4.14 (e)** illustrates that as the concentration of the adsorbates increased, the percentage removed increased and so did the amount adsorbed.

As the amount of *MOSB* was increased from 0.1 to 1 g, the amount adsorbed increased as well from 87.3% to 90.4% (**Figure 4.14(f)).** This corresponds to the rising vacant pores (Aly-Eldeen et al., 2018). When the adsorbent-to-adsorbate concentration ratio is larger, there is swift surface sorption onto the adsorbent, resulting in a lower adsorbate concentration in the solution than when the adsorbent-to-adsorbate concentration ratio is smaller. This is because a specific amount of adsorbent with a fixed number of available binding sites can only adsorb a particular quantity of PGT. Consequently, the higher the adsorbent dose, the greater the concentration of PGT purified by a certain amount of *MOSB.*

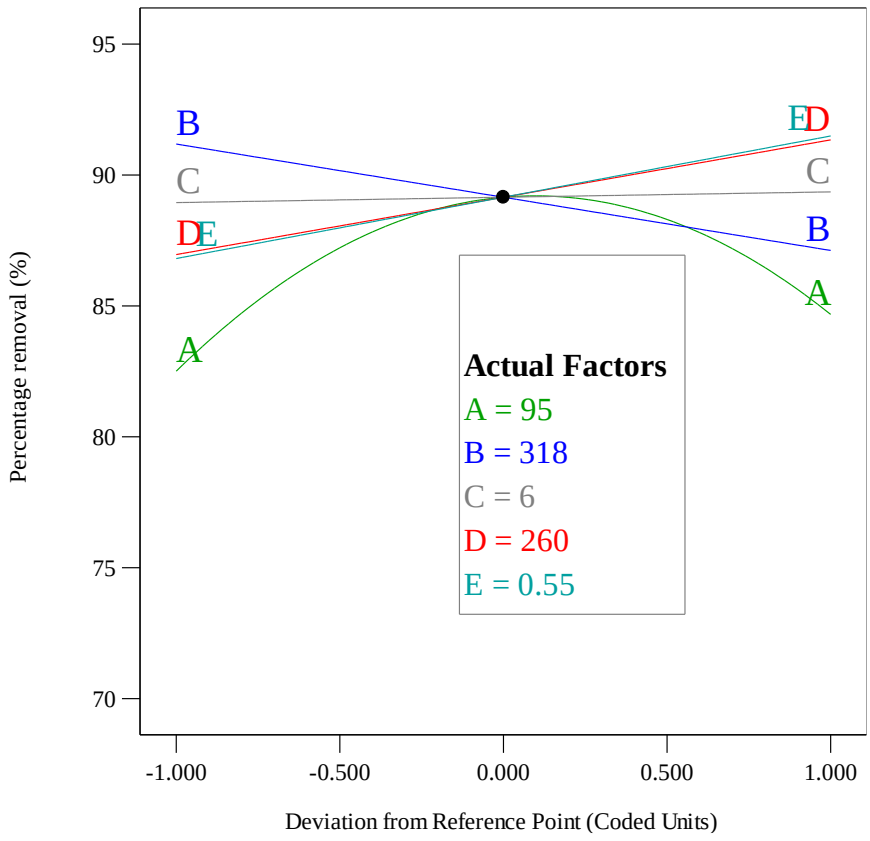

Figure 4.14 (a): Perturbation graph displaying all factor interactions during biosorption of PGT to *MOSB.*

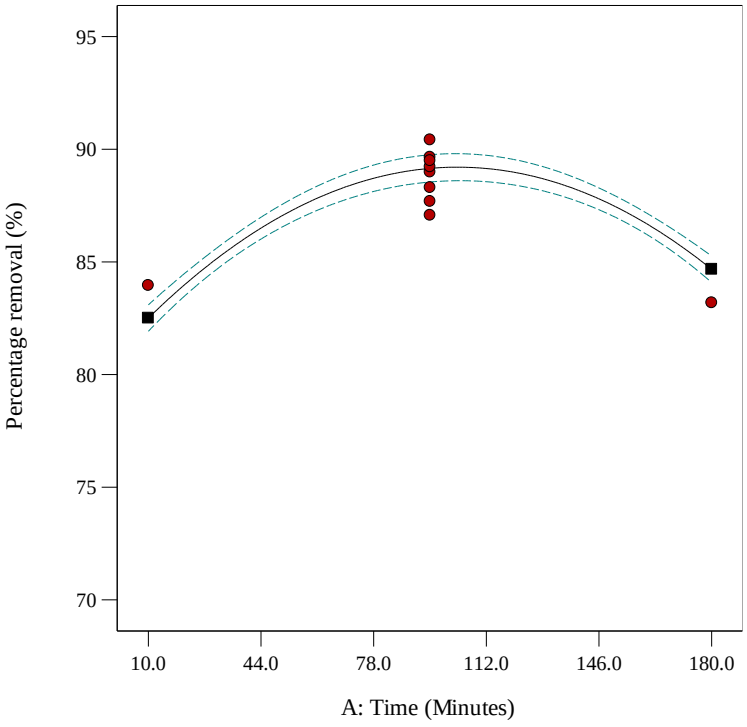

Figure 4.14 (b): Effect of time on percent removal of PGT using *MOSB*.

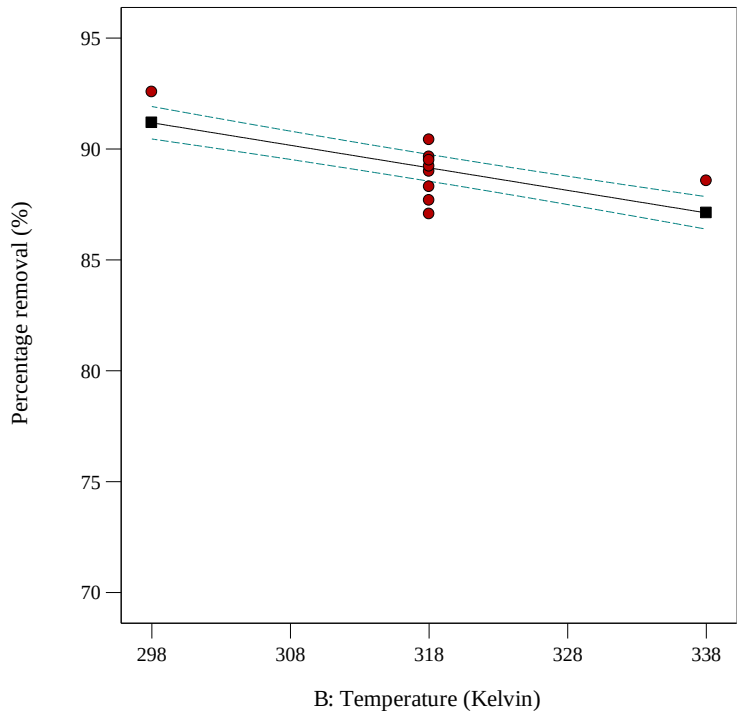

Figure 4.14 (c): Effect of temperature on percent removal of PGT using *MOSB*.

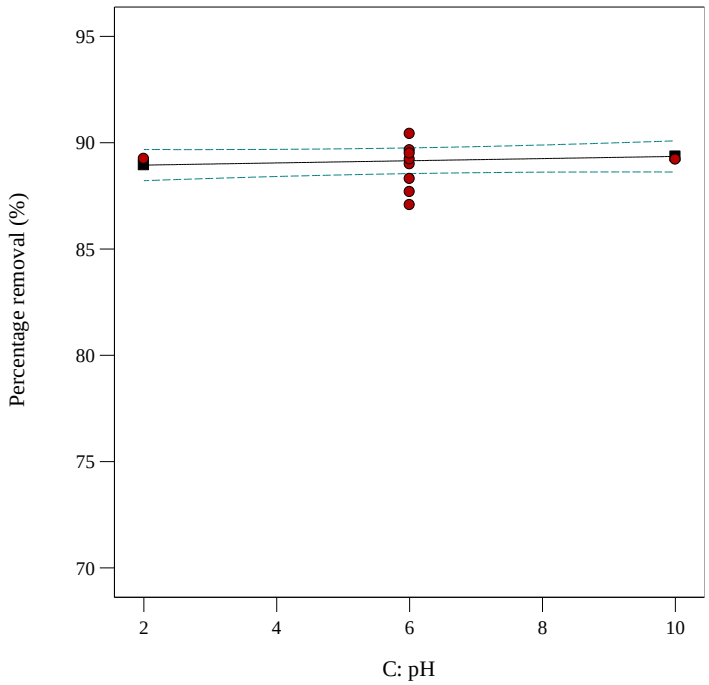

Figure 4.14 (d): Effect of pH on percent removal of PGT using *MOSB*.

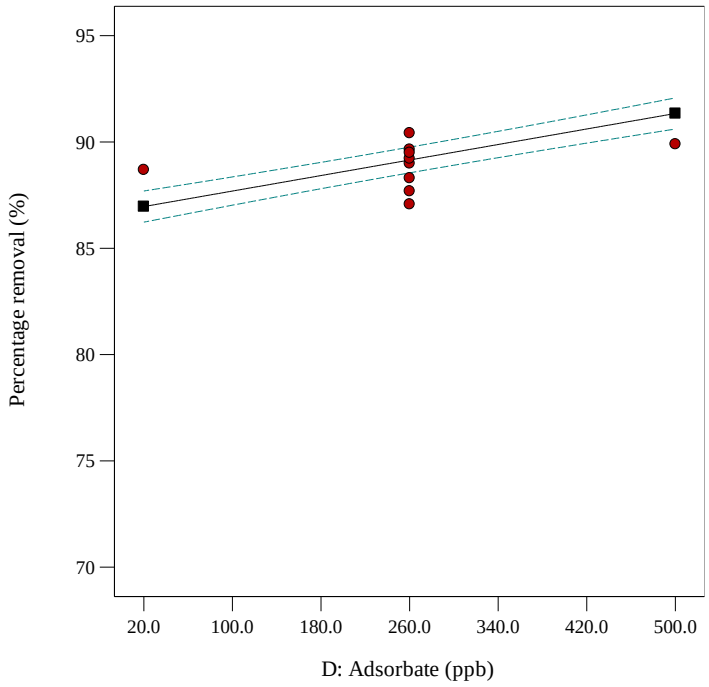

Figure 4.14 (e): Effect of adsorbate concentration on percent removal of PGT using *MOSB*.

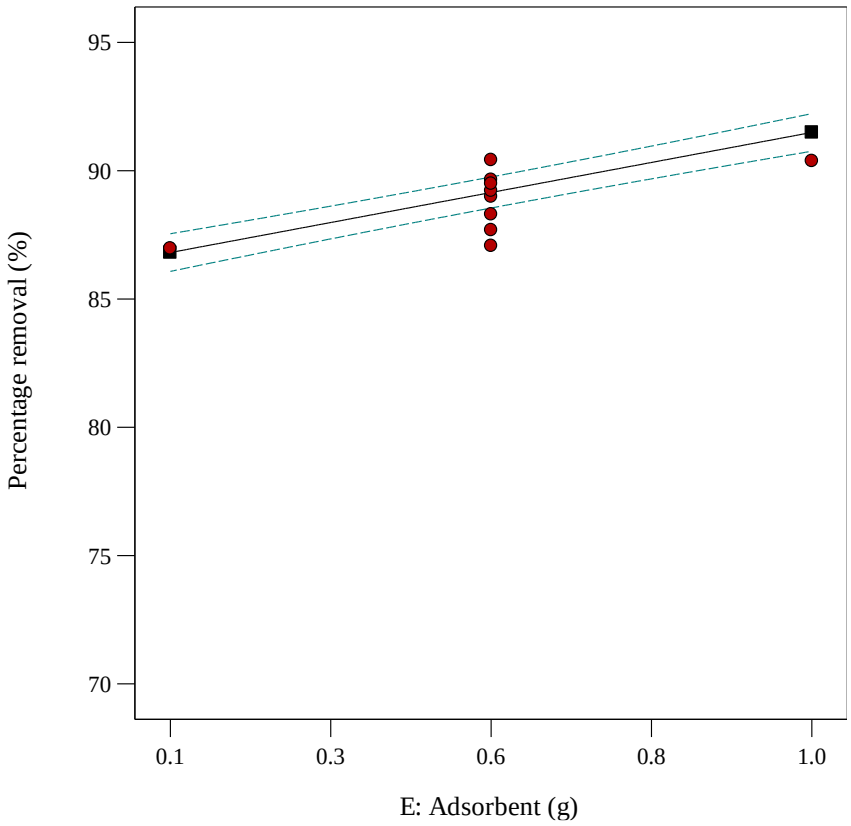

Figure 4.14 (f): Effect of adsorbent dosage on percent removal of PGT using *MOSB.*

4.2.2.3 Three-dimensional surface plots for the adsorption of PGT onto *MOSB*

To estimate the impact of the various interactions of independent factors on adsorption efficiency, three-dimensional (3-D) response surface plots were generated. The plots are shown in **Figures 4.15 (ai-gi).** The contour plots further give a visual representation of the observations. The regions given in red color display optimum efficiency. From **Figures 4.15 (ai & aii),** adsorption efficiency was affected by both contact time and temperature. Closer to room temperature (298 K) was preferable while removal efficiency was observed between 74 min and 163 min and thereafter there was a decrease depicting a possibility of desorption. This therefore implied that room temperature was more

efficient during PGT abstraction making it appropriate during real-life application. The same range of contact time and increased amount of adsorbate and adsorbent improved the adsorption efficiency (**Figures 4.15 bi, bii, ci &cii**). Further, closer to room temperature, increased initial PGT concentration (adsorbate) and adsorbent dosage improved the percentage removal (**Figures 4.15 di, dii, ei & eii)**. In addition, at higher values of initial PGT concentration (adsorbate) and adsorbent, the collective effect was greater (**Figures 4.15 fi &fii**). This was due to increased PGT molecules and a further spike in the number of available vacant sites of the biosorbent when the right contact time and temperature were applied. The pH influence remained relatively constant even as the adsorbent dosage increased the efficiency (**Figures 4.15 gi & gii**). This further corroborates the insignificance of pH in PGT removal and further details pertaining to the mechanism of the biosorption process have been given in section 4.2.2.8.

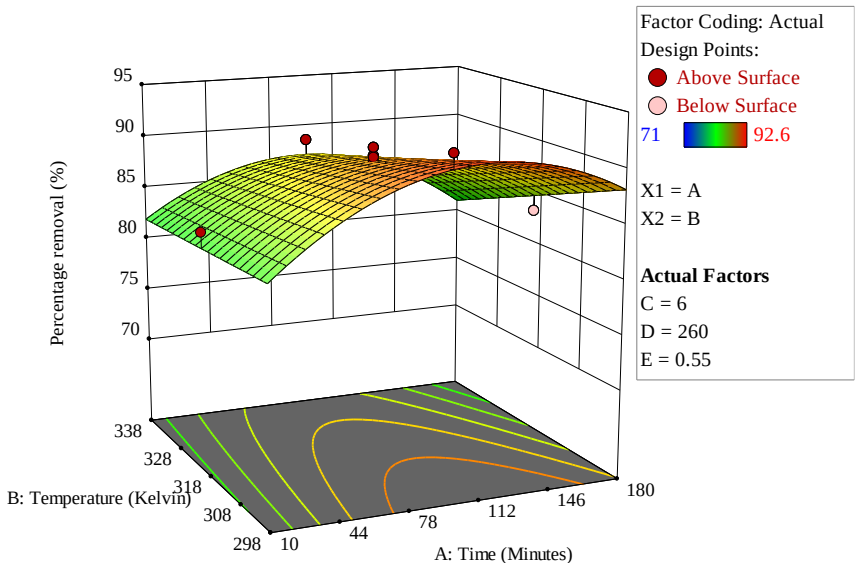

Figure 4.15 (ai): 3-D surface plot displaying the effect of time and temperature on percent removal of PGT using *MOSB.*

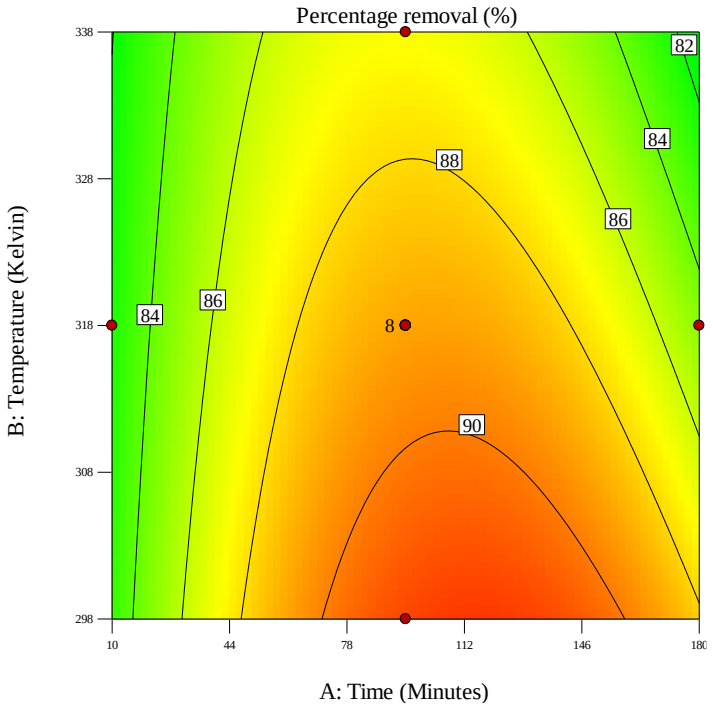

Figure 4.15 (aii): 2-D contour plot displaying the effect of time and temperature on percent removal of PGT using *MOSB.*

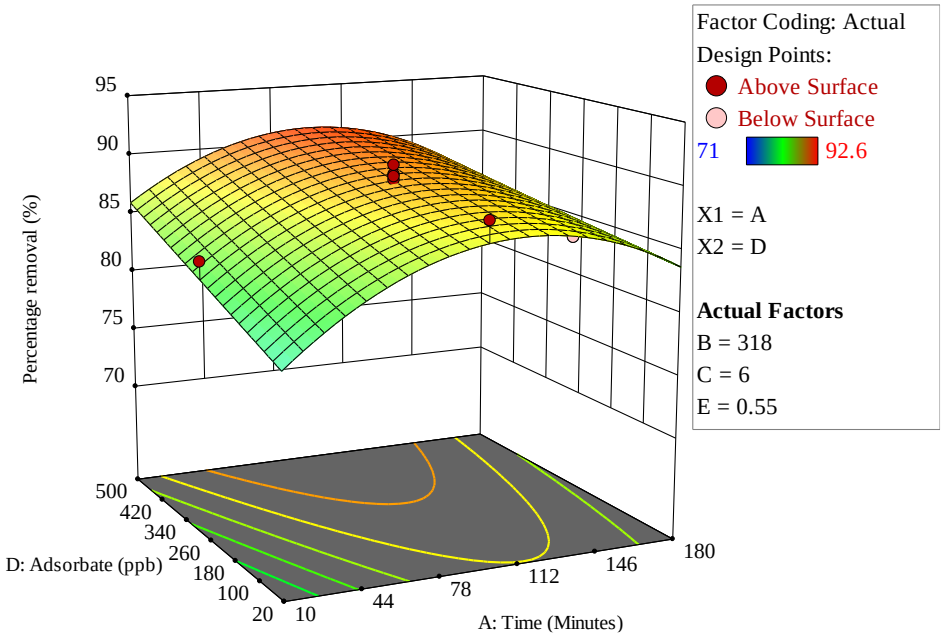

Figure 4.15 (bi): 3-D surface plot displaying the effect of time and adsorbate concentration on percent removal of PGT using *MOSB*.

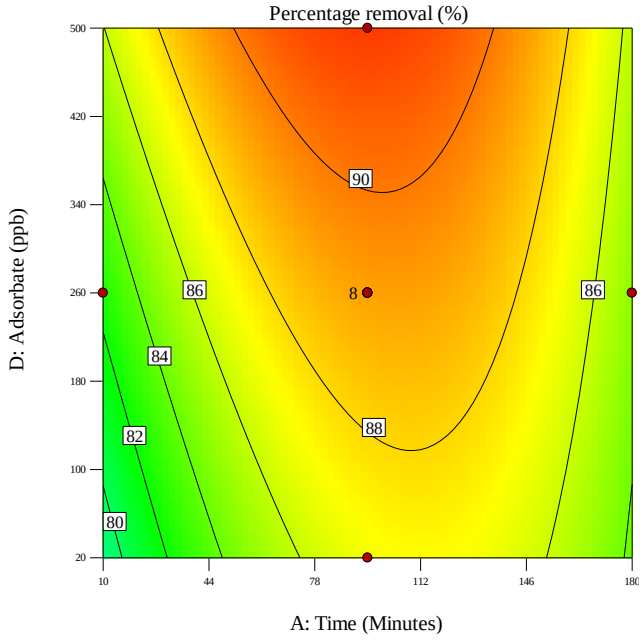

Figure 4.15 (bii): 2-D contour plot displaying the effect of time and adsorbate concentration on percent removal of PGT using *MOSB*.

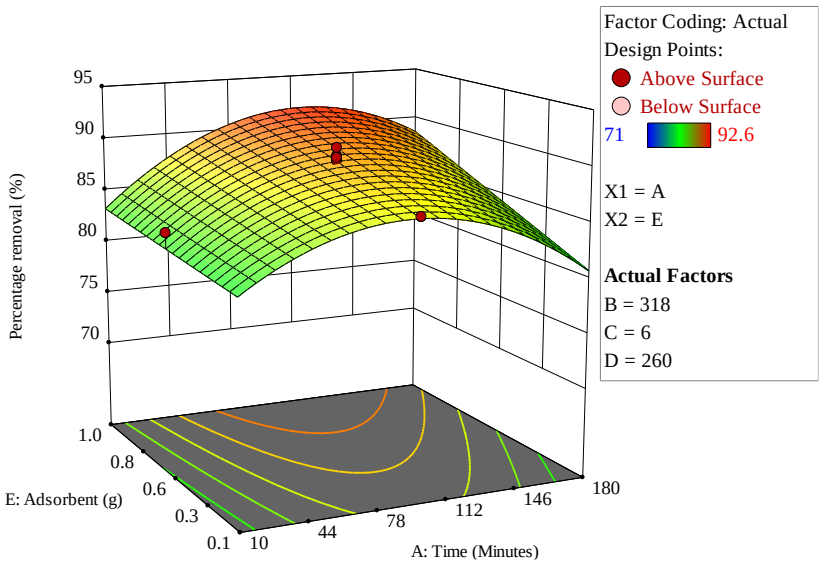

Figure 4.15 (ci): 3-D surface plot displaying the effect of time and adsorbent dosage on percent removal of PGT using *MOSB*.

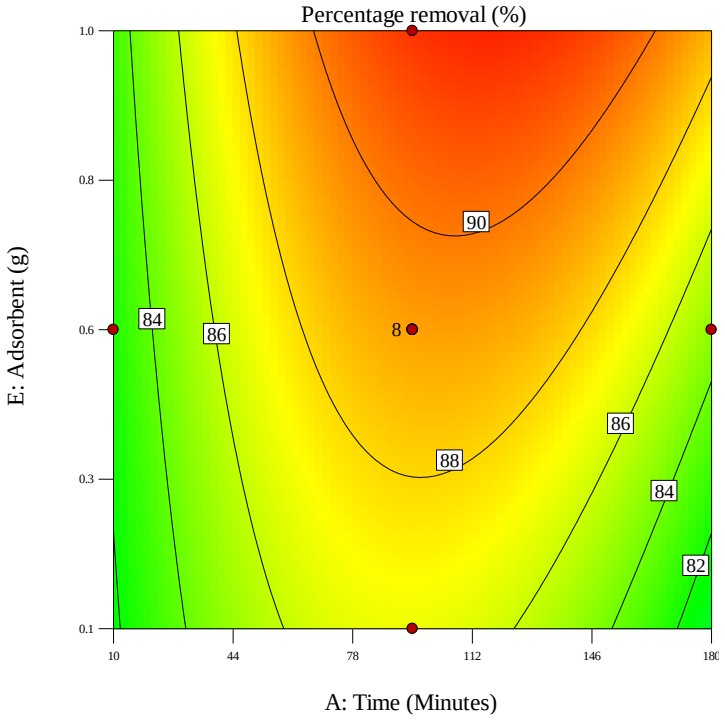

Figure 4.15 (cii): 2-D contour plot displaying the effect of time and adsorbent dosage on percent removal of PGT using *MOSB*.

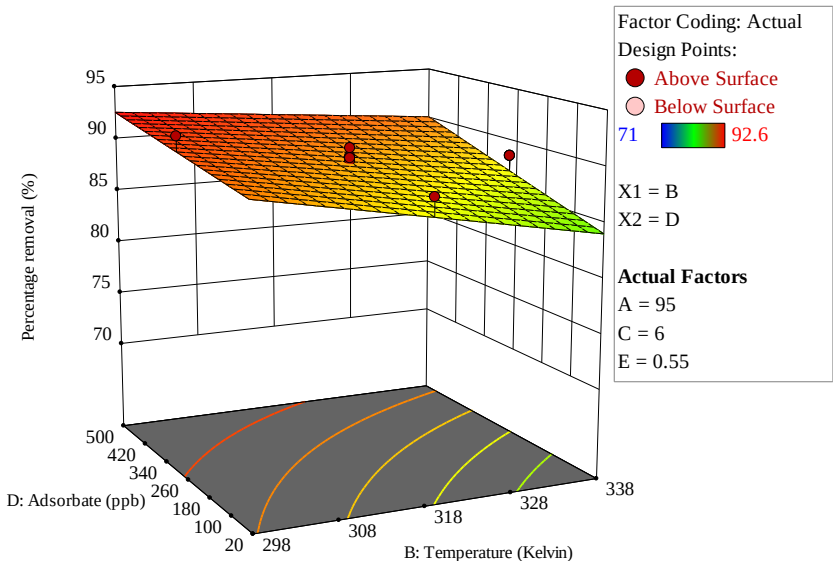

Figure 4.15 (di): 3-D surface plot displaying the effect of temperature and adsorbate concentration on percent removal of PGT using *MOSB*.

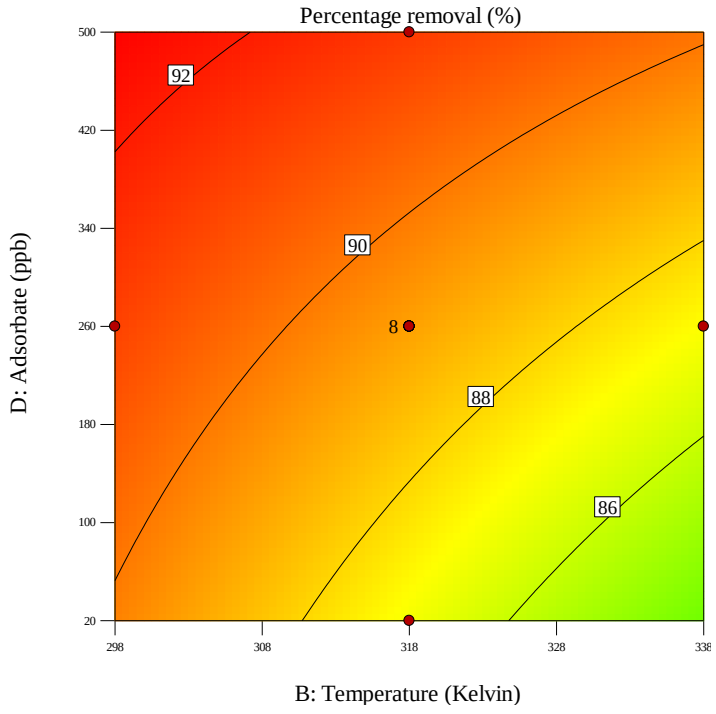

Figure 4.15 (dii): 2-D contour plot displaying the effect of temperature and adsorbate concentration on percent removal of PGT using *MOSB*.

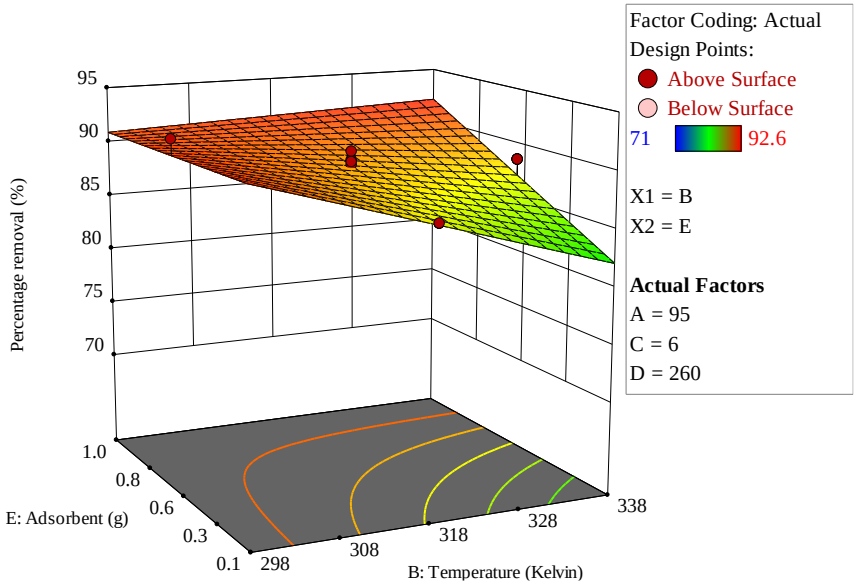

Figure 4.15 (ei): 3-D surface plot displaying the effect of temperature and adsorbent dosage on percent removal of PGT using *MOSB*.

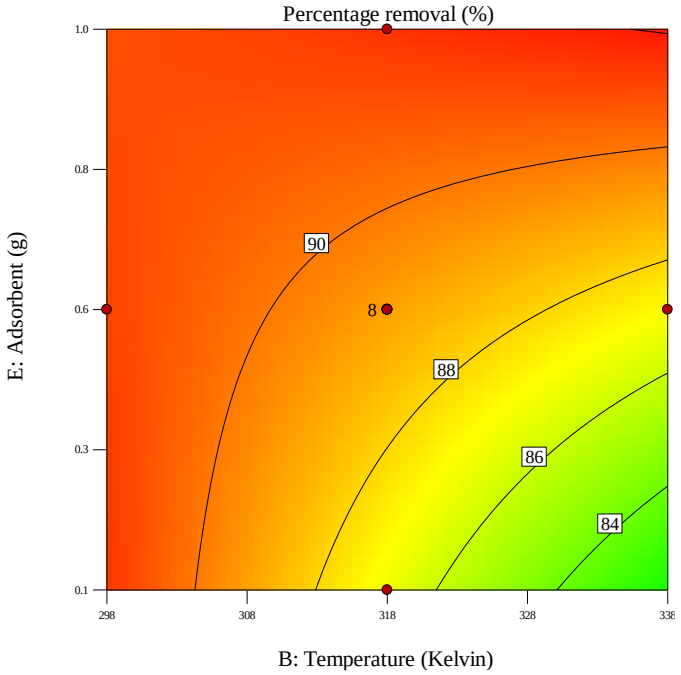

Figure 4.15 (eii): 2-D contour plot displaying the effect of temperature and adsorbent dosage on percent removal of PGT using *MOSB*.

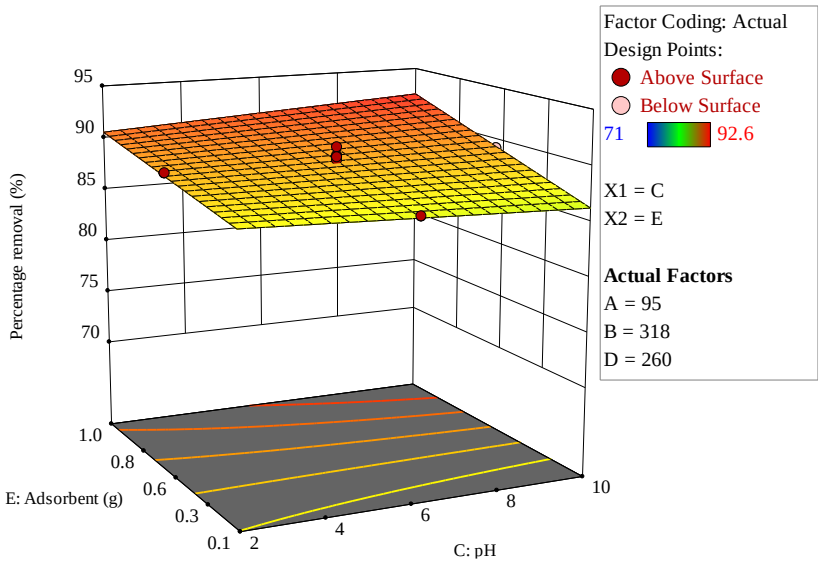

Figure 4.15 (fi): 3-D surface plot displaying the effect of pH and adsorbent dosage on percent removal of PGT using *MOSB*.

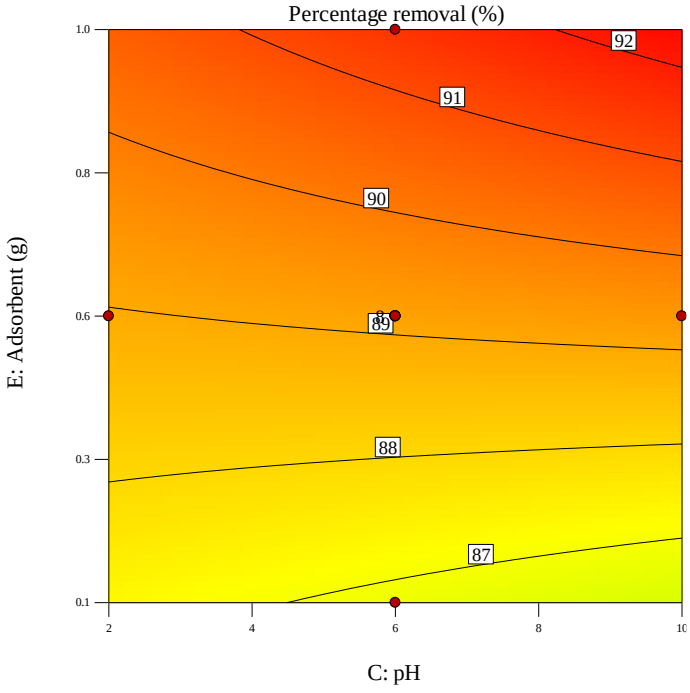

Figure 4.15 (fii): 2-D contour plot displaying the effect of pH and adsorbent dosage on percent removal of PGT using *MOSB*.

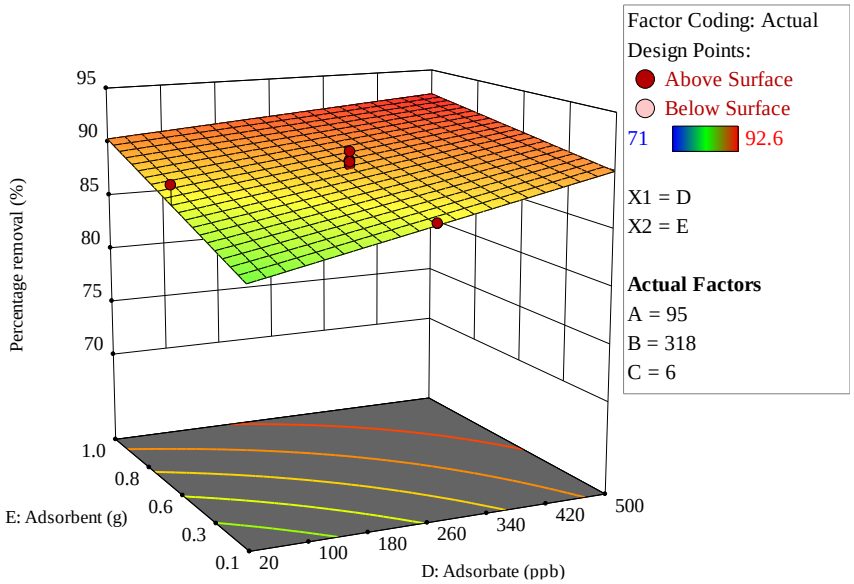

Figure 4.15 (gi): 3-D surface plot displaying the effect of adsorbate concentration and adsorbent dosage on percent removal of PGT using *MOSB*.

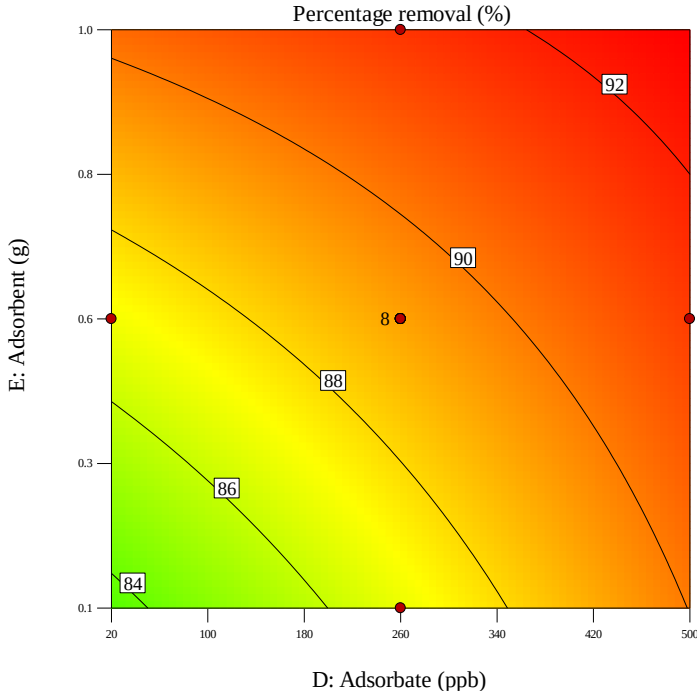

Figure 4.15 (gii): 2-D contour plot displaying the effect of adsorbate concentration and adsorbent dosage on percent removal of PGT using *MOSB*.

4.2.2.4 Optimization of PGT biosorption process

In the optimization analysis, the dependent variables, percentage removal and amount adsorbed (q_e), were set at maximum. For the independent factors, the temperature was minimized to depict experiments carried out at room temperature, and the pH was targeted at 7 to depict near-natural conditions of wastewater treatment; the adsorbent was minimized to ease disposal after use; the adsorbate was maximized while the contact time was left in range. The goal was to find the best settings that would result in the best response. Therefore, by applying the desirability function, the optimum response in terms of percentage removal was found to be 93.71% and 108.97 µg g^{-1} amount adsorbed at a contact time of 86.8 min, pH of 7.0, a temperature of 298 K, adsorbent dosage of 0.1 g and a desirability function of 0.995 (**Figure 4.16**). This confirms the validity of the proposed quadratic model and reliability in predicting the response (R). Acid-activated *MOSB* has been demonstrated to be an inexpensive alternative adsorbent capable of abstracting PGT from aqueous media. Its log K_{OW} of 3.9, as outlined in section 4.1.3, made it have a high sorption potential therefore increasing its adsorbility to *MOSB*.

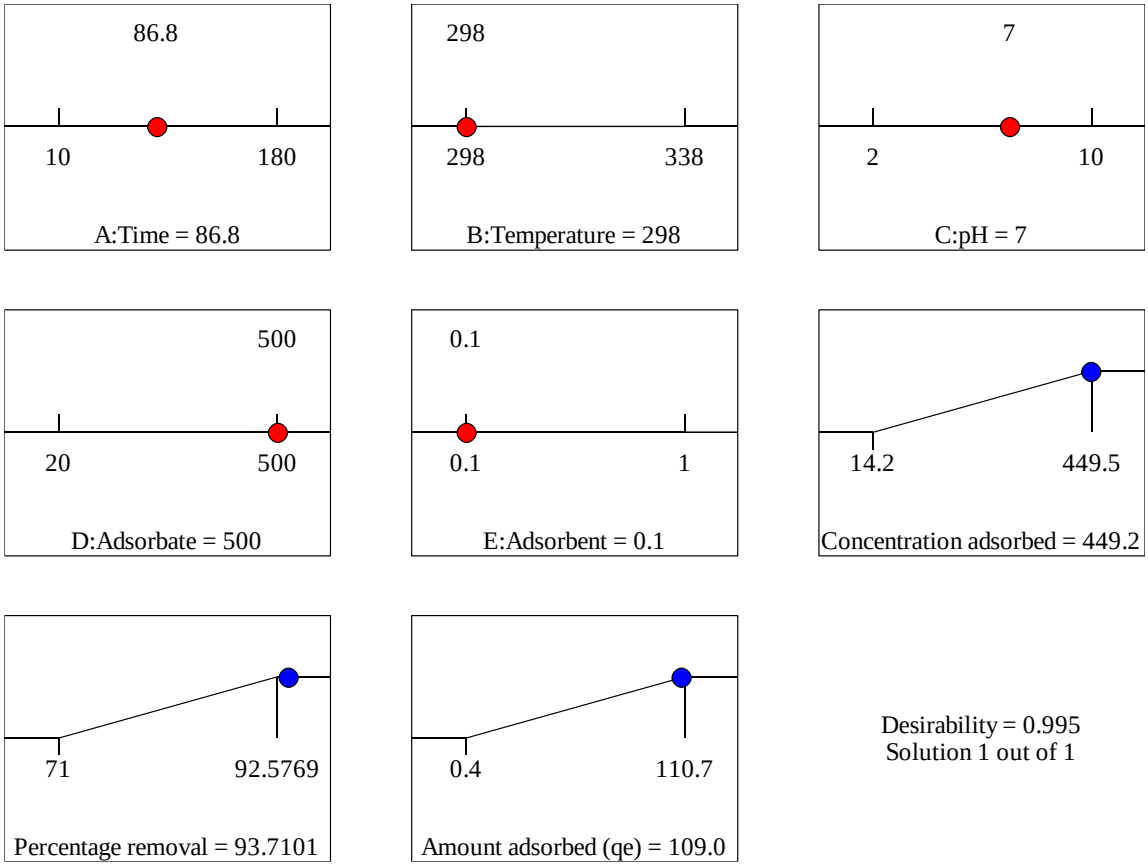

Figure 4.16: Ramps displaying the optimized parameters of PGT biosorption.

4.2.2.5 PGT adsorption isotherm studies

Higher adsorbate concentrations resulted in the rise of both the percentage removed and the amount adsorbed. This implied that more molecules of the adsorbate were being taken up by the vacant pores of the biosorbent. This is because increased concentration levels offer an intense impetus of the concentration gradient, which aids in overcoming the mass transfer resistance of the PGT molecules between the liquid and solid phases (Aly-Eldeen et al., 2018; Bayuo et al., 2020). The non-linearized isotherms are represented in **Figure 4.17** and **Table 4.15** highlights the adsorption isotherm parameters.

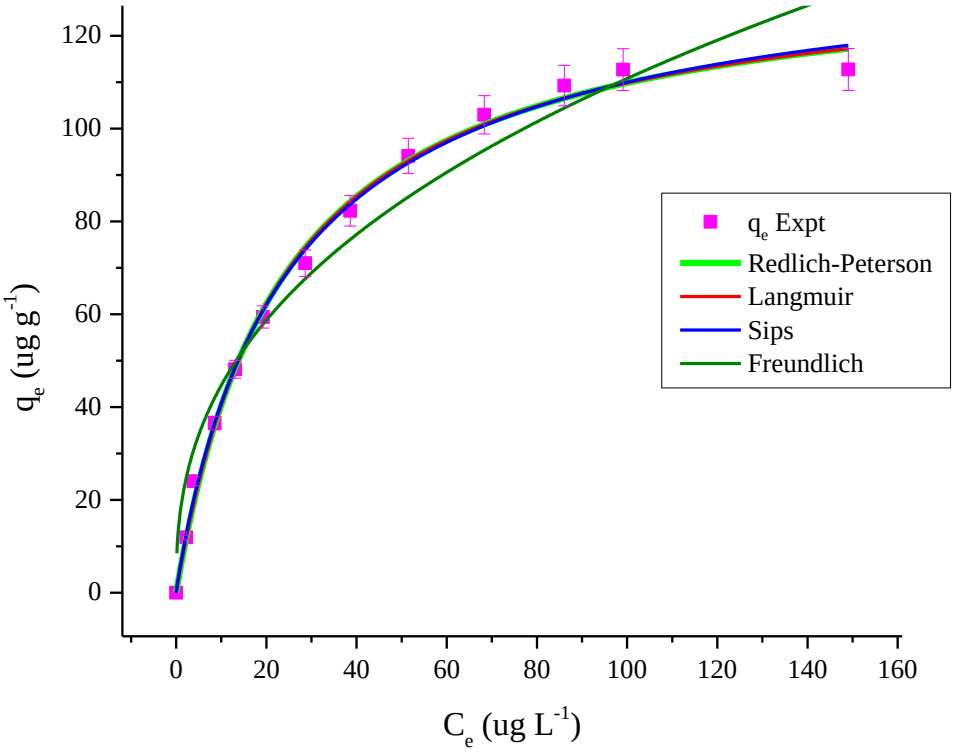

Figure 4.17: Non-linearized isotherms depicting PGT biosorption to *MOSB*.

The Langmuir model was able to adequately describe the experimental sorption data as depicted by the R^2 and the chi-square values (**Table 4.14**) thus implying a monolayer adsorption process; however, other adsorption surfaces were also available and contributed to the adsorption process, hence, the description by Sips model which combines both Langmuir and Freundlich models (Bagheri et al., 2020). This was in agreement with the Redlich-Peterson isotherm model whose g value was unity implying a leaning towards the Langmuir isotherm model. This was further corroborated by the Sips model where when the B_s value is closest to unity (0.950), it implies a monolayer type of adsorption thus corresponding to the Langmuir equation (Shikuku & Jemutai-Kimosop, 2020). The sips model closely followed the Langmuir model predicting a maximum

adsorption capacity of 139.9 µg g^{-1}. Overall, based on the chi-square values (**Table 4.15**), the equilibrium data were described by the isotherms in the order Langmuir > Sips > Redlich-Peterson >Freundlich. All the isotherms gave an $R^2 > 0.94$ thus implying that the biosorption was multi-mechanistic.

Table 4.15: Adsorption isotherm parameters

Isotherm	Langmuir	Freundlich	Redlich-Peterson	Sips
Parameters	Q_{max} = 135.84	1/n = 0.39	A = 5.74	a_s= 0.05
	K_L= 0.042	K_F = 18.03	B = 0.04	q_{MS} = 139.94
			g = 1	B_s = 0.95
Coefficient of determination (R^2)	0.995	0.942	0.995	0.995
Chi-square (χ^2)	7.71	75.04	8.48	8.09

From the Freundlich parameters, according to Treybal (1981), the magnitude of *n* demonstrates the favorability of the biosorption process. He notes that *n* values in the range 2-10 represent favorable, 1-2 moderately unfavorable, and less than 1 a poor adsorptive potential. In this study, the magnitude of *n* (2.54) illustrated a favorable adsorption process. Furthermore, 1/n indicates the strength of the adsorbate-adsorbent bonds. A value less than 1 indicates weak adsorbate-adsorbent forces corresponding to physisorption. The value obtained in this study (0.394) therefore implied that the process was physisorption and the interactions were weak (Shikuku & Jemutai-Kimosop, 2020).

Giles et al. (1974) subdivided isotherms for the adsorption of organic solutes into four main groups depending on their shapes: L, S, H, and C, and thereafter into subgroups. Based on this classification, the isotherm of PGT biosorption displayed an L-type curve,

subgroup 2c (**Figure 4.17**). In L-type curves, also called type 1 or normal curves, the L stands for Langmuir which in essence is consistent with data in this study fitting more into the Langmuir model. In such curves (**Figure 4.17**), the slope steadily falls with a rise in adsorbate concentration because no more vacant sites are available. The subgroup (2c) is majorly displayed by a microporous substrate, further confirming the porosity of *MOSB*.

4.2.2.6 Kinetic studies of PGT biosorption

There was a faster initial uptake reaching a peak before a decrease in percentage removal. PGT's initial rapid biosorption was facilitated by the abundance of vacant binding sites as confirmed by the initial adsorption rate (S_{rate}) and the half-life ($t_{1/2}$). There was no discernible change in the amount in the solid phase depicting achieved equilibrium as time passed. The equilibrium changed towards desorption as a result of saturation of the binding sites, repulsion between adsorbed PGT and those in bulk solution, and inaccessibility of the active inner pore sites**. Figure 4.18** represents the comparative fitting of the experimental data to the kinetic models.

The model's suitability to represent reaction kinetics was determined based on the proximity between experimental (q_{exp}) and model-predicted (q_{cal}) equilibrium adsorption capacities and the R^2 and χ^2 values. The calculated kinetic models' parameters are presented in **Table 4.16.**

Based on the R^2 and χ^2, and the closeness between the experimental (q_{exp}) and the model-predicted (q_{cal}) equilibrium adsorption capacities, both the PFO and PSO model forecasted the adsorption kinetics comparatively well but PFO gave the best fit. The PFO model assumes a physisorption-governed rate-determining step.

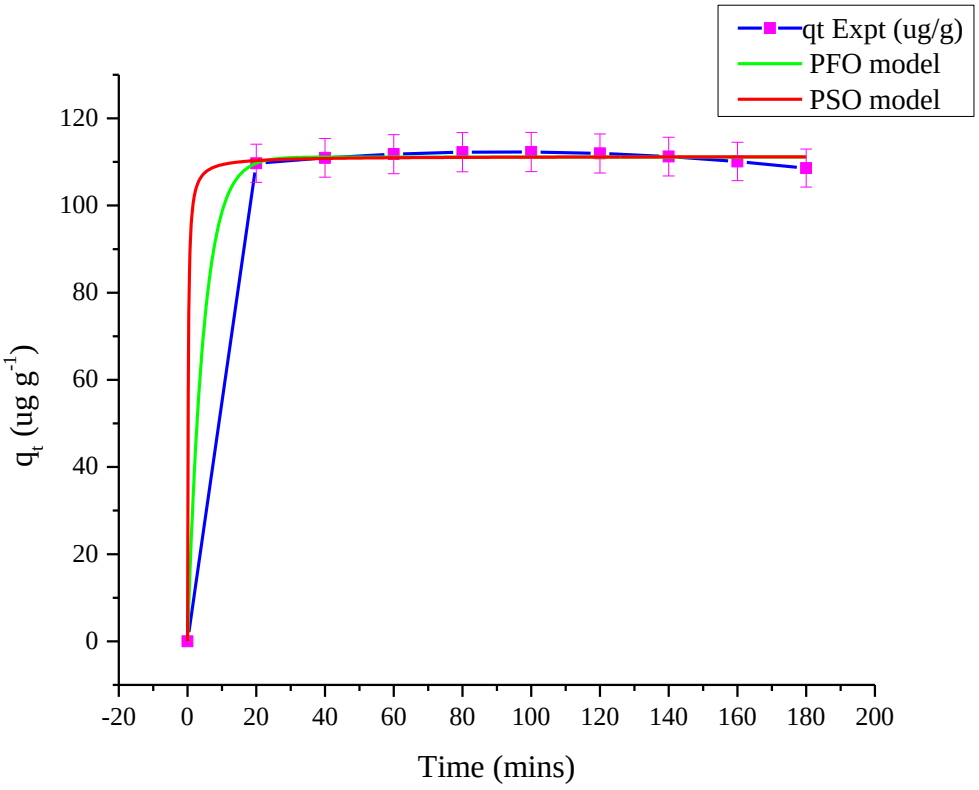

Figure 4.18: Kinetic model graphs for PGT biosorption to *MOSB*.

Table 4.16: Calculated kinetic parameters

Kinetic model	PFO	PSO
Parameters	q_e (cal) (µg g^{-1}) = 111.15	q_e (cal) (µg g^{-1}) = 111.29
	k_1 (min^{-1}) = 0.22	k_2 (min^{-1}) = 0.05
	q_e (expt)(µg g^{-1}) = 111.1	q_e (expt) (µg g^{-1}) = 111.1
S_{rate} (µg g^{-1} min^{-1})	24.12	631.65
$t_{1/2}$ (min^{-1})	3.19	0.18
R^2	0.999	0.999
χ^2	1.399	1.554

4.2.2.7 PGT biosorption thermodynamics

Figure 4.19 displays the Vant Hoff plot while **Table 4.17** depicts the thermodynamic parameters for PGT adsorption onto *MOSB.*

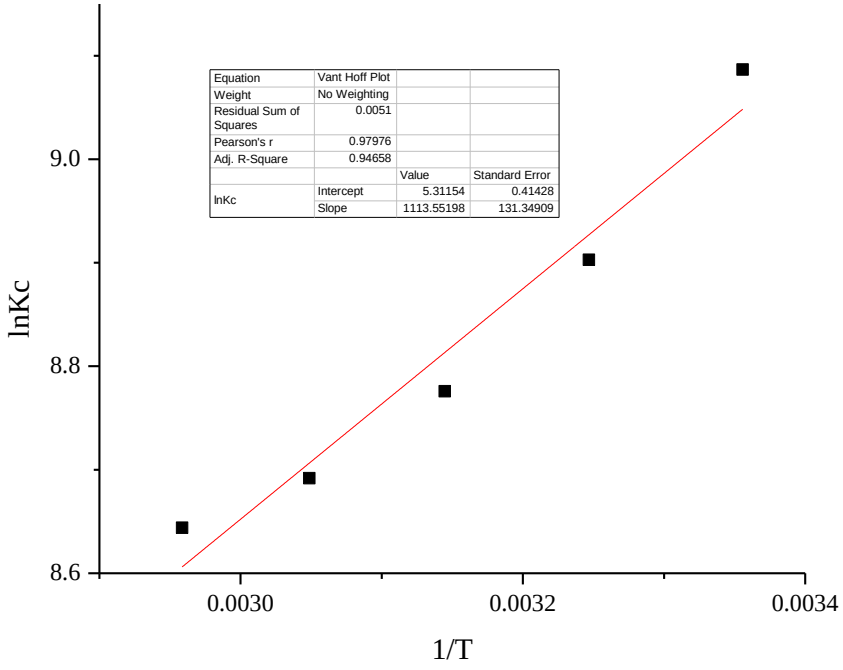

Figure 4.19: Vant Hoff plot for the biosorption of PGT to *MOSB.*

Table 4.17: Thermodynamic parameters for PGT adsorption onto *MOSB*

Compound	Temp. (K)	% removal	ΔG (kJ mol^{-1})	ΔH (kJ mol^{-1})	ΔS (J mol^{-1})
PGT	298	89.8	-22.5	-9.3	+44.2
	308	88.0	-22.8		
	318	86.6	-23.2		
	328	85.6	-23.7		
	338	85.0	-24.3		

From **Table 4.17**, there was a reduction in the percent removal of PGT with every increase in temperature implying an exothermic process. From the test statistics, however, the difference was slightly insignificant ($p > 0.05$). The negative ΔH value (-9.3 kJ mol^{-1}) confirmed exothermicity. The decline in removal with increased temperature is caused by greater water solubility at elevated temperatures by most adsorbates, adsorbate's reduced attraction for the adsorbent surface (Jemutai-Kimosop et al., 2020), and the exothermicity of the reaction which makes it less favorable with increased temperature. The biosorption of PGT to *MOSB* can thus be carried out at room temperature thus suiting utilization in real wastewater treatment systems. The ΔH value (-9.3 kJ mol^{-1}), far below the standard 40–120 kJ mol^{-1} for the chemisorption mechanism, indicates that the adsorption mechanism of PGT onto *MOSB* was physical with no exchange in electrons, thus consistent with the PFO model. Since $\Delta G < 0$ and $\Delta S > 0$ indicate spontaneity, the negative ΔG values and positive ΔS value implied that the adsorption of PGT onto *MOSB* was a spontaneous and favorable process. The physical adsorption mechanism suggested previously was supported by the comparatively small magnitudes of ΔG values. Further confirming exothermicity, the magnitude of ΔG increased with an increase in temperature thus becoming less favorable. The enhanced disorderliness and affinity of the adsorbent for the adsorbate at the liquid-solid interface has been demonstrated by the positive ΔS value (Luttah et al., 2023).

4.2.2.8 Effect of pH during PGT biosorption

The percent removal (R) as a function of pH is depicted in **Figure 4.20**. PGT biosorption was practically unaffected by pH variation with percent removal ranging between 89.8% to 90.1% in the pH range (2-12). The surface charge of the adsorbent (pHzpc) (**Figure**

4.21) was 6.8 (neutral) and the surface charge of the adsorbent was predicted to be positive below this number and negatively charged above it. 44% of *M.O* seeds are proteins of which 53% are globulins and 44% are albumins. These water-soluble proteins in *M.O* have a net positive charge (Militao et al., 2022). However, during modification with H_3PO_4, negatively charged phosphates ($HP\text{-}O^-$) from dissociated H_3PO_4 interacted with the positively charged *MOSB* resulting in a neutral species (Bagheri et al., 2020) thus confirming the neutrality of the adsorbent surface. Focusing on PGT, it is characterized by two pKa values; pKa_1 at -4.8 and pKa_2 at 18.9. Therefore, in the pH range of 2-12 of the study, PGT existed entirely as a neutral species implying that PGT was undissociated under varying pH conditions. As a result, electrostatic attractions were deemed negligible and consequently ruled out as an adsorption mechanism since both the adsorbent and adsorbate were neutral species unaffected by changes in pH. This is supported by similar observations by Moulahcene et al. (2015) as well as the independence of the % removal from solution pH. The mechanism of adsorption could be attributed to π-π interactions due to the presence of oxygen-containing functional groups such as carbonyl in the adsorbate interacting with aromatic rings (π electron receptors) found in the carbonaceous biomass compounds, such as cellulose hemicellulose, and lignin (Araujo et al., 2018). Furthermore, its log K_{OW} of 3.9 and a water solubility of 8.8 mg L^{-1} at 25 °C made it hydrophobic. Consequently, the interaction between the PGT's hydrophobic chain with the hydrophobic regions of the seed powder proteins contributed to the removal mechanism (**Figure 4.22**).

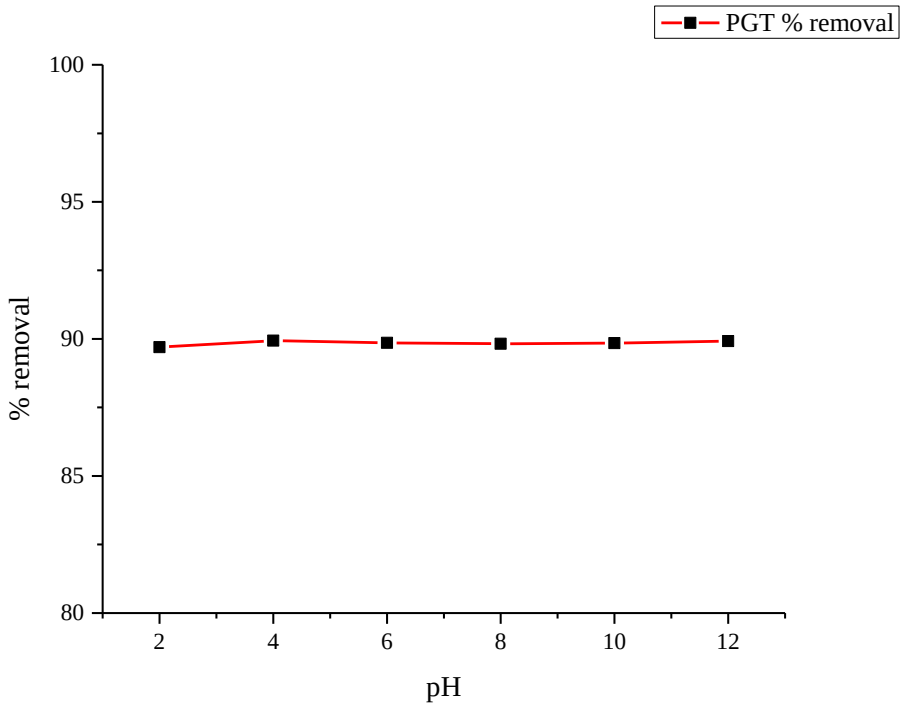

Figure 4.20: Percent removal of PGT by *MOSB* as a function of pH.

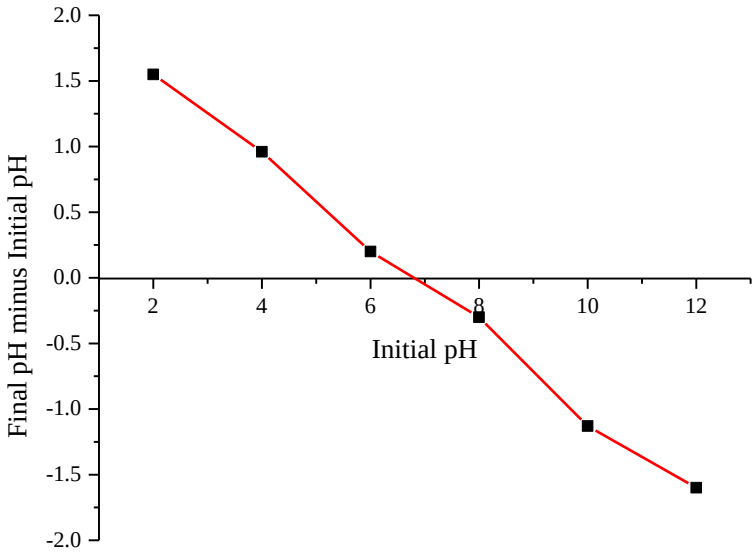

Figure 4.21: Point of zero charge for *MOSB*.

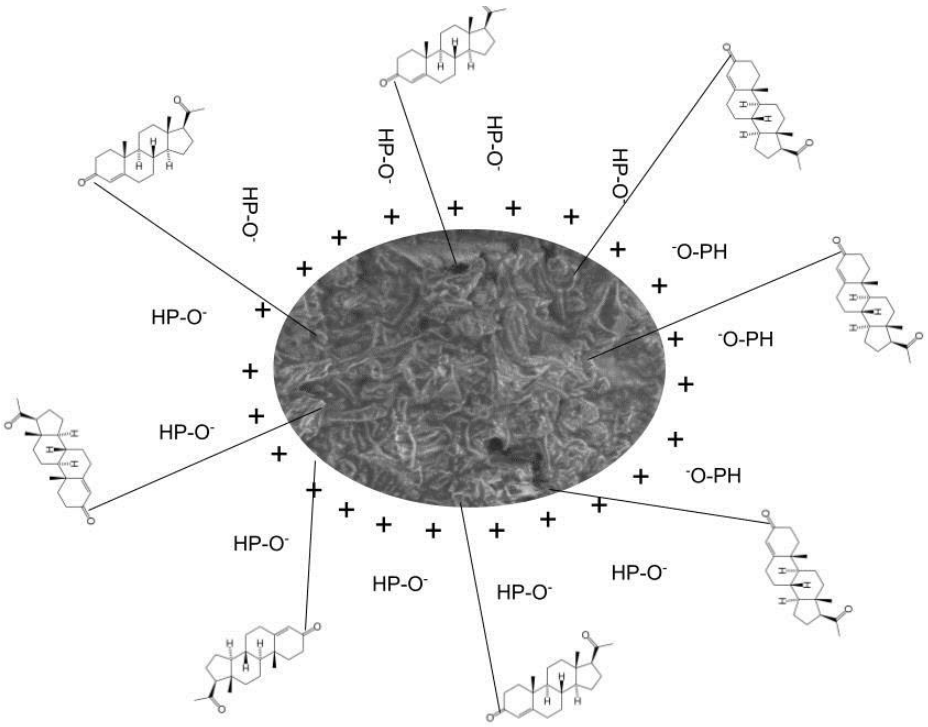

Figure 4.22: Mechanism of PGT biosorption to *MOSB* ($HP\text{-}O^-$ are the negatively charged phosphates while the + charges indicate the net positive caused by the water-soluble proteins in *M.O*).

4.2.3 LNR adsorption results

4.2.3.1 Central composite design (CCD) and data analysis for LNR biosorption

The design plan and results for LNR biosorption are shown in **Table 4.18**. The calibration curves and the chromatograms used for quantification are displayed in **Appendix 14**.

Table 4.18: LNR results obtained from the experimental design matrix

Run	Factor A: Time (Mins)	Factor B: Temperature (K)	Factor C: pH	Factor D: Adsorbate (ppb)	Factor E: Adsorbent (g)	Response 1 Concentration adsorbed (ppb)	Response 2 Percent removal %	Response 3 Amount adsorbed (qe) ug/g
1	180	298	2	20	0.1	17.2	86.1	4.3
2	10	298	2	20	0.1	14.9	74.4	3.7
3	10	298	2	500	0.1	389.1	77.8	97.3
4	95	318	6	260	0.55	238.6	91.8	10.8
5	180	298	10	500	1.0	456.6	91.3	11.4
6	180	298	10	20	0.1	17.4	87.2	4.4
7	180	338	10	20	0.1	15.5	77.4	3.9
8	10	338	10	20	1.0	13.7	68.5	0.3
9	10	338	10	500	1.0	379.3	75.9	9.5
10	95	318	6	260	0.55	237.1	91.2	10.8
11	180	338	10	20	1.0	18.1	90.5	0.5
12	95	298	6	260	0.55	238.6	91.8	10.8
13	180	338	2	500	1.0	446.7	89.3	11.2
14	10	298	10	20	1.0	13.9	69.4	0.3
15	95	318	2	260	0.55	234.5	90.2	10.7
16	10	338	2	500	0.1	393.9	78.8	98.5
17	95	318	6	260	0.1	238.6	91.8	59.6
18	10	318	6	260	0.55	210.3	80.9	9.6

Run	Factor A: Time (Mins)	Factor B: Temperature (K)	Factor C: pH	Factor D: Adsorbate (ppb)	Factor E: Adsorbent (g)	Response 1 Concentration adsorbed (ppb)	Response 2 Percent removal %	Response 3 Amount adsorbed (qe) ug/g
19	95	318	6	20	0.55	17.3	86.6	0.8
20	95	318	6	260	0.55	219.7	84.5	10.0
21	180	338	2	20	0.1	16.3	81.5	4.1
22	95	318	10	260	0.55	232.1	89.3	10.6
23	10	338	10	500	0.1	337.3	67.5	84.3
24	180	338	10	500	0.1	391.8	78.4	98.0
25	10	338	2	20	0.1	11.7	58.3	2.9
26	95	338	6	260	0.55	232.2	89.3	10.6
27	10	298	2	500	1.0	425.8	85.2	10.6
28	180	338	2	20	1.0	18.1	90.5	0.5
29	10	338	2	500	1.0	369.7	73.9	9.2
30	10	298	10	500	0.1	417.7	83.5	104.4
31	180	318	6	260	0.55	234.0	90.0	10.6
32	180	298	2	20	1.0	18.1	90.5	0.5
33	10	338	10	20	0.1	12.6	63.0	3.1
34	10	338	2	20	1.0	12.8	64.0	0.3
35	95	318	6	260	1.0	235.1	90.4	5.9
36	10	298	10	20	0.1	15.4	76.8	3.8
37	180	298	10	20	1.0	17.2	85.8	0.4
38	95	318	6	260	0.55	237.2	91.2	10.8

Run	Factor A: Time (Mins)	Factor B: Temperature (K)	Factor C: pH	Factor D: Adsorbate (ppb)	Factor E: Adsorbent (g)	Response 1 Concentration adsorbed (ppb)	Response 2 Percent removal %	Response 3 Amount adsorbed (qe) ug/g
39	180	338	2	500	0.1	454.7	90.9	113.7
40	180	338	10	500	1.0	454.5	90.9	11.4
41	180	298	2	500	0.1	440.9	88.2	110.2
42	95	318	6	260	0.55	222.1	85.4	10.1
43	95	318	6	260	0.55	232.9	89.6	10.6
44	95	318	6	260	0.55	236.0	90.8	10.7
45	10	298	10	500	1.0	395.9	79.2	9.9
46	180	298	10	500	0.1	452.9	90.6	113.2
47	10	298	2	20	1.0	14.1	70.3	0.4
48	95	318	6	260	0.55	228.7	88.0	10.4
49	180	298	2	500	1.0	458.8	91.8	11.5
50	95	318	6	500	0.55	456.8	91.4	20.8

The proposed model for LNR biosorption to *MOSB* was quadratic and ANOVA was used to determine the significant variation of the model terms and consequently the adequacy of the proposed model **(Table 4.19).**

Table 4.19**:** ANOVA for LNR's quadratic model

Source	Sum of Squares	df	Mean Square	F-value	p-value	
Model	3609.54	20	180.48	15.30	< 0.0001	significant
A-Time	1746.91	1	1746.91	148.10	< 0.0001	
B-Temperature	244.98	1	244.98	20.77	< 0.0001	
C-pH	7.96	1	7.96	0.68	0.42	
D-Adsorbate	315.95	1	315.95	26.79	< 0.0001	
E-Adsorbent	60.15	1	60.15	5.10	0.032	
AB	62.73	1	62.73	5.32	0.03	
AC	9.80	1	9.80	0.8307	0.37	
AD	95.60	1	95.60	8.11	0.01	
AE	36.44	1	36.44	3.09	0.09	
BC	6.99	1	6.99	0.5928	0.45	
BD	0.75	1	0.75	0.0637	0.80	
BE	75.09	1	75.09	6.37	0.02	
CD	14.96	1	14.96	1.27	0.27	
CE	1.84	1	1.84	0.16	0.67	
DE	0.27	1	0.27	0.02	0.88	
A^2	79.41	1	79.41	6.73	0.02	
B^2	0.85	1	0.85	0.07	0.79	
C^2	4.78	1	4.78	0.41	0.53	
D^2	11.13	1	11.13	0.94	0.34	
E^2	0.002	1	0.002	0.0002	0.99	

Source	Sum of Squares	df	Mean Square	F-value	p-value	
Residual	342.07	29	11.80			
Lack of Fit	287.05	22	13.05	1.66	0.25	not significant
Pure Error	55.02	7	7.86			
Cor Total	3951.61	49				

The Model F-value of 15.30 implied that the model was significant. There was only a 0.01% chance that an F-value this large could occur due to noise. P-values less than 0.05 indicate model terms are significant. In this case, A, B, D, E, AB, AD, BE, and A^2 were significant model terms. The lack of fit F-value of 1.66 implied that the lack of fit was not significant relative to the pure error. There was a 25.25% chance that a lack of fit F-value this large could occur due to noise. Non-significant lack of fit is good and therefore the model fitted. Values greater than the p-value of 0.05 indicate the model terms are insignificant. If there are many insignificant model terms (not counting those required to support hierarchy), model reduction is recommended, and Table **4.20** displays the reduced quadratic model.

Table 4.20: ANOVA for Reduced LNR's Quadratic model

Source	Sum of Squares	df	Mean Square	F-value	p-value	
Model	3558.81	10	355.88	35.33	< 0.0001	significant
A-Time	1746.91	1	1746.91	173.45	< 0.0001	
B-Temperature	244.98	1	244.98	24.32	< 0.0001	
D-Adsorbate	315.95	1	315.95	31.37	< 0.0001	
E-Adsorbent	60.15	1	60.15	5.97	0.02	
AB	62.73	1	62.73	6.23	0.02	
AD	95.60	1	95.60	9.49	0.004	
AE	36.44	1	36.44	3.62	0.07	
BE	75.09	1	75.09	7.46	0.01	

Source	Sum of Squares	df	Mean Square	F-value	p-value	
A^2	156.64	1	156.64	15.55	0.0003	
D^2	33.17	1	33.17	3.29	0.08	
Residual	392.80	39	10.07			
Lack of Fit	337.78	32	10.56	1.34	0.36	not significant
Pure Error	55.02	7	7.86			
Cor Total	3951.61	49				

The model F-value of 35.33 implied that the model was significant. There was only a 0.01% chance that an F-value this large could occur due to noise. In this case, A, B, D, E, AB, AD, BE, and A^2 were significant model terms. The lack of fit F-value of 1.34 implied that the lack of fit was not significant relative to the pure error. There was a 36.3% chance that a lack of fit F-value this large could occur due to noise. Non-significant lack of fit implied that the model fitted. From the fit statistics, the R^2 was 0.911. The predicted R^2 of 0.825 was in reasonable agreement with the adjusted R^2 of 0.875; i.e., the difference was less than 0.2. This model can be used to navigate the design space. **Equation 4.2** for the reduced quadratic model can be used to make predictions about the response for given levels of each factor.

$$R = 89.95 + 7.17 * A + -2.68 * B + 3.05 * D + 1.33 * E + 1.40 * AB + -1.73 * AD + 1.07 * AE + 1.53 * BE + -6.57 * A^2 + -3.02 * D^2 \quad \text{(Equation 4. 2)}$$

Figure 4.23 (a), of actual experimental values versus predicted values, displays a reasonable distribution along a straight line implying a good relationship. Diagnostic plots further indicating the fitness of the model by correlating the experimental and predicted values of adsorption of LNR to *MOSB* are shown in **Figures 4.23 (b-f)**. **Figure 4.23 (b)** displays a straight line when the normal percentage probability was plotted against

externally studentized residuals demonstrating that the error terms were normally distributed. This confirmed the goodness of fit of the model predictions. In **Figure 4.23 (c)**, the random scatter along a center line of the residuals of the predicted values of LNR biosorption illustrated that the observed and predicted values were in agreement and this is corroborated by **Figure 4.23 (d)** showing a distribution along a center line in the residuals of the run. The Box-Cox plot (**Figure 4.23 (e)**) for power transform did not recommend any data transformation. Cook's distance (**Figure 4.23 (f)**) is considered high if it is greater than 0.5 and extreme if it is greater than 1. The values in the biosorption of LNR were much less and thus satisfactory.

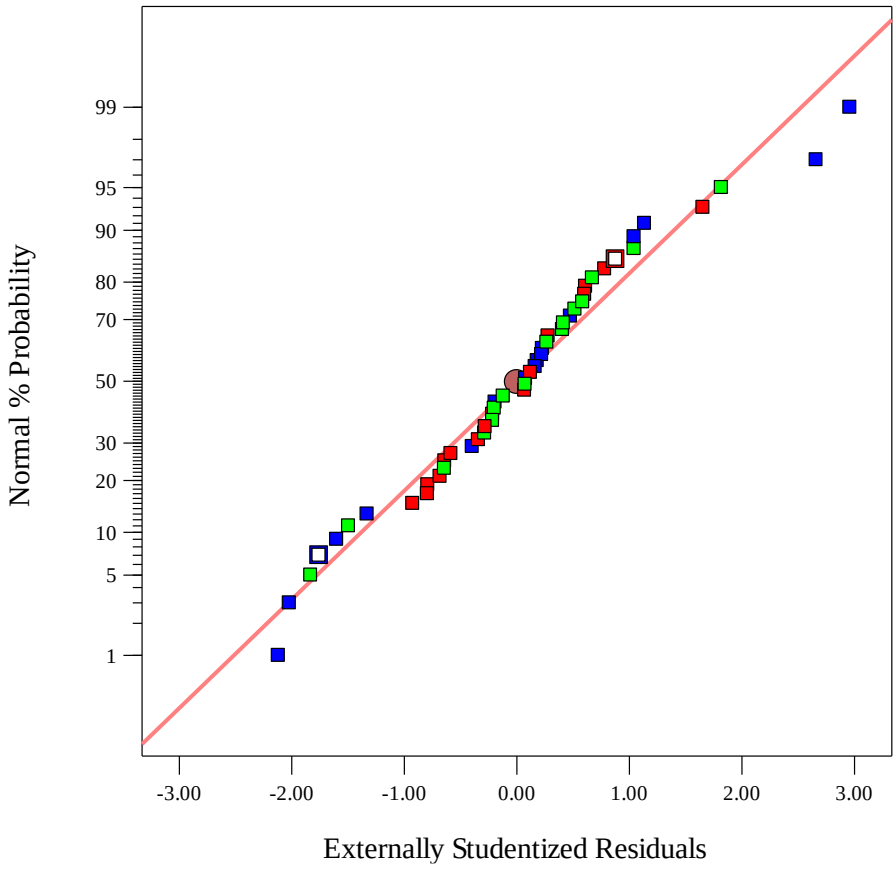

Figure 4.23 (a): Normal plot of residuals for LNR biosorption.

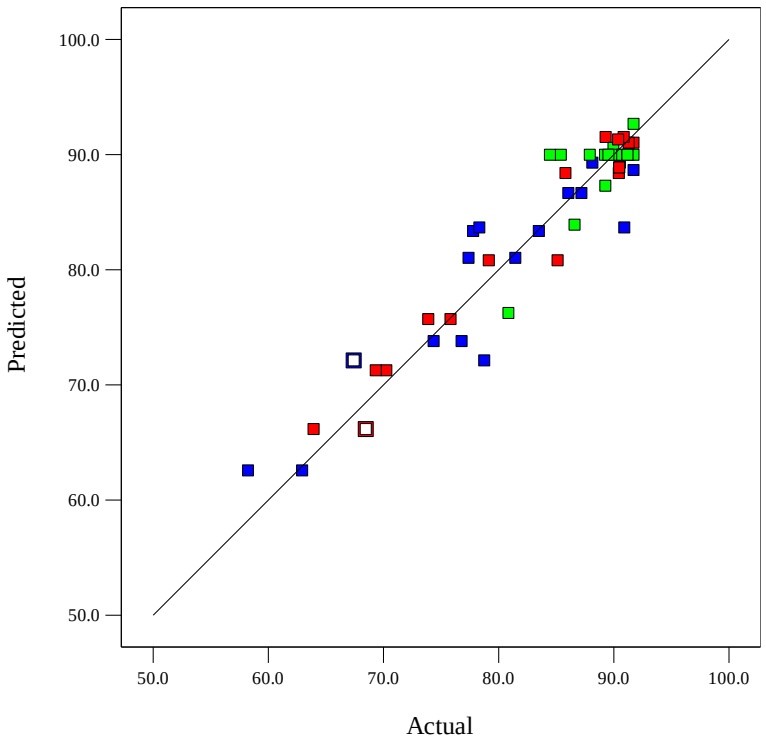

Figure 4.23 (b): Predicted versus actual during LNR biosorption.

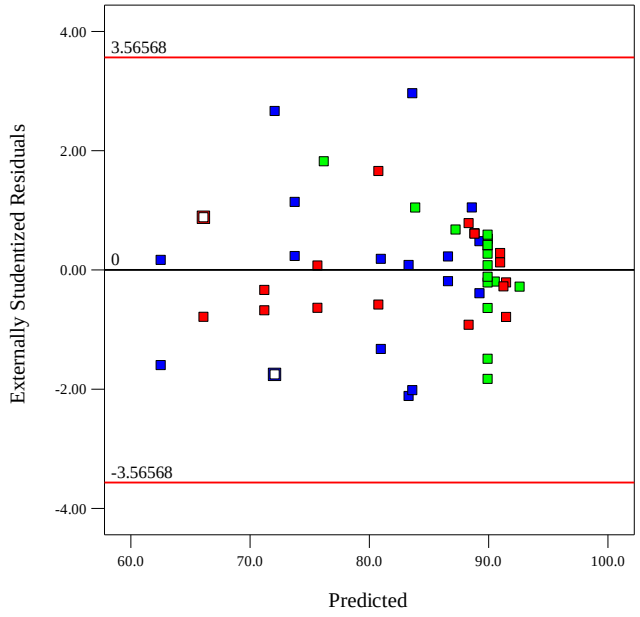

Figure 4.23 (c): Residuals versus predicted during LNR biosorption.

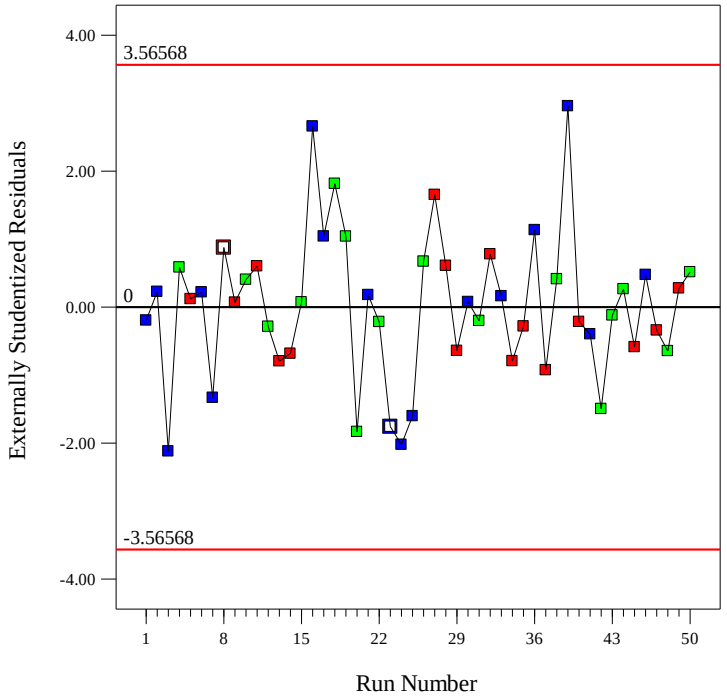

Figure 4.23 (d): Predicted versus run during LNR biosorption.

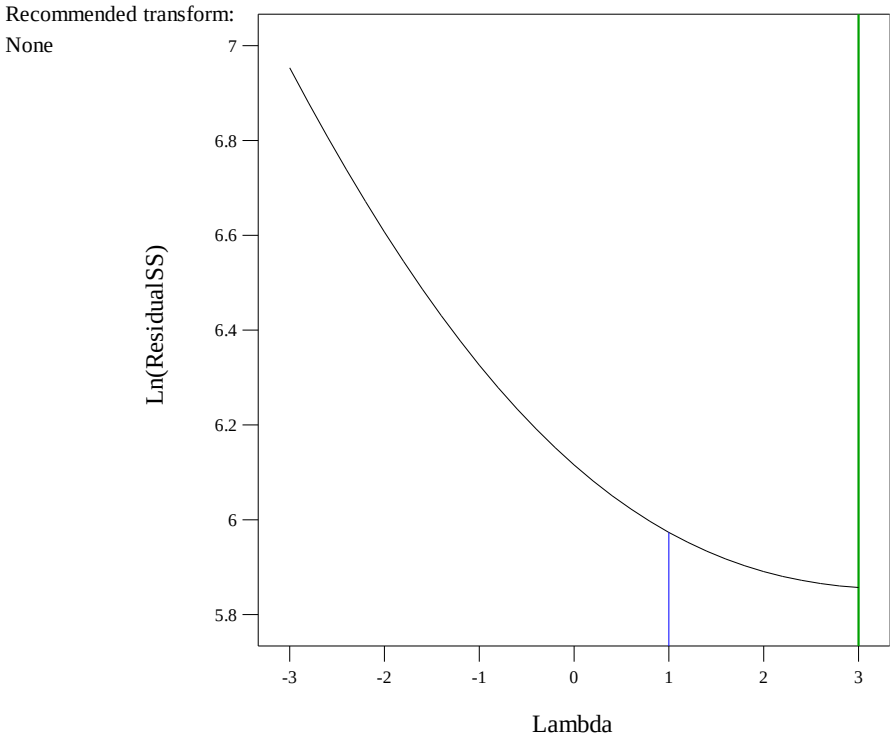

Figure 4.23 (e): Box-Cox plot for power transform for LNR biosorption.

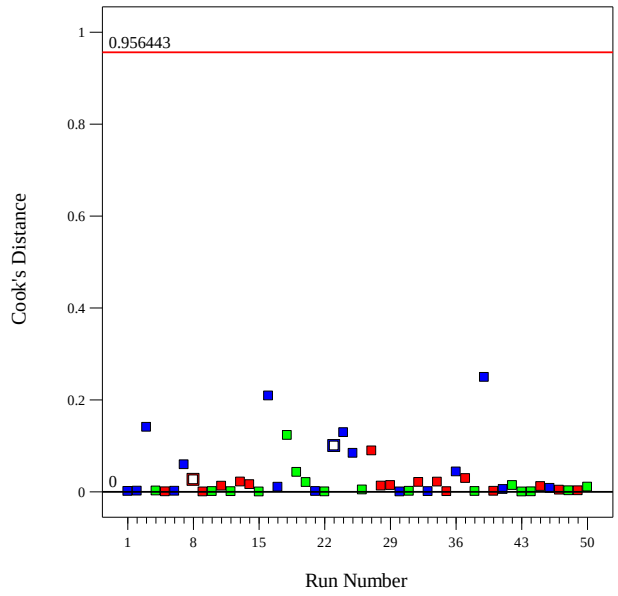

Figure 4.23 (f): Cooks distance for LNR biosorption.

4.2.3.2 Model Graphs for All Factor Interactions

Figure 4.24 (a) displays all factor perturbation around a reference point of contact time-95 min, temperature-318 K, adsorbate concentration of 260 µg L^{-1}, pH-6, and 0.55g of biosorbent. **Figures 4.24 (b-f)** demonstrate how the independent variables affected the biosorption process while accounting for all factor interactions. The percentage removal increased more rapidly initially, peaking before it decreased as contact duration was changed between 10 and 180 min (**Figure 4.24 (b)**). This could be attributed to initial free binding sites before they were all occupied. The removal efficiency declined as the temperature varied from 298 to 338 K, (**Figure 4.24 (c)**). This supports the use of *MOSB* in room temperature conditions in real wastewater applications thus saving energy costs. The results of the ANOVA tests are supported by **Figure 4.24 (d**) which displays a minimal curvature implying that LNR abstraction was not impacted by pH implying that neutral conditions are favourable. Further explanations on the effect of pH and the

mechanism of biosorption are given in **section 4.2.3.8**. The percentage removed and consequently, the amount adsorbed both rose as the concentration of the adsorbates increased, as seen in **Figure 4.24(e)** due to more available molecules for biosorption**.** The amount adsorbed went up from 87.3% to 90.4% when the quantity of *MOSB* was increased from 0.1 to 1 g (**Figure 4.24 (f)**). This is consistent with the number of increasing sites of adsorption (Aly-Eldeen et al., 2018). As the biomass to solute concentration ratio increases, there is a very rapid exterior sorption onto the biosorbent surface consequently reducing the adsorbate concentration in the solution. This is because a constant mass of biomass can only adsorb a definite amount of LNR. Therefore, the more the adsorbent dosage is, the bulkier the pollutant concentration that a fixed mass of *MOSB* can clean up. However, this is limited to the number of vacant sites in the adsorbent.

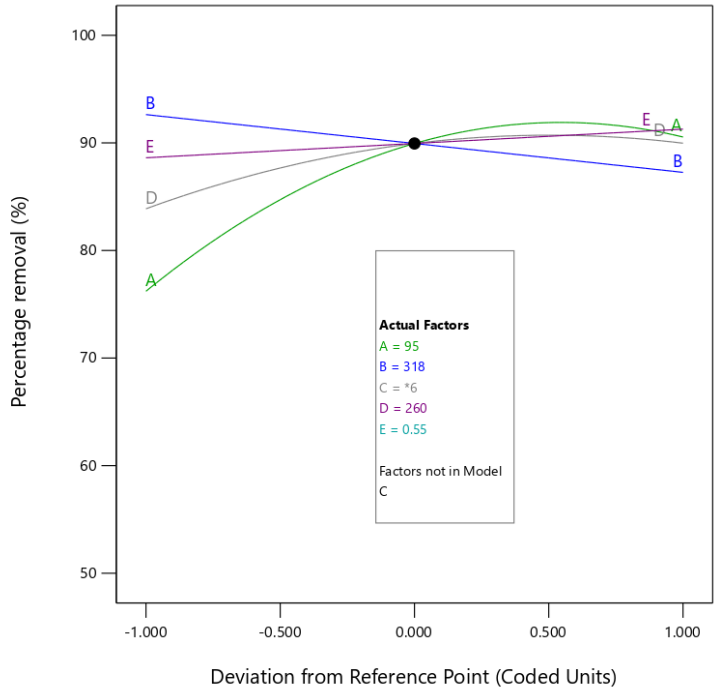

Figure 4.24 (a): Graph depicting all factor perturbation around a reference point during the biosorption of LNR to *MOSB.*

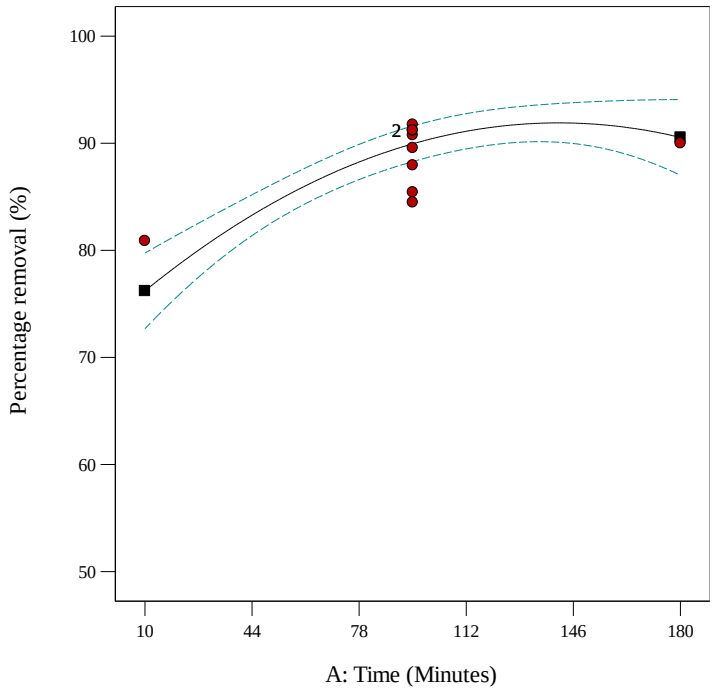

Figure 4.24 (b): Effect of time on percent removal of LNR using *MOSB.*

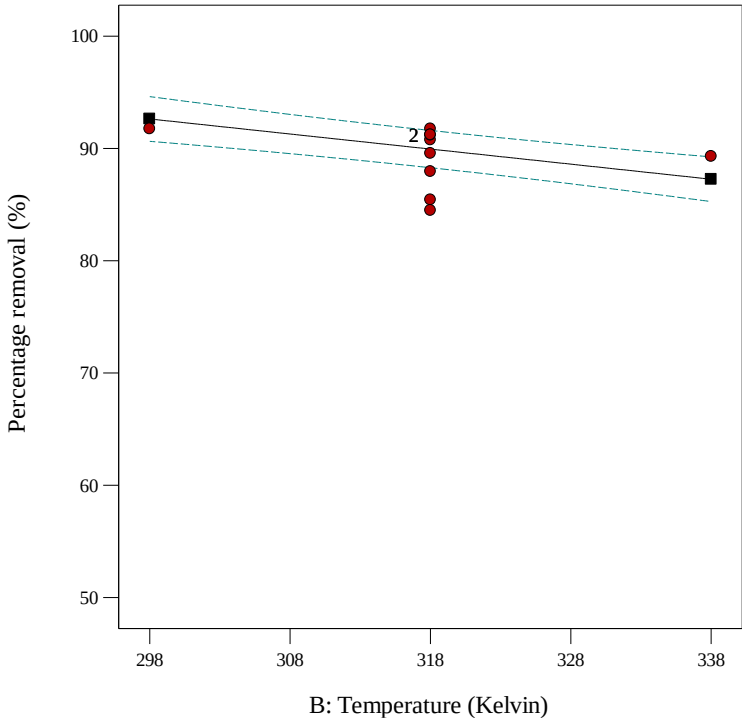

Figure 4.24 (c): Effect of temperature on percent removal of LNR using *MOSB.*

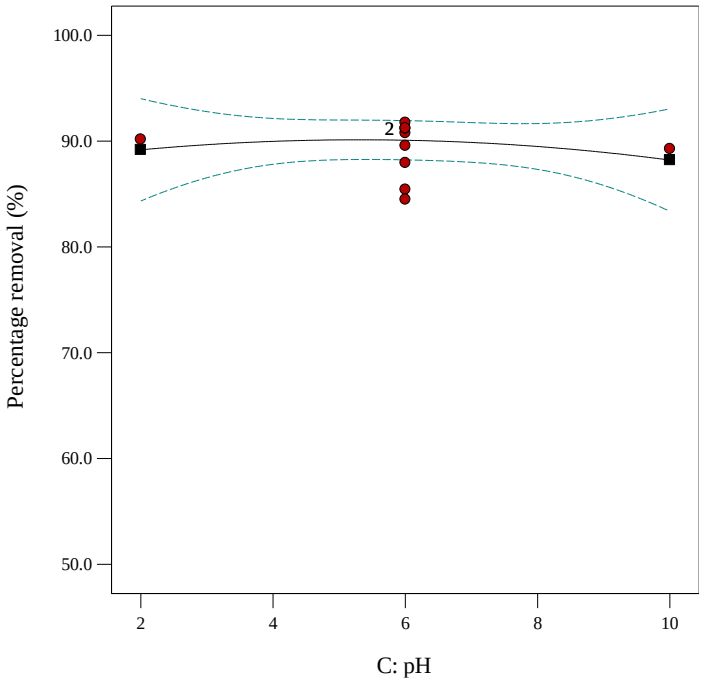

Figure 4.24 (d): Effect of pH on percent removal of LNR using *MOSB.*

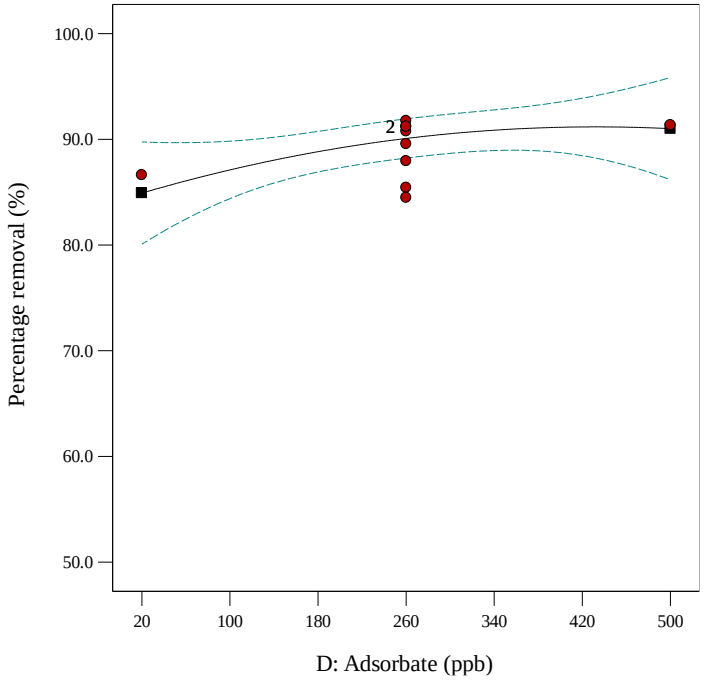

Figure 4.24 (e): Effect of adsorbate concentration on percent removal of LNR using *MOSB.*

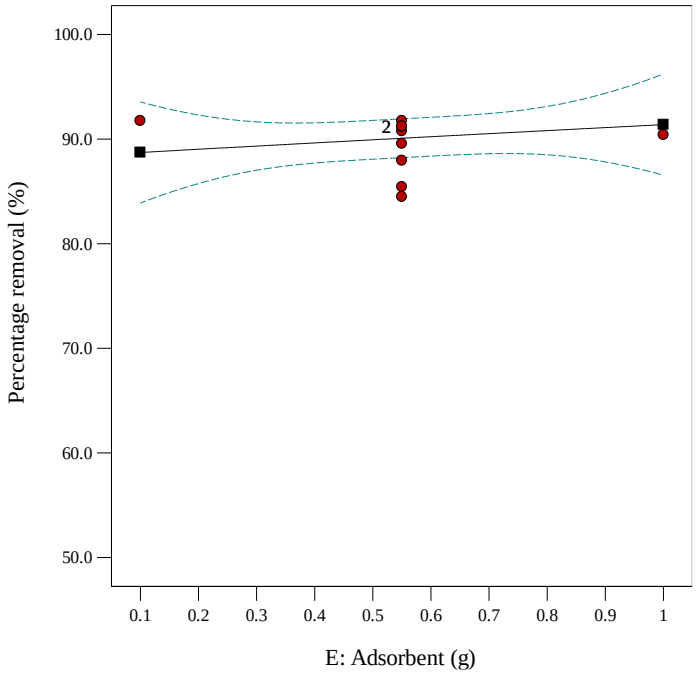

Figure 4.24 (f): Effect of adsorbent dosage on percent removal of LNR using *MOSB.*

4.2.3.3 Three-dimensional surface plots for the adsorption of LNR onto *MOSB*

Figures 4.25 (ai-dii) display 3-D plots and their respective contour plots depicting the effect of the combinations of the independent variables on the adsorption efficiency of *MOSB.* From **Figures 4.25 (ai & aii)**, adsorption efficiency was affected by both contact time and temperature. Closer to room temperature (298 K), suitable for real wastewater treatment, was more favorable while contact time was optimum beyond 78 min. **Figures 4.25 (bi & bii)** show that the influence of pH was not felt in the process even though the longer the contact time, the higher the adsorption efficiency. The same range of contact time and an upsurge of adsorbate and adsorbent augmented the adsorption efficiency (**Figures 4.25 ci, cii, di & dii**). pH was a non-significant variable and most of its interactions with other variables were ignored.

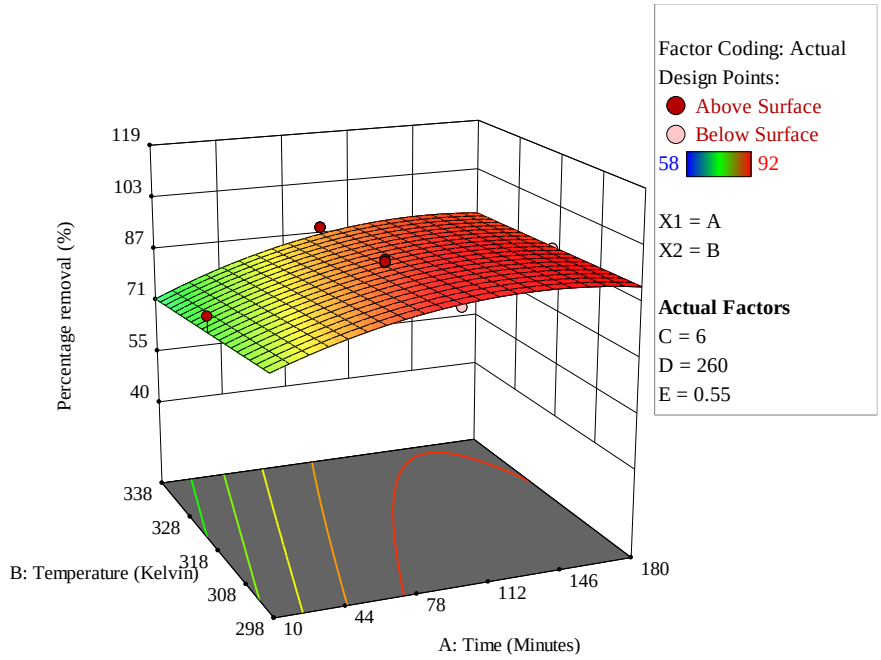

Figure 4.25 (ai): 3-D surface plot displaying the effect of time and temperature on percent removal of LNR using *MOSB.*

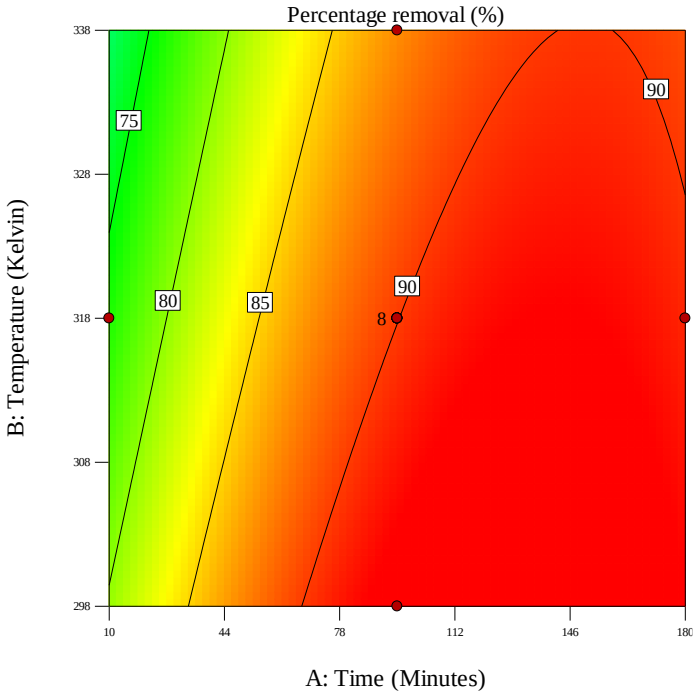

Figure 4.25 (aii): 2-D contour plot displaying the effect of time and temperature on percent removal of LNR using *MOSB.*

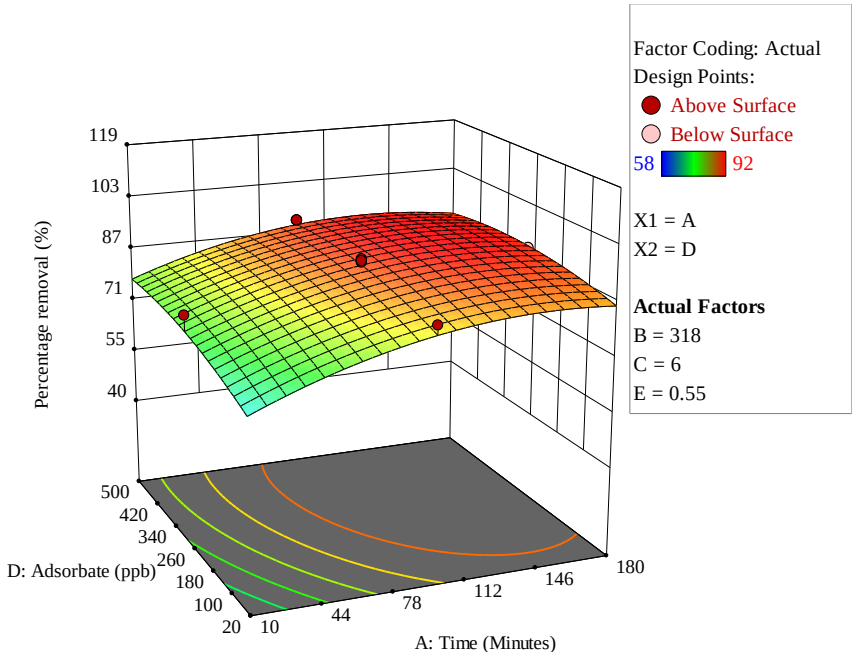

Figure 4.25 (bi): 3-D surface plot displaying the effect of time and adsorbate concentration on percent removal of LNR using *MOSB*.

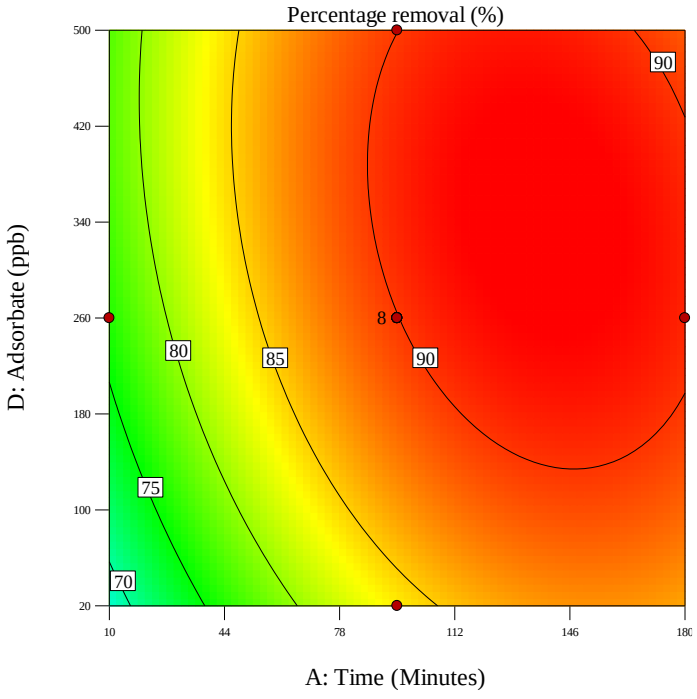

Figure 4.25 (bii): 2-D contour plot displaying the effect of time and adsorbate concentration on percent removal of LNR using *MOSB*.

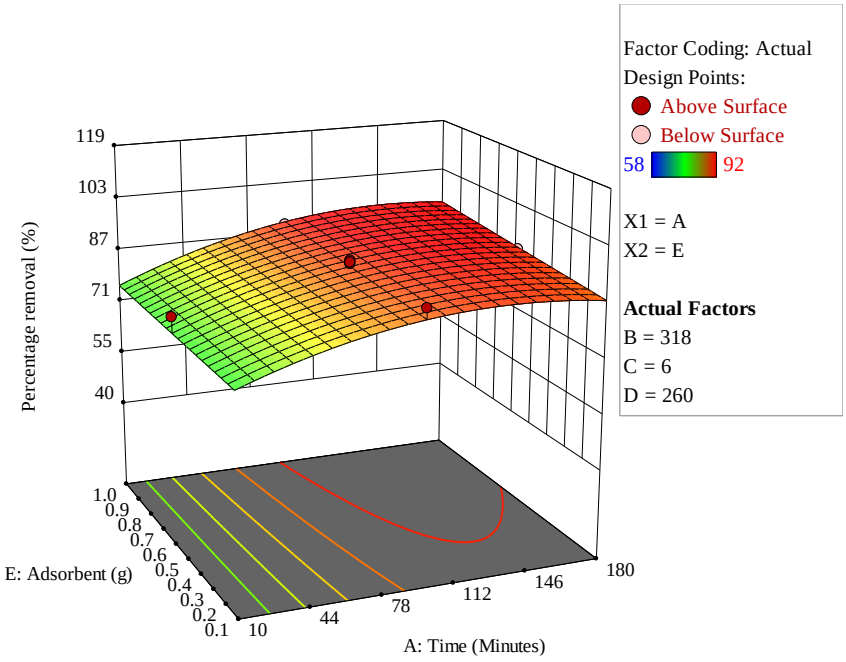

Figure 4.25 (ci): 3-D surface plot displaying the effect of time and adsorbent dosage on percent removal of LNR using *MOSB*.

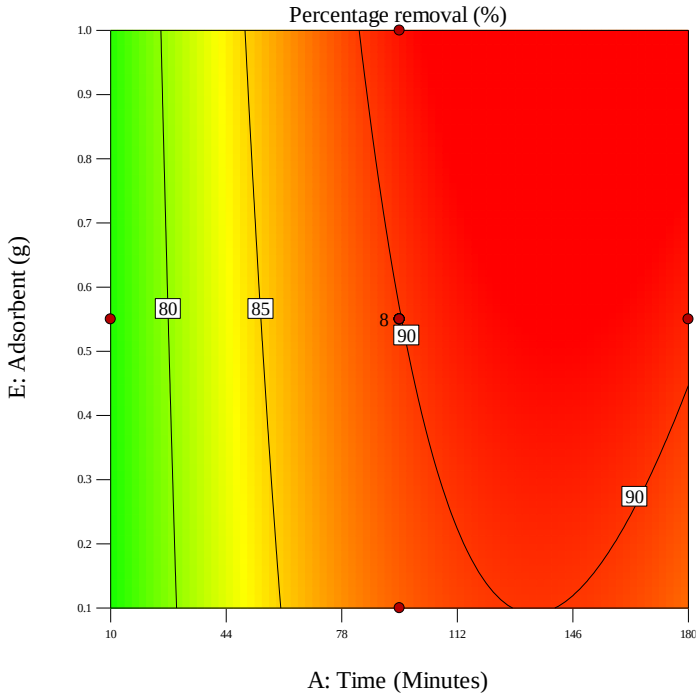

Figure 4.25 (cii): 2-D contour plot displaying the effect of time and adsorbent dosage on percent removal of LNR using *MOSB*.

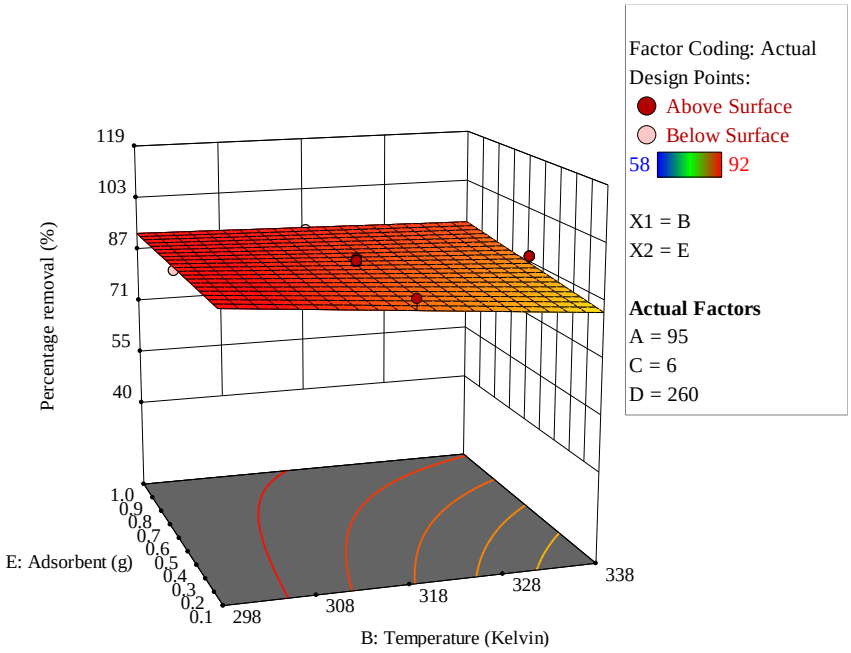

Figure 4.25 (di): 3-D surface plot displaying the effect of temperature and adsorbent dosage on percent removal of LNR using *MOSB.*

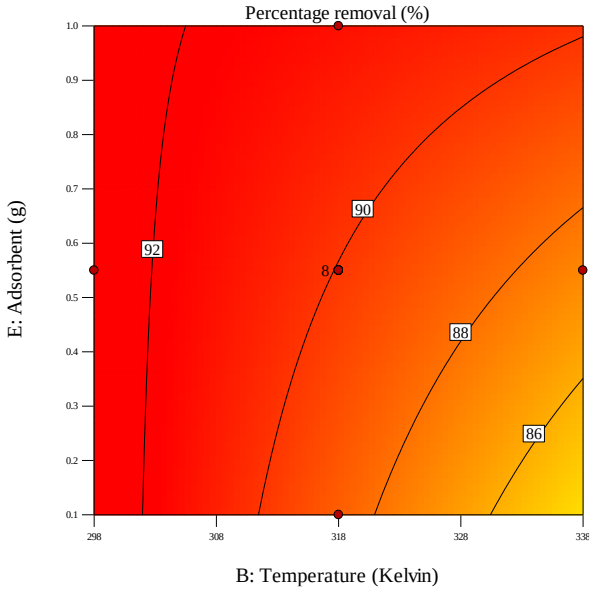

Figure 4.25 (dii): 2-D contour plot displaying the effect of temperature and adsorbent dosage on percent removal of LNR using *MOSB.*

4.2.3.4 Optimization of the biosorption of LNR to *MOSB*

The optimization analysis was carried out as in section 4.2.2.4 to obtain optimum values for which optimum response would be achieved in the biosorption of LNR to *MOSB*. Therefore, by applying the desirability function, the optimum response in terms of percentage removal was found to be 91.8% and 108.9 µg g^{-1} amount adsorbed at a contact time of 154 min, pH of 7.0, a temperature of 298 K, adsorbent dosage of 0.1 g and a desirability function of 0.980 (**Figure 4.26**). This confirmed the validity of the proposed quadratic model and reliability in predicting the response (R).

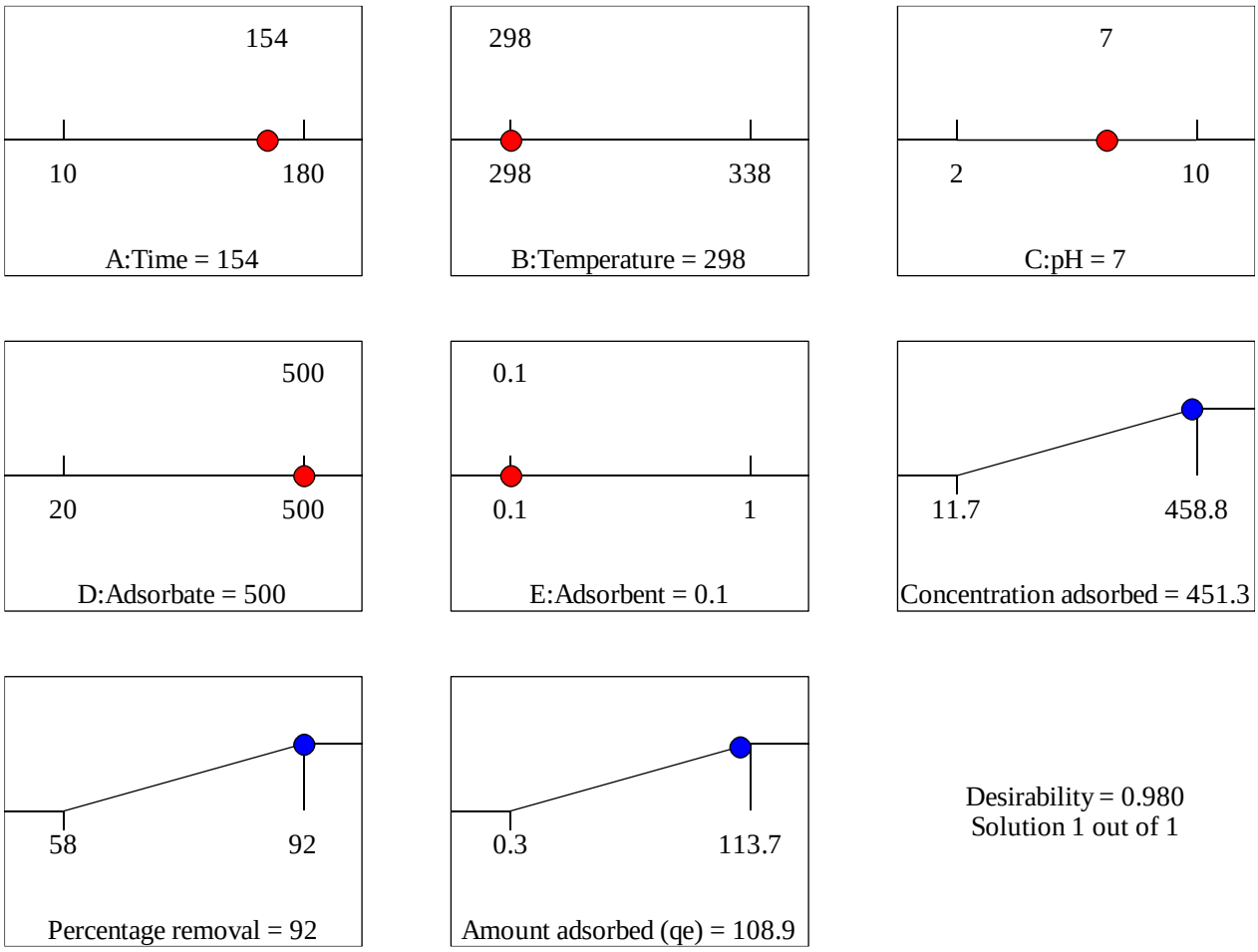

Figure 4.26: Optimization ramps for biosorption of LNR to *MOSB*.

4.2.3.5 LNR biosorption isotherm studies

The adsorption efficiency was boosted with the increase in the concentration of the LNR. This could be attributed to the availability of binding sites in the biosorbent and thus increased interactions between the adsorbate and the biosorbent and mass gradient between the solute and the bulk solution until the maximum adsorption capacity was attained (Luttah et al., 2023). The non-linearized isotherms are represented in **Figure 4.27** and **Table 4.21** highlights the adsorption isotherm parameters.

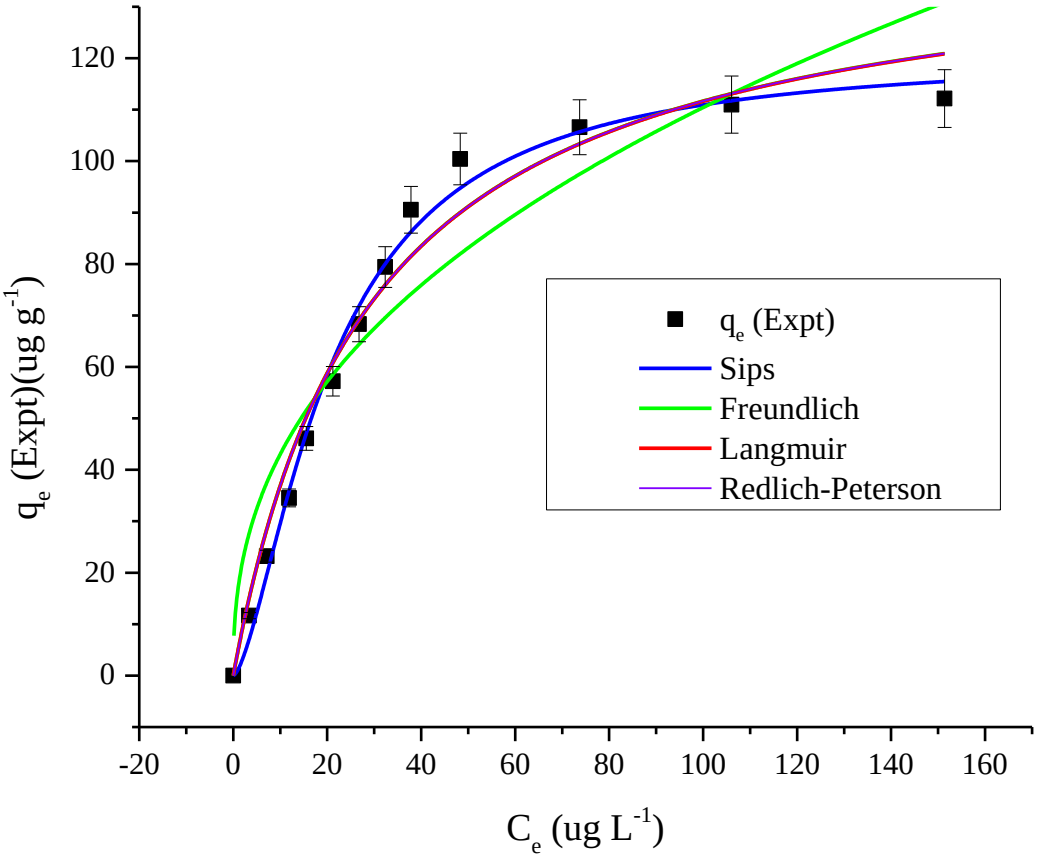

Figure 4.27: Non-linearized isotherms of LNR biosorption.

Table 4.21: Adsorption isotherm parameters for LNR biosorption

Isotherm	Langmuir	Freundlich	Redlich-Peterson	Sips
Parameters	Q_{max} = 144.01	1/n = 0.41	A = 4.98	a_s= 0.01
	K_L= 0.03	K_F = 16.77	B = 0.03	q_{MS} = 121.05
			g = 1	B_s = 1.53
Coefficient of determination (R^2)	0.975	0.858	0.972	0.991
Chi-square (χ^2)	37.80	177.94	41.59	12.97

The experimental sorption data were acceptably describable by the Sips model as depicted by the R^2 and the chi-square values (**Figure 4.27 & Table 4.21**). Sips model is the most applicable 3-parameter isotherm model for monolayer adsorption describing homogeneous or heterogeneous surfaces where the adsorbed molecule has multiple adsorption sites (Wang & Guo, 2020). The monolayer adsorption was predicted by the Sips model to have a maximum capacity of 121.1 ug g^{-1} and was confirmed by data fitting to the Langmuir model. This was also in agreement with the Redlich-Peterson isotherm model whose g value was unity implying a leaning towards the Langmuir isotherm model. The B_s value (>1) was a testament to the heterogeneity of the adsorbent surface. Overall, the equilibrium data were described by the isotherms in the order Sips >Langmuir > Redlich-Peterson >Freundlich. From the Freundlich parameters, according to Treybal (1981), the magnitude of *n* (2.44) demonstrates the favorability of the biosorption process. Further, 1/n (0.41) was less than 1 indicating weak adsorbate-adsorbent forces corresponding to an overall physisorption process (Shikuku & Jemutai-Kimosop, 2020).

The monolayer adsorption was further corroborated by studying the shape of the isotherm. As described by Giles et al. (1974), the isotherm of LNR biosorption displayed an L-type (type 1/normal) curve, subgroup 2c (**Figure 4.27**) which stands for Langmuir. In such kinds of curves, the slope reaches a plateau as adsorbate concentration increases since no more vacant sites are available.

4.2.3.6 Kinetic studies during LNR biosorption to *MOSB*

At the onset, when all adsorption sites are vacant, the *MOSB* had the highest initial adsorption rate due to the highest number of accessible adsorption sites. With time, however, equilibrium was attained as all the bare binding sites were saturated, and thereafter, the equilibrium shifted towards desorption. **Figure 4.28** represents the comparative fitting of the experimental data to the kinetic models.

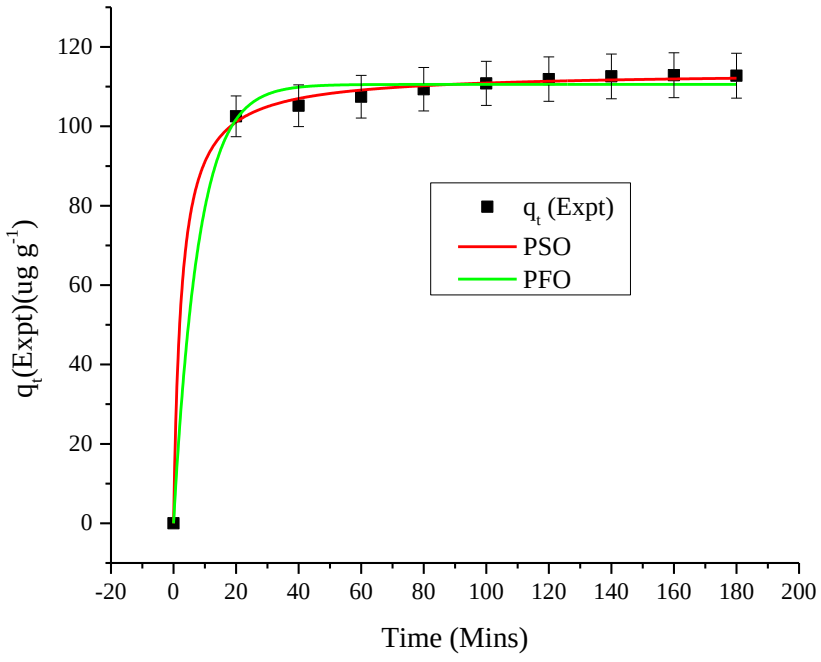

Figure 4.28: Kinetic model graphs for LNR biosorption to *MOSB.*

The applicability of the model to describe the reaction kinetics was decided based on the closeness between experimental (q_{exp}) and model-predicted (q_{cal}) equilibrium adsorption capacities using the R^2 and χ^2. The calculated kinetic models' parameters are presented in **Table 4.22.**

Table 4.22: Calculated kinetic parameters for LNR biosorption

Kinetic model	PFO	PSO
Parameters	q_e (cal) (µg g^{-1}) = 110.56	q_e (cal) (µg g^{-1}) = 113.67
	k_1 (min^{-1}= 0.13	k_2 (min^{-1}) = 0.004
	q_e (expt) (µg g^{-1}) = 112.8	q_e (expt) (µg g^{-1}) = 112.8
S_{rate} (µg g^{-1} min^{-1})	13.93	45.23
$t_{1/2}$ (min^{-1})	5.50	2.51
R^2	0.995	0.999
χ^2	6.14	1.42

Based on the R^2 and χ^2, and the degree of variance between the experimental (q_{exp}) and the model-predicted (q_{cal}) equilibrium adsorption capacities, both the PFO and PSO model predicted the adsorption kinetics comparatively well but PSO gave a better fit relative to the PFO equation. The PSO model postulates chemisorption governed rate-controlling step.

4.2.3.7 LNR biosorption thermodynamics

Figure 4.29 displays the Vant' Hoff plot while **Table 4.23** depicts the thermodynamic parameters for LNR adsorption onto *MOSB.*

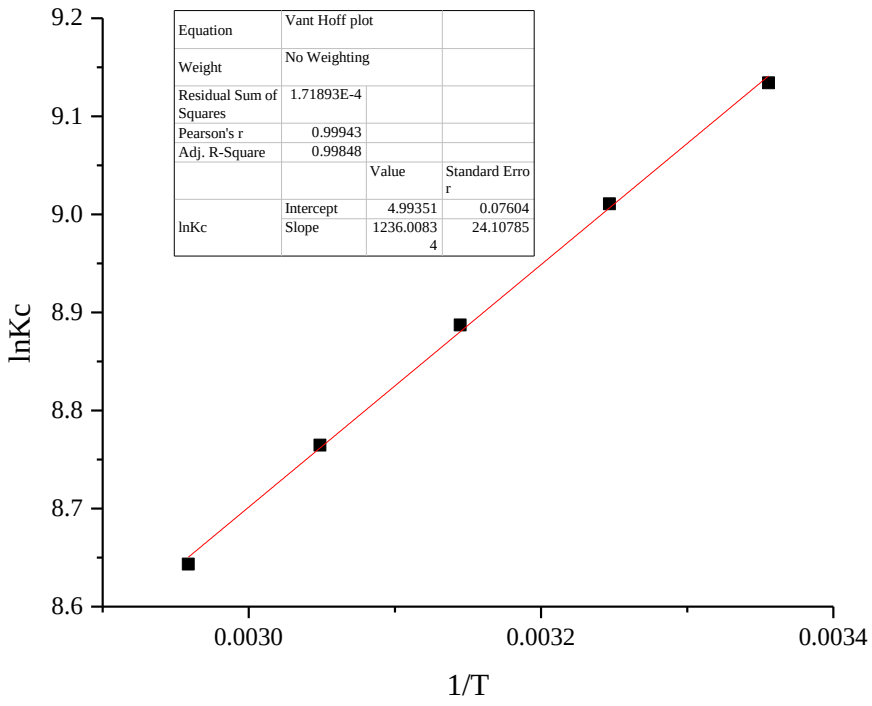

Figure 4.29: Vant' Hoff plot for LNR biosorption.

Table 4.23: Thermodynamic parameters for LNR adsorption onto *MOSB*

Compound	Temp. (K)	% removal	ΔG (kJ mol^{-1})	ΔH (kJ mol^{-1})	ΔS (J mol^{-1})
PGT	298	90.3	-22.6	-10.3	+41.5
	308	89.1	-23.1		
	318	87.9	-23.5		
	328	86.5	-23.9		
	338	85.0	-24.3		

From **Table 4.23**, the percent (%) removal of LNR consistently depreciated with an increase in temperature indicating an exothermic process and was confirmed by the

negative ΔH value (-10.3 kJ mol^{-1}), albeit the difference being slightly insignificant as depicted by the test statistics ($p > 0.05$). This decrease in retention efficiency was due to the weakening of the binding forces between the *MOSB* and the LNR molecules with temperature increase and the equilibrium shifting towards desorption. It could also be attributed to increasing solubility of the LNR and therefore weakening their affinity to the adsorbent surface. The optimum temperature observed was 298 K. The ΔH value (-10.3 kJ mol^{-1}), far below the standard 40–120 kJ mol^{-1} for the chemisorption mechanism, indicated that the overall adsorption mechanism of LNR onto *MOSB* was physical however the rate-determining step involved chemical interactions as observed with its adherence to the PSO kinetic model. The negative ΔG values implied that the adsorption of LNR onto *MOSB* was a spontaneous and favorable process. The magnitude of ΔG values could indicate whether an adsorption process is either physisorption (ΔG = 0 to -20 kJ mol^{-1}) or chemisorption (ΔG = -80 to -400 kJ mol^{-1}) (Owino et al., 2023). The calculated ΔG values (**Table 4.23)** for biosorption of LNR onto *MOSB* ranged from -22.6 to -24.3 kJ mol^{-1}, indicating adsorption process entailed a physisorption mechanism with some slight aspect of chemisorption thereby corroborating the PSO kinetic model. The positive ΔS implied an escalated disorderliness at the adsorbate-adsorbent interphase and thus an affinity for the adsorbate by the adsorbent (Luttah et al., 2023).

4.2.3.8 Effect of pH in LNR biosorption to *MOSB*

The percent removal (R) of LNR as a function of pH is depicted in **Figure 4.30**. There was a minimal increase between pH 5.8-7 but looking at percentages, there was practically no variation as it ranged between 89.9% to 90.9%, a situation observed by Yang et al. (2021a) and Chaara et al. (2012). As reiterated in section 4.2.2.8, the adsorbent surface is

neutral. Even though LNR has a pKa of 12.1 ± 0.7, implying that it is positively charged below this value and negatively charged above it, electrostatic attractions were insignificant due to the neutrality of the adsorbent. The adsorption mechanism in LNR adsorption could be attributed to π-π interactions between the adsorbate and *MOSB* (**Figure 4.31**). This is further corroborated by its log K_{OW} of 3.2 and water solubility of 75 mg L^{-1} at 25 °C (substances with solubilities that are less than 100 mg L^{-1} generally are considered hydrophobic) making it quite hydrophobic implying that adsorption onto an organic adsorbent is an appropriate removal method.

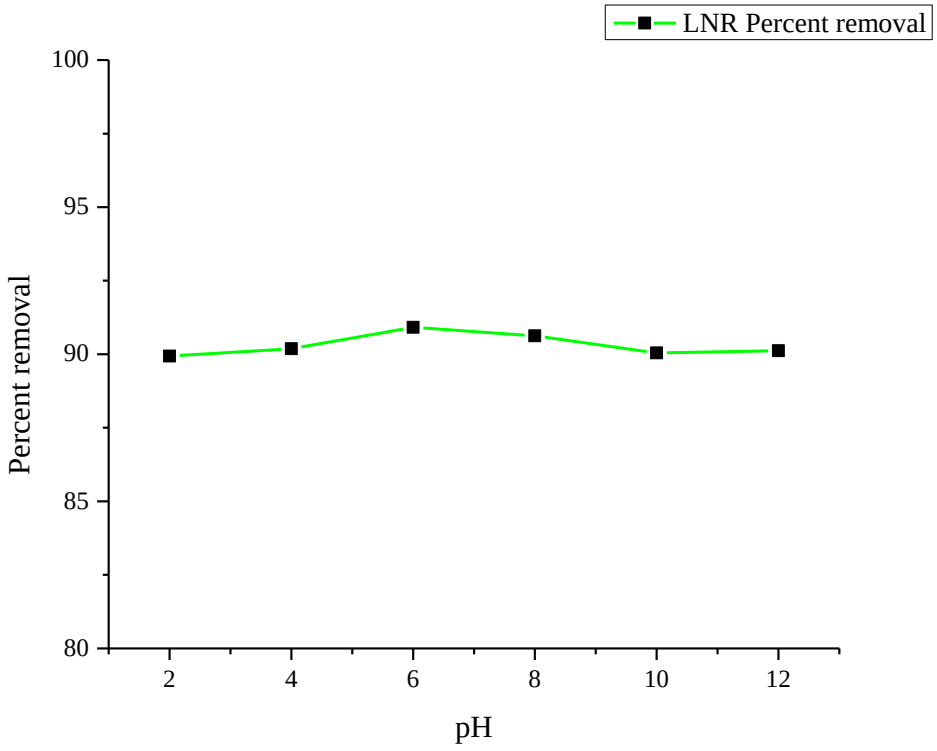

Figure 4.30: Percent removal of LNR as a function of pH.

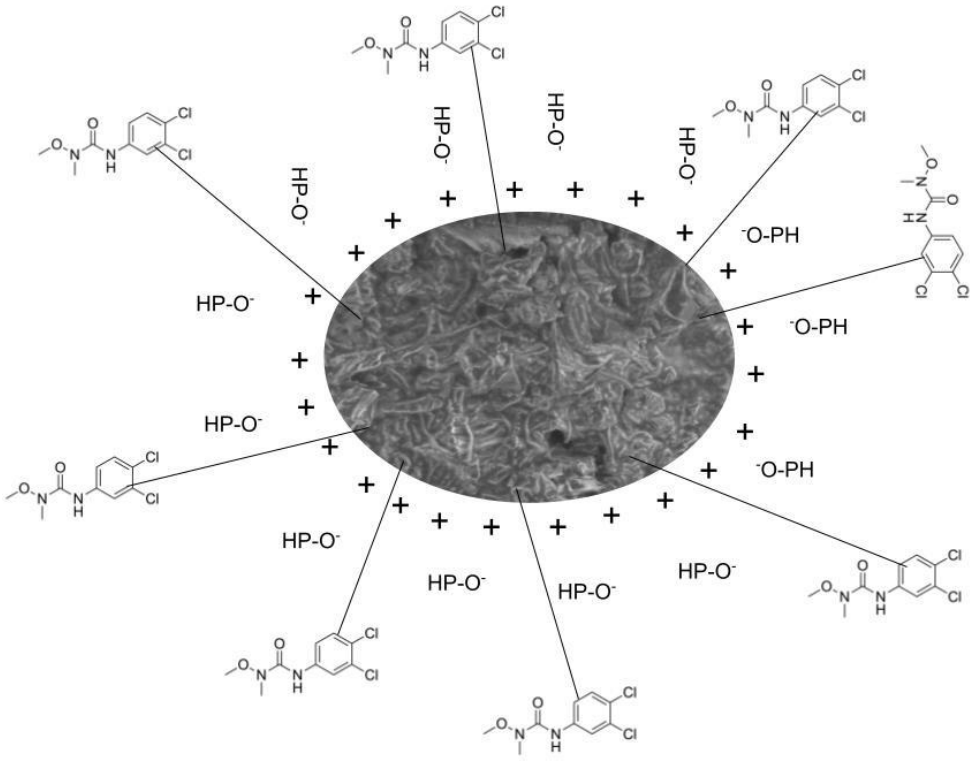

Figure 4.31: LNR-*MOSB* interactions ($HP\text{-}O^-$ are the negatively charged phosphates while the + charges indicate the net positive caused by the water-soluble proteins in *M.O*).

4.2.4 Comparison between PGT and LNR biosorption

The biosorption of the two EDCs had almost similar optimized parameters apart from contact time which was approximately 87 min for PGT and 154 min for LNR. Among other parameters, the adsorption process is affected by the solubility of the molecule. If high, it hinders the affinity of the molecule toward the biosorbent surface (Ngeno et al., 2016). In this sense, the slower adsorption process of LNR was possibly related to its higher solubility (75 mg L^{-1}) when compared to that of PGT (8.8 mg L^{-1}). The hydrophobicity, depicted by the log K_{OW} was also another determining factor. The longer

contact time for LNR may be attributed to its lesser log K_{OW} (3.2) as compared to PGT (3.9) i.e., implying that LNR has more affinity to the water molecule than to the adsorbent's surface while PGT has a greater sorption capacity to carbonaceous materials. This is confirmed by adsorption rates (**Table 4.15 and 4.22**) which were higher for PGT and lower for LNR and which consequently affected their half-lives. Another noted difference was a physisorption rate-determining step for PGT and a chemisorption rate-determining step for LNR.

4.2.5 Comparison of *M.O* byproducts in abstraction of various pollutants

The sequestration of pollutants using *M.O* biosorbents was compared and is shown in **Table 4.24** which displays the performance of *MOSB* as compared to other adsorbents.

Table 4.24**:** M.O by-products' use in the removal of other pollutants

Part of M.O used	Treatment	Pollutants	Optimized parameters	Percentage removal	Adsorption capacity (mg g^{-1})	Reference
Leaves	unmodified	Pb (II) and Zn (II) ions	Initial concentration of metal ions-70 mg/L, adsorbent dosage-0.6 g; pH-3.2	95.6 89.4	51.7 38.5	Jayan et al. (2021)
Leaves	unmodified	Pb (II)	Adsorbent biomass-1.0 g; pH-6.	98.6	45.8	Imran et al. (2019)
Seed powder	Acid treated biochar	Diclofenac	pH-5	82.8	100.9	Bagheri et al. (2020)
Pod husks	unmodified	Crystal violet	pH-6 adsorbent dosage-0.6 g Time-60 mins	86.2	156.3	Keereerak and Chinpa (2020)
Seed powder	Treated with $KMnO_4$	Cadmium and Zinc Ions	pH-4	-	-	Kituyi et al. (2013)
Seed husks	Chemical and thermal treatment	Atrazine	Equilibrium time-1200 mins; pH-5; Temp.-318 K	-	10.3	Cusioli et al. (2021)

Part of M.O used	Treatment	Pollutants	Optimized parameters	Percentage removal	Adsorption capacity (mg g^{-1})	Reference
Seed pods	Both acid-treated and non-treated	lead, cadmium, copper, manganese, iron, zinc, and magnesium	60 min contact time, 1.0 g of sorbent dose, pH 8, 100 μm sorbent particle size, and extraction temp 35°C.	Higher percentages for acid-treated biosorbent	-	Maina et al. (2016)
Seed husks	Chemical and heat treatment	Diclofenac	pH-5 Contact time-12 hours	-	28.7	Araujo et al. (2018)
Seed powder	Modification with $CaCl_2$, NaOH, KMnO4 and HCl	Lead and chromium ions	pH-5; particle size of adsorbent-0.250 mm and adsorbent dosage of 0.6 g.	82 92	- -	(Ongulu et al. (2015))
Pods	Acid treated	Diclofenac	pH-5; Contact time-27 hours		60.8	Viotti et al. (2019)
MOSB	Acid treated	Progesterone	Time-86.8 min; adsorbate concentration-500 µg		135.8 (µg g^{-1})	This study

Part of M.O used	Treatment	Pollutants	Optimized parameters	Percentage removal	Adsorption capacity (mg g^{-1})	Reference
MOSB	Acid treated	Linuron	L^{-1}; Temp-298 K and adsorbent dosage- 0.1 g Contact time-154 min; Adsorbate concentration-500 µg L^{-1}; Temp-298K and adsorbent dosage- 0.1 g		144 (µg g^{-1})	This study

4.3 Phytoremediation of PGT and LNR using *E. Crassipes*

The diagrams displaying the phytoremediation setup are in **Appendix 15**. After analysis of the phytoremediation samples, the concentrations of both PGT and LNR were below the LOQ. The mass spectrometry didn't show fragments for metabolites as well (**Appendix 16**). In this study, negative results are therefore being reported. For plants and the accompanying microorganisms to abstract contaminants, the bioavailability of the contaminant is vital, that is, contact between them is crucial. The physicochemical characteristics of the pollutant, such as its volatility, size, hydrophobicity, water solubility, electric charge, density, and interactions with the surrounding matrix system, all affect its bioavailability. Moreover, the soil ecosystem's properties like pH, bulk density, microbial populations, porosity, nutrient content, and the availability of organic matter have a bigger impact on the movement and immobilization of contaminants (Tripathi et al., 2020). Organic matter concentration in the soil enhances the soil sediment's ability to adsorb hydrophobic organic contaminants. This is so because humus is primarily composed of decomposing plant matter, and plant cell walls comprise lignin, which attaches hydrophobic substances, as well as negatively charged groups that attract cations. Expounding on how hydrophobicity and volatility of a pollutant affect its movement in soils, it is imperative to note that hydrophobicity is typically conveyed as the octanol: water partition coefficient, or log K_{OW}. A high log K_{OW} depicts high hydrophobicity and vice versa. Organic hydrophobic molecules (log $K_{OW} > 3$) are strongly bound to soil organic matter and are insoluble in soil pore water (Pilon-Smits, 2005). Organic hydrophobic molecules are therefore categorized as recalcitrant pollutants due to their limited capacity for phytoremediation as a result of their lack of bioavailability. In this

study, the two pollutants used, PGT and LNR had high K_{OW} (> 3) (**Table 1.1**). This implied that they partitioned more to the soil sediments than to the aqueous portion of the PVC pots used. Additionally, the pollutants may not have been bioavailable because of the root depth of the plants. The used plant is a floating plant and is based on the aqueous portion. Consequently, there was no contact between the plant and the pollutants, and therefore no phytoremediation took place. It is also postulated that the trace concentrations that may have been in the aqueous phase may have been photodegraded via the plant's enzymatic activities, and thus could not be detected. They may have also been taken up into plant tissue but may have dissipated from the plant in volatile form; a process called phytovolatilization. *E. crassipes* has been majorly used for inorganics (Pilon-Smits, 2005) especially metals as they are good metal accumulators in addition to the metals partitioning more to the aqueous phase where the roots of the plant are in contact. Due to their abundance of organic-degrading enzymes, aquatic plants like parrot feather and elodea have been proven to be effective at cleaning up organic waste (Pilon-Smits, 2005).

It's also crucial to point out that organic and inorganic contaminants are absorbed by plant roots in distinct ways. There are no transporters for organic contaminants in plant membranes because they are typically man-made and xenobiotic to plants. As a result, depending on their physical and chemical characteristics, organic contaminants tend to diffuse into and within plant tissues (Tripathi et al., 2020). The organic pollutant's hydrophobicity is again a key factor in plant uptake. Since the transport of organic chemicals through the plant is physical rather than biological, their movement is predictable. Consequently, organic pollutants with a log K_{OW} in the lower range of 0.5 to 3 are hydrophobically capable of permeating through the lipid bilayer of membranes,

while also being hydrophilic enough to be dissolved in the cell fluids. Organic contaminants that are overly hydrophilic (log K_{OW} 0.5) may not penetrate through the plants' cell membranes whereas organic pollutants that are excessively hydrophobic (log $K_{OW} > 3$) become caught in between cell membranes and cell walls on the plant's perimeter and are unable to pass through to the cell fluids (Pilon-Smits, 2005).

By contrast, membrane transporter proteins allow inorganics to be absorbed by biological processes since inorganic contaminants usually exist as ions and cannot pass membranes without the aid of membrane transporter proteins. Inorganic pollutants such as nitrates, phosphates, copper, manganese, and zinc are nutrients and thus contain naturally occurring membrane transporters whereas other inorganic pollutants such as arsenate which is taken up by phosphate transporters, and selenate that is taken up by sulfate transporters are chemically similar to nutrients (Tripathi et al., 2020). The inability of organics not to penetrate cell membranes is yet another reason for the negative results.

CHAPTER FIVE

STRENGTHS, LIMITATIONS, RECOMMENDATIONS AND CONCLUSIONS

5.1 Strengths and limitations

To the best of my knowledge, in Africa, this is the first study to analyze EDCs in UDBS samples obtained from WWTPs and used as fertilizer in agricultural farms. This study also reports PGT and LNR in wastewater and sludge for the first time in East Africa. Related studies have majored in lakes and rivers ignoring the point sources of EDCs such as WWTPs. Nonetheless, there were some study limitations encountered while carrying out the first objective. The major one was financial constraints at the beginning of the study and thus the use of isotope-labeled standards or internal standardization to validate the analytical method was not employed. However, several quality assurance and quality control strategies (such as triplicate analyses, recovery tests, spiked blanks, LODs, and LOQs) were conducted to ensure the robustness, accuracy, and reliability of the analytical method. The quality assurance and control results showed that the analytical method was sufficiently robust and accurate.

The greatest strength during the second and third objectives was investigating, for the first time, acid-activated, fat-free *M.O* seeds for the removal of PGT and LNR from aqueous solutions with RSM as an experimental design tool for the optimization of process parameters. Nonetheless, there were some study limitations encountered at this stage for example; due to the inadequacy of facilities, the biosorbent was not characterized using X-ray photoelectron spectroscopy (XPS). This was however countered by carrying out SEM-EDS which equally gave the elemental composition. Furthermore, biosorption in real wastewater and regeneration of the biosorbent were outside the scope of the study and

future prospective studies may wish to explore these areas. The removal efficiency by *MOSB* was also not 100% implying that some EDCs may still be released to the environment.

For the fourth objective, the major challenge was the poor choice of plant for the selected EDCs.

5.2 Conclusions

This study investigated the levels of DBP, DEHP, DMP, LNR, and PGT in wastewater, sludge, and UDBS samples from WWTPs in western Kenya and Nairobi. The EDCs were detected in all the sludge, UDBS, and wastewater influent samples from all the WWTPs. DEHP and DBP had higher concentrations in all the matrices than other EDCs. There was higher partitioning of the EDCs to the sludge and the UDBS than to the water samples. Notably, DEHP had higher mean concentrations in the sludge and UDBS (3181.2 and 1153.1 ng g^{-1} respectively) in all the sites sampled than the rest of the EDCs. DBP was however higher in the influent wastewater samples as compared to the rest of the EDCs with a mean of 10.12 μg L^{-1}. LNR had the least concentration in the sludge, UDBS, and water samples. The occurrence of some EDCs in the discharged effluents indicates that the WWTPs are not as efficient as desired in completely abstracting organic micropollutants. The abstraction was however through adsorption to the sludge, later detected in UDBS which are used as fertilizers by farmers. This therefore implies that some EDCs can be quite persistent in the environment through UDBS eventually causing bioaccumulation and biomagnification in the food chain. The Dds and high RQs to the receiving water portrayed a potential risk to the environment that policymakers need to put in structures to regulate the uses and disposal of EDCs.

In the second and third objectives, *MOSB* was used for adsorption of PGT and LNR from aqueous solution using Design Expert software where optimization was carried out using RSM. The optimized parameters for PGT, displaying a 93.2% adsorption efficiency were 86.8 min contact time, room temperature (298 K), 500 µg L^{-1} as initial adsorbate concentration, and 0.1 g adsorbent while that for LNR were: 154 min, 500 µg L^{-1} adsorbate concentration, 298K and 0.1 g adsorbent dosage. pH was not a significant factor in the removal of both PGT and LNR. The kinetics, isotherms, and thermodynamics were analyzed further using OriginPro version 9. The equilibrium data were best described by the Langmuir isotherm for PGT and Sips model for LNR, with a maximum monolayer adsorption capacity of 135.8 µg g^{-1} and 144.0 µg g^{-1}, respectively. Adsorption kinetics followed pseudo-first order (PFO) for PGT and pseudo-second order (PSO) for LNR predicting physisorption and a chemisorption rate-determining steps respectively. The thermodynamics functions (PGT: $\Delta G < 0$, ΔH = -9.3 kJ mol^{-1} and ΔS = +44.2 J mol^{-1} and LNR: $\Delta G < 0$, ΔH = -10.3 kJ mol^{-1} and ΔS = +41.5 J mol^{-1}) confirmed that the adsorption of PGT and LNR onto *MOSB* is a spontaneous and exothermic process with randomness and affinity experienced at the surface of the adsorbent. The adsorption mechanism was non-electrostatic and may have involved π-π interactions. The results from this study show that the *MOSB* is a promising alternative for an ecofriendly, low-cost biosorbent that can effectively remove PGT and LNR from aqueous solutions.

Phytoremediation of LNR and PGT using *Eichhornia crassipes* was also carried out as the fourth objective. The uptake was however below the quantification level attributed to the lack of bioavailability of the contaminants to the plants. Pollutant distribution and

concentration are heterogeneous for many sites, the most efficient and cost-effective remediation solution may be a combination of different technologies.

5.3 Recommendations

Not all WWTPs in Kenya were sampled therefore reducing the sample size (N = 60). To generate conclusive findings, future studies may wish to investigate these pollutants in all WWTPs in Kenya. Furthermore, the transformational study of EDCs to analyze their metabolites is also a recommended area in future studies. It is also recommended that a larger scope of EDCs be investigated to give more insights into their occurrence, fate, removal efficiency, mass loading, and toxicity levels. Finally, seasonal variations which will enable the calculation of dissipation kinetics should also be carried out in future studies. This will give more reliable conclusions.

For adsorption studies, more EDCs can be tested for biosorption either using *MOSB* or other biowastes. Further, desorption studies should be carried out to determine the recyclability of *MOSB*. Moreover, the use of CCD and RSM is advisable when carrying out adsorption experiments as it gives more reliable results.

For phytoremediation, proper choice of plant for the targeted pollutants should be taken into consideration. An emergent plant, (rooted in the lake bottom, but their leaves and stems extend out of the water) is recommended to allow for bioavailability to be used for the selected EDCs (PGT and LNR) instead of a floating plant. Alternatively, if *E. crassipes* is to be used, the pollutants to be abstracted should be more hydrophilic. In addition to adding organic fertilizers, the introduction of oxygen to the root zone may increase uptake. Other parameters to be considered involve a detailed site characterization, site management, cost-benefit analysis, time required, and disposal after use. Finally, with

the use of technology, genetically modified plants, incorporated with enzymes capable of enhancing phytoremediation could be another viable option.

REFERENCES

Abdelkader, S., El-Gendy, A., & El-Haggar, S. (2021). Removal of trivalent chromium from tannery wastewater using solid wastes. *Innovative Infrastructure Solutions*, *6*(2), 1-8.

Achieng, G., & Shikuku, V. (2020). Adsorption of copper ions from water onto fish scales derived biochar: Isothermal perspectives. *Journal of Materials and Environmental Science and Pollution Research, Volume 11*(Issue X), 1816-1827.

Adelaja, O. A. (2011). Biosorption of Lead (II) ions from aqueous solution using Moringa oleifera pods.

Adelaja, O. A., Amoo, I. A., & Aderibigbe, A. D. (2011). Biosorption of Lead (II) ions from aqueous solution using Moringa oleifera pods. *Archives of Applied Science Research*, *3*(6), 50-60.

Adeniyi, A. G., & Ighalo, J. O. (2019). Biosorption of pollutants by plant leaves: an empirical review. *Journal of environmental chemical engineering*, *7*(3), 103100.

Adeogun, A. O., Ibor, O. R., Omogbemi, E. D., Chukwuka, A. V., Adegbola, R. A., Adewuyi, G. A., & Arukwe, A. (2015). Environmental occurrence and biota concentration of phthalate esters in Epe and Lagos Lagoons, Nigeria. *bMarine Environmental Research*, *108*, 24-32.

Afolabi, A., Oluyamo, S., & Fuwape, I. (2021). Synthetic characterization and Structural Properties of Nanocellulose from Moringa oleifera seeds. *Journal of the Nigerian Society of Physical Sciences*, *3*, 148–153.

Afolabi, F. O., Musonge, P., & Bakare, B. F. (2021). Evaluation of Lead (II) Removal from Wastewater Using Banana Peels: Optimization Study. *Polish Journal of Environmental Studies*, *30*(2).

Agarry, S. E., Oghenejoboh, K. M., Oghenejoboh, E. O., Owabor, C. N., & Ogunleye, O. O. (2020). Adsorptive remediation of crude oil contaminated marine water using chemically and thermally modified coconut (Cocos nucifera) husks. *J Environ Treat Tech*, *8*, 694-707.

Ahalya, N., Kanamadi, R. D., & Ramachandra, T. V. (2006). Biosorption of iron(III) from aqueous solutions using the husk of Cicer arientinum. *Indian Journal of Chemical Technology*, *13*, 122-127.

Ahmad, S., Kutty, A. A., Raji, F., & Saimy, I. S. (2015). Water quality classification based on water quality index in Sungai Langat, Selangor, Malaysia. *Jurnal Teknologi*, *77*(30).

Ajayi, T. O., & Ogunbayio, A. O. (2012). Achieving Environmental Sustainability in Wastewater Treatment by Phytoremediation with Water Hyacinth (Eichhornia Crassipes). *Journal of Sustainable Development*, *5*(7). https://doi.org/10.5539/jsd.v5n7p80

Akinbiyi, A. (2000). Removal of lead from aqueous solutions by adsorption using peat moss. *A thesis*.

Al-Ghouti, M. A., & Da'ana, D. A. (2020). Guidelines for the use and interpretation of adsorption isotherm models: A review. *Journal of hazardous materials*, *393*, 122383.

Al-Khateeb, L. A., Almotiry, S., & Salam, M. A. (2014). Adsorption of pharmaceutical pollutants onto graphene nanoplatelets. *Chemical Engineering Journal*, *248*, 191-199.

Ali, H., Khan, E., & Sajad, M. A. (2013). Phytoremediation of heavy metals—concepts and applications. *Chemosphere*, *91*(7), 869-881.

Ali, I., Asim, M., & Khan, T. A. (2012). Low cost adsorbents for the removal of organic pollutants from wastewater. *J Environ Manage*, *113*, 170-183. https://doi.org/10.1016/j.jenvman.2012.08.028

Almazrouei, B., Islayem, D., Alskafi, F., Catacutan, M. K., Amna, R., Nasrat, S., . . . Yildiz, I. (2023). Steroid hormones in wastewater: Sources, treatments, environmental risks, and regulations. *Emerging Contaminants*, *9*, 100210.

Aly-Eldeen, M. A., El-Sayed, A. A., Salem, D. M., & El Zokm, G. M. (2018). The uptake of Eriochrome Black T dye from aqueous solutions utilizing waste activated sludge: Adsorption process optimization using factorial design. *The Egyptian Journal of Aquatic Research*, *44*, 179-186.

Amoros, I., Connon, R., Garelick, H., Alonso, J. L., & Carrasco, J. (2000). An assessment of the toxicity of some pesticides and their metabolites affecting a natural aquatic environment using the Microtox™ system. *Water Science and Technology*, *42*(1-2), 19-24.

Ani, J., Okoro, U., Aneke, L., Onukwuli, O., Obi, I., Akpomie, K., & Ofomatah, A. (2019). Application of response surface methodology for optimization of dissolved solids adsorption by activated coal. *Applied Water Science*, *9*, 1-11.

Anwar, F., Latif, S., Ashraf, M., & Gilani, A. H. (2007). Moringa oleifera: a food plant with multiple medicinal uses. *Phytotherapy Research: An International Journal Devoted to Pharmacological and Toxicological Evaluation of Natural Product Derivatives*, *21*(1), 17-25.

Appa, R., Mhaisalkar, V., Bafana, A., Saravana Devi, S., Krishnamurthi, K., Chakrabarti, T., & Naoghare, P. K. (2018). Simultaneous quantitative monitoring of four indicator contaminants of emerging concern (CEC) in different water sources of Central India using SPE/LC-(ESI) MS-MS. *Environmental monitoring and assessment*, *190*(8), 1-12.

Araujo, C. S., Alves, V. N., Rezende, H. C., Almeida, I. L., de Assuncao, R. M., Tarley, C. R., . . . Coelho, N. M. M. (2010). Characterization and use of *Moringa oleifera* seeds as biosorbent for removing metal ions from aqueous effluents. *Water Science and Technology*, *62*, 2198-2203.

Araujo, L. A., Bezerra, C. O., Cusioli, L. F., Silva, M. F., Nishi, L., Gomes, R. G., & Bergamasco, R. (2018). *Moringa oleifera* biomass residue for the removal of pharmaceuticals from water. *Journal of environmental chemical engineering*, *6*, 7192-7199.

Awad, A. M., Jalab, R., Benamor, A., Nasser, M. S., Ba-Abbad, M. M., El-Naas, M., & Mohammad, A. W. (2020). Adsorption of organic pollutants by nanomaterial-based adsorbents: An overview. *Journal of Molecular Liquids*, *301*, 112335.

Bachir, D. H., Boutoumi, H., Khalaf, H., Eloy, P., Schnee, J., & Gaigneaux, E. M. (2021). Influence of Operational Parameters on Photocatalytic Degradation of Linuron in Aqueous TiO2 Pillared Montmorillonite Suspension. *Bulletin of Chemical Reaction Engineering & Catalysis*, *16*(3), 673-685.

Bagheri, A., Abu-Danso, E., Iqbal, J., & Bhatnagar, A. (2020). Modified biochar from Moringa seed powder for the removal of diclofenac from aqueous solution. *Environmental Science and Pollution Research*, *27*, 7318-7327.

Baillie-Hamilton, P. F. (2002). Chemical toxins: a hypothesis to explain the global obesity epidemic. *The Journal of Alternative & Complementary Medicine*, *8*(2), 185-192.

Baldi, I., Lebailly, P., Mohammed-Brahim, B., Letenneur, L., Dartigues, J.-F., & Brochard, P. (2003). Neurodegenerative diseases and exposure to pesticides in the elderly. *American journal of epidemiology*, *157*(5), 409-414.

Bamukyaye, S., & Wanasolo, W. (2017). Performance of egg-shell and fish-scale as adsorbent materials for chromium (VI) removal from effluents of tannery industries in Eastern Uganda. *Open Access Library Journal*, *4*(8), 1-12.

Banasiak, L. J., & Schäfer, A. I. (2010). Sorption of steroidal hormones by electrodialysis membranes. *Journal of Membrane Science*, *365*, 198-205.

Barret, P. E., Joyner, L. G., & Halend, P. P. (1951). The Determination of Pore Volume and Area Distributions in Porous Substances. I. Computations from Nitrogen Isotherms *J. Ame. Chem. Soc.*, *73*(1), 373-380.

Basile, T., Petrella, A., Petrella, M., Boghetich, G., Petruzzelli, V., Colasuonno, S., & Petruzzelli, D. (2011). Review of endocrine-disrupting-compound removal technologies in water and wastewater treatment plants: an EU perspective. *Industrial & Engineering Chemistry Research*, *50*(14), 8389-8401.

Bayuo, J., Abukari, M. A., & Pelig-Ba, K. B. (2020). Optimization using central composite design (CCD) of response surface methodology (RSM) for biosorption of hexavalent chromium from aqueous media. *Applied Water Science*, *10*, 1-12.

Benijts, T., Lambert, W., & De Leenheer, A. (2004). Analysis of multiple endocrine disruptors in environmental waters via wide-spectrum solid-phase extraction and dual-polarity ionization LC-ion trap-MS/MS. *Analytical chemistry*, *76*(3), 704-711.

Bergman, A., Heindel, J. J., Jobling, S., Kid, K. A., & Zoeller, R. T. (2013). *State of the Science of Endocrine Disrupting Chemicals* (An assessment of the state of the

science of endocrine disruptors prepared by a group of experts for the United Nations Environment Programme and World Health Organization., Issue.

Bhatnagar, A., & Sillanpää, M. (2010). Utilization of agro-industrial and municipal waste materials as potential adsorbents for water treatment—a review. *Chemical Engineering Journal*, *157*(2-3), 277-296.

Bider, R.-C., Lluka, T., Himbert, S., Khondker, A., Qadri, S. M., Sheffield, W. P., & Rheinstadter, M. C. (2020). Stabilization of lipid membranes through partitioning of the blood bag plasticizer di-2-ethylhexyl phthalate (DEHP). *Langmuir*, *36*(40), 11899-11907.

Boyle, C. A., Boulet, S., Schieve, L. A., Cohen, R. A., Blumberg, S. J., Yeargin-Allsopp, M., . . . Kogan, M. D. (2011). Trends in the prevalence of developmental disabilities in US children, 1997-2008. *Pediatrics*, *127*(6), 1034-1042. https://doi.org/10.1542/peds.2010-2989

Buasri, A., Chaiyut, N., Tapang, K., Jaroensin, S., & Panphrom, S. (2012). Biosorption of heavy metals from aqueous solutions using water hyacinth as a low cost biosorbent. *Civil Environ Res*, *2*(2), 17-25.

Caioni, G., Merola, C., Perugini, M., d'Angelo, M., Cimini, A. M., Amorena, M., & Benedetti, E. (2021). An experimental approach to study the effects of realistic environmental mixture of linuron and propamocarb on zebrafish synaptogenesis. *International Journal of Environmental Research and Public Health*, *18*(9), 4664.

Calafat, A. M., Ye, X., Wong, L.-Y., Reidy, J. A., & Needham, L. L. (2007). Exposure of the US population to bisphenol A and 4-tertiary-octylphenol: 2003–2004. *Environmental health perspectives*, *116*(1), 39-44.

Çelebi, H., Gök, G., & Gök, O. (2020). Adsorption capability of brewed tea waste in waters containing toxic lead (II), cadmium (II), nickel (II), and zinc (II) heavy metal ions. *Scientific reports*, *10*(1), 17570.

Cevasco, A., Urbatzka, R., Bottero, S., Massari, A., Pedemonte, F., Kloas, W., & Mandich, A. (2008). Endocrine disrupting chemicals (EDC) with (anti) estrogenic and (anti) androgenic modes of action affecting reproductive biology of Xenopus laevis: II. Effects on gonad histomorphology. *Comparative Biochemistry and Physiology Part C: Toxicology & Pharmacology*, *147*(2), 241-251.

Chaara, D., Bruna, F., Draoui, K., Ulibarri, M., Barriga, C., & Pavlovic, I. (2012). Study of key parameters affecting adsorption of the herbicide Linuron on organohydrotalcites. *Applied clay science*, *58*, 34-38.

Chang, H., Wan, Y., Wu, S., Fan, Z., & Hu, J. (2011). Occurrence of androgens and progestogens in wastewater treatment plants and receiving river waters: comparison to estrogens. *Water research*, *45*, 732-740.

Chaudhuri, S. R., Salodkar, S., Sudarshan, M., Mukherjee, I., & Thakur, A. R. (2008). Role of water hyacinth-mediated phytoremediation in waste water purification at east Calcutta wetland. *Environmental Sciences*, *5*(1), 53-62.

Chaukura, N., Gwenzi, W., Tavengwa, N., & Manyuchi, M. M. (2016). Biosorbents for the removal of synthetic organics and emerging pollutants: opportunities and challenges for developing countries. *Environmental Development*, *19*, 84-89.

Chaukura, N., Murimba, E. C., & Gwenzi, W. (2017). Sorptive removal of methylene blue from simulated wastewater using biochars derived from pulp and paper sludge. *Environmental Technology & Innovation*, *8*, 132-140.

Chen, Y., Zhang, H., Luo, Y., & Song, J. (2012). Occurrence and dissipation of veterinary antibiotics in two typical swine wastewater treatment systems in east China. *Environmental monitoring and assessment*, *184*(4), 2205-2217.

Chirikona, F., Filipovic, M., Ooko, S., & Orata, F. (2015). Perfluoroalkyl acids in selected wastewater treatment plants and their discharge load within the Lake Victoria basin in Kenya. *Environmental monitoring and assessment*, *187*(5), 1-12.

Chirikona, F., Quinete, N., Gonzalez, J., Mutua, G., Kimosop, S., & Orata, F. (2022). Occurrence and Distribution of Per-and Polyfluoroalkyl Substances from Multi-Industry Sources to Water, Sediments and Plants along Nairobi River Basin, Kenya. *International Journal of Environmental Research and Public Health*, *19*(15), 8980.

Choina, J., Bagabas, A., Fischer, C., Flechsig, G.-U., Kosslick, H., Alshammari, A., & Schulz, A. (2015). The influence of the textural properties of ZnO nanoparticles on adsorption and photocatalytic remediation of water from pharmaceuticals. *Catalysis Today*, *241*, 47-54.

Christwardana, H. M., & Soetrisnanto, D. (2013). Phytoremediations of Palm Oil Mill Effluent (POME) by using aquatic plants and microalge for biomass production. *International Journal of Sciences: Basic and Applied Research (IJSBAR)*, *13*(2), 31-47.

Cong, B., Li, S., Liu, S., Mi, W., Liu, S., Zhang, Z., & Xie, Z. (2022). Source and Distribution of Emerging and Legacy Persistent Organic Pollutants in the Basins of the Eastern Indian Ocean. *Environmental Science & Technology*, *56*(7), 4199-4209.

Crain, D. A., Janssen, S. J., Edwards, T. M., Heindel, J., Ho, S. M., Hunt, P., . . . Guillette, L. J., Jr. (2008). Female reproductive disorders: the roles of endocrine-disrupting compounds and developmental timing. *Fertil Steril*, *90*(4), 911-940. https://doi.org/10.1016/j.fertnstert.2008.08.067

Cui, X., Shu, H., Wang, L., Chen, G., Han, J., Hu, Q., . . . Zhang, J. (2021). Methacrylic functionalized hybrid carbon nanomaterial for the selective adsorption and detection of progesterone in wastewater. *Environmental Science and Pollution Research*, *28*, 62306-62320.

Cusioli, L. F., Bezerra, C. d. O., Quesada, H. B., Alves Baptista, A. T., Nishi, L., Vieira, M. F., & Bergamasco, R. (2021). Modified Moringa oleifera Lam. Seed husks as low-cost biosorbent for atrazine removal. *Environmental technology*, *42*(7), 1092-1103.

Dar, S., Kumawat, D., Singh, N., & Wani, K. (2011). Sewage treatment potential of water hyacinth (Eichhornia crassipes). *Res J Environ Sci*, *5*(4), 377-385.

Darbre, P. D. (2019). The history of endocrine-disrupting chemicals. *Current Opinion in Endocrine and Metabolic Research*, *7*, 26-33.

De Cock, M., Maas, Y. G., & Van De Bor, M. (2012). Does perinatal exposure to endocrine disruptors induce autism spectrum and attention deficit hyperactivity disorders? Review. *Acta paediatrica*, *101*(8), 811-818.

de Graaf, L., Boulanger, M., Bureau, M., Bouvier, G., Meryet-Figuiere, M., Tual, S., . . . Baldi, I. (2022). Occupational pesticide exposure, cancer and chronic neurological disorders: A systematic review of epidemiological studies in greenspace workers. *Environmental research*, *203*, 111822.

Desimoni, E., & Brunetti, B. (2015). About estimating the limit of detection by the signal to noise approach.

Diamanti-Kandarakis, E., Bourguignon, J. P., Giudice, L. C., Hauser, R., Prins, G. S., Soto, A. M., . . . Gore, A. C. (2009). Endocrine-disrupting chemicals: an Endocrine Society scientific statement. *Endocr Rev*, *30*(4), 293-342. https://doi.org/10.1210/er.2009-0002

Dipu, S., Kumar, A. A., & Thanga, V. S. G. (2011). Phytoremediation of dairy effluent by constructed wetland technology. *The Environmentalist*, *31*(3), 263-278. https://doi.org/10.1007/s10669-011-9331-z

Dong, C.-D., Wang, M.-H., Chen, C.-F., Shih, Y.-J., Chang, K.-L., Lee, S.-H., . . . Chen, C.-W. (2020). Detecting phthalate esters in sludge particulates from wastewater treatment plants. *Journal of Environmental Science and Health, Part A*, *55*(10), 1233-1240. https://doi.org/10.1080/10934529.2020.1780850

Dotto, G. L., & McKay, G. (2020). Current scenario and challenges in adsorption for water treatment. *Journal of environmental chemical engineering*, *8*(4), 103988.

Eldeeb, T. M., Aigbe, U. O., Ukhurebor, K. E., Onyancha, R. B., El-Nemr, M. A., Hassaan, M. A., . . . Balogun, V. A. (2024). Biosorption of acid brown 14 dye to mandarin-CO-TETA derived from mandarin peels. *Biomass Conversion and Biorefinery*, *14*(4), 5053-5073.

Eletta, O., Mustapha, S., Ajayi, O., & Ahmed, A. (2018). Optimization of dye removal from textile wastewater using activated carbon from sawdust. *Nigerian Journal of Technological Development*, *15*(1), 26-32.

Eletta, O. A., & Ighalo, J. O. (2019). A review of fish scales as a source of biosorbent for the removal of pollutants from industrial effluents. *J Res Inf Civ Eng*, *16*(1), 2479-2510.

Epp, J. (2016). X-ray diffraction (XRD) techniques for materials characterization. In *Materials characterization using nondestructive evaluation (NDE) methods* (pp. 81-124). Elsevier.

European Commission. (2003). *Technical Guidance Document in Support of Commission Directive 93/67/EEC on Risk Assessment for New Notified Substances and*

Commission Regulation (EC) No 1488/94 on Risk Assessment for Existing Substances, Part II (Brussels, Belgium).

Farrag, H. F., & Fawzy, M. (2012). Phytoremediation Potentiality of Cyperus articulatus L. *Life Science Journal*, *9*(4).

Fazal, T., Faisal, A., Mushtaq, A., Hafeez, A., Javed, F., Alaud Din, A., . . . Rehman, F. (2021). Macroalgae and coal-based biochar as a sustainable bioresource reuse for treatment of textile wastewater. *Biomass Conversion and Biorefinery*, *11*, 1491-1506.

Fingerhut, M., Nelson, D. I., Driscoll, T., Concha-Barrientos, M., Steenland, K., Punnett, L., . . . Takala, J. (2006). The contribution of occupational risks to the global burden of disease: summary and next steps. *La Medicina del lavoro*, *97*(2), 313-321. http://europepmc.org/abstract/MED/17017364

Freundlich, H. (1906). Over the adsorption in solution. *J. Phys. chem*, *57*, 1100-1107.

Gavrilescu, M., Demnerová, K., Aamand, J., Agathos, S., & Fava, F. (2015). Emerging pollutants in the environment: present and future challenges in biomonitoring, ecological risks and bioremediation. *New biotechnology*, *32*(1), 147-156.

George, M. J., Sichilongo, K. F., Ramabulana, T., Madala, N. E., & Dubery, I. A. (2019). Comparison of Soxhlet and reflux techniques for extraction and characterisation of potential endocrine-disrupting compounds from solid waste dumpsite soil. *Environmental monitoring and assessment*, *191*(3), 1-11.

Ghasemi, A., Khansary, M. A., Marjani, A., & Shirazian, S. (2017). Using quantum chemical modeling and calculations for evaluation of cellulose potential for estrogen micropollutants removal from water effluents. *Chemosphere*, *178*, 411-423.

Gibson, N., Kuchenbecker, P., Rasmussen, K., Hodoroaba, V.-D., & Rauscher, H. (2020). Volume-specific surface area by gas adsorption analysis with the BET method. In *Characterization of Nanoparticles* (pp. 265-294). Elsevier.

Giles, C. H., Smith, D., & Huitson, A. (1974). A general treatment and classification of the solute adsorption isotherm. I. Theoretical. *Journal of colloid and interface science*, *47*, 755-765.

Golovko, O., Šauer, P., Fedorova, G., Kroupová, H. K., & Grabic, R. (2018). Determination of progestogens in surface and wastewater using SPE extraction and LC-APCI/APPI-HRPS. *Science of the Total Environment*, *621*, 1066-1073.

González-Pradas, E., Villafranca-Sánchez, M., Gallego-Campo, A., Ureña-Amate, D., & Fernández-Pérez, M. (1999). Removal of linuron from water by natural and activated bentonite. *Journal of Chemical Technology & Biotechnology: International Research in Process, Environmental & Clean Technology*, *74*(1), 49-54.

Gore, A. C., Crews, D., Doan, L. L., Merrill, M. L., Patisaul, H., & Zota, A. (2014). Introduction to Endocrine Disrupting Chemicals (EDCs). A Guide for Public Interest Organizations and Policy Makers. . *Endocrine Society–IPEN*, *1*(1), 1-76.

Gore, A. C., & Dickerson, S. M. (2012). Endocrine Disruptors and The Developing Brain. *Colloquium Series on The Developing Brain*, *3*(1), 1-114. https://doi.org/10.4199/C00054ED1V01Y201204DBR007

Grandclément, C., Seyssiecq, I., Piram, A., Wong-Wah-Chung, P., Vanot, G., Tiliacos, N., . . . Doumenq, P. (2017). From the conventional biological wastewater treatment to hybrid processes, the evaluation of organic micropollutant removal: a review. *Water research*, *111*, 297-317.

Grassi, M., Rizzo, L., & Farina, A. (2013). Endocrine disruptors compounds, pharmaceuticals and personal care products in urban wastewater: implications for agricultural reuse and their removal by adsorption process. *Environmental Science and Pollution Research*, *20*(6), 3616-3628.

Grosshagauer, S., Pirkwieser, P., Kraemer, K., & Somoza, V. (2021). The future of Moringa foods: A food chemistry perspective. *Frontiers in Nutrition*, *8*, 751076.

Grün, F., & Blumberg, B. (2009). Endocrine disrupters as obesogens. *Molecular and cellular endocrinology*, *304*(1-2), 19-29.

Guillette, L. J. (2000). Organochlorine pesticides as endocrine disruptors in wildlife. *Central European Journal of Public Health*, *8 Suppl*, 34-35. http://europepmc.org/abstract/MED/10943450

Ho, Y.-S. (2006). Review of second-order models for adsorption systems. *Journal of hazardous materials*, *136*, 681-689.

Ho, Y.-S., & McKay, G. (1998). Sorption of dye from aqueous solution by peat. *Chemical Engineering Journal*, *70*, 115-124.

Hodúr, C., Bellahsen, N., Mikó, E., Nagypál, V., Šereš, Z., & Kertész, S. (2020). The adsorption of ammonium nitrogen from milking parlor wastewater using pomegranate peel powder for sustainable water, resources, and waste management. *Sustainability*, *12*(12), 4880.

Huang, C., Wu, L.-H., Liu, G.-Q., Shi, L., & Guo, Y. (2018). Occurrence and ecological risk assessment of eight endocrine-disrupting chemicals in urban river water and sediments of South China. *Archives of environmental contamination and toxicology*, *75*, 224-235.

Ibezute, A. C., & Tawari-Fufeyin, P. (2012). Phytodegradation of Compost Leachate by Water Hyacinth (Eichhornia Crassipes) from Aqueous Solutions. *International Journal of Science and Research (IJSR)*.

Ibisi, N. E., & Asoluka, C. A. (2018). Use of agro-waste (Musa paradisiaca peels) as a sustainable biosorbent for toxic metal ions removal from contaminated water. *Chem. Int*, *4*(1), 52.

Idris, M. A., Jami, M. S., Hammed, A. M., & Jamal, P. (2016). Moringa oleifera seed extract: A review on its environmental applications. *International Journal of Applied Environmental Sciences*, *11*(6), 1469-1486.

Ifelebuegu, A., Ukpebor, J., & Nzeribe-Nwedo, B. (2016). Mechanistic evaluation and reaction pathway of UV photo-assisted Fenton-like degradation of progesterone in

water and wastewater. *International Journal of Environmental Science and Technology*, *13*, 2757-2766.

Igwe, J. C., Abia, A. A., & Ibeh, C. A. (2008). Adsorption kinetics and intraparticulate diffusivities of Hg, As and

Pb ions on unmodified and thiolated coconut fiber. *Int. J. Environ. Sci. Tech.*,, *5*(1), 83-92.

Imran, M., Anwar, K., Akram, M., Shah, G. M., Ahmad, I., Samad Shah, N., . . . Ahmad, S. (2019). Biosorption of Pb (II) from contaminated water onto Moringa oleifera biomass: kinetics and equilibrium studies. *International journal of phytoremediation*, *21*, 777-789.

Inkson, B. J. (2016). Scanning electron microscopy (SEM) and transmission electron microscopy (TEM) for materials characterization. In *Materials characterization using nondestructive evaluation (NDE) methods* (pp. 17-43). Elsevier.

Isichei, T. O., & Okieimen, F. E. (2014). Adsorption of 2-Nitrophenol onto Water Hyacinth Activated Carbon-Kinetics and Equilibrium Studies. *Environment and Pollution*, *3*(4). https://doi.org/10.5539/ep.v3n4p99

Jayan, N., Bhatlu M, L. D., & Akbar, S. T. (2021). Central composite design for adsorption of Pb (II) and Zn (II) metals on PKM-2 *Moringa oleifera* leaves. *ACS omega*, *6*, 25277-25298.

Jemutai-Kimosop, S., Orata, F., Shikuku, V. O., Okello, V. A., & Getenga, Z. M. (2020). Insights on adsorption of carbamazepine onto iron oxide modified diatomaceous earth: kinetics, isotherms, thermodynamics, and mechanisms. *Environmental research*, *180*, 108898.

Jiang, D., Amano, Y., & Machida, M. (2017). Removal and recovery of phosphate from water by calcium-silicate composites-novel adsorbents made from waste glass and shells. *Environmental Science and Pollution Research*, *24*(9), 8210-8218.

Johnson, R. A., Harris, R. E., & Wilke, R. A. (2000). Are pesticides really endocrine disruptors? *WMJ : official publication of the State Medical Society of Wisconsin*, *99*(8), 34-38. http://europepmc.org/abstract/MED/11149256

K'Oreje, K. O., Demeestere, K., De Wispelaere, P., Vergeynst, L., Dewulf, J., & Van Langenhove, H. (2012). From multi-residue screening to target analysis of pharmaceuticals in water: development of a new approach based on magnetic sector mass spectrometry and application in the Nairobi River basin, Kenya. *Sci Total Environ*, *437*, 153-164. https://doi.org/10.1016/j.scitotenv.2012.07.052

K'oreje, K. O., Kandie, F. J., Vergeynst, L., Abira, M. A., Van Langenhove, H., Okoth, M., & Demeestere, K. (2018). Occurrence, fate and removal of pharmaceuticals, personal care products and pesticides in wastewater stabilization ponds and receiving rivers in the Nzoia Basin, Kenya. *Science of the Total Environment*, *637*, 336-348.

K'oreje, K. O., Okoth, M., Van Langenhove, H., & Demeestere, K. (2020). Occurrence and treatment of contaminants of emerging concern in the African aquatic

environment: Literature review and a look ahead. *Journal of environmental management*, *254*, 109752.

Kairigo, P., Ngumba, E., Sundberg, L.-R., Gachanja, A., & Tuhkanen, T. (2020). Occurrence of antibiotics and risk of antibiotic resistance evolution in selected Kenyan wastewaters, surface waters and sediments. *Science of the Total Environment*, *720*, 137580.

Kan, Y., Yue, Q., Li, D., Wu, Y., & Gao, B. (2017). Preparation and characterization of activated carbons from waste tea by H3PO4 activation in different atmospheres for oxytetracycline removal. *Journal of the Taiwan Institute of Chemical Engineers*, *71*, 494-500.

Kanamarlapudi, S., Chintalpudi, V. K., & Muddada, S. (2018). Application of biosorption for removal of heavy metals from wastewater. *Biosorption*, *18*, 69-116.

Karri, R. R., Sahu, J., & Meikap, B. (2020). Improving efficacy of Cr (VI) adsorption process on sustainable adsorbent derived from waste biomass (sugarcane bagasse) with help of ant colony optimization. *Industrial Crops and Products*, *143*, 111927.

Kasonga, T. K., Coetzee, M. A., Kamika, I., Ngole-Jeme, V. M., & Momba, M. N. B. (2021). Endocrine-disruptive chemicals as contaminants of emerging concern in wastewater and surface water: A review. *Journal of environmental management*, *277*, 111485.

Kebede, T. G., Dube, S., & Nindi, M. M. (2019). Removal of multi-class antibiotic drugs from Wastewater using water-soluble protein of Moringa stenopetala seeds. *Water*, *11*(3), 595.

Keereerak, A., & Chinpa, W. (2020). A potential biosorbent from *Moringa oleifera* pod husk for crystal violet adsorption: Kinetics, isotherms, thermodynamic and desorption studies. *Science Asia*, *46*, 186–194.

Kelly, C. (2000). Analysis of steroids in environmental water samples using solid-phase extraction and ion-trap gas chromatography–mass spectrometry and gas chromatography–tandem mass spectrometry. *Journal of chromatography A*, *872*(1-2), 309-314.

Kenya Population Census. (2019). Kenya population and housing census. In.

Khan, S. A., Khan, S. B., Khan, L. U., Farooq, A., Akhtar, K., & Asiri, A. M. (2018). Fourier transform infrared spectroscopy: fundamentals and application in functional groups and nanomaterials characterization. *Handbook of materials characterization*, 317-344.

Khazri, H., Boczkaj, G., Ghorbel-Abid, I., & Trabelsi-Ayadi, M. (2022). Determination of phenylbutazone, sulfamethazine, carbendazim and linuron using a novel pine bark biosorbent for solid-phase extraction (SPE) with high-performance liquid chromatography (HPLC). *Instrumentation Science & Technology*, 1-13.

Kimosop, S. J., Getenga, Z. M., Orata, F., Okello, V., & Cheruiyot, J. (2016). Residue levels and discharge loads of antibiotics in wastewater treatment plants (WWTPs),

hospital lagoons, and rivers within Lake Victoria Basin, Kenya. *Environmental monitoring and assessment, 188*(9), 1-9.

Kituyi, J. L., Foulkes, M., Worsfold, P., Ongulu, R. A., Kiplagat, A., & Gachanja, A. (2013). Efficiency of pre-treated *Moringa oleifera* for the removal of Cd^{2+} and Zn^{2+} ions from wastewaters. *Ecohydrology & Hydrobiology, 13*, 267-271.

Korde, S., Deshmukh, S., Tandekar, S., & Jugade, R. (2021). Implementation of response surface methodology in physi-chemisorption of Indigo carmine dye using modified chitosan composite. *Carbohydrate Polymer Technologies and Applications, 2,* 100081.

Kumar, M., Gogoi, A., & Mukherjee, S. (2020). Metal removal, partitioning and phase distributions in the wastewater and sludge: Performance evaluation of conventional, upflow anaerobic sludge blanket and downflow hanging sponge treatment systems. *Journal of Cleaner Production*, *249*, 119426.

Kumar, M., Ngasepam, J., Dhangar, K., Mahlknecht, J., & Manna, S. (2022). Critical review on negative emerging contaminant removal efficiency of wastewater treatment systems: Concept, consistency and consequences. *Bioresource Technology*, *352*, 127054. https://doi.org/https://doi.org/10.1016/j.biortech.2022.127054

Kumar, P., Anand, B., Tsang, Y. F., Kim, K.-H., Khullar, S., & Wang, B. (2019). Regeneration, degradation, and toxicity effect of MOFs: Opportunities and challenges. *Environmental research*, *176*, 108488.

Landrigan, P. J., & Etzel, R. A. (2013). *Textbook of children's environmental health*. Oxford University Press.

Langmuir, I. (1916). The constitution and fundamental properties of solids and liquids. Part I. Solids. *Journal of the American Chemical society*, *38*, 2221-2295.

Lee, I., & Ji, K. (2022). Identification of combinations of endocrine disrupting chemicals in household chemical products that require mixture toxicity testing. *Ecotoxicology and Environmental Safety*, *240*, 113677.

Liao, S.-W., & Chang, W.-L. (2004). Heavy metal phytoremediation by water hyacinth at constructed wetlands in Taiwan. *Journal of Aquatic*, Plan-t.

Liu, L., Liu, Y. H., Wang, Z., Liu, C. X., Huang, X., & Zhu, G. F. (2014). Behavior of tetracycline and sulfamethazine with corresponding resistance genes from swine wastewater in pilot-scale constructed wetlands. *J Hazard Mater*, *278*, 304-310. https://doi.org/10.1016/j.jhazmat.2014.06.015

Loha, K. M., Lamoree, M., Weiss, J. M., & de Boer, J. (2018). Import, disposal, and health impacts of pesticides in the East Africa Rift(EAR) zone: A review on management and policy analysis. *Crop Protection*, *112*, 322-331. https://doi.org/10.1016/j.cropro.2018.06.014

Longnecker, M. P., Klebanoff, M. A., Brock, J. W., Zhou, H., Gray, K. A., Needham, L. L., & Wilcox, A. J. (2002). Maternal Serum Level of 1,1-Dichloro-2,2-bis(p-chlorophenyl)ethylene and Risk of Cryptorchidism, Hypospadias, and Polythelia

among Male Offspring. *American journal of epidemiology*, *155*(4), 313-322. https://doi.org/10.1093/aje/155.4.313

Luttah, I., Onunga, D. O., Shikuku, V. O., Otieno, B., & Kowenje, C. O. (2023). Removal of endosulfan from water by municipal waste incineration fly ash-based geopolymers: Adsorption kinetics, isotherms, and thermodynamics. *Frontiers in Environmental Chemistry*, *4*, 1164372.

Madhurina, M., Bidisha, M., Shekhar, M. M., Sankar, C., Amitava, G., & Arunabha, M. (2014). Study on the Phytoremediation Potential of Pharmaceutical Wastewater Spiked with Nutrients through Municipal Wastewater–A Case Study in Indian Context. *International Research Journal of Environment Sciences*, *3*(1), 83-89.

Maia, L. S., da Silva, A. I., Carneiro, E. S., Monticelli, F. M., Pinhati, F. R., & Mulinari, D. R. (2021). Activated carbon from palm fibres used as an adsorbent for methylene blue removal. *Journal of Polymers and the Environment*, *29*, 1162-1175.

Maina, I. W., Obuseng, V., & Nareetsile, F. (2016). Use of *Moringa oleifera* (Moringa) seed pods and Sclerocarya birrea (Morula) nut shells for removal of heavy metals from wastewater and borehole water. *Journal of Chemistry*, *2016*, 9312952.

Martín-Pozo, L., del Carmen Gómez-Regalado, M., Moscoso-Ruiz, I., & Zafra-Gómez, A. (2021). Analytical methods for the determination of endocrine disrupting chemicals in cosmetics and personal care products: A review. *Talanta*, *234*, 122642.

Marttinen, S. K., Kettunen, R. H., Sormunen, K. M., & Rintala, J. A. (2003). Removal of bis(2-ethylhexyl) phthalate at a sewage treatment plant. *Water research*, *37*(6), 1385-1393. https://doi.org/https://doi.org/10.1016/S0043-1354(02)00486-4

Mashile, P. P., Mpupa, A., & Nomngongo, P. N. (2018). Adsorptive removal of microcystin-LR from surface and wastewater using tyre-based powdered activated carbon: Kinetics and isotherms. *Toxicon*, *145*, 25-31.

Meeker, J. D. (2012). Exposure to environmental endocrine disruptors and child development. *Archives of pediatrics & adolescent medicine*, *166*(10), 952-958.

Metcalfe, C., Bayen, S., Desrosiers, M., Muñoz, G., Sauvé, S., & Yargeau, V. (2022). Methods for the analysis of endocrine disrupting chemicals in selected environmental matrixes. *Environmental research*, *206*, 112616.

Michelini, L., Meggio, F., Rocca, N. L., Ferro, S., & Ghisi, R. (2012). Accumulation and effects of sulfadimethoxine in Salix fragilis L. plants: a preliminary study to phytoremediation purposes. *International journal of phytoremediation*, *14*(4), 388-402.

Mihayo, D., Vegi, M. R., & Vuai, S. A. H. (2021). Defluoridation of aqueous solution using raw and surface modified biosorbents prepared from adansonia digitata fruit pericarp. *Journal of Dispersion Science and Technology*, 1-13.

Militao, I. M., Roddick, F., Bergamasco, R., & Fan, L. (2022). Rapid adsorption of PFAS: Application of *Moringa oleifera* seed powder encapsulated in alginate beads. *Environmental Technology & Innovation*, *28*, 102761.

Moulahcene, L., Skiba, M., Senhadji, O., Milon, N., Benamor, M., & Lahiani-Skiba, M. (2015). Inclusion and removal of pharmaceutical residues from aqueous solution using water-insoluble cyclodextrin polymers. *Chemical Engineering Research and Design*, *97*, 145-158.

Moura, F. C., Rios, R. D., & Galvão, B. R. (2018). Emerging contaminants removal by granular activated carbon obtained from residual Macauba biomass. *Environmental Science and Pollution Research*, *25*, 26482-26492.

Mukherjee, S., Mehta, D., Dhangar, K., & Kumar, M. (2021). Environmental fate, distribution and state-of-the-art removal of antineoplastic drugs: A comprehensive insight. *Chemical Engineering Journal*, *407*, 127184.

Nantaba, F., Palm, W.-U., Wasswa, J., Bouwman, H., Kylin, H., & Kuemmerer, K. (2021). Temporal dynamics and ecotoxicological risk assessment of personal care products, phthalate ester plasticizers, and organophosphorus flame retardants in water from Lake Victoria, Uganda. *Chemosphere*, *262*, 127716.

National Centre for Biotechnology Information. (2022). *PubChem Compound Summary*. https://www.ncbi.nlm.nih.gov/

Ndoun, M. C., Elliott, H. A., Preisendanz, H. E., Williams, C. F., Knopf, A., & Watson, J. E. (2021). Adsorption of pharmaceuticals from aqueous solutions using biochar derived from cotton gin waste and guayule bagasse. *Biochar*, *3*, 89-104.

Ng, B., Quinete, N., Maldonado, S., Lugo, K., Purrinos, J., Briceño, H., & Gardinali, P. (2021). Understanding the occurrence and distribution of emerging pollutants and endocrine disruptors in sensitive coastal South Florida Ecosystems. *Science of the Total Environment*, *757*, 143720.

Ngeno, E. C., Orata, F. O., Baraza, L. D., Shikuku, V. O., & Kimosop, S. J. (2016). Adsorption of Caffeine and Ciprofloxacin onto Pyrolitically Derived Water Hyacinth Biochar: Isothermal, Kinetic and Thermodynamic Studies. *Journal of Chemistry and Chemical Engineering*, *10*, 185-194.

Ngigi, A. N., Magu, M. M., & Muendo, B. M. (2020). Occurrence of antibiotics residues in hospital wastewater, wastewater treatment plant, and in surface water in Nairobi County, Kenya. *Environmental monitoring and assessment*, *192*(1), 1-16.

Nguyen, V.-H., Smith, S. M., Wantala, K., & Kajitvichyanukul, P. (2020). Photocatalytic remediation of persistent organic pollutants (POPs): A review. *Arabian Journal of Chemistry*. https://doi.org/10.1016/j.arabjc.2020.04.028

NORMAN Network. (2023). *Network of reference laboratories, research centres and related organisations for monitoring of emerging environmental substances* https://doi.org/https://www.norman-network.net/?q=node/4

Nyagah, C. N. (2013). Non-financial constraints hindering growth of SME'S in Kenya: the case of plastic manufacturing companies in industrial area in Nairobi County. *MBA Project*.

Ojoghoro, J., Scrimshaw, M., & Sumpter, J. (2021). Steroid hormones in the aquatic environment. *Science of the Total Environment*, *792*, 148306.

Okello, V. A., Kimosop, S. J., Getenga, Z. M., Orata, F., & Shikuku, V. O. (2017). Green remediation of carbamazepine from water using novel magnetic iron modified carbonized baggasse: kinetics, equilibrium and mechanistic studies.

Olaniyan, L. W., & Okoh, A. I. (2020). Determination and ecological risk assessment of two endocrine disruptors from River Buffalo, South Africa. *Environmental monitoring and assessment*, *192*(12), 1-15.

Olisah, C., Okoh, O. O., & Okoh, A. I. (2019). Global evolution of organochlorine pesticides research in biological and environmental matrices from 1992 to 2018: A bibliometric approach. *Emerging Contaminants*, *5*, 157-167.

Olker, J. H., Elonen, C. M., Pilli, A., Anderson, A., Kinziger, B., Erickson, S., Skopinski, M., Pomplun, A., LaLone, C. A., Russom, C. L., & Hoff, D. (2022). The ECOTOXicology Knowledgebase: A Curated Database of Ecologically Relevant Toxicity Tests to Support Environmental Research and Risk Assessment. *Environmental Toxicology and Chemistry*, *41*(6), 1520-1539. https://doi.org/https://doi.org/10.1002/etc.5324

Olujimi, O., Fatoki, O. S., Odendaal, J. P., & Daso, A. P. (2012). *Chemical monitoring and temporal variation in levels of endocrine disrupting chemicals (priority phenols and phthalate esters) from selected wastewater treatment plant and freshwater systems in Republic of South Africa*.

Omo-Okoro, P. N., Daso, A. P., & Okonkwo, J. O. (2018). A review of the application of agricultural wastes as precursor materials for the adsorption of per-and polyfluoroalkyl substances: a focus on current approaches and methodologies. *Environmental Technology & Innovation*, *9*, 100-114.

Omwoma, S., Lalah, J. O., Virani, M., Schramm, K.-W., & Henkelmann, B. (2015). Dioxin-like PCBs and PCDD/Fs in surface sediments near the shore of Winam Gulf, Lake Victoria. *Chemosphere*, *118*, 143-147.

Onchiri, R., Mayaka, A., Majanga, A., Ongulu, R., Orata, F., Getenga, Z., & Gichumbi, J. (2021). Phthalate Levels in Wastewater Treatment Plants of Lake Victoria Basin.

Ong, S.-T., Khoo, E.-C., Keng, P.-S., Hii, S.-L., Lee, S.-L., Hung, Y.-T., & Ha, S.-T. (2011). Plackett–Burman design and response surface methodological approach to optimize basic dyes removal using sugarcane bagasse. *Desalination and Water Treatment*, *25*, 310-318.

Ongulu, R. A., Kituyi, J. L., & Getenga, Z. M. (2015). Biosorption of Pb^{2+} and Cr^{2+} Using *Moringa oleifera* and their Adsorption Isotherms. *Science Journal of Analytical Chemistry*, *3*, 100-108.

Onwuka, J. C., Agbaji, E. B., Ajibola, V. O., & Okibe, F. G. (2016). Kinetic studies of surface modification of lignocellulosic Delonix regia pods as sorbent for crude oil spill in water. *Journal of applied research and technology*, *14*(6), 415-424.

Orata, F. (2018). Conventional Wastewater Treatment Plants as a Discharge and Source Point for Biota Exposure to Micro-pollutants. In *Ecotoxicology: Perspectives on Key Issues* (pp. 213). CRC Press.

Owino, E. K., Shikuku, V. O., Nyairo, W. N., Kowenje, C. O., & Otieno, B. (2023). Valorization of solid waste incinerator fly ash by geopolymer production for removal of anionic bromocresol green dye from water: Kinetics, Isotherms and Thermodynamics studies. *Sustainable Chemistry for the Environment*, *3*, 100026.

Oyewo, O. A., Onyango, M. S., & Wolkersdorfer, C. (2016). Application of banana peels nanosorbent for the removal of radioactive minerals from real mine water. *Journal of environmental radioactivity*, *164*, 369-376.

Padhiyar, H., Thanki, A., Singh, N. K., Pandey, S., Yadav, M., & Yadav, T. C. (2020). Parametric and kinetic investigations on segregated and mixed textile effluent streams using Moringa oleifera seed powders of different sizes. *Journal of Water Process Engineering*, *34*, 101159.

Park, C. M., Han, J., Chu, K. H., Al-Hamadani, Y. A., Her, N., Heo, J., & Yoon, Y. (2017). Influence of solution pH, ionic strength, and humic acid on cadmium adsorption onto activated biochar: experiment and modeling. *Journal of Industrial and Engineering Chemistry*, *48*, 186-193.

Pilon-Smits, E. (2005). PHYTOREMEDIATION. *Annual Review of Plant Biology*, *56*(1), 15-39. https://doi.org/10.1146/annurev.arplant.56.032604.144214

Prüss-Üstün, A., & Corvalán, C. (2006). *Preventingdisease through healthy environments* (92 4 159382 2). (Towards an estimate of the environmental burden of disease, Issue.

Rachoń, D. (2015). Endocrine disrupting chemicals (EDCs) and female cancer: Informing the patients. *Reviews in Endocrine and Metabolic Disorders*, *16*(4), 359-364.

Ragab, D., Gomaa, H., Sabouni, R., Salem, M., Ren, M., & Zhu, J. (2016). Micropollutants removal from water using microfiltration membrane modified with ZIF-8 metal organic frameworks (MOFs). *Chemical Engineering Journal*, *300*, 273-279.

Ramutshatsha-Makhwedzha, D., Munyengabe, A., Mavhungu, M. L., Mbaya, R., & Baloyi, J. (2023). Breakthrough studies for the sorption of methylene blue dye from wastewater samples using activated carbon derived from waste banana peels. *Biomass Conversion and Biorefinery*, 1-13.

Redlich, O., & Peterson, D. L. (1959). A useful adsorption isotherm. *Journal of physical chemistry*, *63*, 1024-1024.

Rissouli, L., Benicha, M., & Chabbi, M. (2016). Contribution to the elimination of Linuron by the adsorption process using Chitin and Chitosan biopolymers. *J Mater Environ Sci*, *7*, 531-540.

Rivera-Utrilla, J., Ocampo-Pérez, R., Méndez-Díaz, J. D., & Sánchez-Polo, M. (2012). Environmental impact of phthalic acid esters and their removal from water and sediments by different technologies–a review. *Journal of environmental management*, *109*, 164-178.

Rossner, A., Snyder, S. A., & Knappe, D. R. (2009). Removal of emerging contaminants of concern by alternative adsorbents. *Water Res*, *43*(15), 3787-3796. https://doi.org/10.1016/j.watres.2009.06.009

Rwiza, M. J., Oh, S.-Y., Kim, K.-W., & Kim, S. D. (2018). Comparative sorption isotherms and removal studies for Pb (II) by physical and thermochemical modification of low-cost agro-wastes from Tanzania. *Chemosphere*, *195*, 135-145.

Sahbaz, D. A., Dandil, S., & Acikgoz, C. (2019). Removal of crystal violet dye by a novel adsorbent derived from waste active sludge used in wastewater treatment. *Water Quality Research Journal*, *54*(4), 299-308.

Salaudeen, T., Okoh, O., Agunbiade, F., & Okoh, A. (2018). Fate and impact of phthalates in activated sludge treated municipal wastewater on the water bodies in the Eastern Cape, South Africa. *Chemosphere*, *203*, 336-344.

Sanz-Santos, E., Álvarez-Torrellas, S., Ceballos, L., Larriba, M., Águeda, V. I., & García, J. (2021). Application of sludge-based activated carbons for the effective adsorption of neonicotinoid pesticides. *Applied Sciences*, *11*(7), 3087.

Sarkingobir, Y., Dikko, M., & Ladan, Z. A. (2020). Removal of Lead, Copper, and Colour from Wastewater Using Raw Coconut Shell, Activated Carbon and Activated Nanocomposite. *Int. J. Med. Biosci.*, *3*(1), 1-9.

Šauer, P., Stará, A., Golovko, O., Valentová, O., Bořík, A., Grabic, R., & Kroupová, H. K. (2018). Two synthetic progestins and natural progesterone are responsible for most of the progestagenic activities in municipal wastewater treatment plant effluents in the Czech and Slovak republics. *Water research*, *137*, 64-71.

Schoutteten, K. (2012). *Adsorption of pharmaceuticals on activated carbon: measurements, mechanisms and modeling* Master's thesis, Universiteit Gent].

Schug, T. T., Janesick, A., Blumberg, B., & Heindel, J. J. (2011). Endocrine disrupting chemicals and disease susceptibility. *The Journal of steroid biochemistry and molecular biology*, *127*(3-5), 204-215.

Shah, R. A., Kumawat, D., Singh, N., & Wani, K. A. (2010). Water hyacinth (Eichhornia crassipes) as a remediation tool for dye effluent pollution. *International Journal Science and Nature*, *1*(2), 172-178.

Sharma, P. K., & Ayub, S. (2019). The Cost Analysis and Economic Feaibility of AGRO Wastes to Adsorb Chromium (VI) From Wastewater. *International Journal of Civil Engineering and Technology (IJCIET)*, *10*(2), 2387-2402.

Sharpe, R. M. (2011). Pediatrics: endocrine disruption and human health effects—a call to action. *Nature Reviews Endocrinology*, *7*(11), 633.

Shikuku, V. O., Achieng, G. O., Ngeno, E. C., Okowa, G. M., Masitsa, G. A., & Owuor, J. J. (2017). Distribution and removal efficiency activated sludge at a municipal wastew. *Research Journal of Chemical, 7*(8), 19-25.

Shikuku, V. O., Donato, F. F., Kowenje, C. O., Zanella, R., & Prestes, O. D. (2015). A comparison of adsorption equilibrium, kinetics and thermodynamics of aqueous phase clomazone between faujasite X and a natural zeolite from Kenya. *South African Journal of Chemistry*, *68*, 245-252.

Shikuku, V. O., & Jemutai-Kimosop, S. (2020). Efficient removal of sulfamethoxazole onto sugarcane bagasse-derived biochar: Two and three-parameter isotherms, kinetics and thermodynamics. *South African Journal of Chemistry*, *73*, 111-119.

Siddiqua, A., Hahladakis, J. N., & Al-Attiya, W. A. K. (2022). An overview of the environmental pollution and health effects associated with waste landfilling and open dumping. *Environmental Science and Pollution Research*, *29*(39), 58514-58536.

Singh, B., Kumar, A., & Malik, A. K. (2014). Recent advances in sample preparation methods for analysis of endocrine disruptors from various matrices. *Crit Rev Anal Chem*, *44*(3), 255-269. https://doi.org/10.1080/10408347.2013.859981

Sips, R. J. (1948). On the structure of a catalyst surface. *J. Chem. Phys.*, *16,*, 490-495.

Sirival, R., Patdhanagul, N., Preecharram, S., Nantaphan, P., & Mahem, R. (2020). The performance of synthetic zeolite combined with activated carbon for removal of linuron herbicide. *Suranaree J Sci Technol*, *27*.

Škrbić, B. D., Ji, Y., Đurišić-Mladenović, N., & Zhao, J. (2016). Occurence of the phthalate esters in soil and street dust samples from the Novi Sad city area, Serbia, and the influence on the children's and adults' exposure. *Journal of hazardous materials*, *312*, 272-279.

So, L., Chu, L., & Wong, P. (2003). Microbial enhancement of Cu2+ removal capacity of Eichhornia crassipes (Mart.). *Chemosphere*, *52*(9), 1499-1503.

Soto, A. M., & Sonnenschein, C. (2010). Environmental causes of cancer: endocrine disruptors as carcinogens. *Nature Reviews Endocrinology*, *6*(7), 363.

Souza, I. P., Cazetta, A. L., Pezoti, O., & Almeida, V. C. (2017). Preparation of biosorbents from the Jatoba (Hymenaea courbaril) fruit shell for removal of Pb (II) and Cd (II) from aqueous solution. *Environmental monitoring and assessment*, *189*, 1-16.

Spagnoli, A. A., Giannakoudakis, D. A., & Bashkova, S. (2017). Adsorption of methylene blue on cashew nut shell based carbons activated with zinc chloride: The role of surface and structural parameters. *Journal of Molecular Liquids*, *229*, 465-471.

Spirhanzlova, P., De Groef, B., Nicholson, F. E., Grommen, S. V. H., Marras, G., Sébillot, A., . . . Du Pasquier, D. (2017). Using short-term bioassays to evaluate the endocrine disrupting capacity of the pesticides linuron and fenoxycarb. *Comparative Biochemistry and Physiology Part C: Toxicology & Pharmacology*, *200*, 52-58. https://doi.org/https://doi.org/10.1016/j.cbpc.2017.06.006

Ssebugere, P., Sillanpää, M., Matovu, H., Wang, Z., Schramm, K.-W., Omwoma, S., . . . Odongo, S. (2020). Environmental levels and human body burdens of per-and poly-fluoroalkyl substances in Africa: A critical review. *Science of the Total Environment*, *739*, 139913.

Staples, C. A., Dorn, P. B., Klecka, G. M., O'Block, S. T., & Harris, L. R. (1998). A review of the environmental fate, effects, and exposures of bisphenol A. *Chemosphere*, *36*(10), 2149-2173.

Stevens, M., & Batlokwa, B. (2017). Removal of nickel (II) and cobalt (II) from wastewater using vinegar-treated eggshell waste biomass. *Journal of Water Resource and Protection*, *9*(08), 931.

Sudarsan, J., Thattai, D., & Das, A. (2012). Phyto-remediation of dairy-waste water using constructed wetland. *Int Pharm Bio Scie*, *3*(3).

Sukumaran, D., Anilkumar, A., & Thanga, S. G. (2013). Phytoremediation of latex effluent by constructed wetland technology. *Science and Education*, *1*(6), 104-109.

Tarley, C. R., & Arruda, M. A. (2004). Biosorption of heavy metals using rice milling by-products. Characterisation and application for removal of metals from aqueous effluents. *Chemosphere*, *54*(7), 987-995. https://doi.org/10.1016/j.chemosphere.2003.09.001

To, M.-H., Hadi, P., Hui, C.-W., Lin, C. S. K., & McKay, G. (2017). Mechanistic study of atenolol, acebutolol and carbamazepine adsorption on waste biomass derived activated carbon. *Journal of Molecular Liquids*, *241*, 386-398.

Tome, S., Etoh, M.-A., Etame, J., & Kumar, S. (2020). Improved reactivity of volcanic ash using municipal solid incinerator fly ash for alkali-activated cement synthesis. *Waste and biomass valorization*, *11*, 3035-3044.

Tong, D. S., Zhou, C. H., Lu, Y., Yu, H., Zhang, G. F., & Yu, W. H. (2010). Adsorption of Acid Red G dye on octadecyl trimethylammonium montmorillonite. *Applied clay science*, *50*(3), 427-431. https://doi.org/10.1016/j.clay.2010.08.018

Trenholm, R. A., Vanderford, B. J., Holady, J. C., Rexing, D. J., & Snyder, S. A. (2006). Broad range analysis of endocrine disruptors and pharmaceuticals using gas chromatography and liquid chromatography tandem mass spectrometry. *Chemosphere*, *65*(11), 1990-1998.

Treybal, R. (1981). Mass-transfer operations, McGraw-Hill. Using tree fern as a biosorbent. *Process Biochem*, *40*, 119-124.

Tripathi, S., Singh, V. K., Srivastava, P., Singh, R., Devi, R. S., Kumar, A., & Bhadouria, R. (2020). Phytoremediation of organic pollutants: current status and future directions. *Abatement of environmental pollutants*, 81-105.

Trueman, R. J., & Erber, L. (2013). Invasive species may offer advanced phytoremediation of endocrine disrupting chemicals in aquatic ecosystems. *Emirates Journal of Food and Agriculture*, *25*(9), 648. https://doi.org/10.9755/ejfa.v25i9.16393

Tyler, C. R., Spary, C., Gibson, R., Santos, E. M., Shears, J., & Hill, E. M. (2005). Accounting for Differences in Estrogenic Responses in Rainbow Trout (Oncorhynchus mykiss: Salmonidae) and Roach (Rutilus rutilus: Cyprinidae) Exposed to Effluents from Wastewater Treatment Works. *Environmental Science & Technology*, *39*(8), 2599-2607. https://doi.org/10.1021/es0488939

Uhrovčík, J. (2014). Strategy for determination of LOD and LOQ values–Some basic aspects. *Talanta*, *119*, 178-180.

Van Thuan, T., Quynh, B. T. P., Nguyen, T. D., & Bach, L. G. (2017). Response surface methodology approach for optimization of Cu2+, Ni2+ and Pb2+ adsorption using KOH-activated carbon from banana peel. *Surfaces and interfaces*, *6*, 209-217.

Vanderford, B. J., Pearson, R. A., Rexing, D. J., & Snyder, S. A. (2003). Analysis of endocrine disruptors, pharmaceuticals, and personal care products in water using liquid chromatography/tandem mass spectrometry. *Analytical chemistry*, *75*(22), 6265-6274.

Viotti, P. V., Moreira, W. M., dos Santos, O. A. A., Bergamasco, R., Vieira, A. M. S., & Vieira, M. F. (2019). Diclofenac removal from water by adsorption on Moringa oleifera pods and activated carbon: Mechanism, kinetic and equilibrium study. *Journal of Cleaner Production*, *219*, 809-817.

Volesky, B. (1999). Biosorption for the Next Century *Process Metallurgy*, *9*(1999), 161-170.

Volza Grow Global. (2021). Kenya Import data of progesterone. https://www.volza.com/imports-kenya/kenya-import-data-of-progesterone

Vymazal, J. (2002). The use of sub-surface constructed wetlands for wastewater treatment in the Czech Republic: 10 years experience. *Ecological Engineering*, *18*(5), 633-646.

Wang, B., Zhang, W., Li, H., Fu, H., Qu, X., & Zhu, D. (2017). Micropore clogging by leachable pyrogenic organic carbon: a new perspective on sorption irreversibility and kinetics of hydrophobic organic contaminants to black carbon. *Environmental Pollution*, *220*, 1349-1358.

Wang, J., & Guo, X. (2020). Adsorption isotherm models: Classification, physical meaning, application and solving method. *Chemosphere*, *258*, 127279.

Wang, Y., Wang, S.-l., Xie, T., & Cao, J. (2020). Activated carbon derived from waste tangerine seed for the high-performance adsorption of carbamate pesticides from water and plant. *Bioresource Technology*, *316*, 123929.

Wanyonyi, W. C., Onyari, J. M., & Shiundu, P. M. (2013). Adsorption of methylene blue dye from aqueous solutions using Eichhornia crassipes. *Bulletin of environmental contamination and toxicology*, *91*(3), 362-366.

Weizel, A., Schlüsener, M. P., Dierkes, G., & Ternes, T. A. (2018). Occurrence of Glucocorticoids, Mineralocorticoids, and Progestogens in Various Treated Wastewater, Rivers, and Streams. *Environmental Science & Technology*, *52*(9), 5296-5307. https://doi.org/10.1021/acs.est.7b06147

Wong, S., Ghafar, N. A., Ngadi, N., Razmi, F. A., Inuwa, I. M., Mat, R., & Amin, N. A. S. (2020). Effective removal of anionic textile dyes using adsorbent synthesized from coffee waste. *Scientific reports*, *10*(1), 2928.

Yang, J., Sun, H., Liu, Y., Wang, X., & Valizadeh, K. (2021a). The sorption of tebuconazole and linuron from an aqueous environment with a modified sludge-based biochar: Effect, mechanisms, and its persistent free radicals study. *Journal of Chemistry*, *2021*, 1-15.

Yang, J., Sun, H., Liu, Y., Wang, X., & Valizadeh, K. (2021b). The sorption of Tebuconazole and Linuron from an Aqueous Environment with a Modified Sludge-Based Biochar: Effect, Mechanisms, and Its Persistent Free Radicals Study. *Journal of Chemistry*, *2021*, 2912054. https://doi.org/10.1155/2021/2912054

Zeenat, Elahi, A., Bukhari, D. A., Shamim, S., & Rehman, A. (2021). Plastics degradation by microbes: A sustainable approach. *Journal of King Saud University - Science*, *33*(6), 101538. https://doi.org/https://doi.org/10.1016/j.jksus.2021.101538

Zhu, Q., Jia, J., Zhang, K., Zhang, H., & Liao, C. (2019). Spatial distribution and mass loading of phthalate esters in wastewater treatment plants in China: an assessment of human exposure. *Science of the Total Environment*, *656*, 862-869.

Zoeller, R. T., Brown, T. R., Doan, L. L., Gore, A. C., Skakkebaek, N. E., Soto, A. M., . . . Vom Saal, F. S. (2012). Endocrine-disrupting chemicals and public health protection: a statement of principles from The Endocrine Society. *Endocrinology*, *153*(9), 4097-4110. https://doi.org/10.1210/en.2012-1422

APPENDICES

Appendix 1: Sampling in of Kariobangi WWTP

Appendix 2: Sampling in Kisii WWTP

Appendix 3: Picking UDBS samples

Appendix 4: Clean-up and extraction using SPE

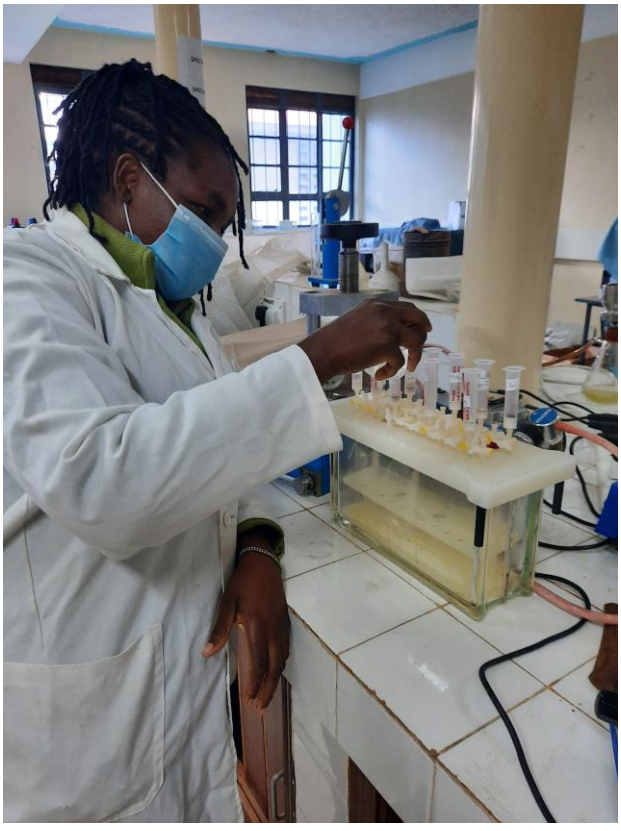

Appendix 5: Clean-up and extraction using soxhlet

(g)

Appendix 6: Calibration curves for concentration levels

Batch Path	D:\MassHunter\Data\Food and Dugs\GE 074-2021\QuantResults\GE 074-2021 DBP Batch.batch.bin		
Analysis Time	3/26/2021 7:58:52 AM	**Analyst Name**	DGAL-PC\Admin
Report Time	3/26/2021 8:00:22 AM	**Reporter Name**	Admin
Last Calib Update	3/26/2021 7:58:51 AM	**Batch State**	Processed
Quant Batch Version	B.07.01	**Quant Report Version**	B.07.01

DBP

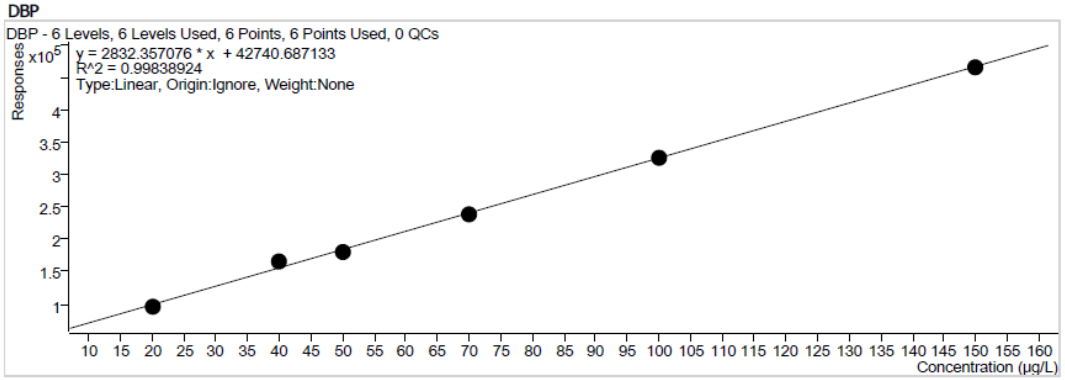

Batch Path	D:\MassHunter\Data\Food and Dugs\GE 074-2021\QuantResults\GE 074-2021 BATCH.batch.bin		
Analysis Time	3/23/2021 4:38:49 PM	**Analyst Name**	DGAL-PC\Admin
Report Time	3/23/2021 4:42:39 PM	**Reporter Name**	Admin
Last Calib Update	3/23/2021 4:38:48 PM	**Batch State**	Processed
Quant Batch Version	B.07.01	**Quant Report Version**	B.07.01

DMP

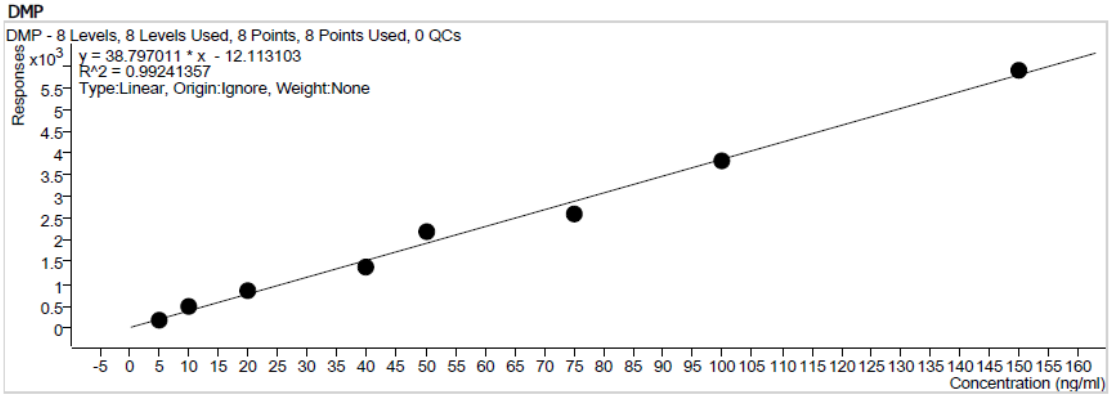

Batch Path	D:\MassHunter\Data\Food and Dugs\GE 074-2021\QuantResults\GE 074-2021 BATCH.batch.bin		
Analysis Time	3/23/2021 4:38:49 PM	**Analyst Name**	DGAL-PC\Admin
Report Time	3/23/2021 4:42:39 PM	**Reporter Name**	Admin
Last Calib Update	3/23/2021 4:38:48 PM	**Batch State**	Processed
Quant Batch Version	B.07.01	**Quant Report Version**	B.07.01

DEHP

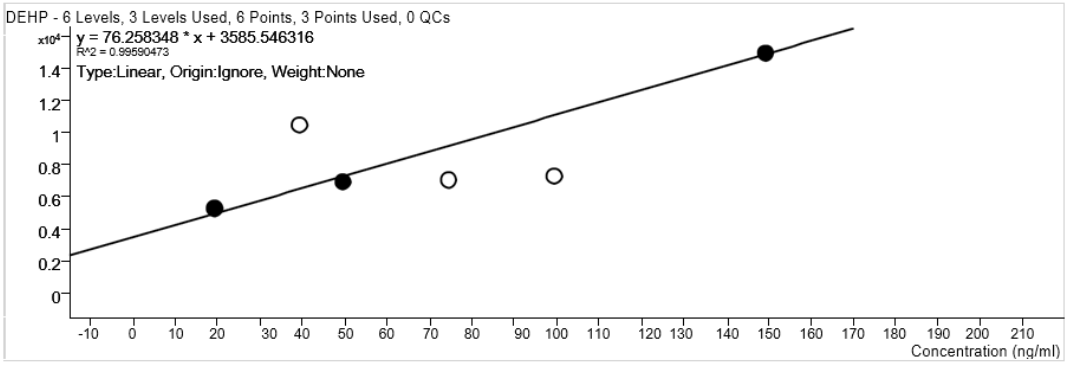

Batch Path	D:\MassHunter\Data\Food and Dugs\GE 074-2021\QuantResults\GE 074-2021 BATCH.batch.bin		
Analysis Time	3/23/2021 4:38:49 PM	**Analyst Name**	DGAL-PC\Admin
Report Time	3/23/2021 4:42:39 PM	**Reporter Name**	Admin
Last Calib Update	3/23/2021 4:38:48 PM	**Batch State**	Processed
Quant Batch Version	B.07.01	**Quant Report Version**	B.07.01

Linuron

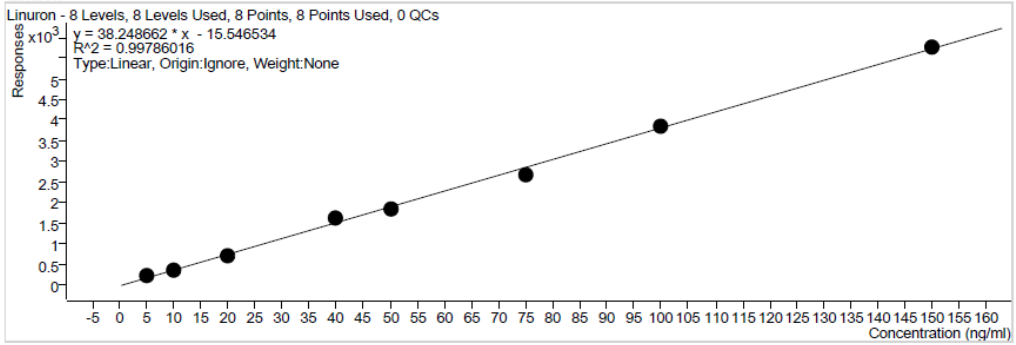

Batch Path	D:\MassHunter\Data\Food and Dugs\GE 074-2021\QuantResults\GE 074-2021 Progesterone Batch.batch.bin		
Analysis Time	3/26/2021 7:52:07 AM	Analyst Name	DGAL-PC\Admin
Report Time	3/26/2021 7:53:05 AM	Reporter Name	Admin
Last Calib Update	3/26/2021 7:52:07 AM	Batch State	Processed
Quant Batch Version	B.07.01	Quant Report Version	B.07.01

Progesterone

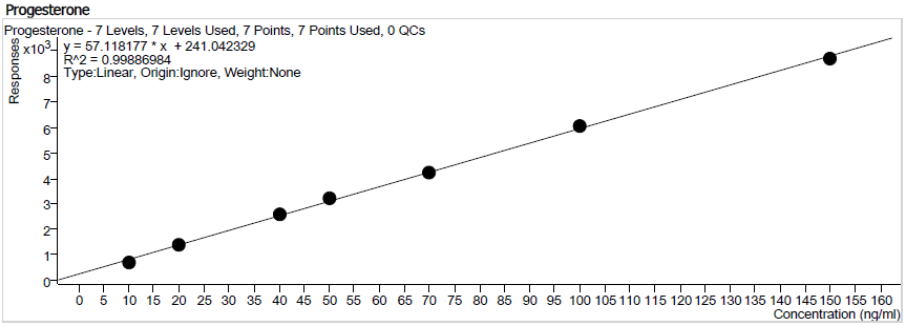

Appendix 7: Some chromatograms for real samples

Sample Chromatogram

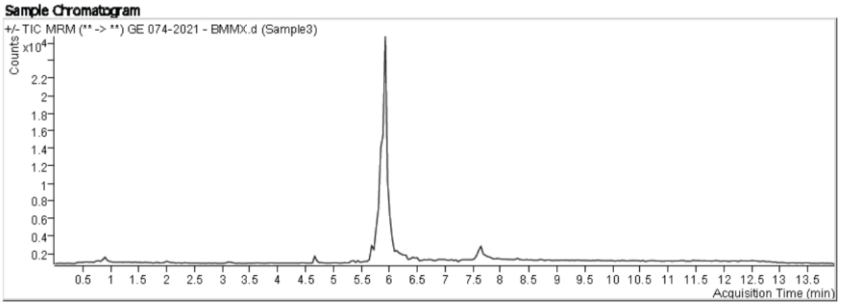

DMP

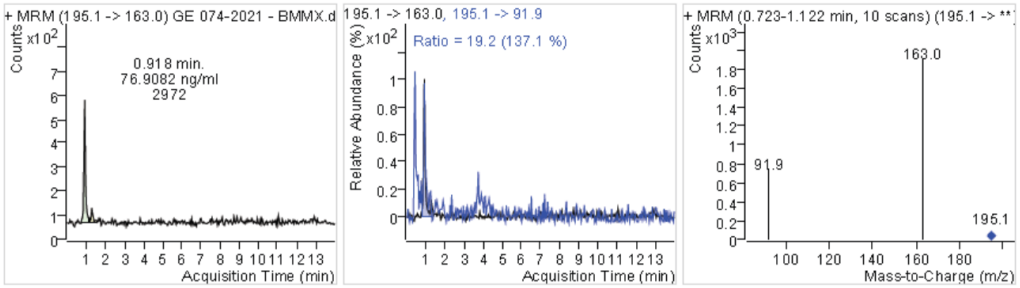

DEHP

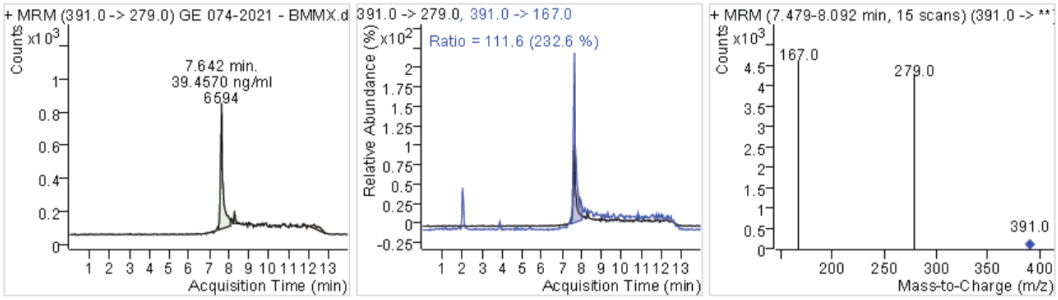

Linuron

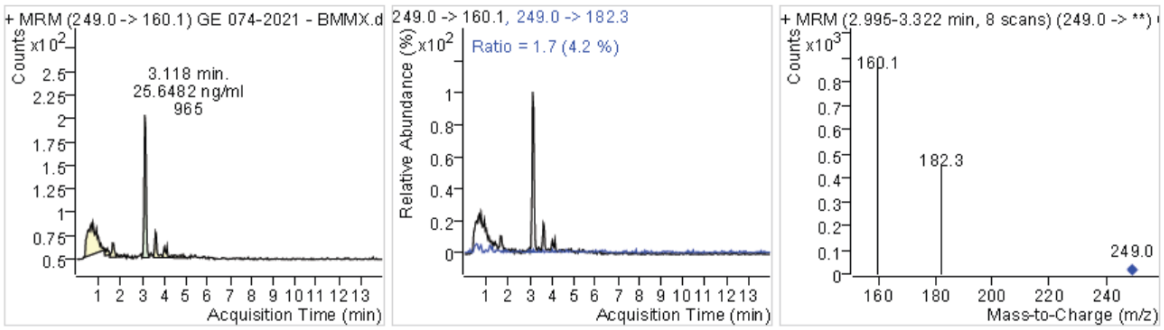

Progesterone

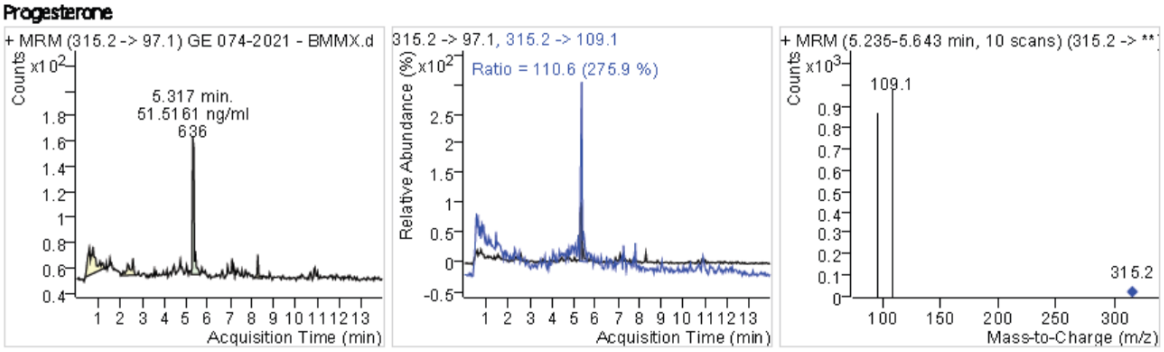

DBP

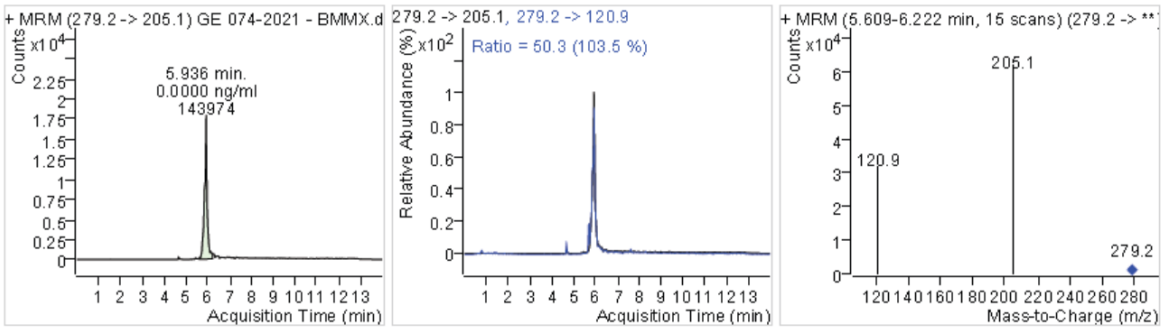

Sample Chromatogram

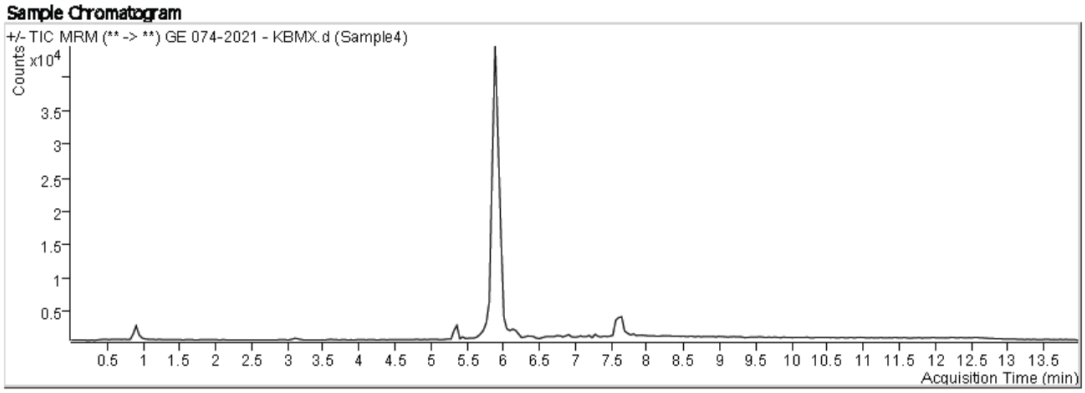

DMP

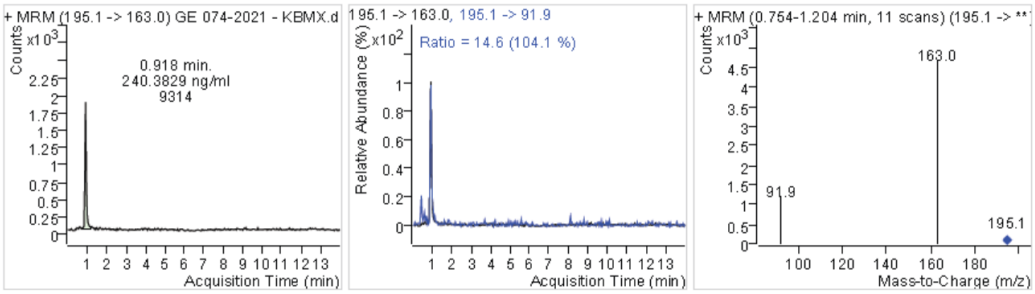

Linuron

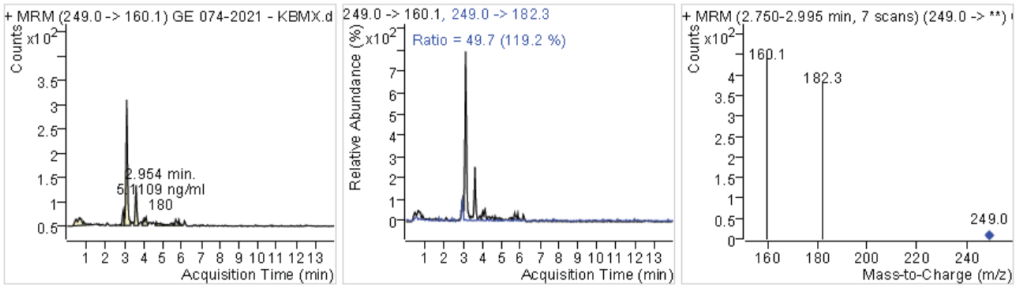

Progesterone

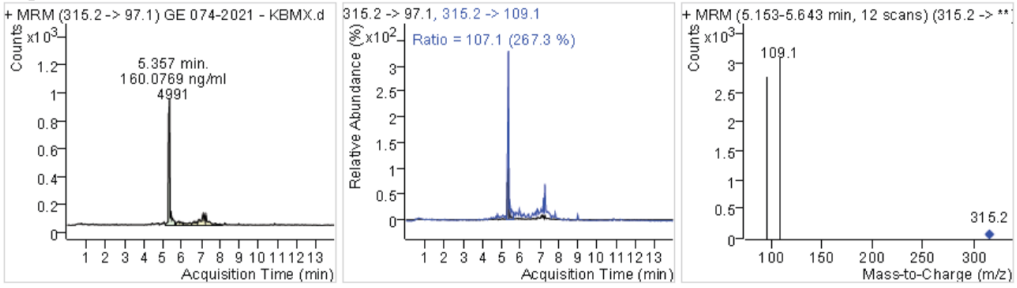

DBP

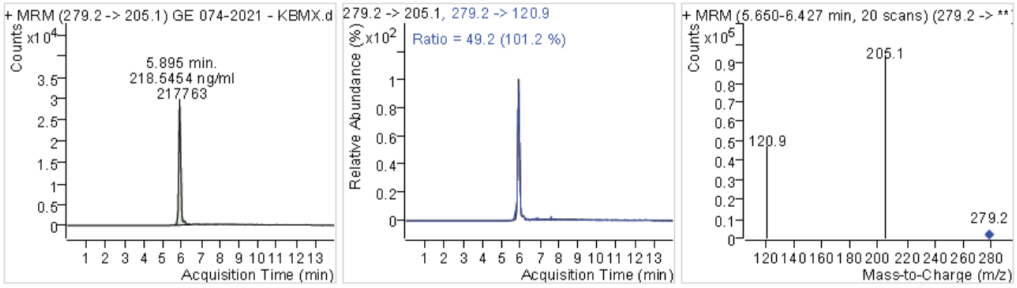

DEHP

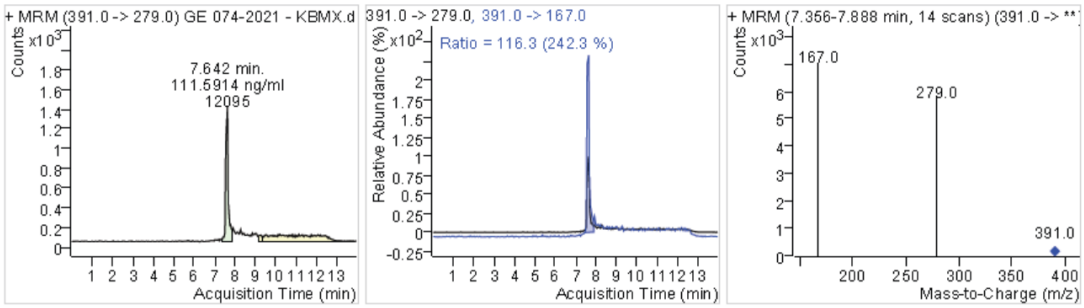

Sample Chromatogram

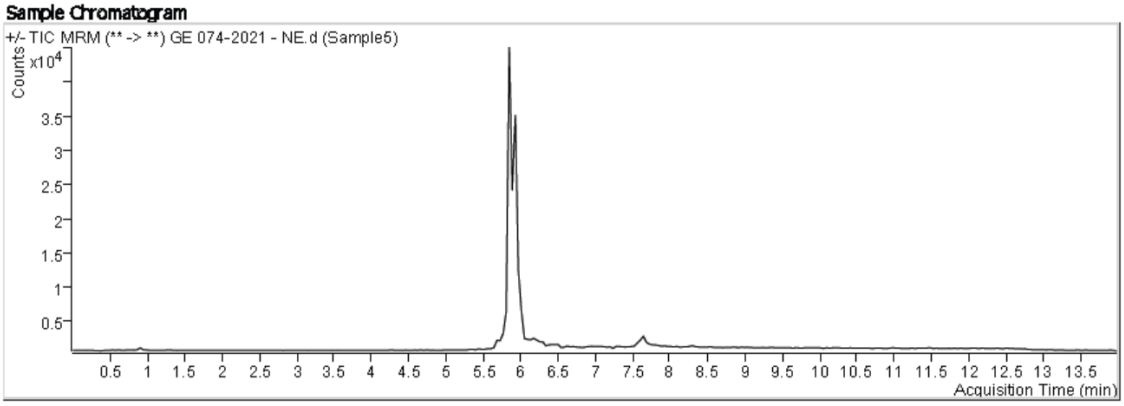

DMP

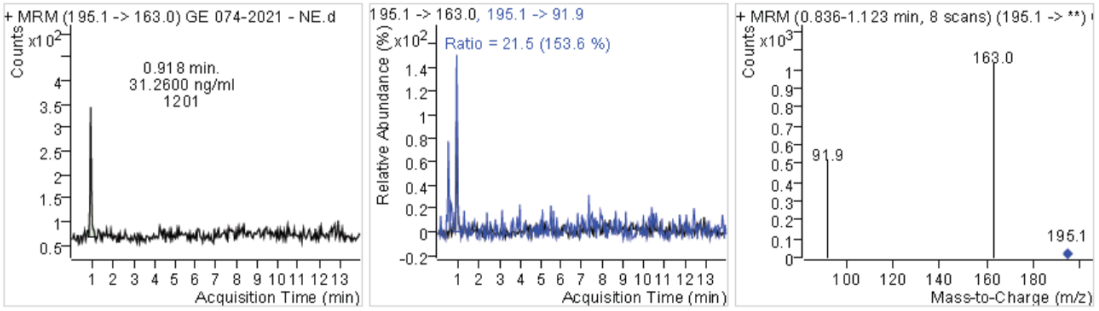

DEHP

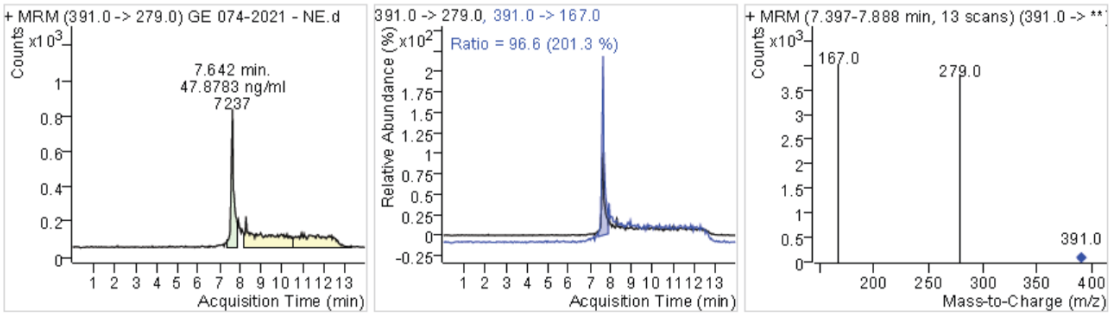

Linuron

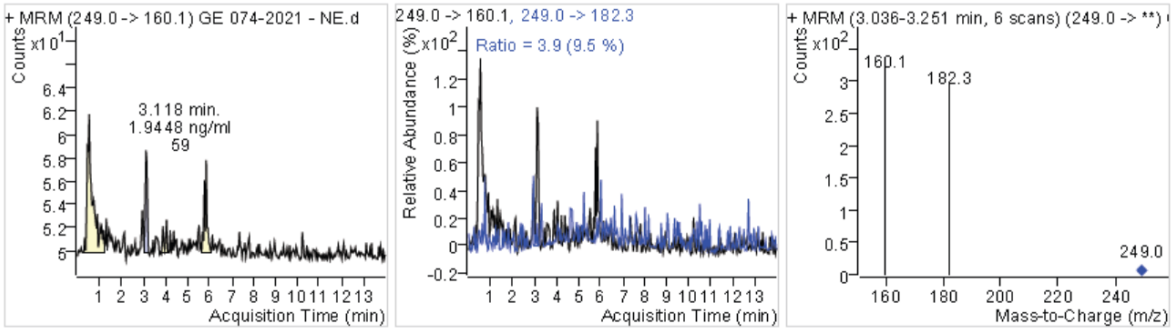

Progesterone

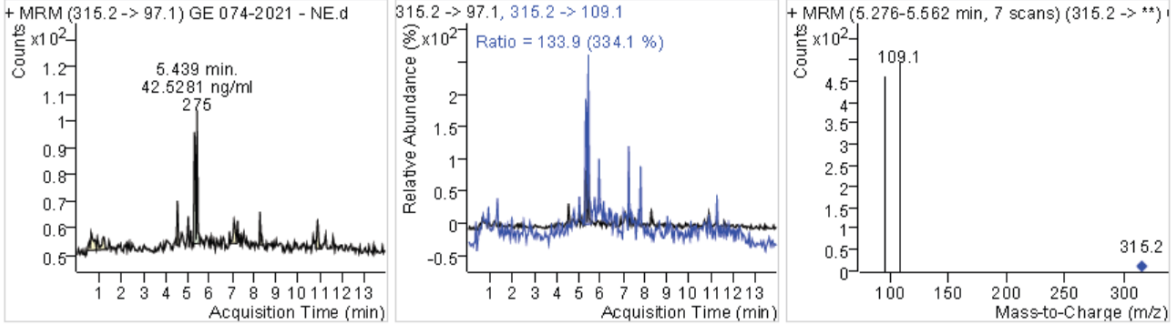

DBP

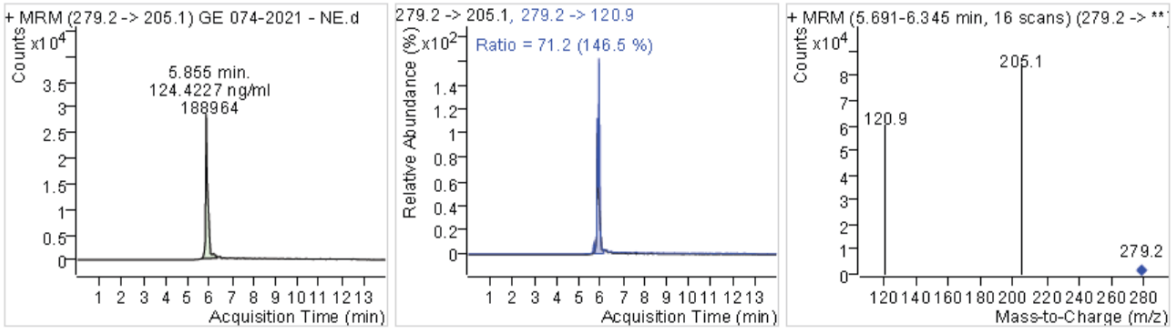

Sample Chromatogram

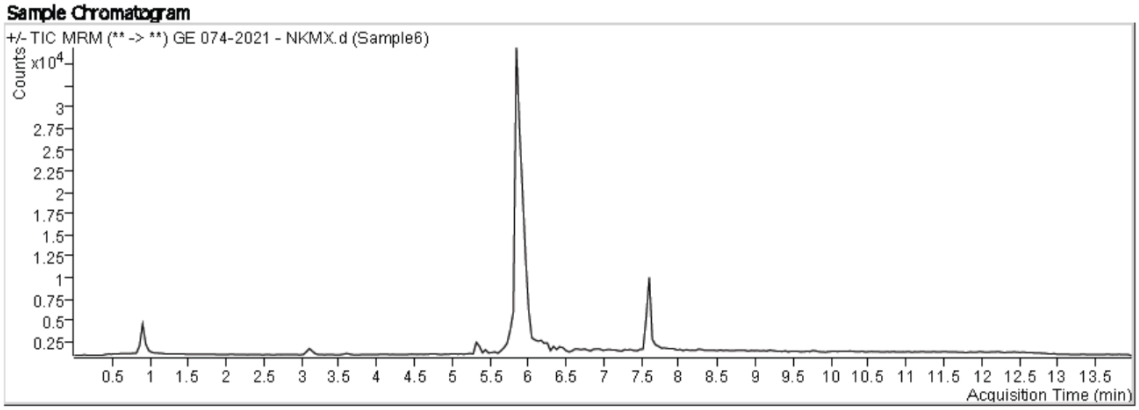

DMP

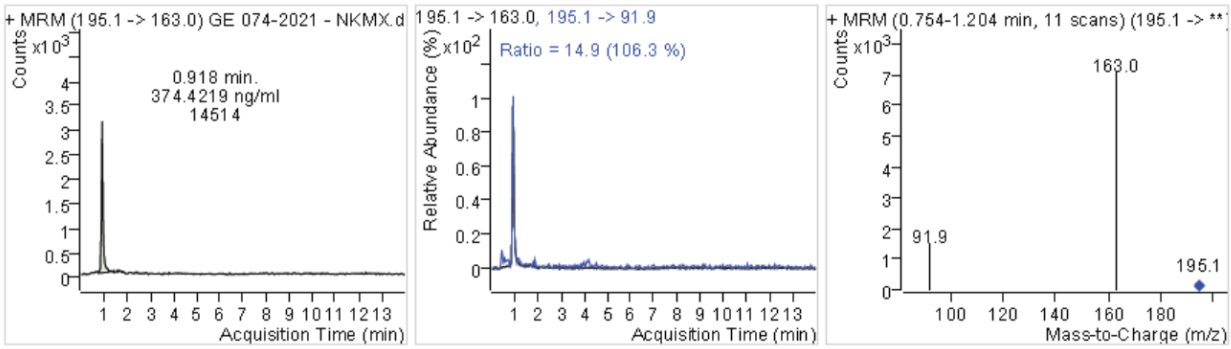

Linuron

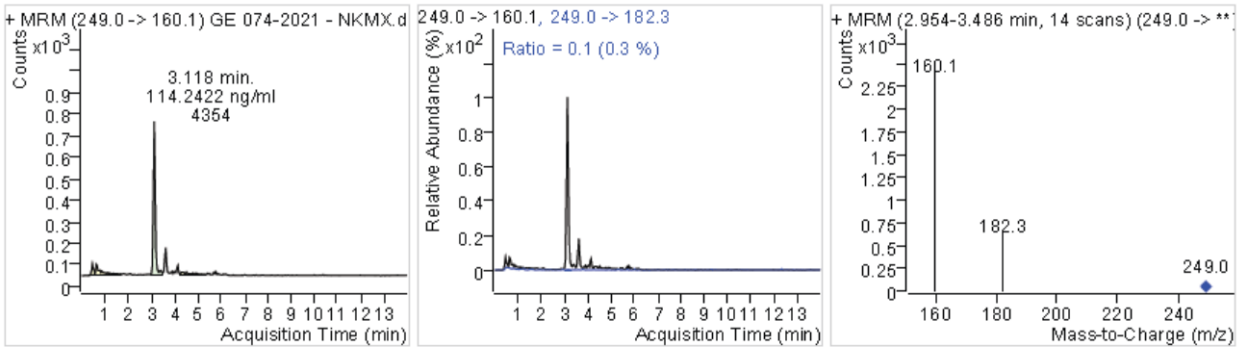

Progesterone

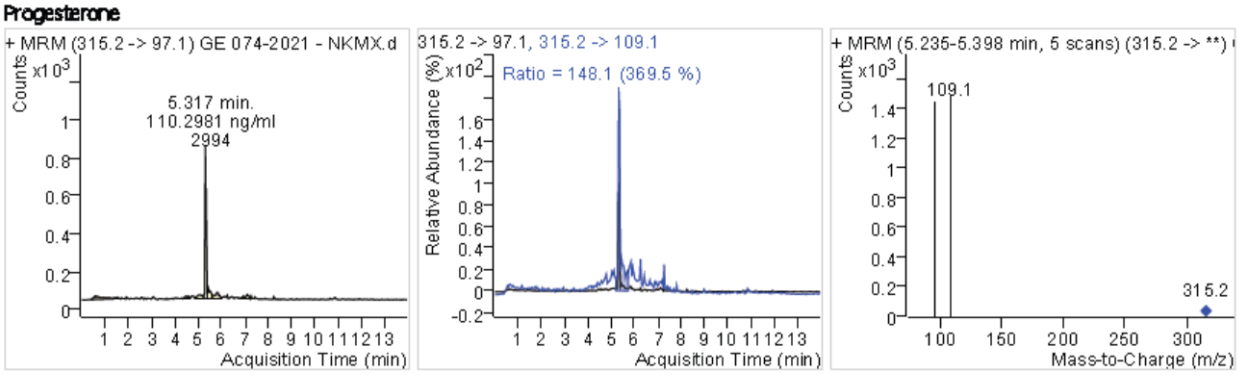

DBP

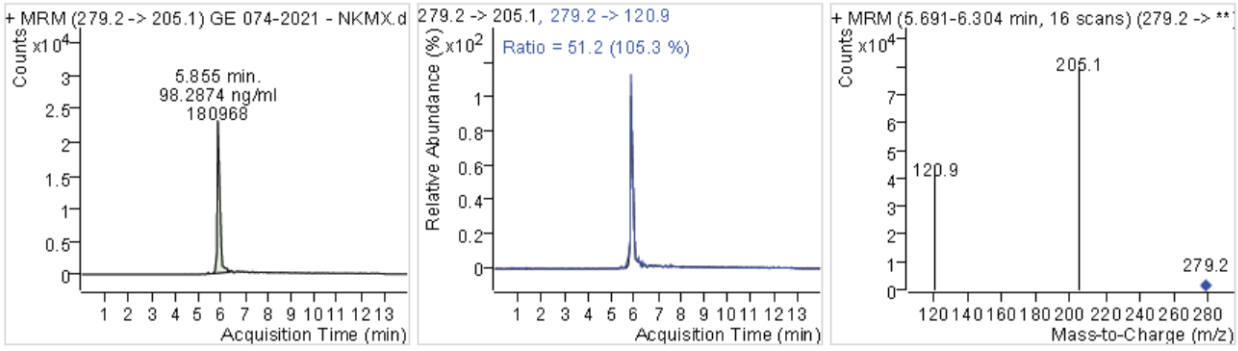

DEHP

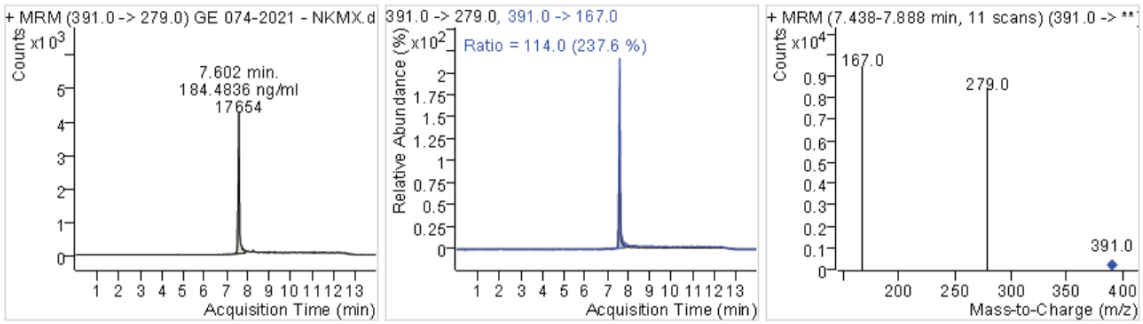

Sample Chromatogram

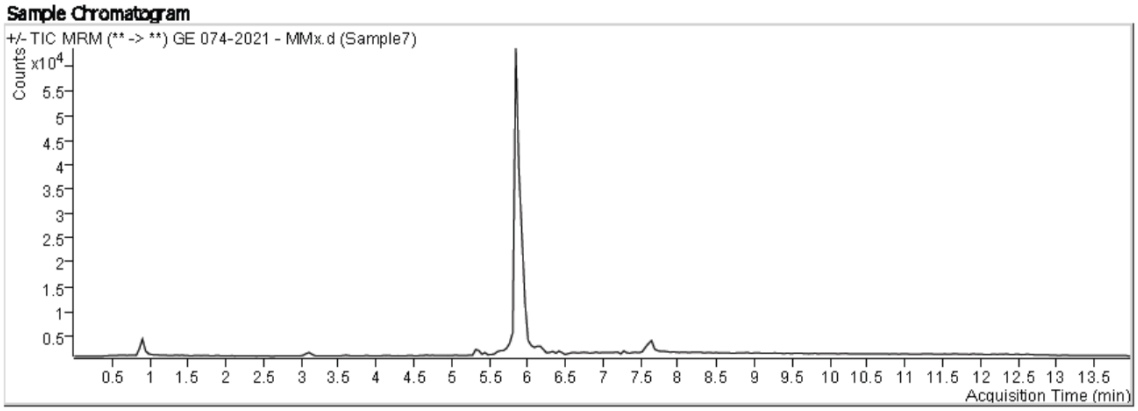

DMP

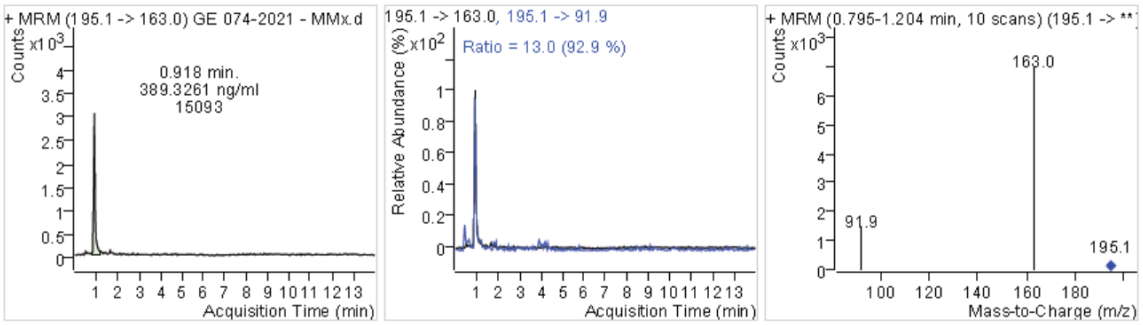

DEHP

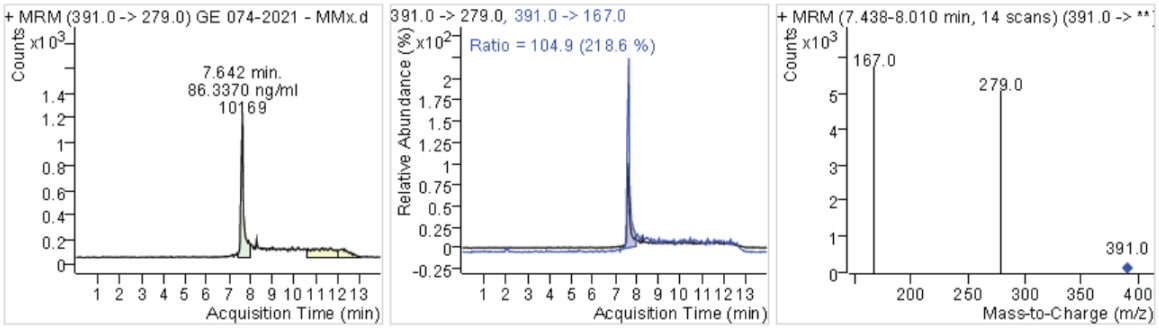

Linuron

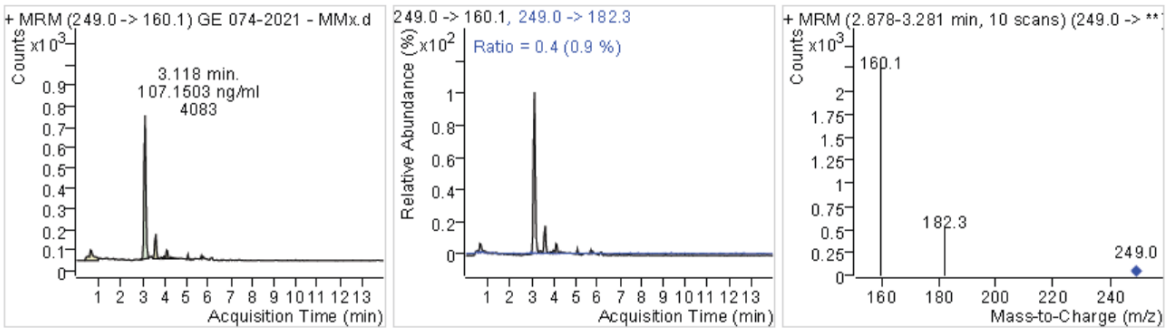

Progesterone

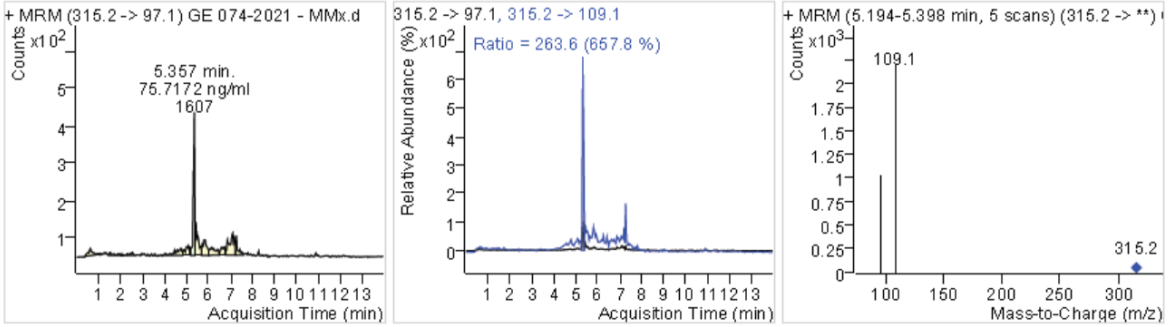

DBP

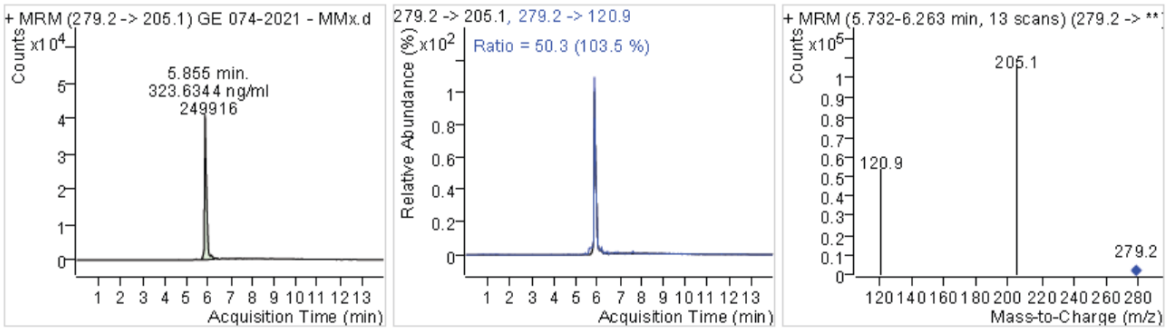

Sample Chromatogram

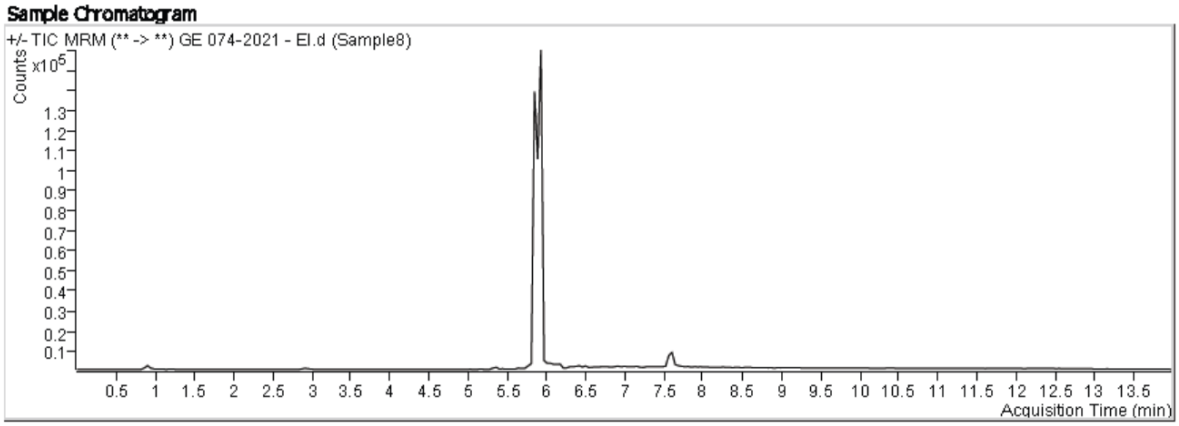

DEHP

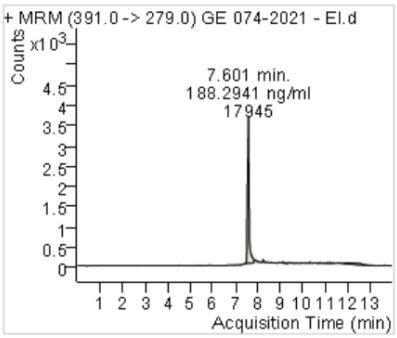

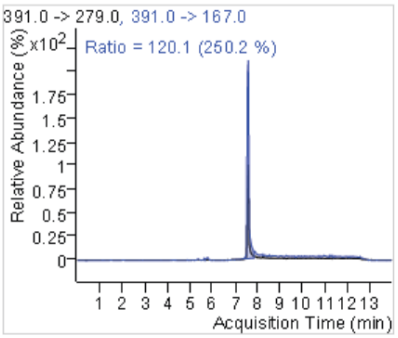

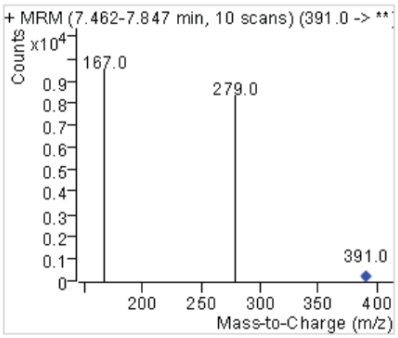

Linuron

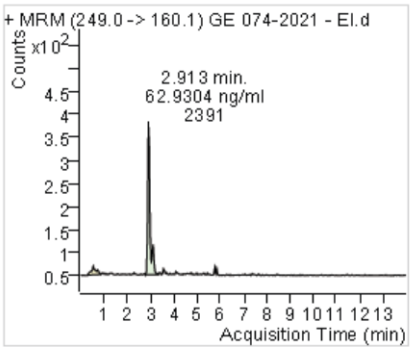

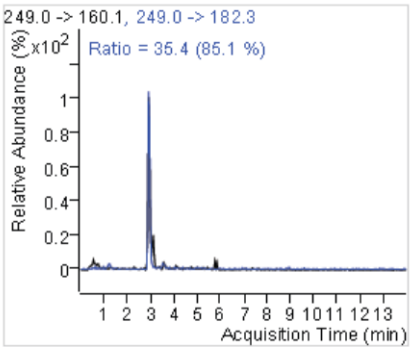

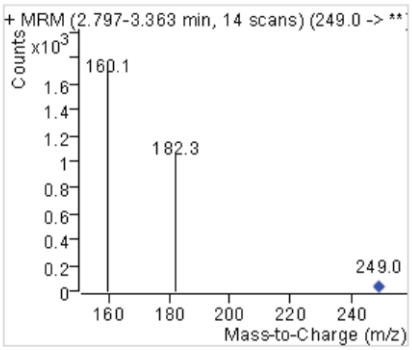

Progesterone

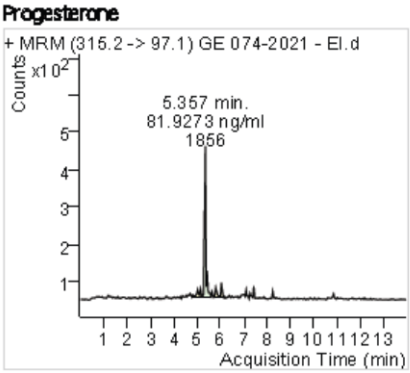

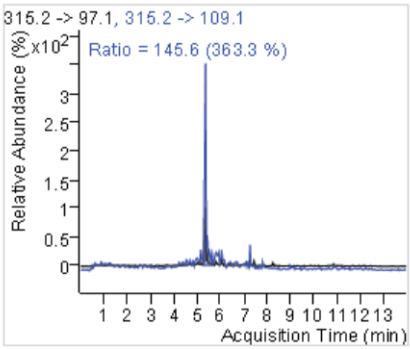

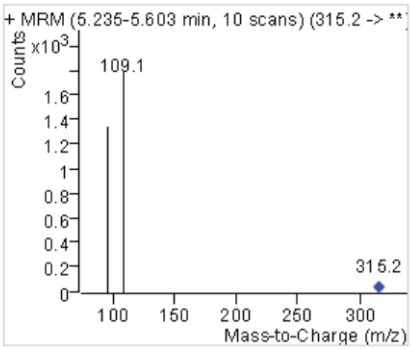

DBP

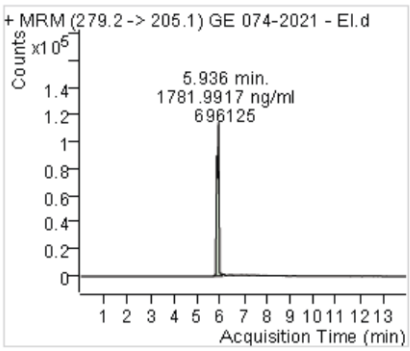

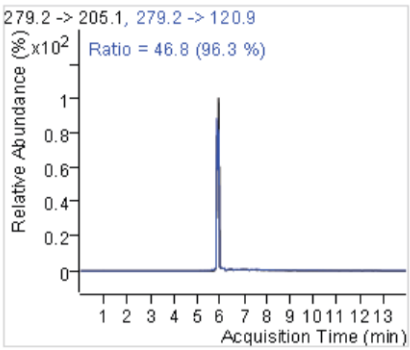

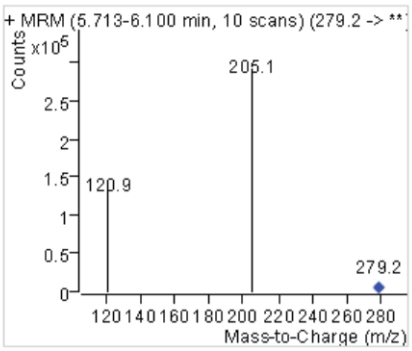

DMP

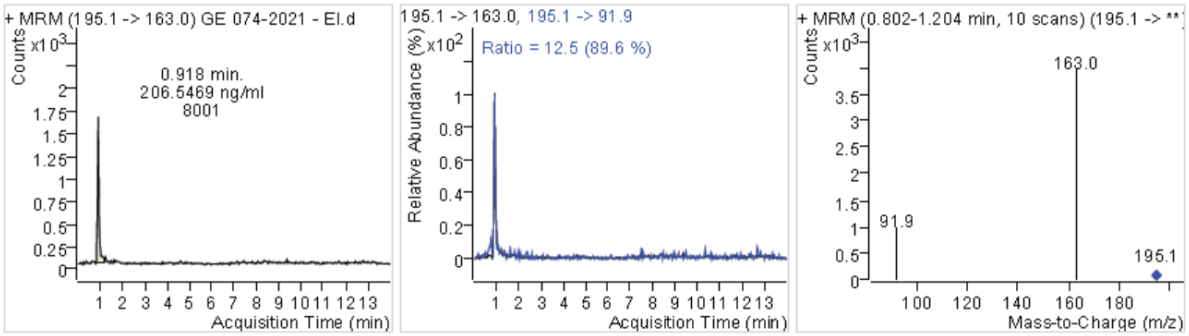

Sample Chromatogram

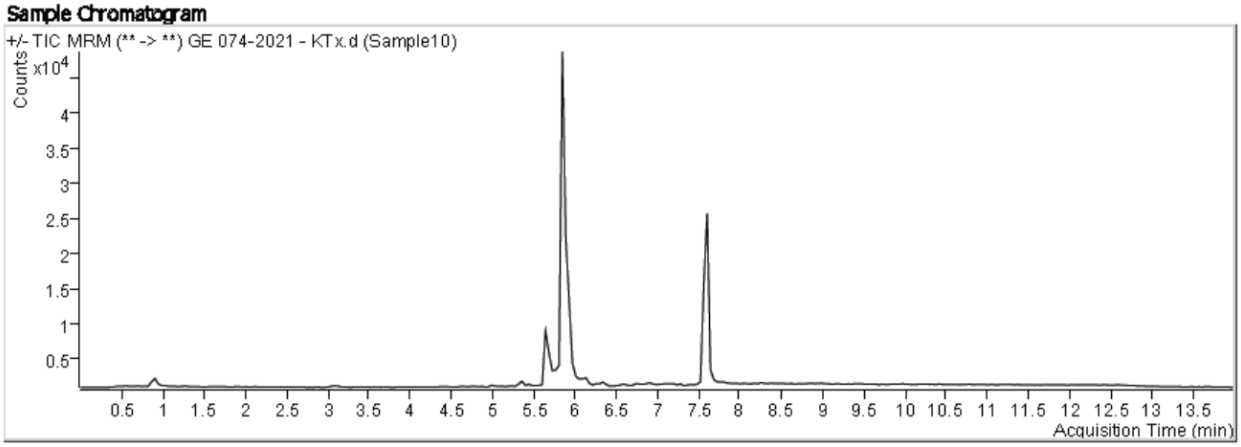

DMP

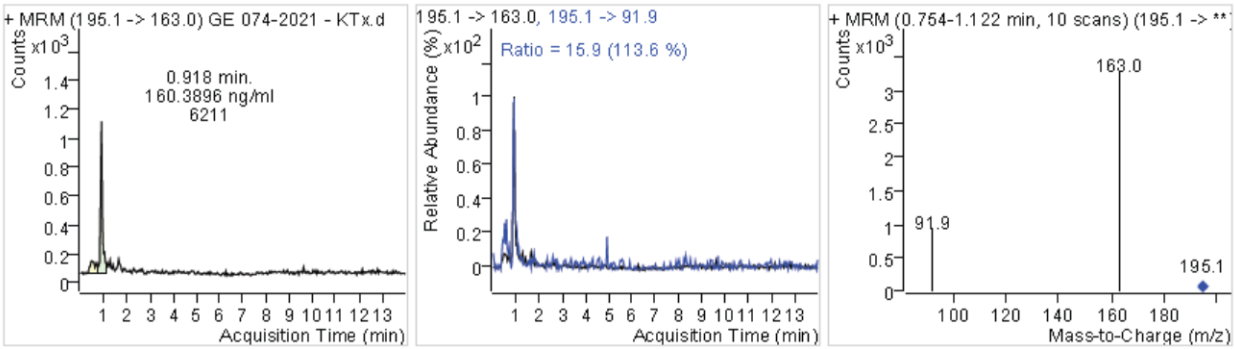

DEHP

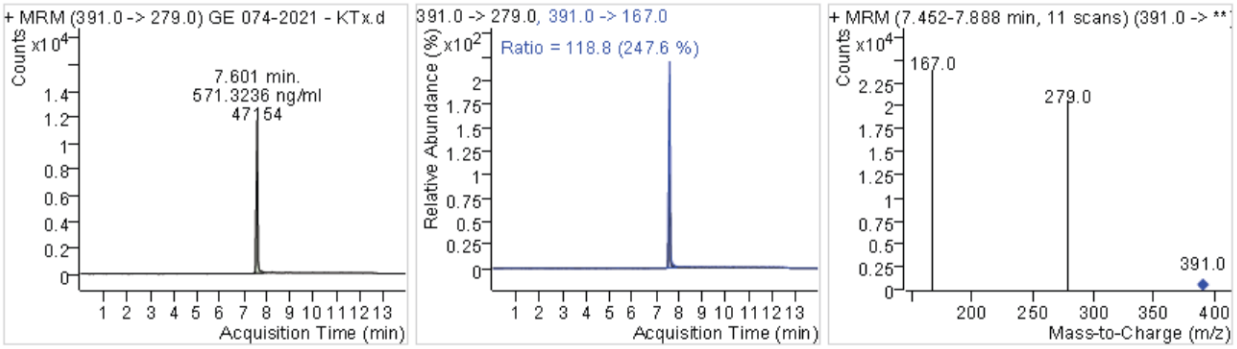

Linuron

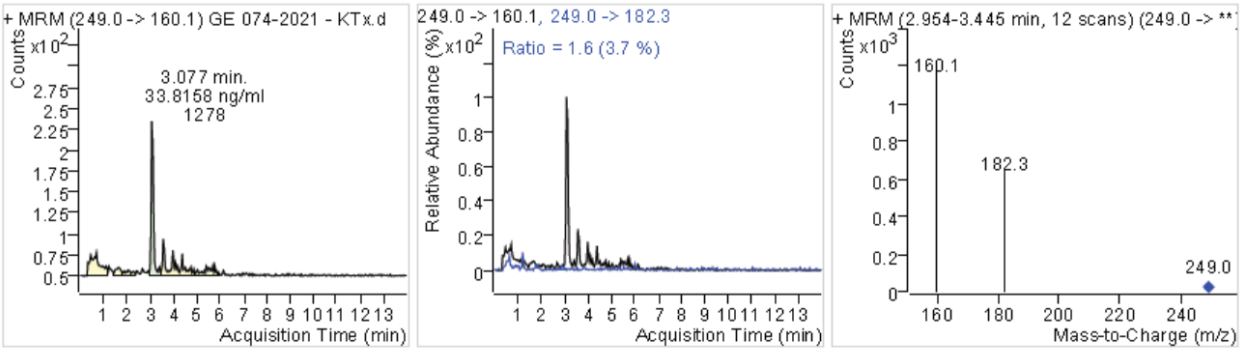

Progesterone

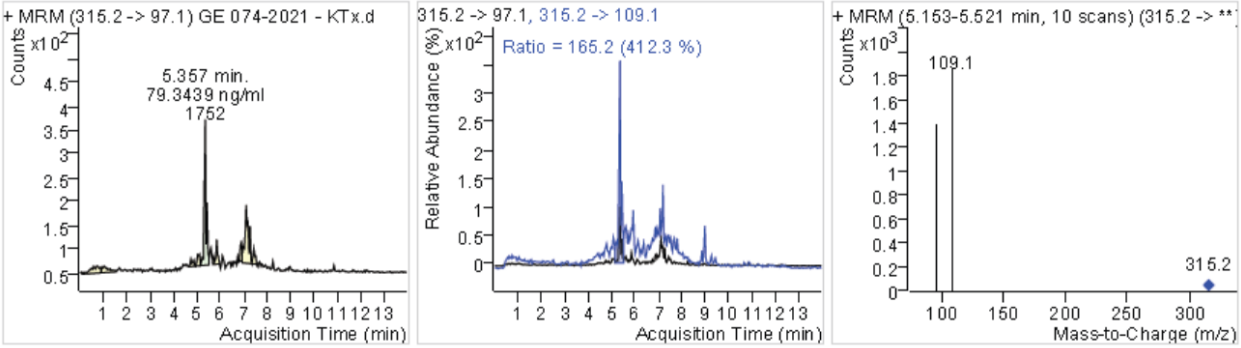

DBP

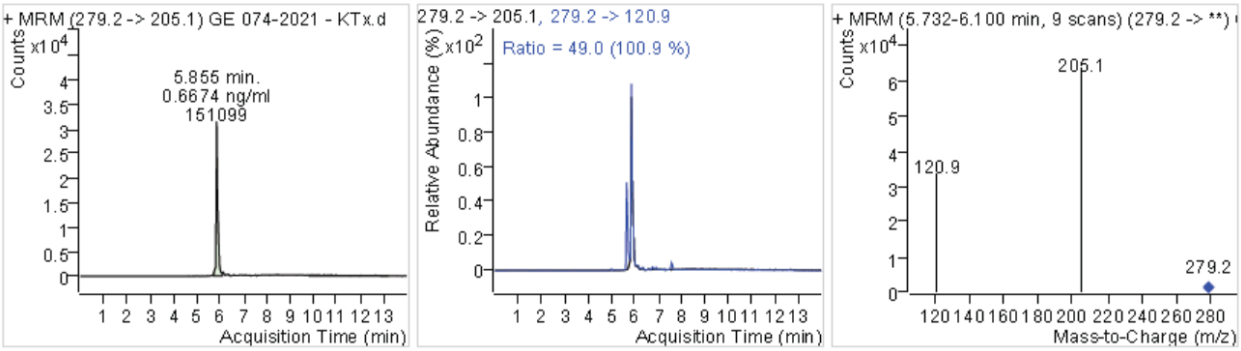

Appendix 8: Levels of EDCs (μgl^{-1}) in the wastewater samples

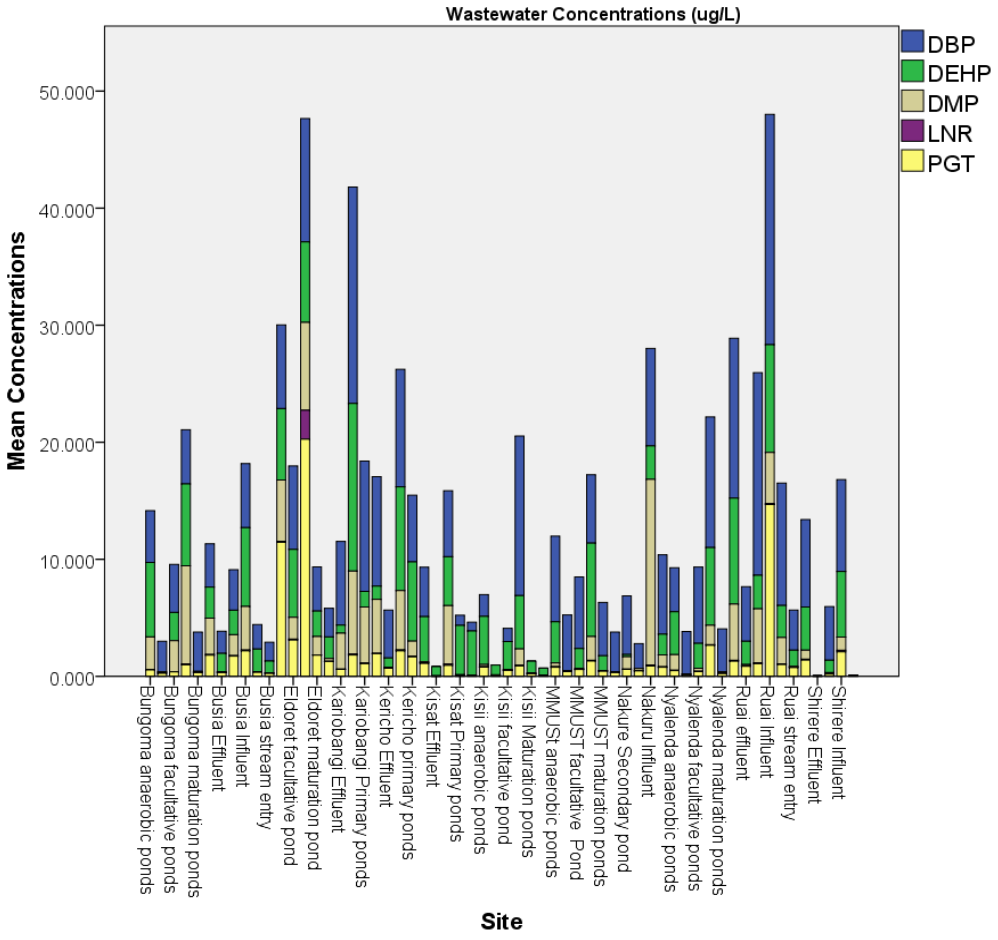

Appendix 9: Characterization of the adsorbent-SEM-EDS at different magnifications for untreated *MOSB*

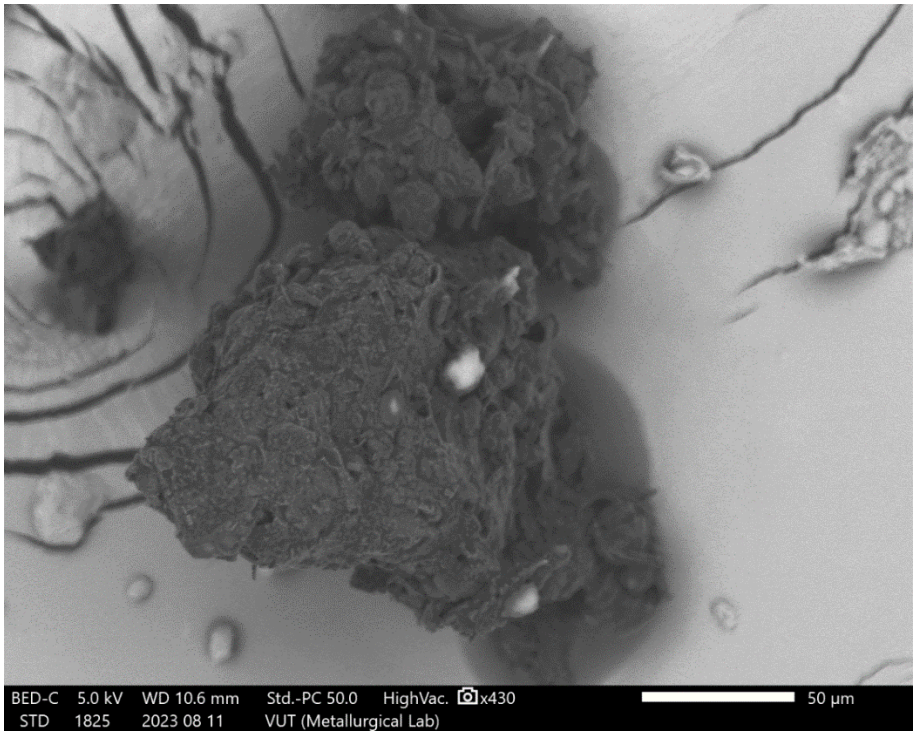

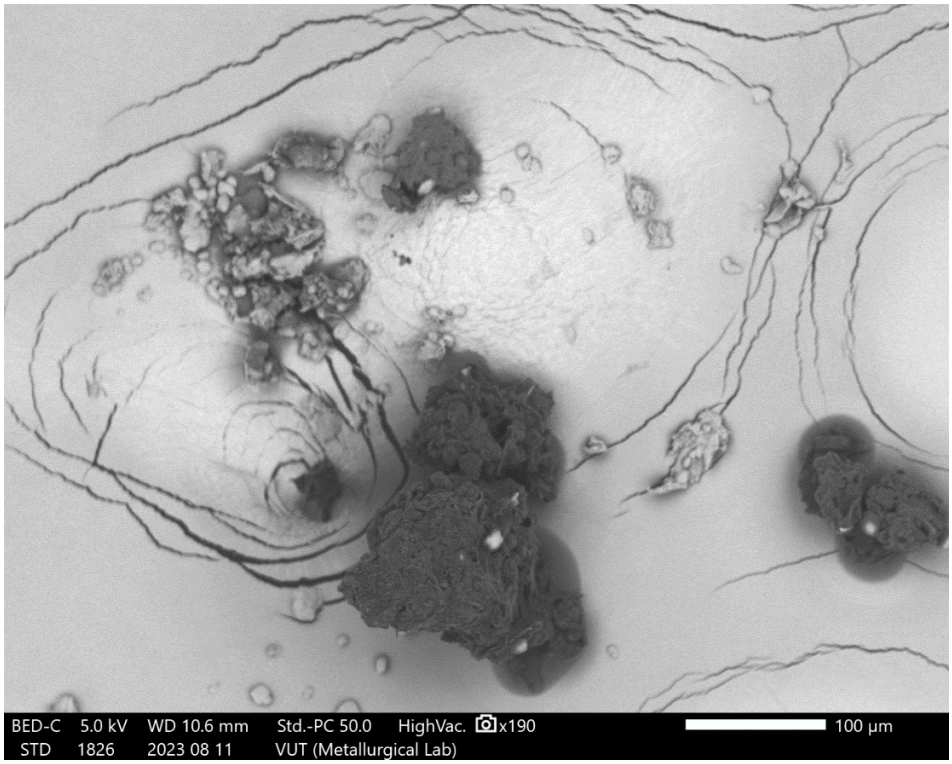

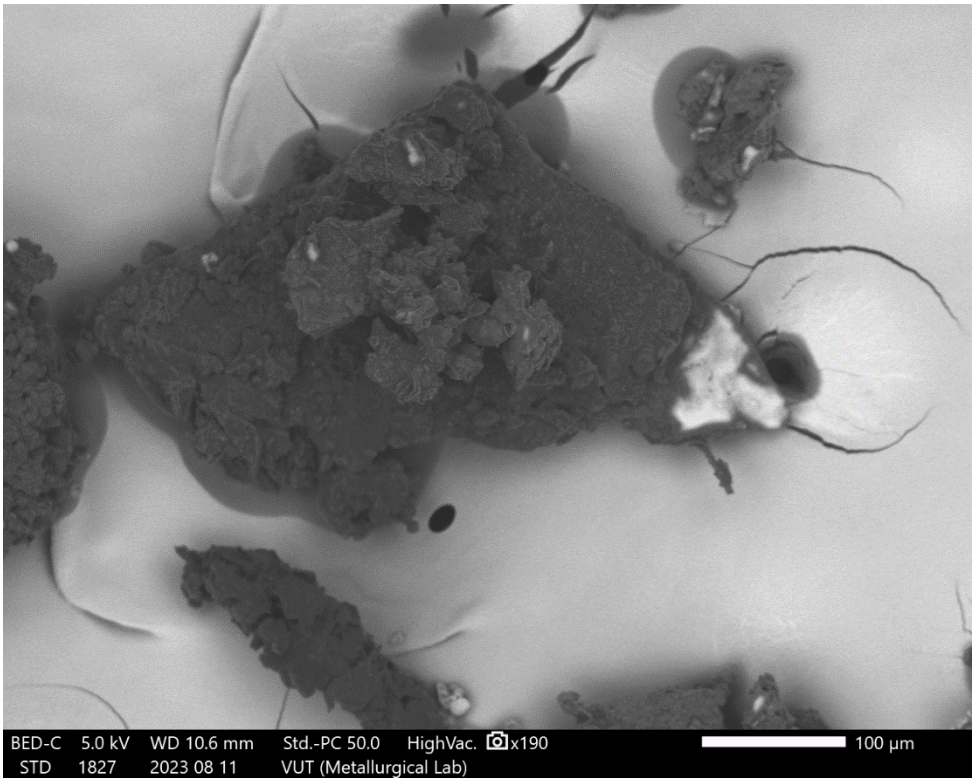
BED-C 5.0 kV WD 10.6 mm Std.-PC 50.0 HighVac. x190 100 µm
STD 1827 2023 08 11 VUT (Metallurgical Lab)

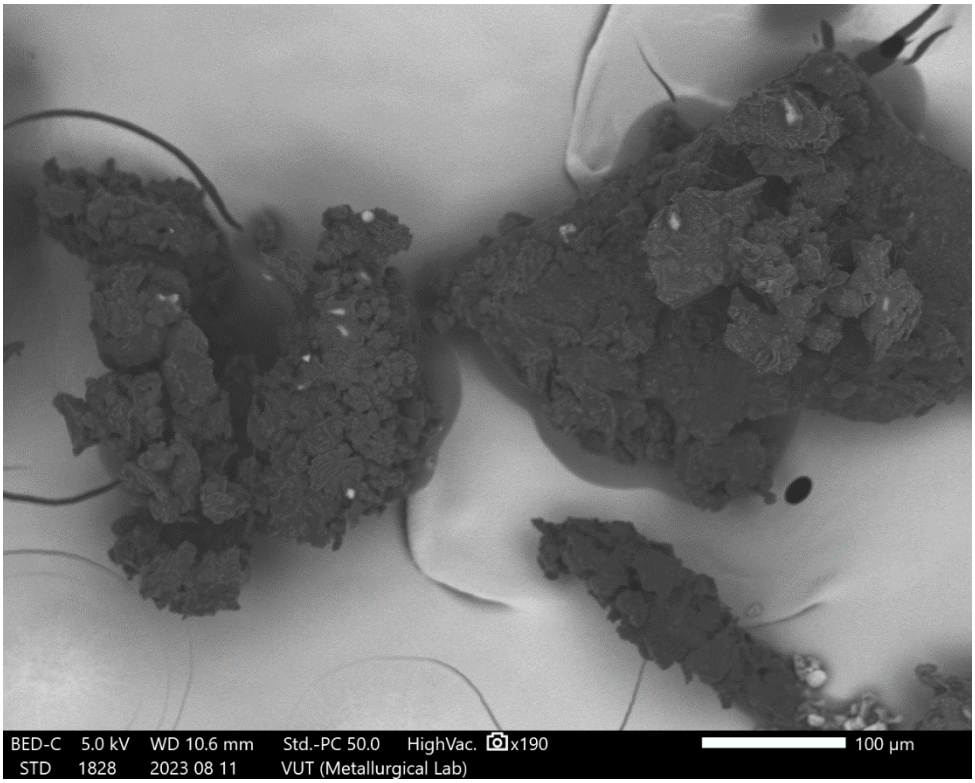
BED-C 5.0 kV WD 10.6 mm Std.-PC 50.0 HighVac. x190 100 µm
STD 1828 2023 08 11 VUT (Metallurgical Lab)

Appendix 10: SEM-EDS at different magnifications for treated *MOSB*

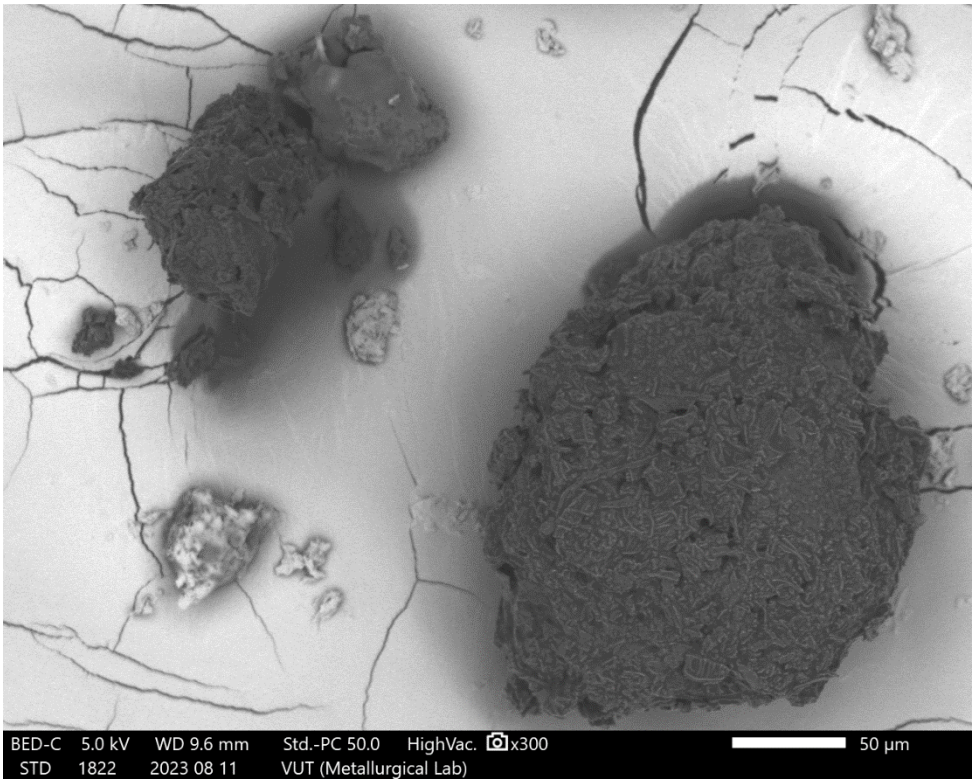

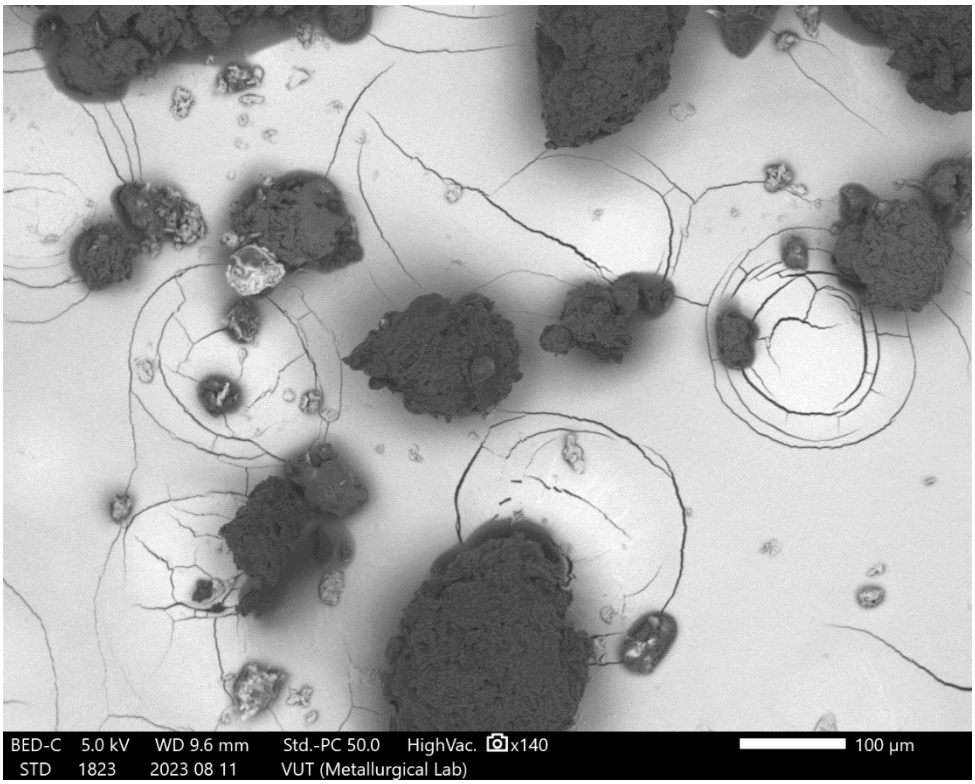

Appendix 11: *MOSB*-PGT SEM-EDS

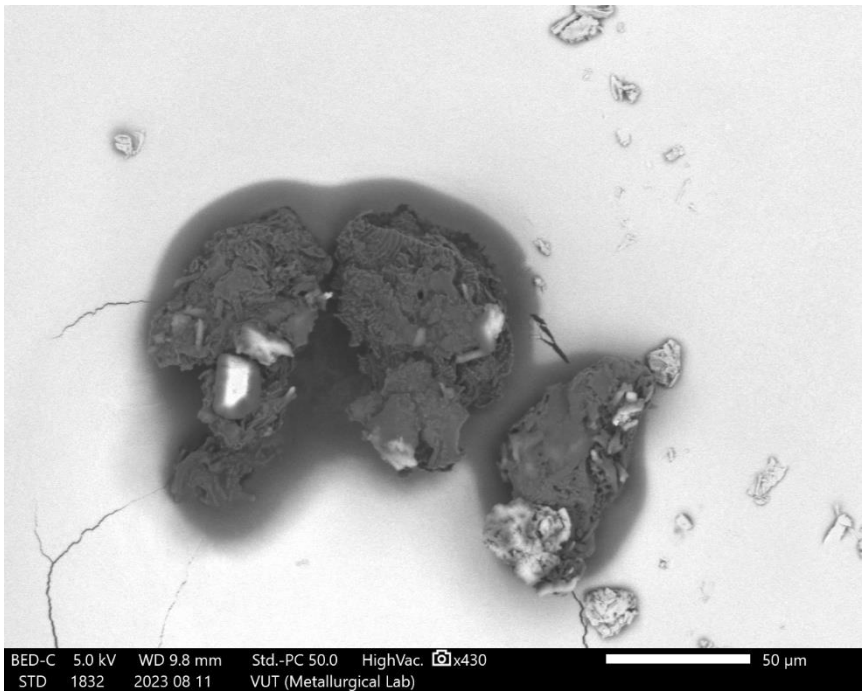

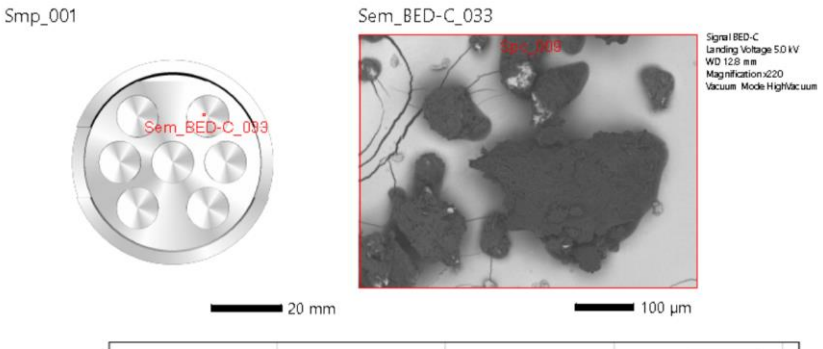

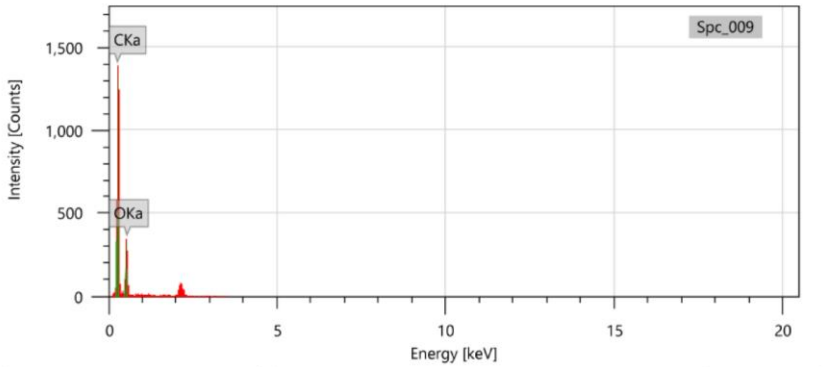

Items	Value
measurement conditions	
Acceleration voltage	5.00 kV
Probe current	-
Magnification	x 220
Process time	T3
Measurement detector	First
Live time	30.00 seconds
Real time	30.17 seconds
Dead time	1.00 %
Count rate	548.00 CPS

Display name	Standard data	Quantification method	Result Type
Spc_009	Standardless	ZAF	Metal

Element	Line	Mass%	Atom%
C	K	71.37±0.35	76.86±0.37
O	K	28.63±0.53	23.14±0.43
Total		100.00	100.00
Spc_009			Fitting ratio 0.0406

Appendix 12: *MOSB*-LNR SEM-EDS

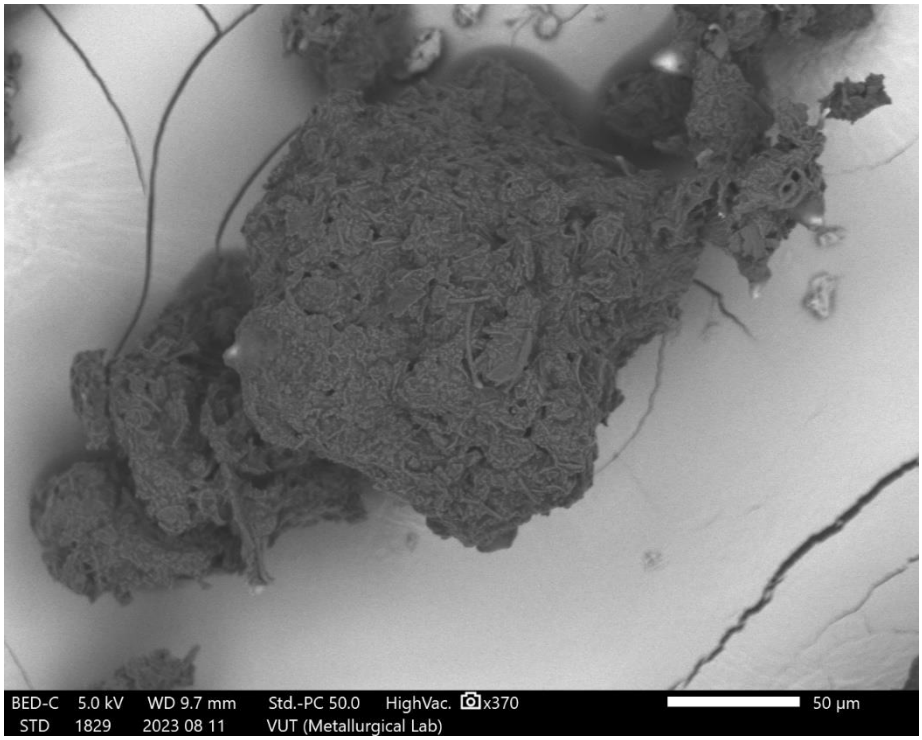

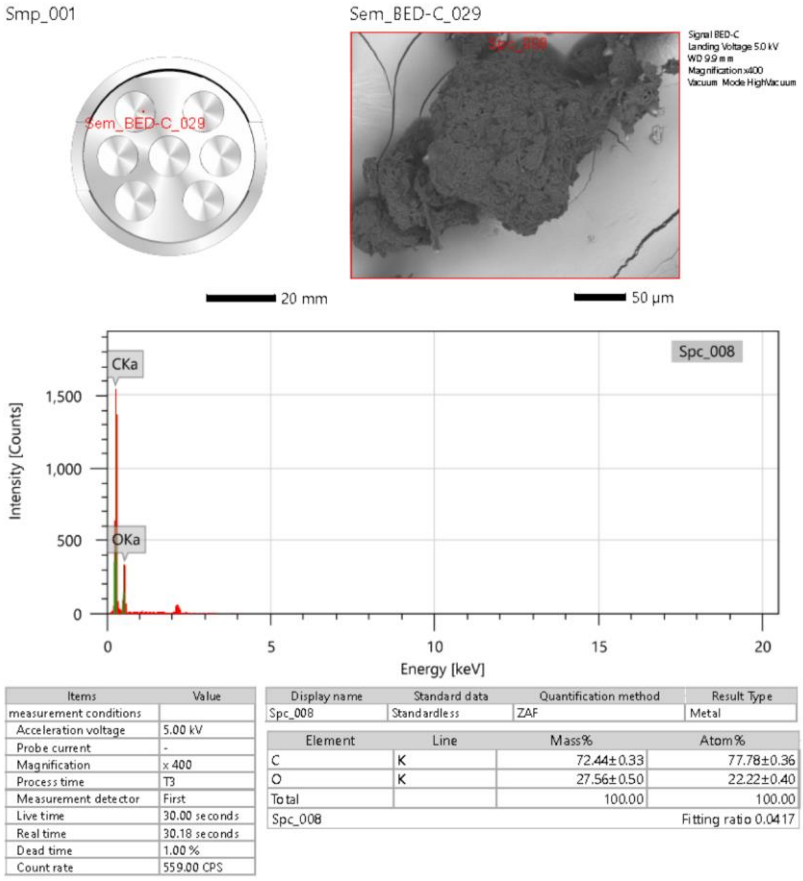

Items	Value
measurement conditions	
Acceleration voltage	5.00 kV
Probe current	-
Magnification	x 400
Process time	T3
Measurement detector	First
Live time	30.00 seconds
Real time	30.18 seconds
Dead time	1.00 %
Count rate	559.00 CPS

Display name	Standard data	Quantification method	Result Type
Spc_008	Standardless	ZAF	Metal

Element	Line	Mass%	Atom%
C	K	72.44±0.33	77.78±0.36
O	K	27.56±0.50	22.22±0.40
Total		100.00	100.00
Spc_008			Fitting ratio 0.0417

Appendix 13: Calibration curve and sample chromatograms for PGT biosorption

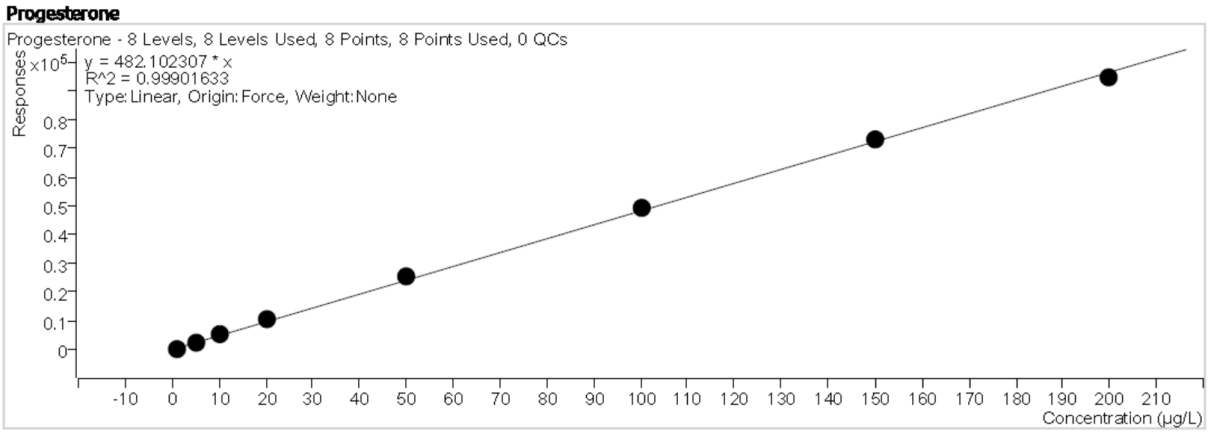

Sample Chromatogram

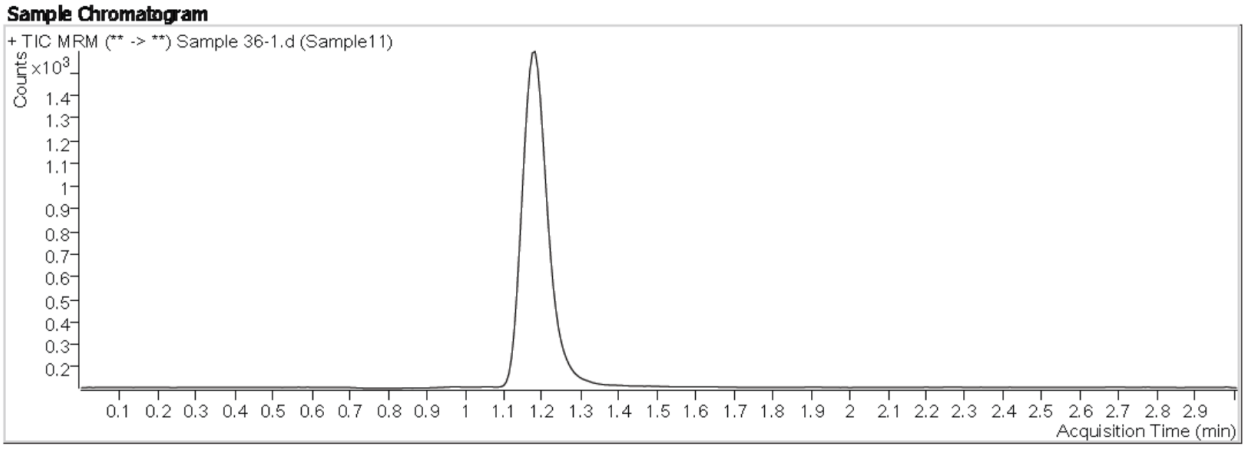

Progesterone

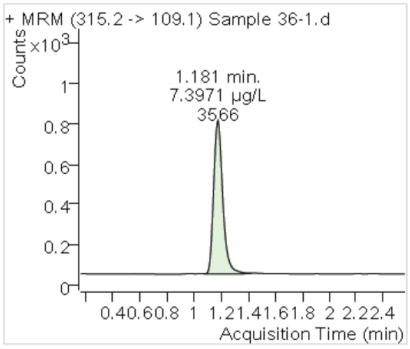

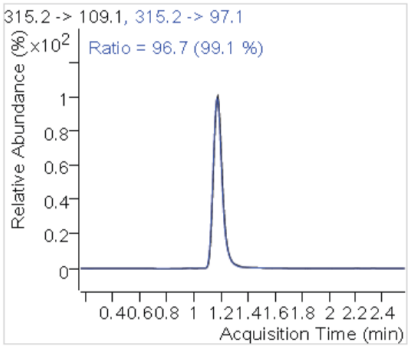

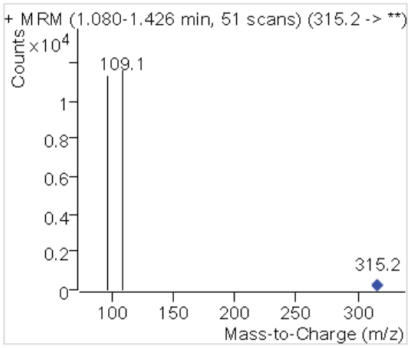

Progesterone

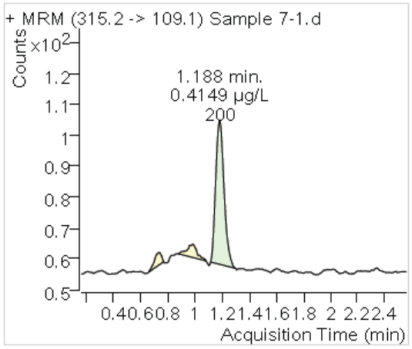

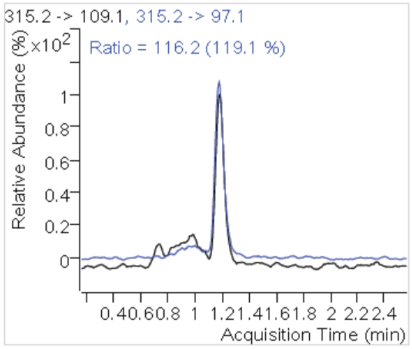

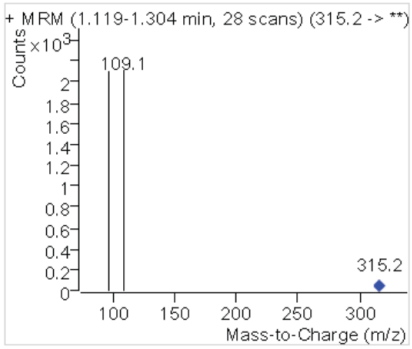

Progesterone

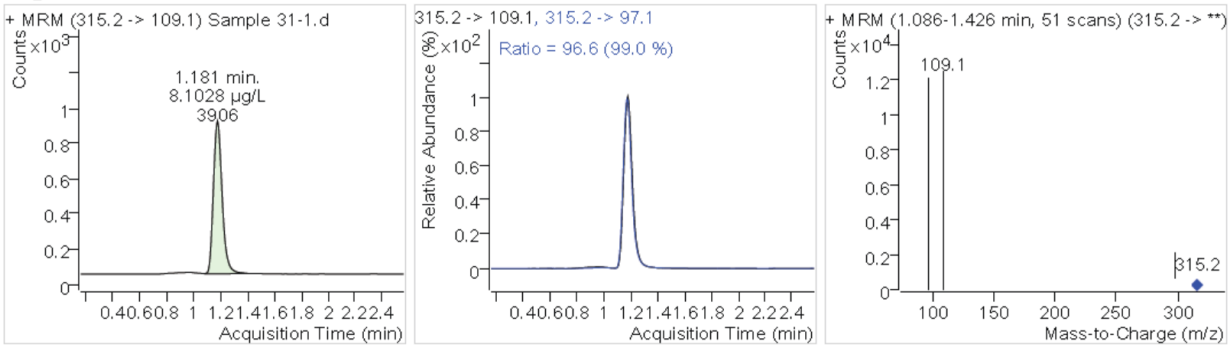

Progesterone

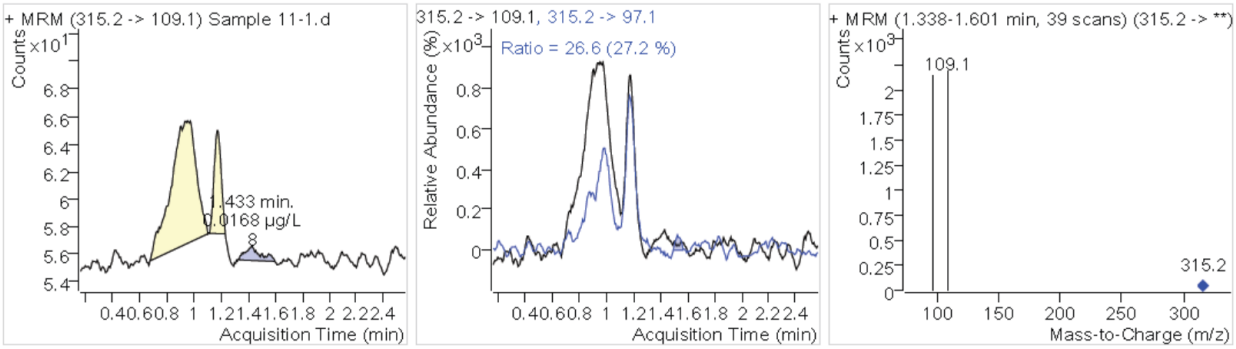

Progesterone

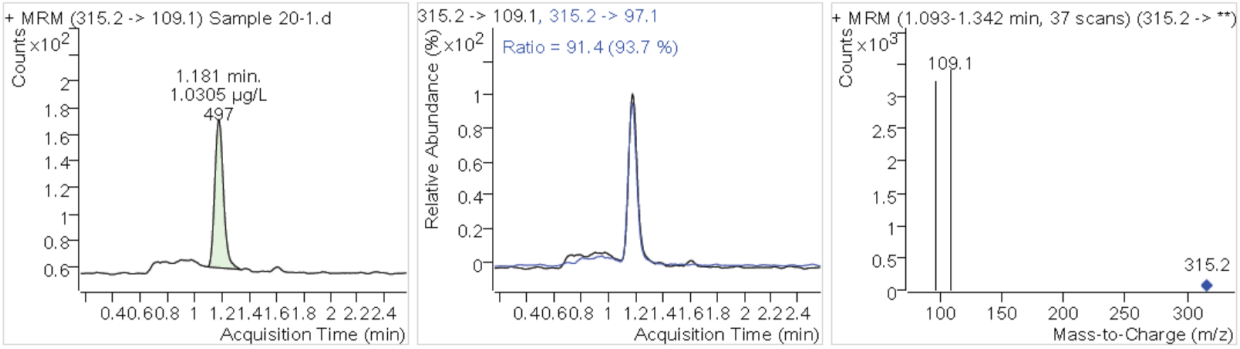

Progesterone

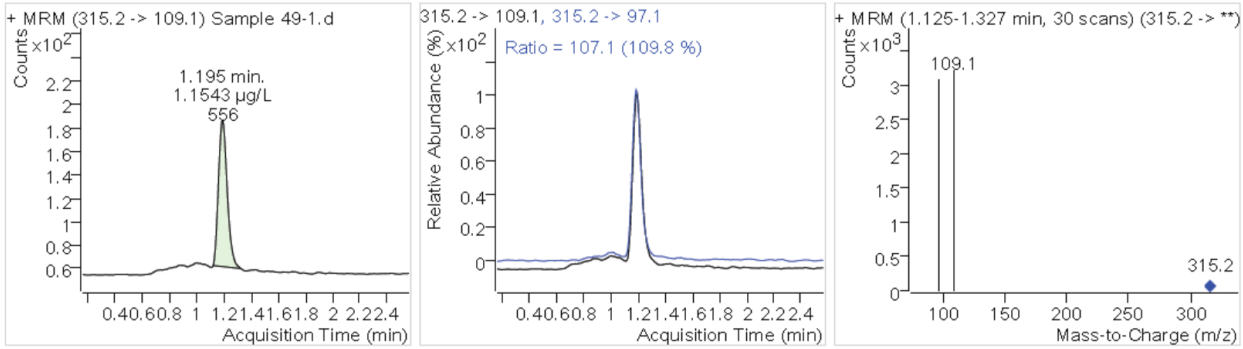

Progesterone

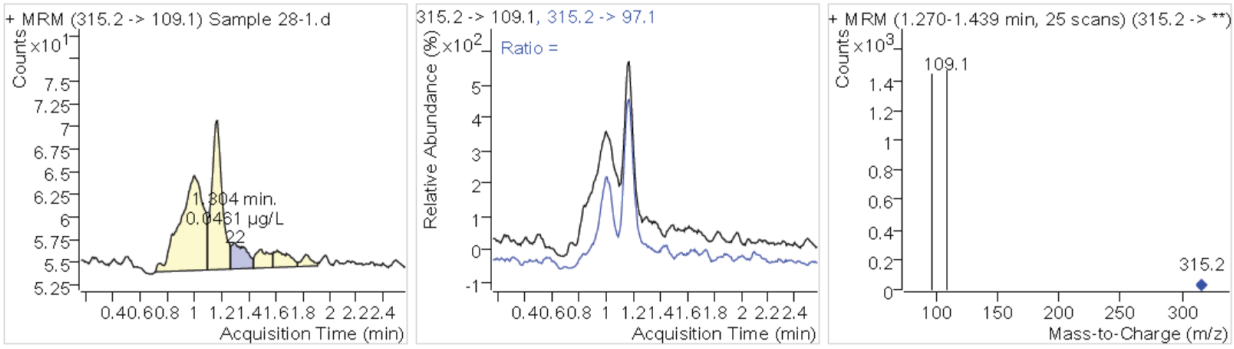

Progesterone

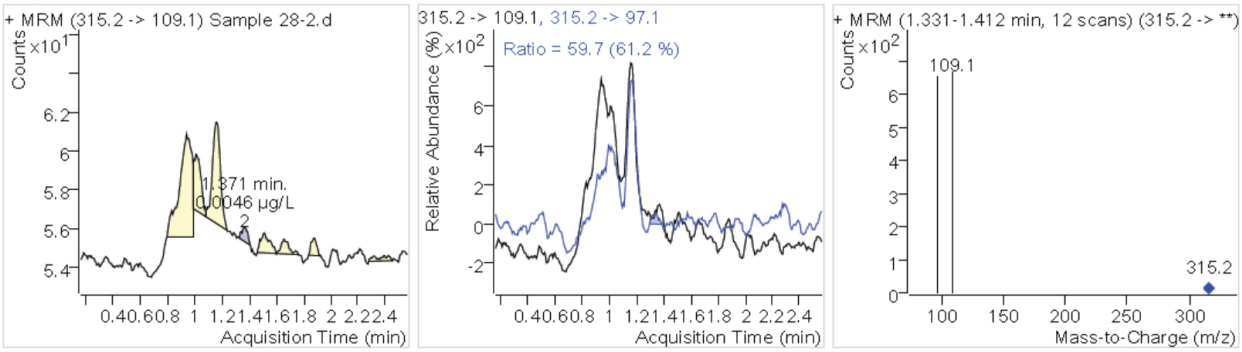

Progesterone

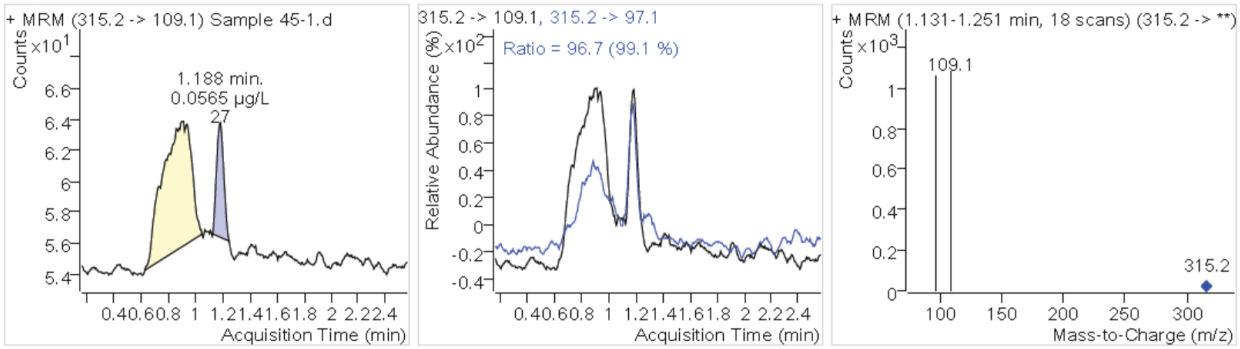

Progesterone

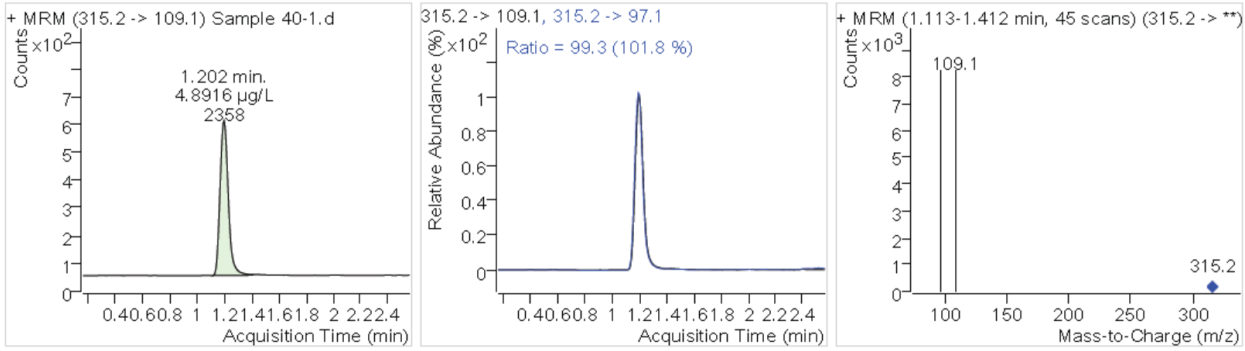

Progesterone

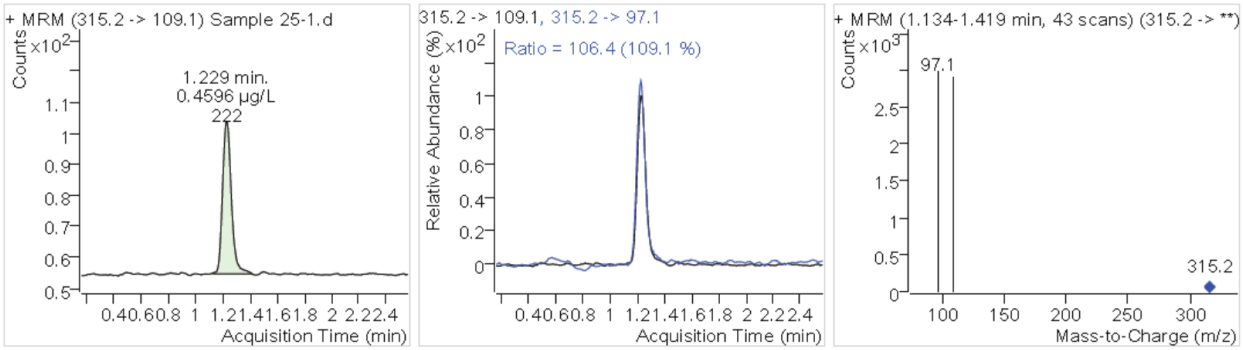

Progesterone

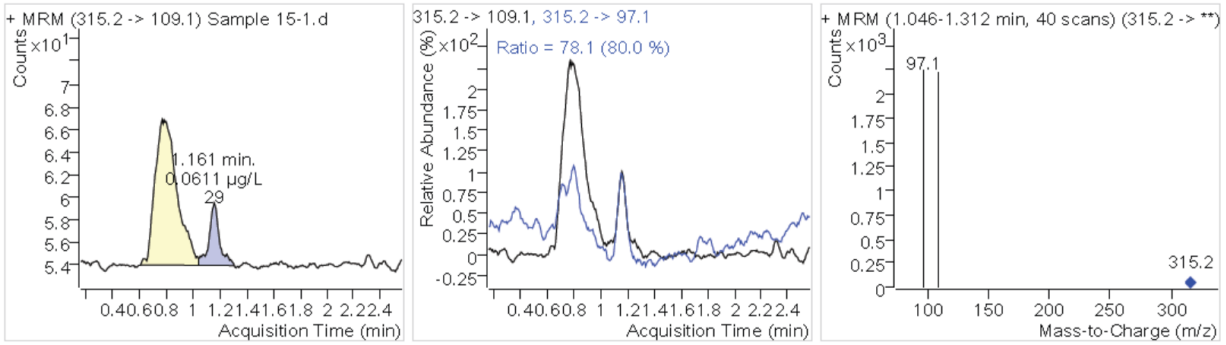

Progesterone

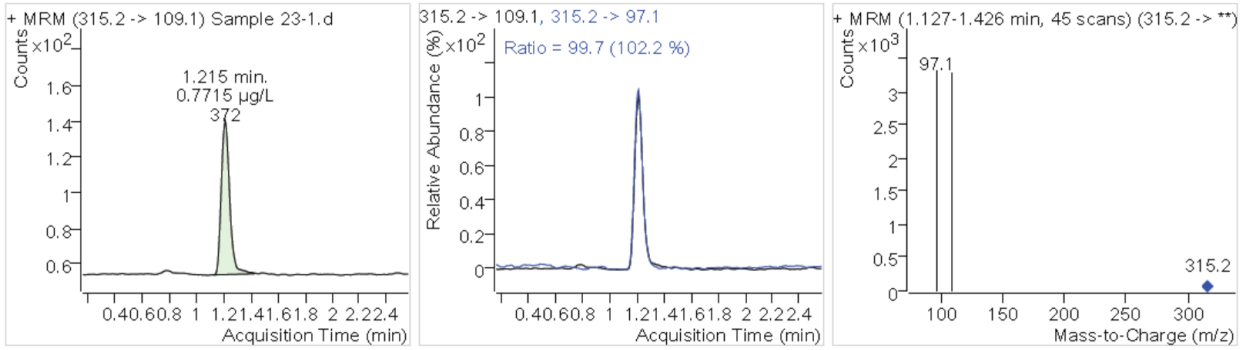

Progesterone

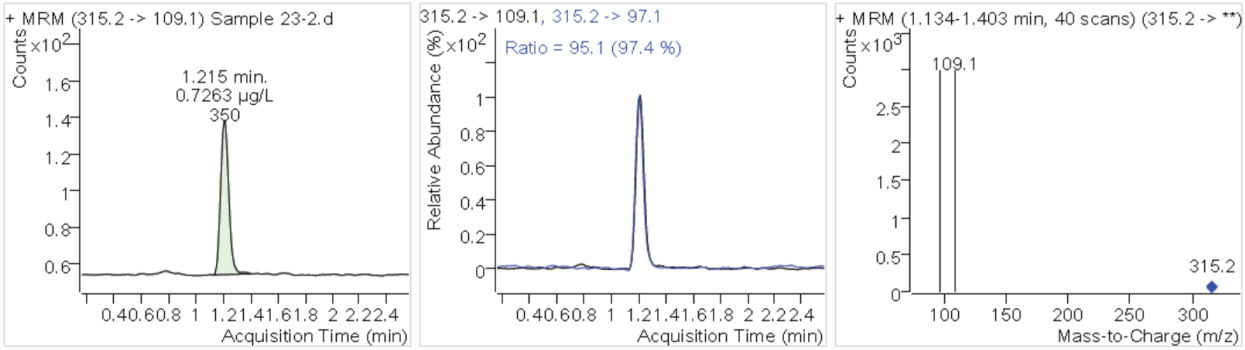

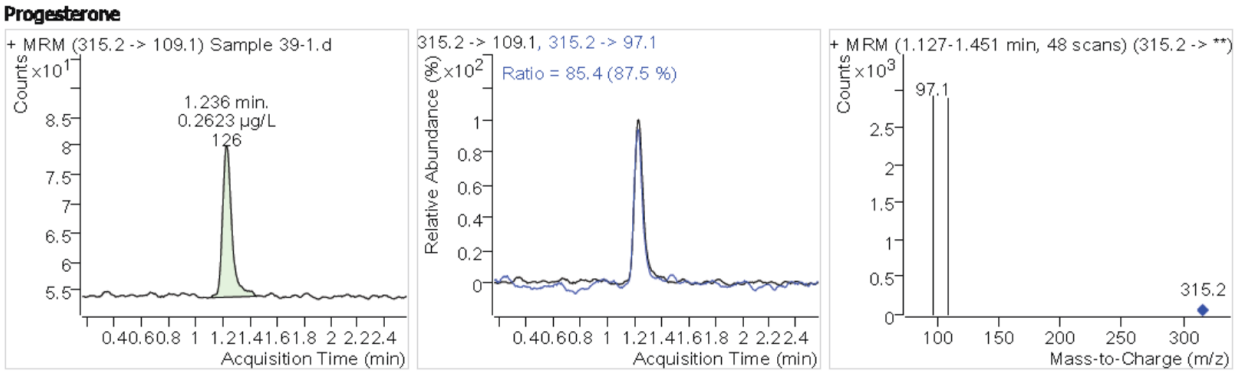

Appendix 14: Calibration curve and sample chromatograms for LNR adsorption

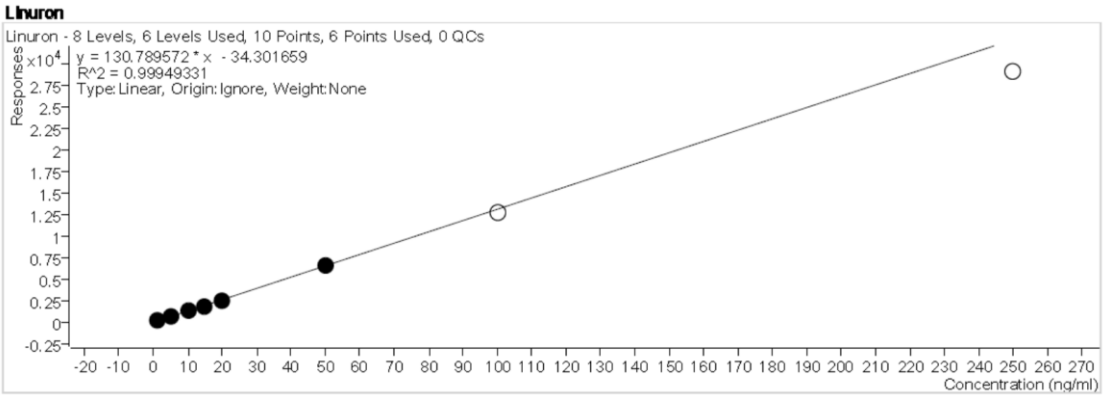

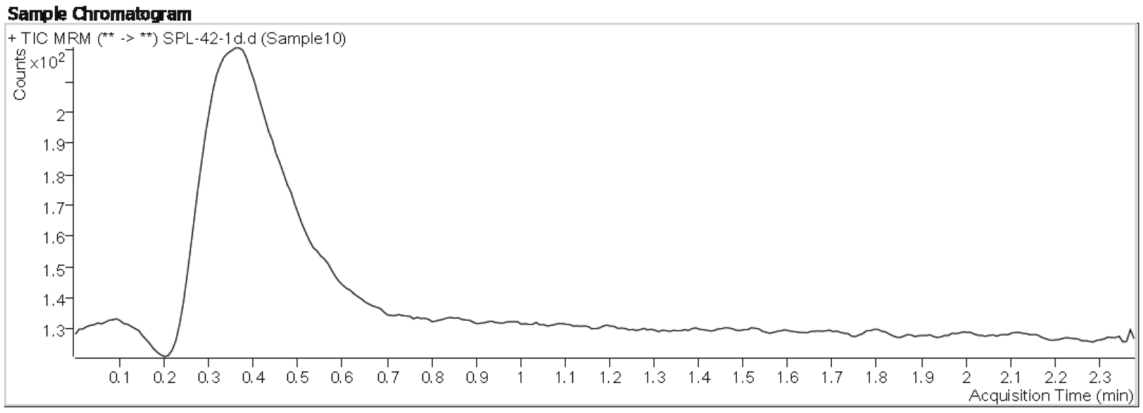

Linuron

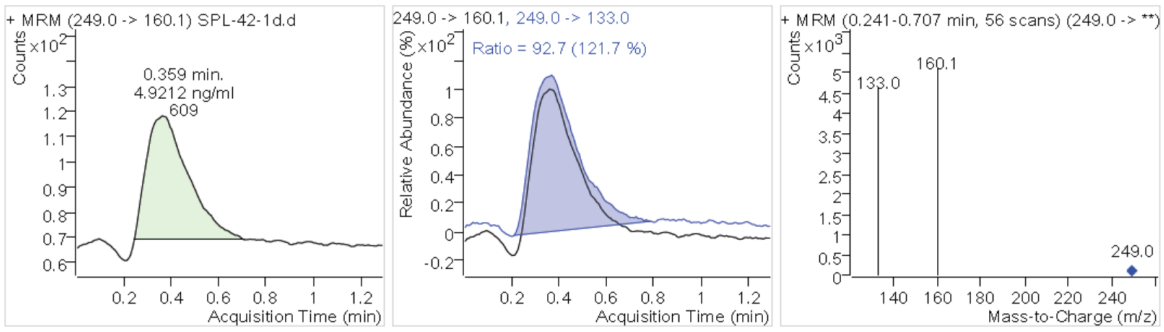

Linuron

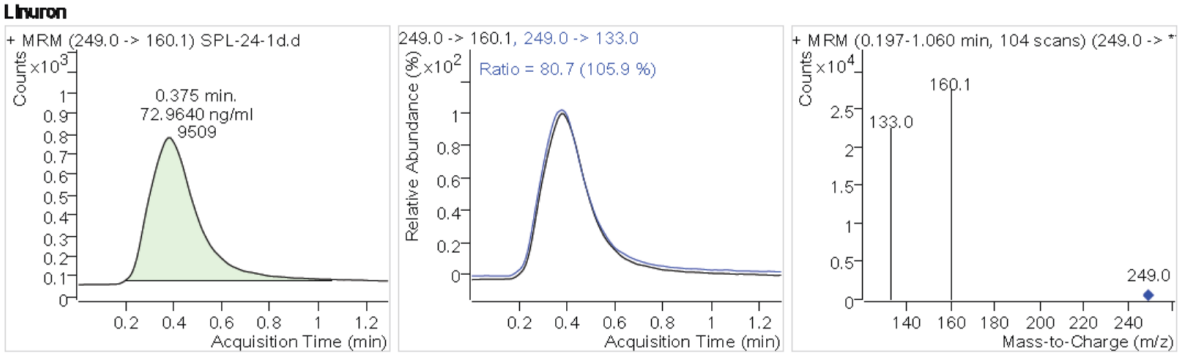

Linuron

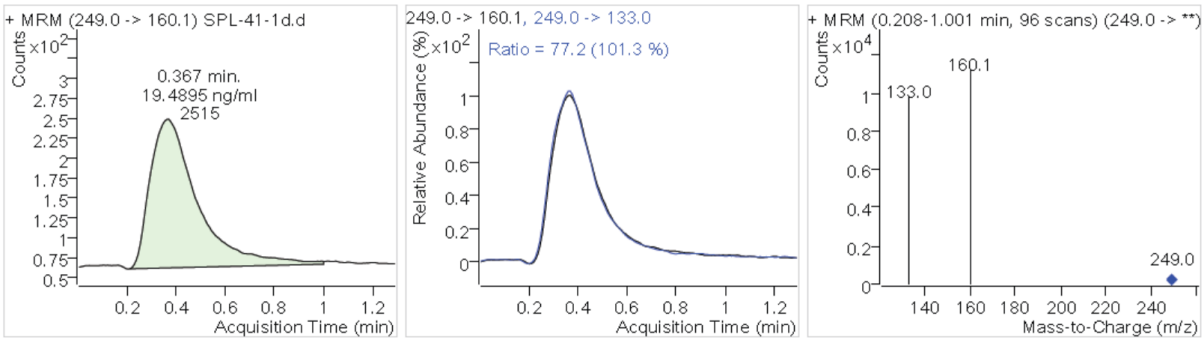

Linuron

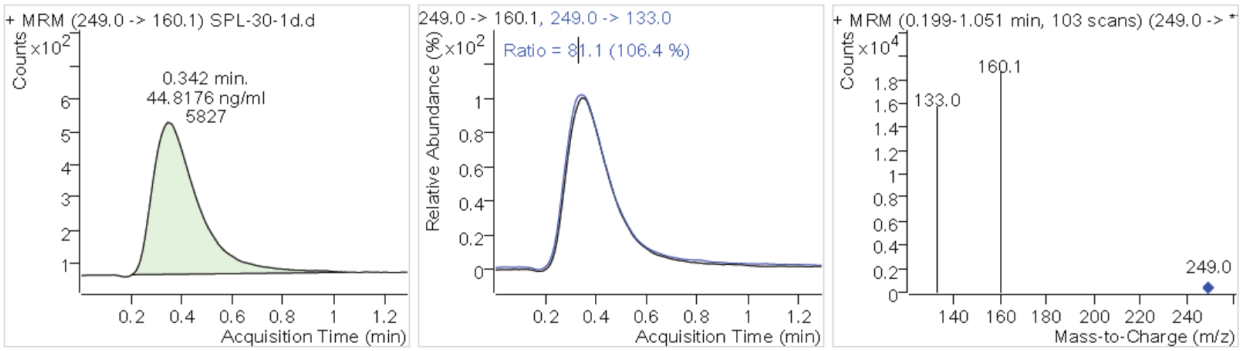

Linuron

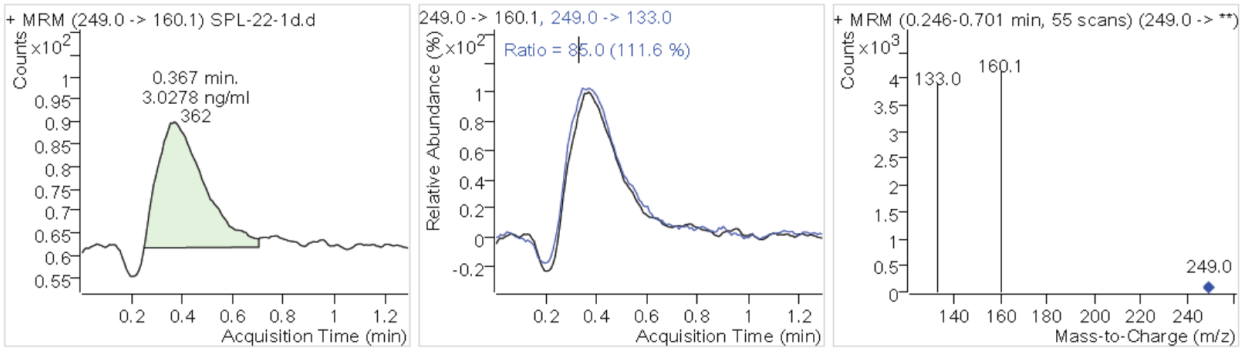

Linuron

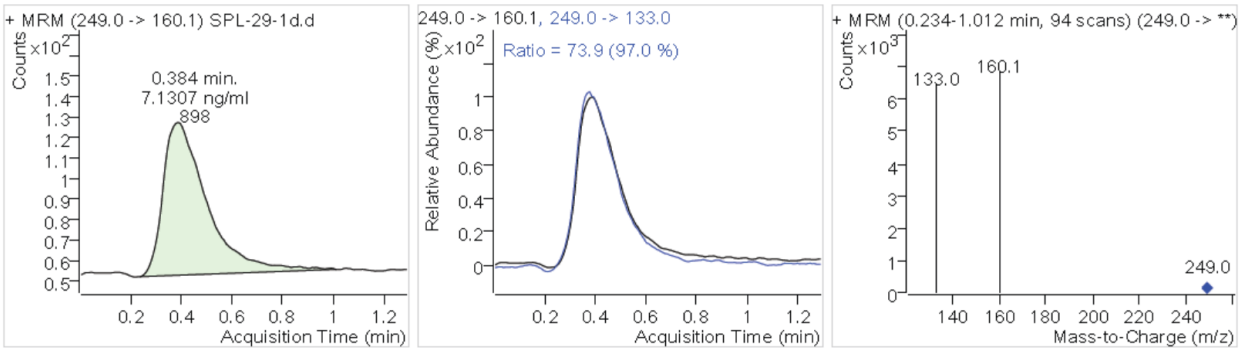

Linuron

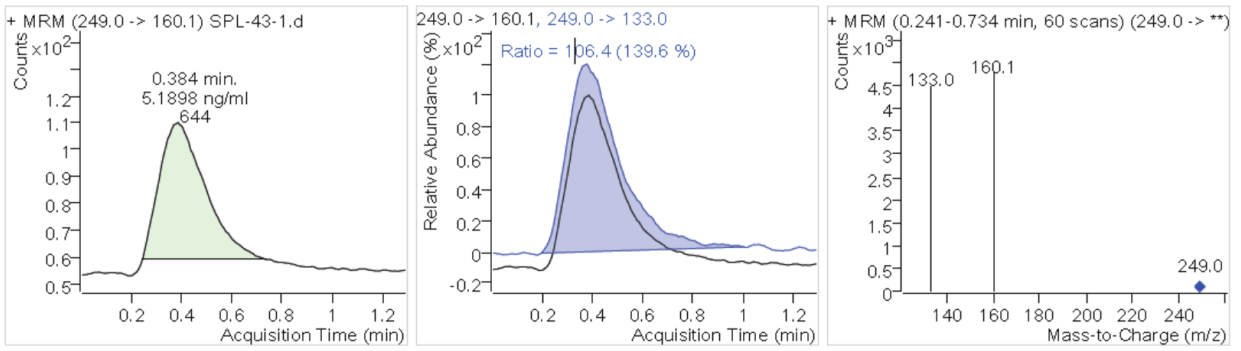

Linuron

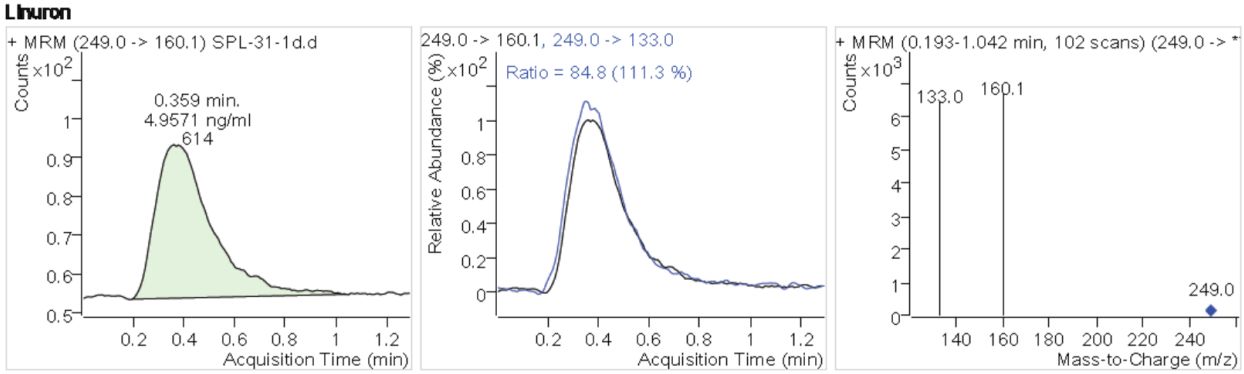

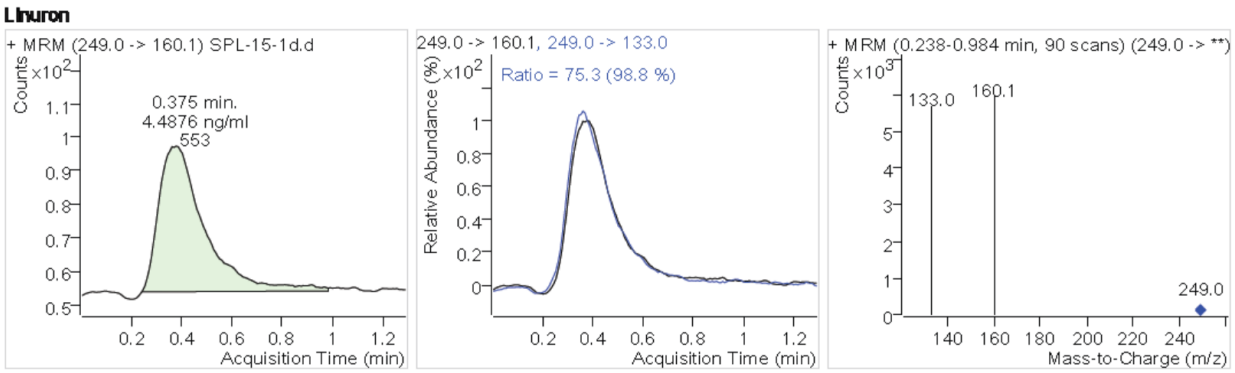

Appendix 15: Pictures from phytoremediation experiments


stem


P1
P2
P3

Appendix 16: Some sample chromatograms

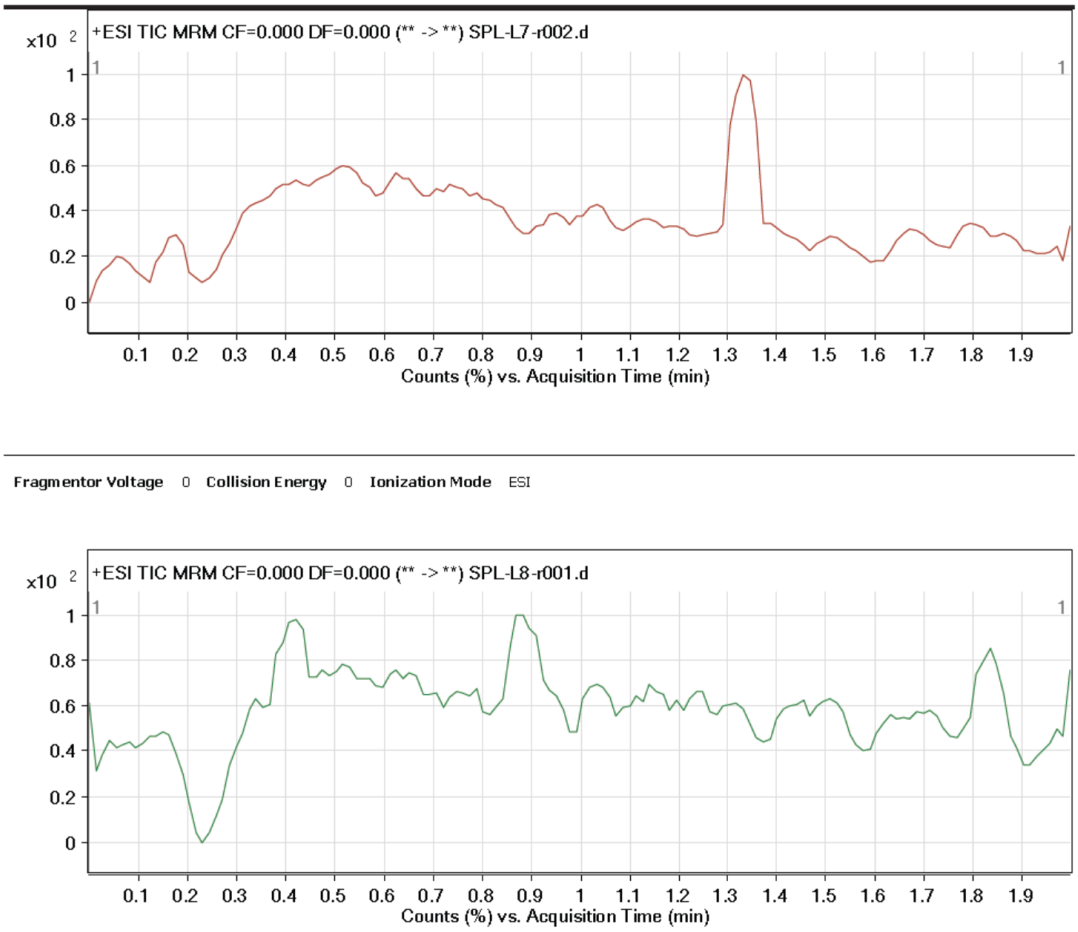

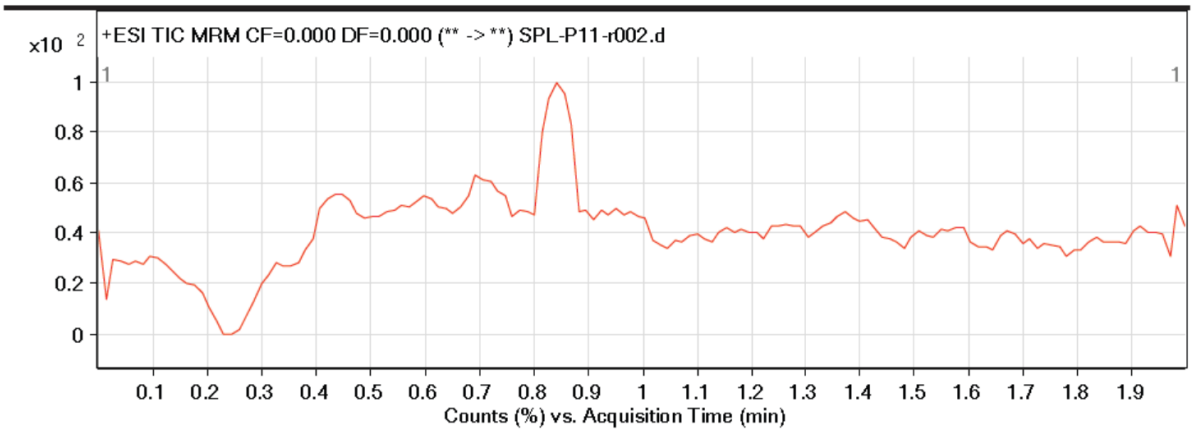

Fragmentor Voltage 0 Collision Energy 0 Ionization Mode ESI

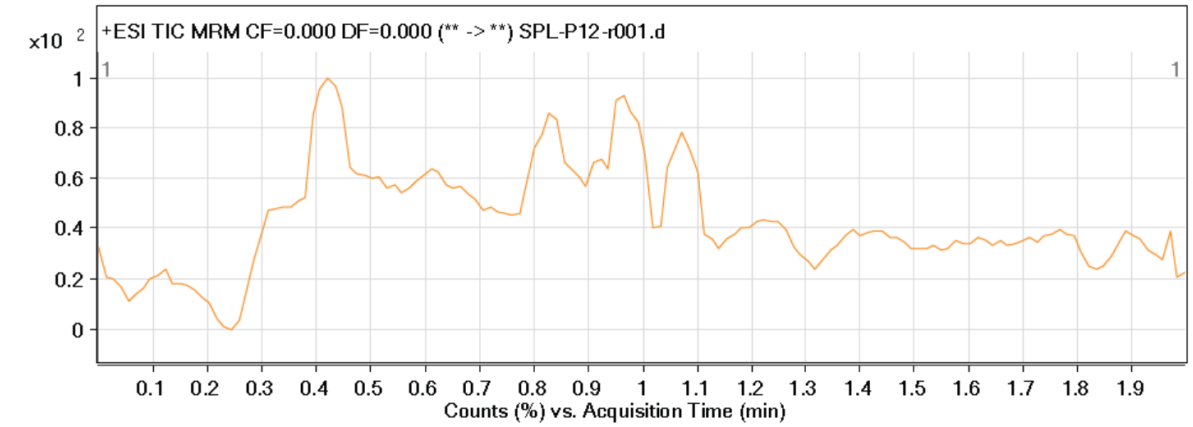

Appendix 17: First published paper

Environmental Advances 9 (2022) 100282

Contents lists available at ScienceDirect

Environmental Advances

journal homepage: www.sciencedirect.com/journal/environmental-advances

Sustainable re-utilization of waste materials as adsorbents for water and wastewater treatment in Africa: Recent studies, research gaps, and way forward for emerging economies

Emily Chelangat Ngeno [a,b,d], Kinyua E. Mbuci [a], Mohamed Chaker Necibi [c,*], Victor Odhiambo Shikuku [d], Chijioke Olisah [e], Roselyn Ongulu [a], Henry Matovu [b,f], Patrick Ssebugere [b,j,**], Almotasembellah Abushaban [c], Mika Sillanpää [g,h,i]

[a] Department of Pure and Applied Chemistry, Masinde Muliro University of Science and Technology, P. O. Box 190, Kakamega, Kenya
[b] Department of Chemistry, Makerere University, P. O. Box 7062, Kampala, Uganda
[c] International Water Research Institute, Mohammed VI Polytechnic University (UM6P), Green City Ben-Guerir 43150, Morocco
[d] Department of Physical Sciences, Kaimosi Friends University College, P. O. Box 385, Kaimosi, Kenya
[e] Department of Botany, Institute of Coastal and Marine Research, Nelson Mandela University, Port Elizabeth, South Africa
[f] Department of Chemistry, Gulu University, P. O. Box 166, Gulu, Uganda
[g] Department of Chemical Engineering, School of Mining, Metallurgy and Chemical Engineering, University of Johannesburg, P. O. Box 17011, Doornfontein 2028, South Africa
[h] Faculty of Sciences, Department of Chemistry, Biochemistry and Environmental Protection, University of Novi Sad, Trg Dositeja Obradovića 3, Novi Sad 21000, Serbia
[i] Department of Biological and Chemical Engineering, Aarhus University, Nørrebrogade 44, Aarhus C 8000, Denmark
[j] Department of Analytical Environmental Chemistry, Helmholtz Centre for Environmental Research—UFZ, Leipzig D-04318, Germany

ARTICLE INFO

Keywords:
Wastewater treatment
Pollutants
Adsorption
Waste materials
Africa

ABSTRACT

Access to clean water is a fundamental human right. However, due to the rapid urbanization and industrialization in many African countries, the emergence of a plethora of new classes of water contaminants coupled with aging wastewater treatment infrastructure and technologies, access to clean water has remained elusive especially to rural communities. Additionally, most countries in Africa cannot afford the capital investment associated with advanced and specialized treatment technologies. The solution seems to be the valorization of locally-sourced waste materials and their use as adsorbents, flocculants/coagulants, or photocatalysts, to be included in current and future wastewater treatment facilities. The present review presents a concise and comprehensive compilation, and critique of recent research water purification studies in Africa using waste-based adsorbents. While the abundance of industrial and agricultural wastes presents opportunity for sustainable exploitation for water treatment, several gaps warrant further research. Specifically, future research should include life cycle assessment (LCA) of the wastewater treatment plants (WWTPs) and proposed technologies, in-depth cost analysis, use of environmentally relevant concentrations in simulated studies or real wastewaters and examination of removal efficiencies for biological contaminants such as viruses, bacteria among others. Waste materials are shown to be suitable candidates for delivery of effective and techno-economic adsorbents for water purification in African countries.

Appendix 18: Second published paper

Environmental Research

journal homepage: www.elsevier.com/locate/envres

Endocrine disrupting chemicals in wastewater treatment plants in Kenya, East Africa: Concentrations, removal efficiency, mass loading rates and ecological impacts

Emily Ngeno [a, b, c], Roselyn Ongulu [a], Francis Orata [a], Henry Matovu [d], Victor Shikuku [b], Richard Onchiri [e], Abel Mayaka [f], Eunice Majanga [g], Zachary Getenga [h], Joel Gichumbi [i], Patrick Ssebugere [c, j, k, *]

[a] Department of Pure and Applied Chemistry, Masinde Muliro University of Science and Technology, P.O Box 190–50100, Kakamega, Kenya
[b] Department of Physical Sciences, Kaimosi Friends University, P.O Box 385–50309, Kaimosi, Kenya
[c] Department of Chemistry, Makerere University, P.O Box 7062, Kampala, Uganda
[d] Department of Chemistry, Gulu University, P.O Box 166, Gulu, Uganda
[e] Department of Civil Engineering, Technical University of Mombasa, P.O Box 000–80100, Mombasa, Kenya
[f] Faculty of Engineering, Multimedia University, P.O Box 15653–00503, Nairobi, Kenya
[g] Department of Social Sciences, Masinde Muliro University of Science and Technology, P.O Box 190–50100, Kakamega, Kenya
[h] Department of Physical Sciences, Machakos University, P.O Box 136–90100, Machakos, Kenya
[i] Department of Physical Sciences, Chuka University, P.O Box 109–60400, Chuka, Kenya
[j] Department of Cell Toxicology, Helmholtz Centre for Environmental Research–UFZ, 04318, Leipzig, Germany
[k] Department of Analytical Environmental Chemistry, Helmholtz Centre for Environmental Research–UFZ, 04318, Leipzig, Germany

ARTICLE INFO

Keywords:
Wastewater
Exogenous chemicals
Health effects
Aquatic organisms
Sub-Saharan Africa

ABSTRACT

This study investigated the levels, mass loadings, removal efficiency, and associated ecotoxicological risks of selected endocrine disrupting chemicals (EDCs), namely, dibutylphthalate (DBP), diethylhexylphthalate (DEHP), dimethylphthalate (DMP), linuron (LNR) and progesterone (PGT) in wastewater, sludge, and untreated dry biosolid (UDBS) samples from twelve wastewater treatment plants (WWTPs) in nine major towns in Kenya. Analysis was done using high-performance liquid chromatography coupled with triple quadrupole mass spectrometry (LC-MS/MS). All the wastewater influents had quantifiable levels of EDCs with DBP being the most abundant (37.49%) with a range of 4.33 ± 0.63 to 19.68 ± 1.24 μg L^{-1}. DEHP was the most abundant in sludge and accounted for 48.2% ranging between 278.67 and 9243.49 ng g^{-1} dry weight (dw). In the UDBS samples, DEHP was also the most abundant (40%) of the total EDCs detected with levels ranging from 78.77 to 3938.54 ng g^{-1} dw. The average removal efficiency per pollutant was as follows: DMP (98.7%) > DEHP (91.7%) > PGT (83.4%) > DBP (77.9%) > LNR (72.2%) which can be attributed to sorption onto the biosolid, biological degradation, photolysis, and phytoremediation. The pH was negatively correlated to the EDC concentrations while total dissolved solids (TDS), chemical oxygen demand (COD), biochemical oxygen demand (BODs), and electrical conductivity (EC) were positively correlated. The mass loadings were as high as 373.33 g day^{-1} of DBP in the treatment plants located in densely populated cities. DEHP and PGT had their Risk Quotients (RQs) > 1, posing a high risk to biota. DMP, DBP, and LNR posed medium risks as their RQ values were between 0.1 and 1. EDCs are therefore loaded to environmental compartments through either the effluent that loads these pollutants into the receiving aquatic ecosystem or through the UDBS, which are used as fertilizers in agricultural farmlands causing potential toxicological risks to aquatic and terrestrial life.

Appendix 19: Third published paper

Chemosphere 360 (2024) 142457

Contents lists available at ScienceDirect

Chemosphere

journal homepage: www.elsevier.com/locate/chemosphere

Response surface methodology directed modeling of the biosorption of progesterone onto acid activated *Moringa oleifera* seed biomass: Parameters and mechanisms

Emily Ngeno [a,b,c], Roselyn Ongulu [a], Victor Shikuku [b], Deo Ssentongo [c], Benton Otieno [d], Patrick Ssebugere [c,e,f,*], Francis Orata [a,**]

[a] Department of Pure and Applied Chemistry, Masinde Muliro University of Science and Technology, P.O Box 190–50100, Kakamega, Kenya
[b] Department of Physical Sciences, Kaimosi Friends University, P.O Box 385–50309, Kaimosi, Kenya
[c] Department of Chemistry, Makerere University, P. O Box 7062, Kampala, Uganda
[d] Department of Chemical and Metallurgical Engineering, Vaal University of Technology, Vanderbijlpark, South Africa
[e] Department of Cell Toxicology, Helmholtz Centre for Environmental Research–UFZ, 04318, Leipzig, Germany
[f] Department of Analytical Environmental Chemistry, Helmholtz Centre for Environmental Research–UFZ, 04318, Leipzig, Germany

HIGHLIGHTS

GRAPHICAL ABSTRACT

Appendix 20: MMUST Approval letters

MASINDE MULIRO UNIVERSITY OF SCIENCE AND TECHNOLOGY (MMUST)

Tel: 056-30870
Fax: 056-30153
E-mail: dps@mmust.ac.ke
Website: www.mmust.ac.ke

P.O Box 190
Kakamega – 50100
Kenya

Directorate of Postgraduate Studies

Ref: MMU/COR: 509099

Date: 11TH November, 2020

Emily Chelangat Ngeno,
SCH/H/01-56335/2017,
P.O. Box 190-50100
KAKAMEGA

Dear Ms. Ngeno,

RE: APPROVAL OF PROPOSAL

I am pleased to inform you that the Directorate of Postgraduate Studies has considered and approved your Ph.D. Proposal entitled: "***Occurrence, Adsorption and Phytoremediation of Selected Endocrine Disrupting Chemicals from Wastewater using Moringa Oleifera and Eicchornia Crassipes***" and appointed the following as supervisors:

1. Dr. Francis Orata – SONAS, MMUST
2. Dr. Roseline Ongulu - SONAS, MMUST
3. Dr. Patrick Sebugere - Makerere University

You are required to submit through your supervisor(s) progress reports every three months to the Director of Postgraduate Studies. Such reports should be copied to the following: Chairman, School of Natural Sciences Graduate Studies Committee; Chairman, Department of Pure and Applied Chemistry & Departmental Graduate Studies Committee. Kindly adhere to research ethics consideration in conducting research.

It is the policy and regulations of the University that you observe a deadline of three years from the date of registration to complete your Ph.D. thesis. Do not hesitate to consult this office in case of any problem encountered in the course of your work.

We wish you the best in your research and hope the study will make original contribution to knowledge.

Yours Sincerely,

DEAN
SCHOOL OF GRADUATE STUDIES
MASINDE MULIRO UNIVERSITY
OF SCIENCE & TECHNOLOGY

Prof. John Obiri
DIRECTOR, DIRECTORATE OF POSTGRADUATE STUDIES

MASINDE MULIRO UNIVERSITY OF SCIENCE AND TECHNOLOGY (MMUST)

Tel: 056-30870
Fax: 056-30153
E-mail: dps@mmust.ac.ke
Website: www.mmust.ac.ke

P.O Box 190
Kakamega – 50100
Kenya

Directorate of Postgraduate Studies

Ref: MMU/COR: 509099 **Date:** 23 September, 2024

Emily Chelangat Ngeno,
SCH/H/01-56335/2017,
P.O. Box 190-50100
KAKAMEGA

Dear Ms. Ngeno,

RE: APPROVAL OF PROPOSAL

I am pleased to inform you that the Directorate of Postgraduate Studies has considered and approved your Ph.D. Proposal entitled: "***Occurrence, Adsorption and Phytoremediation of Selected Endocrine Disrupting Chemicals from Wastewater using Moringa Oleifera and Eicchornia Crassipes"*** and appointed the following as supervisors:

1. Prof. Francis Orata - SONAS, MMUST
2. Dr. Roseline Ongulu - SONAS, MMUST
3. Dr. Patrick Sebugere - Makerere University

You are required to submit through your supervisor(s) progress reports every three months to the Director of Postgraduate Studies. Such reports should be copied to the following: Chairman, School of Natural Sciences Graduate Studies Committee; Chairman, Department of Pure and Applied Chemistry & Departmental Graduate Studies Committee. Kindly adhere to research ethics consideration in conducting research.

It is the policy and regulations of the University that you observe a deadline of three years from the date of registration to complete your Ph.D. thesis. Do not hesitate to consult this office in case of any problem encountered in the course of your work.

We wish you the best in your research and hope the study will make original contribution to knowledge.

Yours Sincerely,

MASINDE MULIRO UNIVERSITY OF SCIENCE AND TECHNOLOGY

Dr. Consolata Ngala
DEPUTY DIRECTOR, DIRECTORATE OF POSTGRADUATE STUDIES

Appendix 21: NACOSTI Research Permit

REPUBLIC OF KENYA

NATIONAL COMMISSION FOR SCIENCE,TECHNOLOGY & INNOVATION

Ref No: **220411**

Date of Issue: **11/October/2024**

RESEARCH LICENSE

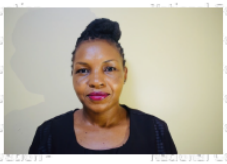

This is to Certify that Ms.. Emily Chelangat Ngeno of Masinde Muliro University of Science and Technology, has been licensed to conduct research as per the provision of the Science, Technology and Innovation Act, 2013 (Rev.2014) in Kakamega on the topic: OCCURRENCE, ADSORPTION AND PHYTOREMEDIATION OF SELECTED ENDOCRINE DISRUPTING CHEMICALS FROM WASTEWATER USING MORINGA OLEIFERA AND EICCHORNIA CRASSIPES for the period ending : 11/October/2025.

License No: **NACOSTI/P/24/40565**

220411

Applicant Identification Number

Director General
NATIONAL COMMISSION FOR SCIENCE,TECHNOLOGY & INNOVATION

Verification QR Code

NOTE: This is a computer generated License. To verify the authenticity of this document, Scan the QR Code using QR scanner application.

See overleaf for conditions